Optimisation of the Operation of the Ramspol Barrier

Thesis Report

MSc Thesis

S.D. (Selma) Prins

Delft University of Technology

TU Delft

Rijkswaterstaat
Ministerie van Infrastructuur en Milieu

Optimisation of the Operation of the Ramspol Barrier

Thesis Report

by

S.D. (Selma) Prins

to obtain the degree of Master of Science
at the Delft University of Technology,
to be defended publicly on Thursday April 3, 2024 at 11:30 AM.

Student number:	5088844	
Project date:	March 2025	
Thesis committee:	Dr. ir. B. C. (Bram) Van Prooijen,	TU Delft
	Mr. dr. ir. C. (Cong) Mai Van,	TU Delft
	Dr. ir. A. M. R. (Alexander) Bakker,	TU Delft and Rijkswaterstaat
	T. (Tycho) Busnach,	Rijkswaterstaat

Cover:	Closure of the Ramspol Barrier during closure (Rijkswaterstaat, 2024a).
Style:	TU Delft Report Style, with modifications by Daan Zwaneveld, Maaike van Agtmaal and Selma Prins.

An electronic version of this thesis is available at http://repository.tudelft.nl/.

TU Delft

Acknowledgements

This thesis marks the completion of my master's degree in Civil Engineering, but also the end of my life as a student in Delft. Five and a half years ago, I came to Delft without knowing anyone or anything about what lay ahead. It proved to be an amazing time that shaped me both academically and personally. I met countless wonderful people from all parts of the Netherlands and beyond, with whom I shared numerous nights, tennis and bouldering sessions, and unforgettable vacations. For my studies, I always let my curiosity guide my choices, leading to countless lectures about all aspects of hydraulic structures and overseas to California for a multidisciplinary project. Although not as a design as in most courses, this interest is also present in my thesis as an operational question. I'm grateful for this period and look forward to my next chapter and more memorable moments with the people I met here.

To my committee, I would like to express my sincere gratitude for your guidance and enthusiasm throughout this thesis. Alexander, I am grateful for your extensive guidance and feedback during our weekly meetings and for your enthusiastic ideas. Furthermore, your expertise in data analysis has helped me with my own analysis, resulting in a profound understanding of the system. Tycho, thank you for sharing your practical insights into the operation of the Ramspol Barrier and the broader system. Your input helped me complete this project and deepened my understanding of the real-world challenges of flood defense operations beyond their design. Bram, I appreciate your guidance in structuring my hydraulic model and your sharp remarks during our meetings. This helped me identify the shortcomings of my project.

S.D. (Selma) Prins
Delft, March 2025

Abstract

The Ramspol Barrier, an inflatable storm surge barrier, is an integral component of the flood protection system for the Zwarte Meer and its hinterland. However, its current operational procedure faces several challenges that compromise flood safety, cause disruptions for the shipping industry, and significantly burden the operation team. The current operational procedure activates specific steps based on predefined water level thresholds, often mobilizing the operation team and disrupting shipping without ultimately leading to a barrier closure. It is also questioned whether closures are always the best strategy for optimizing flood safety in the system.

This thesis aims to improve the operational procedure of the Ramspol Barrier by balancing flood safety, operational burden, and disruptions to vessel navigation.

A comprehensive system and data analysis were conducted to understand the dynamics of high-water events, which are primarily driven by onshore winds, precipitation, and wind-induced water setups. These conditions, coupled with restricted drainage at the Afsluitdijk and increased discharges from the Zwarte Water and IJssel, result in rapid water level rises at the barrier. The current operation protocol triggers closure at +0.50 m NAP and an inland flow, protecting the Vecht Delta. However, this blocks outflow, delays vessel movements, and causes water accumulation in the Zwarte Meer. The analysis further revealed a strong correlation between higher water levels and wind setup. In comparison, the impact of discharges from the IJssel and Zwarte Water on higher water levels was minimal. The findings also highlighted the growing strain on the operation team and the disruptions faced by the shipping industry over recent years.

Nine scenarios were simulated using a developed reservoir model to assess the system's sensitivity to wind setups and discharges, the effect of adjustments to the operation procedure, and the model's predictive capabilities. The simulations revealed that closures during receding or stagnating water levels, or when wind setup was already developed, sometimes resulted in higher water levels than non-closure scenarios. In cases where water levels were between +0.40 m NAP and +0.50 m NAP, navigation could often be maintained, provided wind setups were reducing or stagnating, and no significant discharge peaks were predicted. Moreover, minor wind events at initial water levels above +0.50 m NAP frequently triggered unnecessary closures, which could elevate water levels, highlighting the need for more robust closure criteria based on sustained flow rather than momentary fluctuations. When multiple peaks occurred, the timing and proximity of these peaks played a crucial role in determining the impact on water levels. Earlier closures reduced water levels but extended operational disruptions, while higher discharges led to faster water level rises post-closure, requiring earlier openings. Lastly, enhancing the ability to predict critical water levels and closure and opening criteria can significantly benefit both operational teams and the shipping industry. Implementing 24- to 48-hour forecasts would enhance planning by ensuring teams are on-site when needed, minimizing unnecessary disruptions, predicting the timing and likelihood of Ramspol Barrier closures, and enabling the shipping industry to adjust schedules to reduce waiting times.

The results indicate that an adaptive, forecast-driven approach to barrier operation could potentially improve flood protection, reduce disruptions for the shipping industry, and alleviate the team's operational burden.

Contents

List of Figures

List of Tables

1

Introduction

Approximately 60 per cent of the Netherlands is susceptible to flooding, while this region accounts for 70 per cent of the nation's gross domestic product and houses around 9 million residents (Rijksoverheid, 2024). This vulnerability, combined with predictions of sea level rise and increasingly extreme weather events, underscores the importance of effective flood protection measures.

A key component of Dutch flood defenses is storm surge barriers: movable hydraulic structures that temporarily close waterways during high water events. One such structure is the Ramspol Barrier, located near Zwolle in the province of Overijssel. This inflatable barrier is deployed to close off the Zwarte Meer from the Ketelmeer and IJsselmeer during high water levels of +0.50 m NAP [1] and a current from the Ketelmeer towards the Zwarte Meer. Completed in 2002, the Ramspol Barrier has been vital in safeguarding the western part of Overijssel—home to approximately 190,000 people—against flooding (Vergouwe, 2014). On average, it closes once or twice per year (Rijkswaterstaat, 2024a).

1.1. Problem Analysis

Despite its critical role in flood protection, the operation of the Ramspol Barrier faces several challenges that compromise its ability to ensure flood safety and increase hindrance for both the operation team and the shipping industry. The operation team of Rijkswaterstaat is frequently mobilised in anticipation of conditions meeting the current closing criteria: a water level of +0.50 m NAP coinciding with water flow towards the Zwarte Meer (Rijkswaterstaat, 2024a). However, due to uncertainties in the water level and wind predictions, the team is activated more frequently than the number of actual closures of the Ramspol Barrier, meaning that they often oversee situations at the barrier location without ultimately closing it. Additionally, vessel passages are prohibited after the water level reaches +0.40 m NAP, causing significant hindrances, especially when the barrier does not close.

Crucially, the current operation procedure does not always guarantee optimal flood safety within the system. For example, it may not adequately account for more complex weather conditions, such as peaks just exceeding the closure criteria of +0.50 m NAP or multiple subsequent peaks, which may require various closures or extended periods of closures. Since the closure or opening procedure, once initiated, must be completed before it can be reversed, improper operation can result in suboptimal protection. In some cases, this could expose the system to unnecessary risks during critical weather conditions.

Addressing these shortcomings is crucial to enhance the barrier's operational performance and ensure the procedure is efficient and fully aligned to protect the system against flooding. An evaluation of the current approach is required to develop an optimised operation procedure that minimises disruptions and provides the highest level of protection during adverse weather conditions.

[1] NAP: Normaal Amsterdams Peil: A reference level used to express the elevation in The Netherlands. The elevation of +0 m NAP is equivalent to the average sea level (Rijkswaterstaat, 2024d).

1.2. Objective and Research Questions

This research aims to optimise the Ramspol Barrier's operation procedures to balance the demands on the operation team, minimise disruptions to vessels, and ensure flood safety within the system. The corresponding research question is as follows:

How can the Ramspol Barrier be optimally operated under current conditions to balance the operational challenges faced by the team, minimise disruptions to the shipping industry, and ensure compliance with flood safety regulations?

To answer this question, the following sub-questions will need to be addressed:

1. *What are the characteristics of the Ramspol Barrier water system, including its layout, meteorological and hydrological conditions, operation, and flood safety requirements?*
2. *How can the system be modelled and how will changes in operation procedures of the Ramspol Barrier affect water levels within the system?*
3. *How can the operation procedure of the Ramspol Barrier be improved?*

1.3. Method

Various methods are required to answer the questions presented in section 1.3 and achieve the goal of improving the Ramspol Barrier's operational procedure. An overview of the method, inputs and outputs is shown in Figure 1.1.

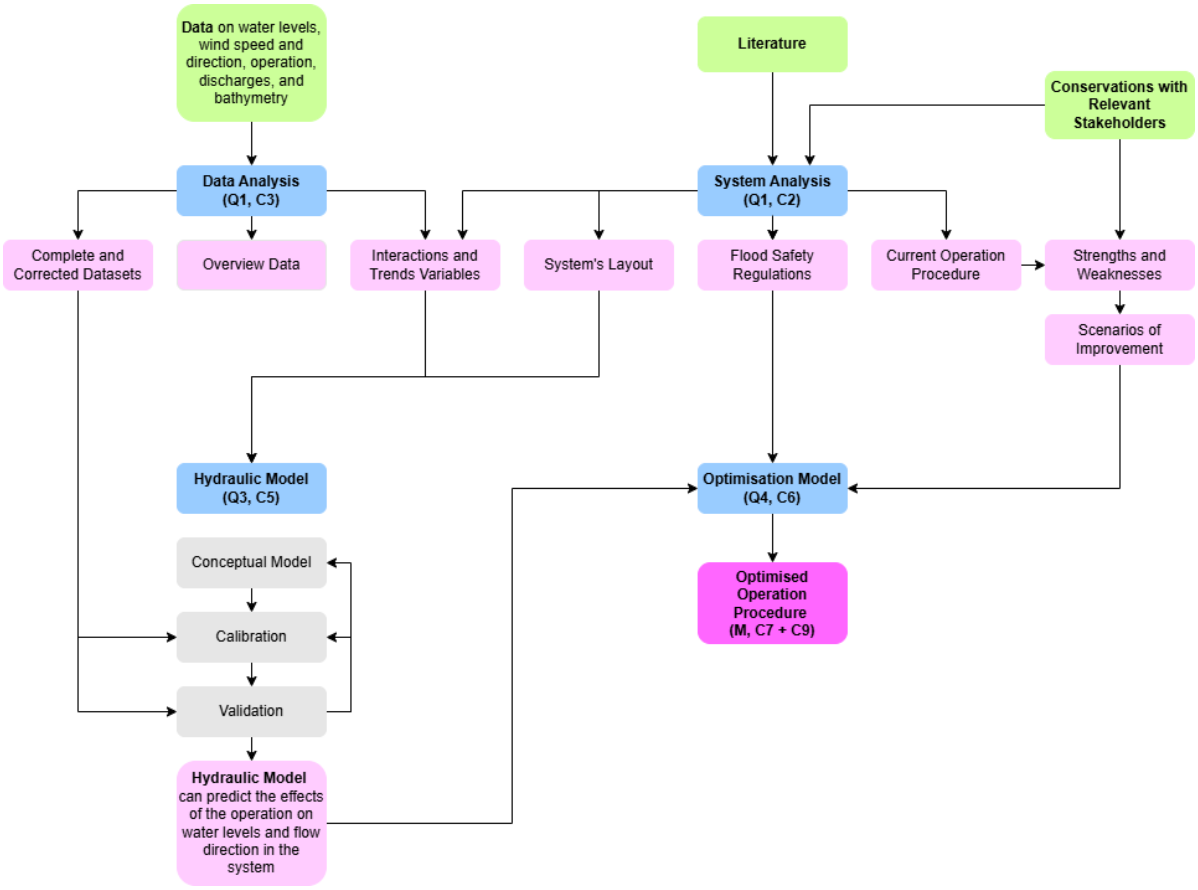

Figure 1.1: Overview of the method, including research questions (Q), chapters (C), steps (blue), input (green) and output(pink).

Firstly, to achieve a thorough understanding of the layout, interactions, and management of the IJsselmeer and Vecht- and IJssel delta system, two analyses are done: a system analysis (chapter 2) and a data analysis (chapter 3). The first will describe the layout, flood safety management, and current operation of the Ramspol Barrier based on a literature study and meetings with the system's managers. The data analyses will focus more on cleaning, corrections, trends, and interactions of observations of the water levels, discharges, wind speed and direction in the water system. Additionally, possible changes in weather conditions and water levels under climate change are considered here.

Subsequently, the gathered descriptive knowledge is used to create a hydraulic model of the IJsselmeer and IJssel and Vecht Delta water system. This model should estimate the water levels in the system and water flow direction at the Ramspol Barrier based on the following inputs: the wind speed and direction, the river and drainage discharges, initial water levels, and operation of the Ramspol Barrier (closed or not). The ultimate goal of the model is to rapidly run scenarios with enough certainty such that it can be used to support the decision of whether or not a closure is necessary (Tycho).

The development of the hydraulic model will start with an inventory of the existing models and their availability since these may be used as a baseline for the to-be-developed model. The model has the following requirements:

- A robust simplified model: the primary aim is to develop a hydraulic model which can predict water levels in the system and flow direction at the barrier with enough certainty. Therefore, a more simple reservoir model will be developed and attention to its 'correctness' will be given by validating it with data and/or existing models.
- Must be able to run improvement scenarios automatically through commands in Python.
- Must be able to take prediction uncertainty into account.
- Limited run time such that it can consider numerous cases during the improvement process and quickly run scenarios during the operation procedure. More complex models are less qualified for this purpose since the implementation and running time are longer.
- Easy to understand and implement for people without prior knowledge of Python code.

The final hydraulic model is thus a balance between its accuracy, development and simulation time, accessibility and adaptability.

Initially, the model will focus on the IJsselmeer, Zwarte Meer, Ketelmeer, Zwarte Water, Vecht, IJssel, and the Ramspol Barrier. Additions of smaller water bodies such as bypasses, sluices, and streams may be added at a later stage if considered useful and when time allows. Furthermore, the model will not focus on the structural response of hydraulic structures (Ramspol Barrier, levees, sluices, etc.) to hydraulic loads.

Subsequently, simulations in the hydraulic model are used to propose a proper operation procedure for specific scenarios, considering statistical uncertainty and balancing the system's flood safety with the hindrances for the operation team and shipping industry. These scenarios are formulated by interviewing the Ramspol Barrier's operation team, about what they consider the benefits or disadvantages of the current operation procedures and what their wishes are for the improvement of the operation procedure and specify which weather conditions require the most improvement. This will be combined into potential optimisation areas and relevant weather scenarios.

1.4. Layout Report

The layout of the report is as follows:

- **Chapter 1** introduces the problem, the research goal and questions, and the methods.
- **Chapter 2** describes the layout and workings of the IJsselmeer and IJssel- and Vecht Delta.
- **Chapter 3** discusses the available data, and their trends, interactions and corrections.
- **Chapter 4** presents the conceptual hydraulic model and its calibration and validation.
- **Chapter 5** identifies potential areas and scenarios for operational improvement and analyses their results following simulations with the hydraulic model.
- **Chapter 6** reflects on the applied methods, assumptions and results.
- **Chapter 7** concludes the thesis by answering the research questions and offering recommendations for additional research.

2

Water System and Ramspol Barrier Operation

The Vecht-IJssel Delta and the IJsselmeer, situated in the northern part of the Netherlands, are the focus for optimising the operation of the Ramspol Barrier, as shown in Figure 2.1. This chapter provides an overview of the water system, the Ramspol Barrier, its operation, and the associated flood safety standards.

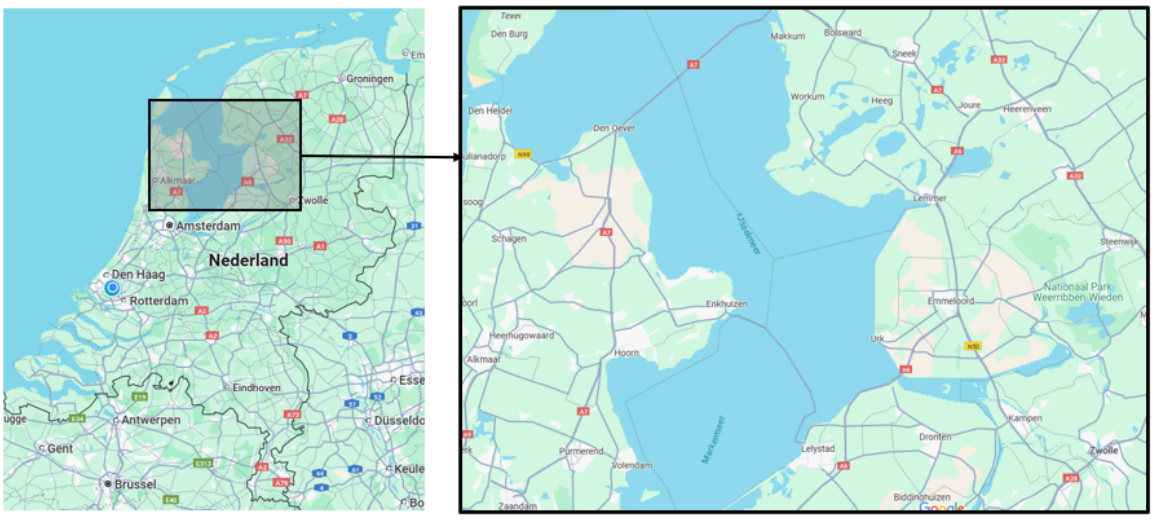

Figure 2.1: Location of the water system of interest within the Netherlands (Google Maps, 2024).

2.1. The Water System

As mentioned, the studied water system consists of the IJsselmeer and the Vecht-IJssel Delta. The latter contains the Ketelmeer, Zwarte Meer, Zwarte Water, Vecht, IJssel, Vossemeer, and Reevediep. An overview of the system is shown in Figure 2.2.

The IJssel, Vecht, and Zwarte Water feed the system. Precipitation from parts of Overijssel, Drenthe, and the western part of Germany drains into local streams and canals, which flow into the Vecht and Zwarte Water. The discharge of these rivers is highly precipitation-dependent, and their outlet is located on the east end of the Zwarte Meer. The IJssel is a branch of the river Rhine and discharges into the Ketelmeer at its eastern side.

Figure 2.2: Map of the water system of interest.

The Zwarte Meer is located between Overijssel and the Noord-Oostpolder, and the Noord-Oostpolder bounds the Ketelmeer in the North, the Flevopolder in the South, and the IJsselmeer on the West. The divide between the two lakes is the Ramspol Barrier, an inflatable storm surge barrier that can be closed in case of high water levels and inland stream conditions. It then protects the Vecht Delta against flooding. More information on the Ramspol Barrier can be found in section 2.2 and section 2.3.

Downstream from the Zwarte Meer and Ketelmeer, the water is stored in the IJsselmeer. The Afsluitdijk bounds the lake in the North, the province of Friesland in the Northeast, the Province of North-Holland in the West, the Province of Flevoland in the Southeast, and the Houtribdijk in the South. The Afsluitdijk closes the IJsselmeer off from the Wadden Sea, and the Houtribdijk, located between Enkhuizen, North-Holland, and Lelystad, Flevoland, closes the IJsselmeer off from the Markermeer.

Alongside the discharges from the Vecht and IJssel Delta, the IJsselmeer is fed with precipitation and water inflow from pumps and locks along the lake.

The water level is regulated by the Lorentz and Stevin Locks in the Afsluitdijk, located on the north side of the IJsselmeer. These drainage locks discharge water (free decay) into the Wadden Sea when opened, but only if the water level in the Wadden Sea is lower than that of the IJsselmeer. These locks could thus be used to mitigate droughts and high water levels to a certain extent by respectively storing or releasing water (Rijkswaterstaat, 2024e). The current maximum drain capacity through the Afsluitdijk is about 5000 cubic metres per second, but options to increase the drain and pump capacity are investigated (Grevers & Zwaneveld, 2011). About two-thirds of this capacity is located at the Lorentz locks (two times five shafts of 12 metres) and the other one-third at the Stevin Locks (five shafts of 12 metres) (Rijkswaterstaat, 2023).

As decided in the Nieuwe Peilbesluit 2018, the target water levels of the IJsselmeer have since February 2019 been set to -0.40 m NAP in winter and between -0.30 and -0.10 m NAP in summer. The higher water level in summer mainly accommodates drier weather and an increased water demand (Rijkswaterstaat, 2024e). However, annual deviations from these targets are observed.

2.1.1. Flood Defences and Hydraulic Structures

Various flood defences and hydraulic structures are in place to protect the water system against floods and manage the water levels and navigation in the system. The flood defences mainly consist of levees and a few flood barriers. In the Netherlands, flood defences are part of a so-called dike ring, which protects its enclosed area through a combination of levees, structures and in some cases naturally high terrain. Each dike ring is further divided into smaller segments, each with its safety standards (see section 2.4). Within the water system of interest, the following dike rings are located: Dike Ring 7, the Northeast Polder, Dike Ring 8, the Flevoland, Dike Ring 9, Vollenhove, Dike Ring 10, Kampen, Dike Ring 11, IJssel Delta, and Dike Ring 53, Zwolle. The locations of the dike rings are indicated in Figure 2.3,

and an overview of the locks and barriers in the system is given in Table 2.1. As illustrated in Figure 2.3, north of Dike Ring 10 lies an area not protected with primary flood defences. This area functions as a retention area, but also locates houses and farmland, meaning that flooding is still undesirable. The area is protected by a small levee with a height of approximately 1 metre.

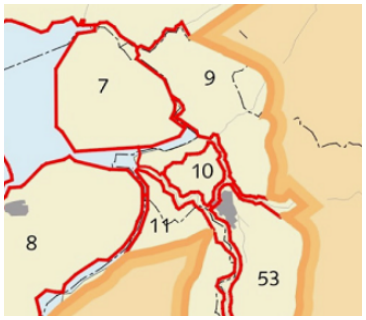

Figure 2.3: Map of the location of the dike rings within the Vecht-IJsseldelta (Rijksoverheid, 2015).

Table 2.1: Overview of the locks and barriers in the Vecht-IJsseldelta (Pfaff-Wagenaar et al., 2016).

Structure	**Location**	**Function**
Keersluis Zwolle	Zwarte Water/Weteringen	Floodgate; protects the centre of Zwolle and its hinterland against high water levels on the Zwarte Water and Vecht. Closes when the water level exceeds +1.0 m NAP and the water flow direction is towards the city centre of Zwolle.
Gemaal Zedemuden	Zwarte Water/Meppelerdiep	Pumping station; discharges water from Meppelerdiep into Zwarte Water in case of high water levels.
Meppelerdiepsluis	Zwarte Water/Meppelerdiep	Ship lock. Open passage if water levels are between -0.50 m NAP and +0.50 m NAP, closed if water levels are higher or lower.
Grote Kolksluis	Zwarte Water/Meppelerdiep	Ship lock.
Kadoelerkeersluis	Zwarte Meer/Kadoelermeer	Floodgate; closes off Kadoelermeer from Zwarte Meer when water level at Zwarte Meer side exceeds +1.0 m NAP.
Ramspol Barrier	Zwarte Meer/Ketelmeer	Storm surge barrier; closes off Zwarte Meer from the Ketelmeer and IJsselmeer to protect its hinterland against flooding. Closes in case of water levels over +0.5 m NAP and inland flow direction. Maximum retention height is +3.5 m NAP.
Reevesluis	Reevediep/Drontermeer	Ship and drainage lock.
Scheeresluis	IJssel/Reevediep	Ship lock and spillway; normally used as a lock, but can, in case of high water conditions on the IJssel, be opened to use the Reevediep as a bypass to increase the discharge capacity and thus increase flood safety.
Spooldersluis	IJssel/Zwarte Water	Floodgate; closes off the IJssel from the Zwolle-IJssel Canal.
Ganzensluis	IJssel/Ganzendiep	Ship lock. It is used as a floodgate if the Ramspol Barrier is closed.

2.1.2. Hydrological Conditions

Although there is a target water level, the IJsselmeer's actual water level can deviate from this due to various factors. The water levels in the system are influenced by the initial water level of the IJsselmeer, the wind setup over the IJsselmeer, Ketelmeer and Zwartemeer, the discharges of the IJssel, Vecht and Zwarte Water, the drain capacity through the Afsluitdijk, and the local precipitation (Pfaff-Wagenaar et al., 2016).

The water level at the IJsselmeer is significantly affected by the drain capacity of the Lorentz and Stevin Locks in the Aflsuitdijk, as well as the inflow from rivers, locks and precipitation. Drainage through these locks depends heavily on the water level of the Wadden Sea, as drainage is only possible when the Wadden Sea's water level is lower than that of the IJsselmeer. Due to tidal variations and setups over the Wadden Sea, drainage is only possible part of the time. The Wadden Sea experiences semi-diurnal tides, meaning there are two high and two low tides every 24 hours. The tidal range usually varies between 1.5 and 3 metres, with significant spatial variations. For example, the average tidal range at Kornwederzand is 1.8 metres and at Den Oever 1.5 metres (Rijkswaterstaat, 2023).

The inflow of the IJsselmeer largely consists of the discharges of the Vecht, Zwarte Water, and IJssel. The Vecht and Zwarte Water discharges are largely driven by regional precipitation and runoff, with peaks often arriving in the Zwarte Meer about a day later. In extreme wet conditions, the Zwarte Water discharges about 500 to 800 m^3/s (Pfaff-Wagenaar et al., 2016). The discharge from the IJssel accounts for about 14 to 17 per cent of the Rhine's discharge at Lobith, with peaks at Lobith taking two to three days to reach Kampen. Downstream from Olst, where the IJssel's discharge is measured, the lateral inflow is negligible since the river is bordered by high terrain on both sides (Salland and Veluwe). During extreme wet conditions, the IJssel discharges about 1500 to 2000 m^3/s (Pfaff-Wagenaar et al., 2016)).

High water scenarios in the system often result from comparable weather conditions: onshore winds from the North Sea causing precipitation in the water system and water set up along the coast. High setups at the Wadden Sea side of the Afsluitdijk can limit the drainage of the IJsselmeer. Additionally, high precipitation in the region further increases the discharges of the Zwarte Water and IJssel, contributing to higher inflow and water levels in the system.

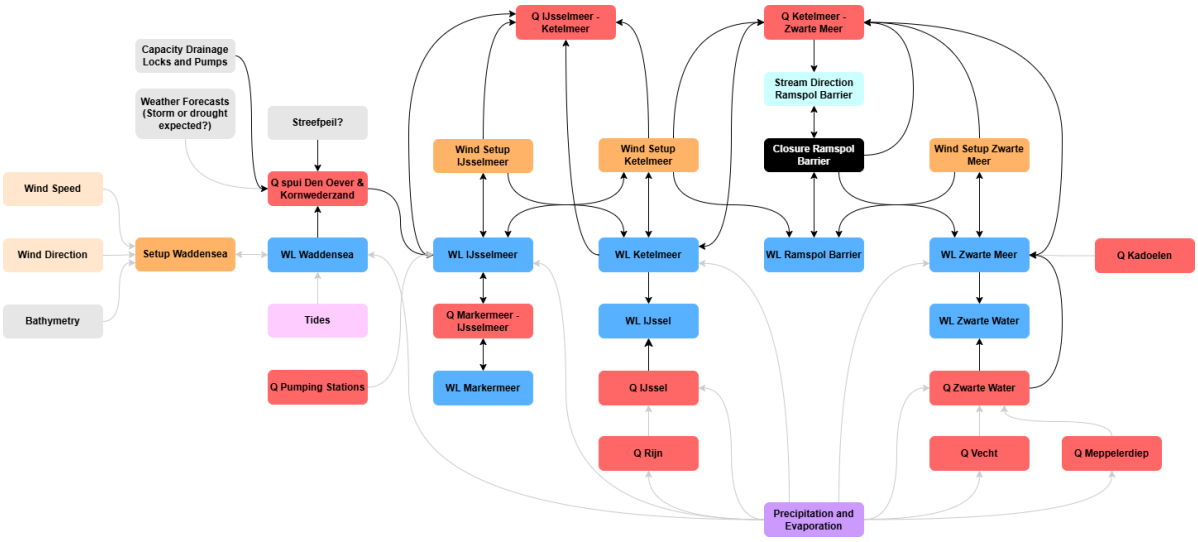

Figure 2.4: The interactions between variables in the water system. The black lines represent the processes included in the model, while the grey lines indicate processes that exist but are not accounted for.

In such scenarios, significant wind setup is also developed, since the northwestern winds push the water over the funnel-shaped IJsselmeer, and the connected Ketelmeer and Zwarte Meer. This leads to rapid water level rise at the Ramspol Barrier. When the water level at the Ramspol Barrier reaches +0.50 metres NAP and the flow direction is land inwards, the barrier closes to prevent the Vecht Delta against high water levels and wind setups. However, the closure also prevents water outflow of the Zwarte Meer, which combined with increased inflow from the Zwarte Water, leads to water level rise (Pfaff-Wagenaar et al., 2016). As described in subsection 2.1.1, levees and various hydraulic structures are in place to protect the hinterland and regulate the water levels in the system.

2.1.3. Shipping Industry

Under normal conditions, the Ramspol Barrier remains open, allowing ships to pass freely. This creates a continuous water system connecting the Zwarte Meer, Zwarte Water and Vecht to the Ketelmeer and IJssel. However, when the Ramspol Barrier is closed, this connection is interrupted, and vessels must bypass the barrier by navigating through the Spooldersluis and Zwolle-IJsselkanaal. This adds up to a full day of delays for the shipping industry (Pfaff-Wagenaar et al., 2016). No precise data is available on the scale of the shipping industry or the extent of the disruption.

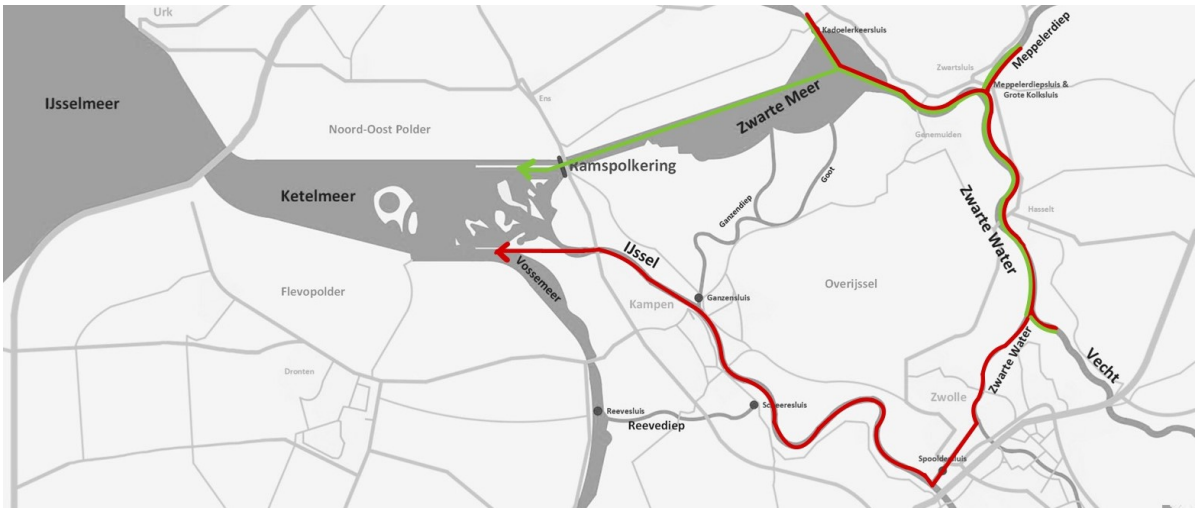

Figure 2.5: Normal shipping route (green) and its alternative when the Ramspol Barrier is closed (red).

2.2. Ramspol Barrier

The Ramspol Barrier is an inflatable rubber storm surge barrier between the Ketelmeer and Zwartemeer. Designed to provide temporary flood protection, it only closes when water levels reach +0.50 m NAP and there is a northwestern current. During such closures, it protects the western part of Overijssel against flooding. When open, the barrier allows for navigation and water exchange between the lakes.

The barrier comprises three rubber dams, each 80 meters long, 10 meters high, with a rubber thickness of 16 millimetres and a water retaining height of +3.5 m NAP. During closures, each dam is inflated with 3.5 million litres of both water and air, resembling a gigantic bicycle tyre. Between closures, the rubber fabric is stored in a sill at the bottom, enabling navigation and water exchange. One of the rubber dams is situated in the Ramsdiep, serving as a fairway for commercial vessels, while the other two are located in the Ramsgeul. The northern Ramsgeul dam is used by recreational boats, whereas the southern dam is completely closed to all shipping (Rijkswaterstaat, 2024a). Additionally, there is a permanent rock barrier section in the middle. The layout of the Ramspol Barrier is shown in Figure 1.

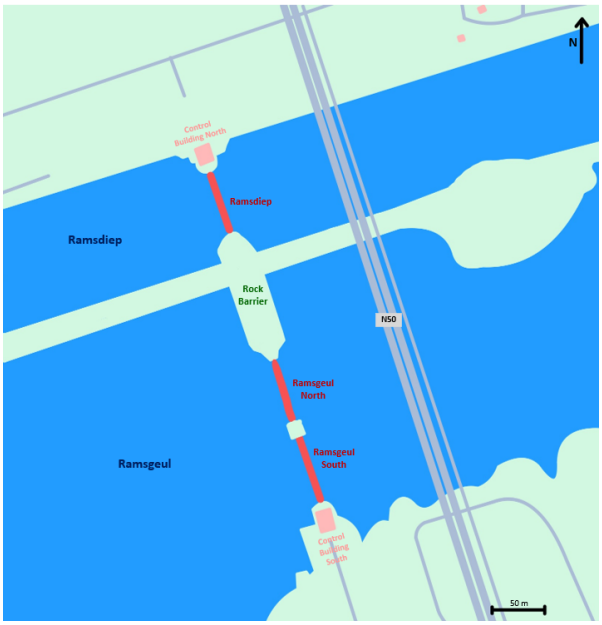

Figure 2.6: Layout of the Ramspol Barrier.

The choice for a storm surge barrier stemmed from a cost-benefit analysis favouring this solution over strengthening 115 kilometres of levees along the Zwarte Meer. The inflatable design also integrates well with the landscape, fulfilling aesthetic requirements, and fulfilling its destined functions: flood protection, navigation and water exchange.

Completed in December 2002, the Ramspol Barrier was initially managed by the Waterschap Groot-Salland (now merged into Waterschap Drents Overijsselse Delta) until July 1, 2014, when management was transferred to Rijkswaterstaat. Since its completion, the barrier has been deployed once or twice annually on average, with an additional annual closure for testing (Rijkswaterstaat, 2024a). Inspections of the rubber barrier take place once every four years. The annual number of closures since 2012 is visualised in Figure 2.7.

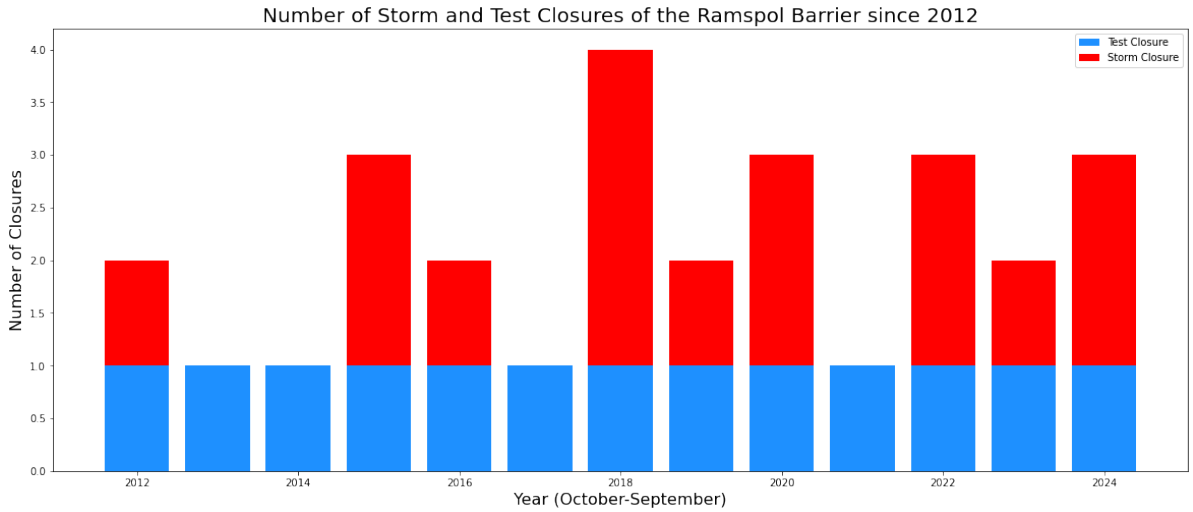

Figure 2.7: Annual number of test and storm closures of the Ramspol Barrier since 2012.

2.3. Current Operation of the Ramspol Barrier

The current operation procedure is motivated by the water levels at both sides of the barrier and the current direction. The Ramspol Barrier automatically closes when the local water level exceeds +0.50 m NAP and water flow towards the Zwarte Meer occurs. This is influenced by the discharges of the IJssel and Zwarte Water, water levels and wind setup over the funnel-shaped IJsselmeer and Ketelmeer (roughly 65 kilometres) in case of northwestern winds (Google Maps, 2024). However, the closure procedure is activated far before the actual closure of the barrier at a water level of +0.20 m NAP. Subsequently, the passage of ships is blocked when the water level increases to +0.40 m NAP. Ultimately, the barrier is closed when a further increased water level of +0.50 m NAP and a land inwards current coincide. An overview of this procedure is given in Figure 2.8. Closing takes approximately an hour during which air is pumped (3.5 million litres) and water (also 3.5 million litres) flows into the inflatable rubber barrier (Rijkswaterstaat, 2024a). The activation team is present throughout the process, regardless of whether the barrier closes.

During closure, navigation and water outflow of the Zwarte Meer to the Ketelmeer are hindered, causing delays for the shipping industry and discharge accumulation at the Zwarte Meer. The Ramspol Barrier opens when the water level at the Zwarte Meer equals the water level at the Zwarte Meer. The procedure takes approximately 3 hours during which the air and water are pumped out, and the rubber is properly stored in the sill at the bottom. A dive inspection ensures the rubber is correctly positioned (Rijkswaterstaat, 2024a). Once the closure or opening procedure is initiated, it must be completed before it can be reversed.

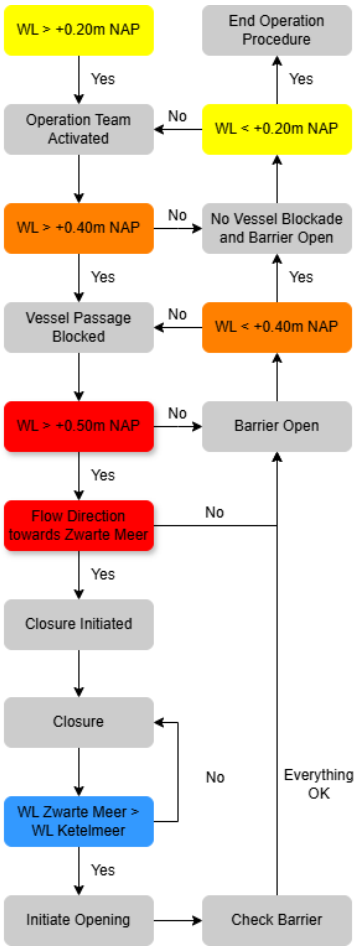

Figure 2.8: Flowchart of the data analysis.

2.4. Flood Safety Regulations

Extensive flood regulations protect the Netherlands from flooding. Flood safety standards are expressed in terms of flood probability: the probability that a barrier will lose its retaining function. These standards are determined for the expected situation of 2050, accounting for socioeconomic developments and climate change.

Currently, two standards are in place: the signalling norm and the lower limit norm. The signalling norm helps to identify the need for reinforcements promptly, while the lower limit standard sets the maximum allowable flood probability a flood defence must meet at a minimum. Under these definitions, the signalling norm can be exceeded for a certain period, but the lower limit must always be maintained. In general, the signalling standards are about three times less strict than the lower limit standard. These standards are currently included in the Environmental and Planning Act (in Dutch: Omgevingswet)

The allowable flood probability is determined by a combination of the Local Individual Risk (LIR, in Dutch: Lokaal Individueel Risico), a Social Cost-Benefit Analysis (SCBA) and the group risk (Slootjes & van der Most, 2016).

- The LIR ensures that all individuals are protected against flooding by a minimum safety level. It was politically decided that the maximum probability that an individual at a specific location could die as a result of flooding is 1 in 100000. For the signalling norm, the probability is set at $5 \cdot 10^{-6}$.
- The SCBA determines the optimal economic flood probability by balancing the potential damage from flooding with the cost of improving flood protection. This means that areas with a high population density, high economic value, or critical national infrastructure are assigned stricter standards.
- Lastly, the group risk provides insights into the areas where large numbers of casualties are most likely in the event of flooding. The risk is higher for densely populated areas or regions where large sections could flood simultaneously. A dike segment's standard can be tightened if the standard based on LIR and SCBA is relatively low compared to the group risk.

Flood probabilities are classified into intervals ranging from 1 in 10 to 1 in 100,000, with steps increasing by factors of 10, including specific thresholds at 1 in 300, 1 in 3,000, and so on. The standards of the levees in the water system of interest are shown in Figure 2.9 and Table 2. Currently, not all flood defences meet these standards, which presents a challenge to achieve compliance by 2050. Flood defences are assessed every six years, with the most recent assessment conducted between 2017 and 2023.

Figure 2.9: Lower Limit Standard of Primary Flood Defences in the Water System (van Infrastructuur en Waterstaat, n.d.).

Table 2.2: Overview of the safety standards of the primary flood defences in the system.

Dike Ring	Location	Lower Limit Standard	Signalling Standard
6.1	Stavoren-Lemmer	1/1000	1/3000
6.2	Kornwederzand-Stavoren	1/1000	1/3000
7.1	Ramspol-Kadoelen	1/1000	1/3000
7.2	Lemmer-Ramspol	1/1000	1/3000
8.3	Lelystad-Ketelbrug	1/10000	1/30000
8.4	Ketelbrug-Reevesluis	1/10000	1/30000
9.1	Zwartsluis-Ommen	1/300	1/1000
9.2	Kadoelen-Zwartsluis	1/1000	1/3000
10.1	Genemuiden-Katerveer	1/1000	1/3000
10.2	IJsselmuiden-Genemuiden	1/1000	1/3000
10.3	IJsselmuiden-Katerveer	1/3000	1/10000
11.1	Reevesluis-Hattem	1/1000	1/3000
11.2	Kampen	1/1000	1/3000
12.2	Den Oever-Enkhuizen	1/1000	1/3000
13.6	Medemblik-Enkhuizen	1/1000	1/3000
53.3	Zwolle	1/3000	1/10000
201	Afsluitdijk	1/3000	1/1000
204b	Houtribdijk	1/300	1/1000
225	Ramspol- IJsselmuiden	1/10000	1/30000
227	Reevesluis	1/1000	1/3000

3

Data Analysis

The data analysis aims to enhance the understanding of the water system's behaviour under normal and extreme conditions by identifying trends and interactions between key variables, such as water levels, discharges, and wind conditions.

To achieve this, the chapter provides an overview of the measurement locations (section 3.1) and compiles complete and consistent datasets for all relevant variables. The trend analysis (section 3.3) examines long-term changes in the system, identifying seasonal patterns, peak values, and potential shifts in trends. Additionally, the cross-correlation analysis (section 3.4) quantifies interactions between key variables, such as wind speed and direction, water levels, and discharges, while also exploring time lags between external forcing and system response.

The insights and datasets obtained from this chapter will not only improve the understanding of the physical behaviour of the water system but also provide a robust foundation for further modelling and scenario analysis (chapter 4 and chapter 5).

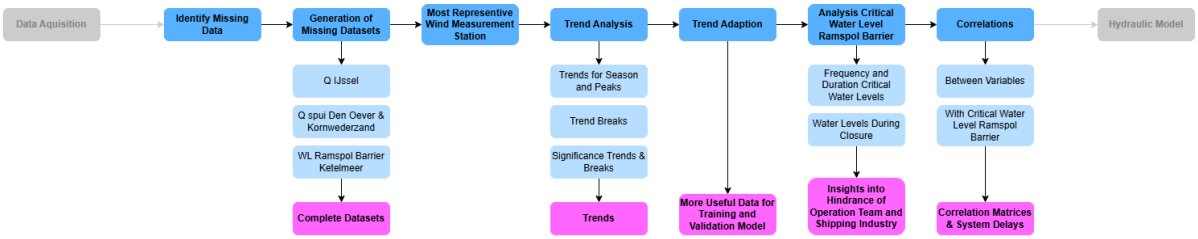

Figure 3.1: Flowchart of the data analysis.

3.1. Overview of the Measurement Locations

Water levels, discharges, and wind conditions are measured across the IJsselmeer and the IJssel-Vecht Delta at various stations. An overview of the selected stations and measured variables is provided in Figure 3.2 and Table 3.1. As detailed in Appendix A, these observations span different periods and measurement frequencies—some dating back decades, while others were introduced as recently as 2024. This variation implies that certain key variables for the hydraulic model lack long-term records and must be inferred from relationships with other measurements (see section 3.2). Additionally, data not recorded at 10-minute intervals must be resampled to ensure consistency across datasets.

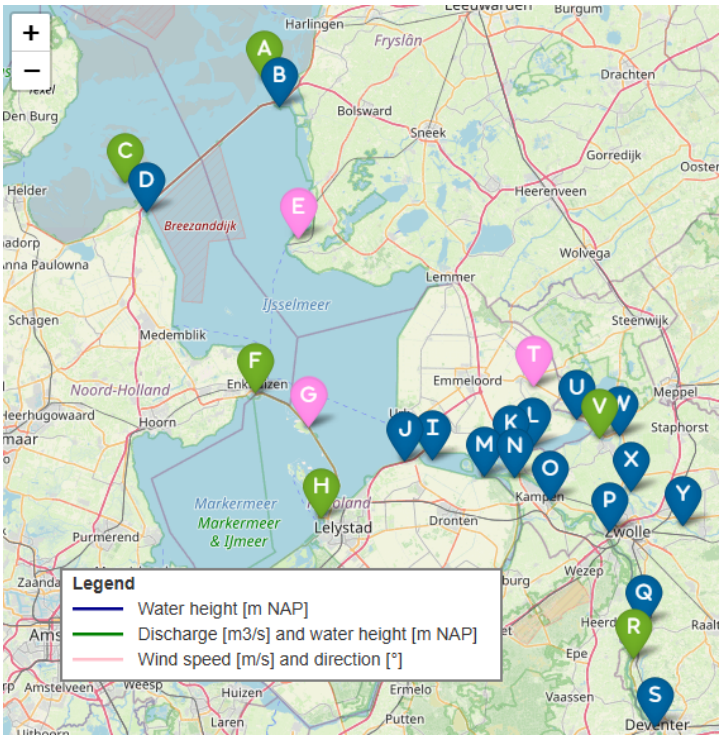

Figure 3.2: Locations of all analysed measurement stations.

Table 3.1: An overview of the used measurement stations, variables and the intended use.

Label	Measurement Station	Variable	Units	Frequency	Use	Source
A	Kornwederzand Buiten	Water level	m NAP	10 minutes	Drainage discharge and water level IJsselmeer	Rijkswaterstaat(Rijkswaterstaat, 2024c)
		Discharge	m^3/s	10 minutes	Validation model	Rijkswaterstaat(Rijkswaterstaat, 2024c)
B	Kornwederzand Binnen	Water level	m NAP	10 minutes	Drainage discharge and water level IJsselmeer	Rijkswaterstaat(Rijkswaterstaat, 2024c)
C	Den Oever Buiten	Water level	m NAP	10 minutes	Drainage discharge and water level IJsselmeer	Rijkswaterstaat(Rijkswaterstaat, 2024c)
		Discharge	m^3/s	10 minutes	Validation model	Rijkswaterstaat(Rijkswaterstaat, 2024c)
D	Den Oever Binnen	Water level	m NAP	10 minutes	Drainage discharge and water level IJsselmeer	Rijkswaterstaat(Rijkswaterstaat, 2024c)
E	Stavoren	Wind speed	m/s	10 minutes	Wind setup IJsselmeer, Ketelmeer and Zwarte Meer	KNMI (Institute), 2023)
		Wind direction	◦	10 minutes	Wind setup IJsselmeer, Ketelmeer and Zwarte Meer	KNMI (Institute), 2023)
F	Krabbersgatsluizen Noord	Water level	m NAP	10 minutes	Discharge Markermeer-IJsselmeer	Rijkswaterstaat(Rijkswaterstaat, 2024c)
		Discharge	m^3/s	10 minutes	Validation model	Rijkswaterstaat(Rijkswaterstaat, 2024c)
G	Houribdijk	Wind speed	m/s	10 minutes	Wind setup IJsselmeer, Ketelmeer and Zwarte Meer	KNMI (Institute), 2023)
		Wind direction	◦	10 minutes	Wind setup IJsselmeer, Ketelmeer and Zwarte Meer	KNMI (Institute), 2023)
H	Houtribsluizen Noord	Water level	m NAP	10 minutes	Discharge Markermeer-IJsselmeer	Rijkswaterstaat(Rijkswaterstaat, 2024c)
		Discharge	m^3/s	10 minutes	Validation model	Rijkswaterstaat(Rijkswaterstaat, 2024c)
I	Ketelmeer West	Water level	m NAP	10 minutes	Validation model	Rijkswaterstaat(Rijkswaterstaat, 2024c)
J	Kamperhoek	Water level	m NAP	10 minutes	Validation model	Rijkswaterstaat(Rijkswaterstaat, 2024c)
K	Ramspol Ketelmeerzijde	Water level	m NAP	10 minutes	Validation model	Rijkswaterstaat(Rijkswaterstaat, 2024c)
		Water flow velocity	m/s	10 minutes	Validation model	Operational data
L	Ramspolbrug	Water level	m NAP	10 minutes	Validation model	Rijkswaterstaat(Rijkswaterstaat, 2024c)
M	Ketelmond	Water level	m NAP	10 minutes	Validation model	Rijkswaterstaat(Rijkswaterstaat, 2024c)
N	Keteldiep	Water level	m NAP	10 minutes	Validation model	Rijkswaterstaat(Rijkswaterstaat, 2024c)
O	Kampen	Water level	m NAP	10 minutes	Validation model	Rijkswaterstaat(Rijkswaterstaat, 2024c)
P	Katerveer	Water level	m NAP	10 minutes	Validation model	Rijkswaterstaat(Rijkswaterstaat, 2024c)
Q	Wijhe	Water level	m NAP	10 minutes	Validation model	Rijkswaterstaat(Rijkswaterstaat, 2024c)
R	Olst	Discharge	m^3/s	10 minutes	Water levels IJssel and lakes	Rijkswaterstaat(Rijkswaterstaat, 2024c)
		Water level	m NAP	10 minutes	Validation model	Rijkswaterstaat (Rijkswaterstaat, 2024c)
S	Deventer	Water level	m NAP	10 minutes	Validation model	Rijkswaterstaat (Rijkswaterstaat, 2024c)
T	Marknesse	Wind speed	m/s	10 minutes	Wind setup IJsselmeer, Ketelmeer and Zwarte Meer	KNMI (Institute), 2023)
		Wind direction	◦	10 minutes	Wind setup IJsselmeer, Ketelmeer and Zwarte Meer	KNMI (Institute), 2023)
U	Kadoelen	Water level	m NAP	10 minutes	Validation model	Rijkswaterstaat(Rijkswaterstaat, 2024c)
V	Genemuiden	Discharge	m^3/s	10 minutes	Water levels Zwarte Water and inflow Zwarte Meer	Rijkswaterstaat(Rijkswaterstaat, 2024c)
		Water level	m NAP	10 minutes	Validation model	Rijkswaterstaat (Rijkswaterstaat, 2024c)
W	Zwartsluis Buiten	Water level	m NAP	10 minutes	Validation model	Rijkswaterstaat(Rijkswaterstaat, 2024c)
X	Mond der Vecht	Water level	m NAP	10 minutes	Validation model	Rijkswaterstaat(Rijkswaterstaat, 2024c)
Y	Vechterweerd Beneden	Water level	m NAP	10 minutes	Validation model	Rijkswaterstaat(Rijkswaterstaat, 2024c)

3.2. Data Completion: Estimating Missing Discharge and Selecting Wind Stations

3.2.1. Estimation Discharge IJssel

The discharge data for the IJssel, measured at Olst, has only been available since January 2024 (Rijkswaterstaat, 2024c). However, a more extended time series is necessary for the trend analysis and the training and validation of the hydraulic model. Therefore, the discharge data between 2000 and 2024 has been estimated through the determined Q/H-relation between the observations of the discharge at Olst and the water level at Wijhe in 2024.

For this purpose, an upstream measurement station with long-term observations (at least since the start of the operation of the Ramspol Barrier in 2002) is required to acquire a sufficiently long estimation for the IJssel discharge and have a clear exponential Q/H-relation since the effect of the downstream water level in the Ketelmeer is minimised. The water level measurement stations of Wijhe and Deventer qualified for this purpose. Subsequently, the exponential relation between the discharge and water level was quantified for both stations through regression of Equation 3.1, over the first part of the randomly split 2024 data. The results with the water level at Wijhe are visualised in Figure 3.3.

$$Q = a_1 + a_2 \cdot H^{a_3} \tag{3.1}$$

Where:

- Q is the discharge in m^3/s,
- H is the water level in $mNAP$,
- a_1, a_2, a_3 regression parameters.

The results were subsequently validated with the second part of the 2024 data, demonstrating a slightly improved fit while using the water level at Wijhe compared to Deventer. The test statistics are presented in Table 3.2. The final Q/WL-relation is described by Equation 3.2 and, together with the historical water level at Wijhe, it can be used to estimate historical discharges at the IJssel.

$$Q_{Olst} = 208.89 + 79.05 \cdot H_{Wijhe}^{1.56} \tag{3.2}$$

Table 3.2: Comparison of the validation test statistics between Wijhe and Deventer.

Test Statistic	Wijhe	Deventer
R^2 training	0.9980	0.9924
R^2 validation	0.9981	0.9923
RMSE training	6.85	13.33
RMSE validation	6.86	13.65
RMSE cross-validation	6.86	13.43

Figure 3.3: The fitted Power Law compared to the water level observations at Wijhe.

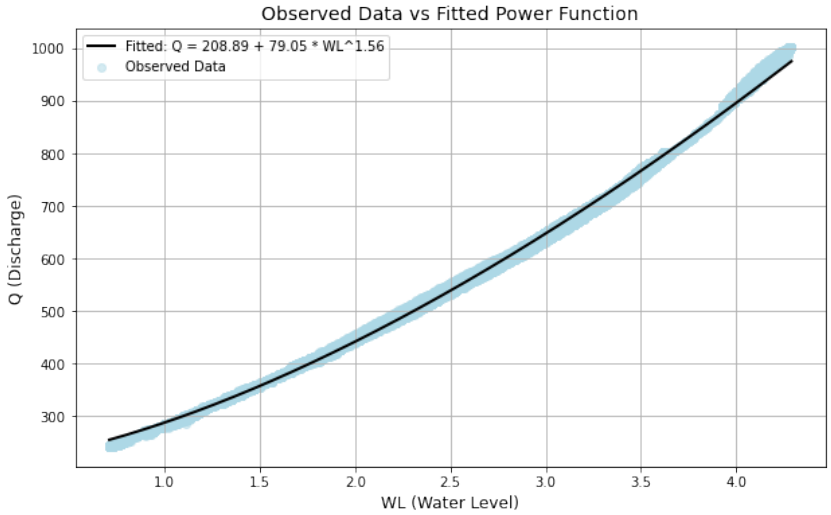

3.2.2. Representative Wind Measurement Station

In the studied water system, consisting of the IJssel— and Vecht Delta and the IJsselmeer, there are three wind speed and direction measurement stations: Stavoren, Houtribdijk and Marknesse. The locations of these stations are indicated in Figure 3.2.

To determine the most representative wind measurement station for wind-driven setup across the IJsselmeer, Ketelmeer, and Zwarte Meer, the theoretical setup is calculated for each lake using Equation 3.3. Only northwestern winds are considered, as they generate the highest setups and contribute to high water levels at the Ramspol Barrier (subsection 2.1.2). The computed setup is then compared to water levels at Ketelbrug (IJsselmeer), the Ramspol Barrier (Ketelmeer), and Kadoelen (Zwarte Meer) by calculating the Spearman cross-correlation (see section 3.4). This analysis identifies both the correlation strength and the physical lag in the system, as the cross-correlation determines the time shift that maximizes correlation. The station with the highest correlation is assumed to be the most relevant for wind measurements.

$$S = \frac{0.5\kappa \cdot F \cdot u_{10}^2}{g \cdot d_{avg}} cos(\phi) \tag{3.3}$$

In which κ is a frictional constant, $u_{10,i}$ is the wind speed at time step i in [m/s], F the fetch in [m], g the gravitational constant in $[\frac{m}{s^2}]$, d the average lake depth along the fetch in [m], and ϕ_i the wind angle at time step i in degrees. It was decided that $\kappa = 3.4 \cdot 10^{-6}$ [-] for the IJsselmeer by (Deltacommissie, 1961).

The results of this calculation are presented in Figure 3.4. As shown, relatively low cross-correlations are found between the observed water levels and the calculated wind-driven setup. This indicates that the water levels at the Ketelbrug, Ramspol Barrier and Kadoelen are likely dependent on other variables, such as the incoming and outcoming discharges in the system and the initial water levels on the lake. Despite the relatively low cross-correlations, it was decided that, based on the highest correlations and the best proximity to the water level measurement points in the IJssel- and Vechtdelta, the measurement stations at Houtribdijk would be the most relevant.

3.3. Trend Analysis

Identifying trends and trend breaks in the complete time series, and seasonal and extreme observations, is valuable for understanding how the system has changed over time, the variation between summer and winter, as well as shifts driven by external factors such as water management policies, climate change, or structural modification to the system. Furthermore, for the calibration and validation of the hydraulic model (chapter 4), it is crucial to ensure that all observations are consistent, meaning they

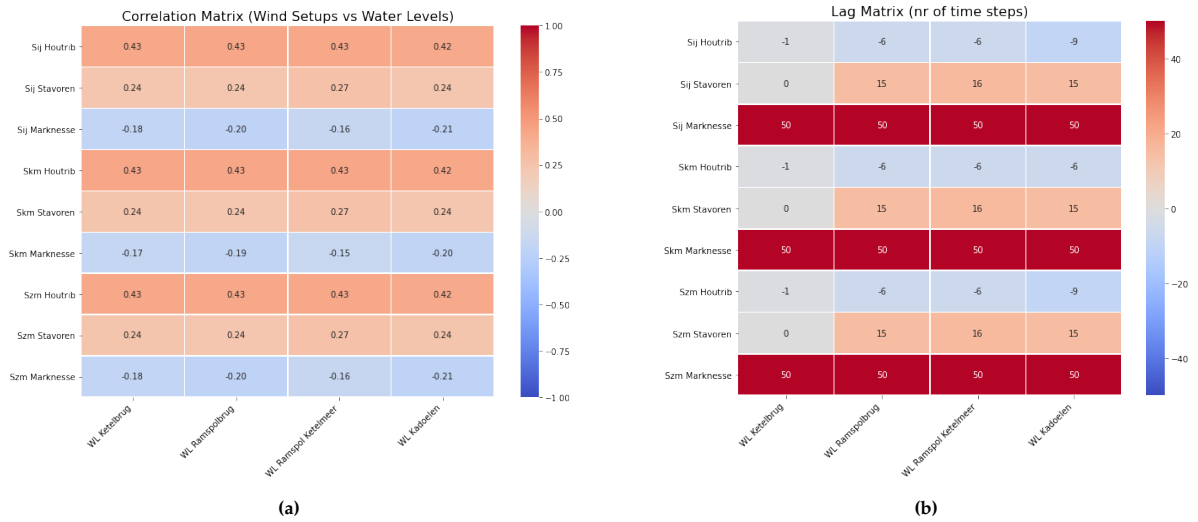

Figure 3.4: The cross-correlation (a) and lag matrix (b) between the theoretical wind setup and the observed water levels, only considering northwestern winds.

should be accurate, reliable, and not conflict with each other. Additionally, the observations must be homogeneous and free from trends for the optimisation (chapter 5), ensuring that it is done for the current operational climate.

3.3.1. Seasonal Trends

For the evaluation of seasonal differences and trends, the data is divided into two seasons as defined by the Peilbesluit IJsselmeer (Rijkswaterstaat, 2024e): winter (October through March) and summer (April through September). Two methods are used to assess the trends and their significance: linear regression and the Mann-Kendall test. The first provides a direct estimate for a linearized and fitted slope. While the second is non-parametric test which detects monotonic trends without assuming a specific distribution or linearity. Linear regression facilitates an easier quantification and visualisation of potential trends, while the Mann-Kendall test provides a more robust evaluation of their significance. The results for the water level at the Ramspolbrug are visualised in Figure 3.5, and an overview of all measurement stations is given in Table A.5.

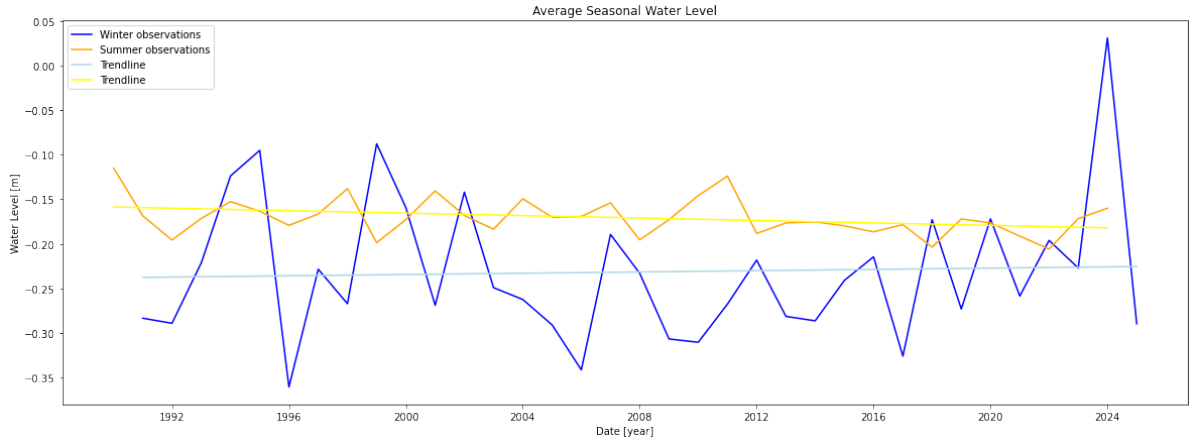

Figure 3.5: Seasonal trends in the average water level at the Ramspolbrug (95-percentile threshold is +0.08 m NAP).

3.3.2. Trends Extreme Observations

To analyse trends in the seasonal number of peaks and the average peak height, the data is separated into summer and winter seasons. Focusing on the most significant peaks, a peak-over-threshold approach is applied, using the 95th percentile as the threshold. A one-week declustering time is implemented. On one side, this is long for a fast-reacting system (subsection 3.4.3), but on the other hand, water level throughout the system can remain high for a week due to weather depressions. The one-week declustering time is considered a balance. For each year and season, the total number of peaks and the average peak height are calculated. To quantify these trends and assess their robustness, linear regression is used to estimate the rate of change, while the Mann-Kendall test evaluates the statistical significance of the trends. The results for the water level at the Ramspolbrug are visualised in Figure 3.6, and an overview of all measurement stations is given in Table A.5.

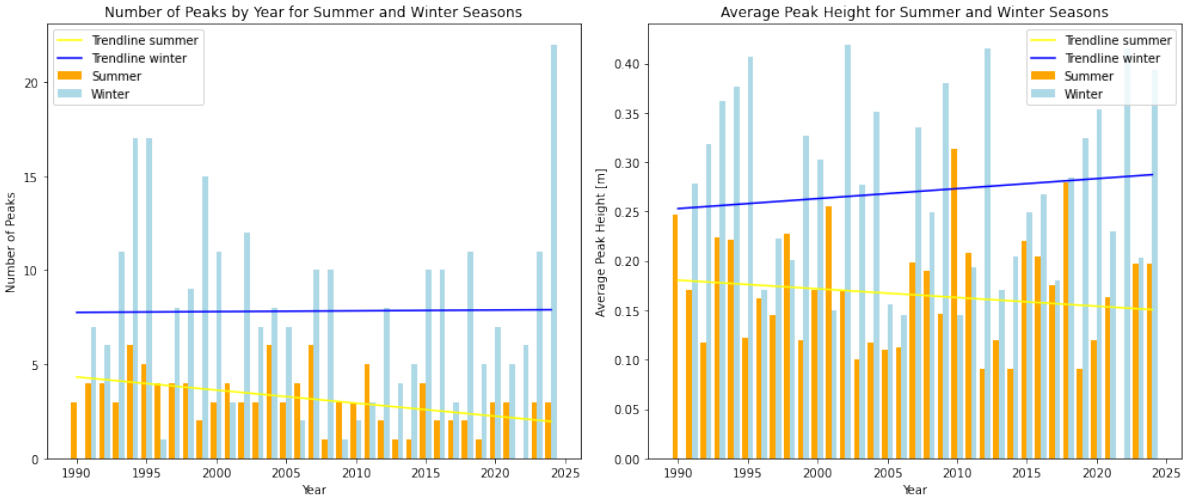

Figure 3.6: Number of peaks and average peak height for the water level at the Ramspolbrug.

3.3.3. Trend Breaks

Trend breaks or abrupt changes in historical time series can occur due to structural, management and environmental changes in the water system. Potential examples in the IJsselmeer and IJssel- and Vechtdelta system include the creation of the Noordoostpolder and Flevopolder, the construction of the Ramspol Barrier, changes in the target water level of the IJsselmeer, and climate change.

Since it is unknown if, how many and when these breaks occur, the PELT (Pruned Exact Linear Time) algorithm was used to detect these breaks. The algorithm checks for all possible splits in the dataset while remaining computationally efficient by discarding dead ends. The optimal breakpoint(s) are identified by minimising the cost function, described by Equation 3.4.

$$C_{total} = \sum_{i=1}^{m+1} \left[C\left(y_{(\tau_{i-1}+1):\tau_i} \right) \right] + \beta m. \tag{3.4}$$

In which:

- β is a penalty for adding more breakpoints. This prevents overfitting and is taken as $2 * lengthdataset$.
- m is the number of breakpoints.
- $\left[C\left(y_{(\tau_{i-1}+1):\tau_i} \right) \right]$ is the cost function for an individual segment. Taken as twice the negative log-likelihood (Killick et al., 2012).
- C_{total} is the total, to be minimised, cost.

After detecting the trends, the validity of the breaks and segmented trends is evaluated using the Chow test and the Mann-Kendall test, respectively. The Chow test evaluates the significance of the breakpoint by comparing the linear regression models before and after the break. This is described by Equation 3.5. However, no significant breaks were found in the data.

$$F = \frac{(S_{tot} - (S_1 + S_2))/k}{(S_1 + S_2)/(n_1 + n_2 - 2k)} \tag{3.5}$$

In which:

- S_{tot}, S_1, S_2 are the residual sums of squares for the total time series, the first segment and the second segment.
- n_1, n_2 are the lengths of the segments.

3.4. Intervariable and Temporal Correlations

A cross-correlation analysis is conducted to quantify the relationships between variables in the water system and identify the time lags corresponding to physical processes such as wind-driven setup and discharge propagation.

The cross-correlation method examines how well two variables are related at different time lags. More specifically, it computes the correlation between variable X at timestep i and variable Y at timestep. The lag j-i, set at a maximum of 100 time steps, corresponding to the maximum correlation, identifies the physical lag between two variables. The Spearman Rank correlation is used for this process since it helps identify all monotonic relationships, not just linear ones, and has a relatively fast computational speed. This correlation is described by Equation 3.6.

$$\rho(X, Y) = \frac{cov[R(X), R(Y)]}{\sigma_{R(X)}\sigma_{R(Y)}} \tag{3.6}$$

Two separate analyses were performed to achieve an understanding of both the general workings of the system (subsection 3.4.1) and its workings under high water conditions (subsection 3.4.2). The first uses all observed and estimated data of all variables in 2024, and the latter selects the data based on the water level threshold at the Ramspol Barrier.

3.4.1. Between Variables

The analysis of the cross-correlations, as shown in Figure 3.7, provides insights into the dynamics of the interconnected IJsselmeer and IJssel- and Vecht Delta system under normal conditions. These insights are described below.

Firstly, a strong negative correlation is observed between the Wadden Sea water levels and the drainage discharges of the Stevin and Lorentz Locks at Den Oever and Kornwederzand. This relationship reflects the operational dynamics of the system: lower water levels in the Wadden Sea allow for increased drainage from the IJsselmeer by enhancing its head difference when the IJsselmeer water level is maintained above the target level. The close correlation between the discharges and outer water levels at Den Oever and Kornwederzand (0.96 and 0.99) highlights a similar operation of these locks.

Secondly, at upstream locations along the IJssel, such as Deventer, Olst and Wijhe, the discharge shows an exceptionally strong correlation with the discharge (0.99-1.00). This implies that the water levels at these points are primarily governed by the discharge. However, as water moves downstream to, for example, Kampen or Genemuiden, the correlation with the discharge weakens to approximately 0.70. At these locations, the influence of the downstream lake water level becomes more pronounced, with correlation varying between 0.95 to 1.00. This indicates that downstream water levels are influenced by both upstream river discharges and the interconnected lake system.

Interesting to note is the divergence between the discharges of the IJssel (Q_{Olst}) and the Zwarte Water ($Q_{Genemuiden}$). With 0.57, this correlation is only moderate and underscores the different water sources for both rivers. The IJssel is largely influenced by the upstream discharge of the Rijn, which has a large

and diverse catchment area, while the Zwarte Water and, thus, the Vecht are mostly influenced by regional precipitation.

Despite its varying driving factors, the system's connectivity is impressive. Water levels along the same rivers and between lakes show an incredibly strong positive correlation of 0.90 to 1.00. This coherence shows that water level fluctuations typically occur system-wide.

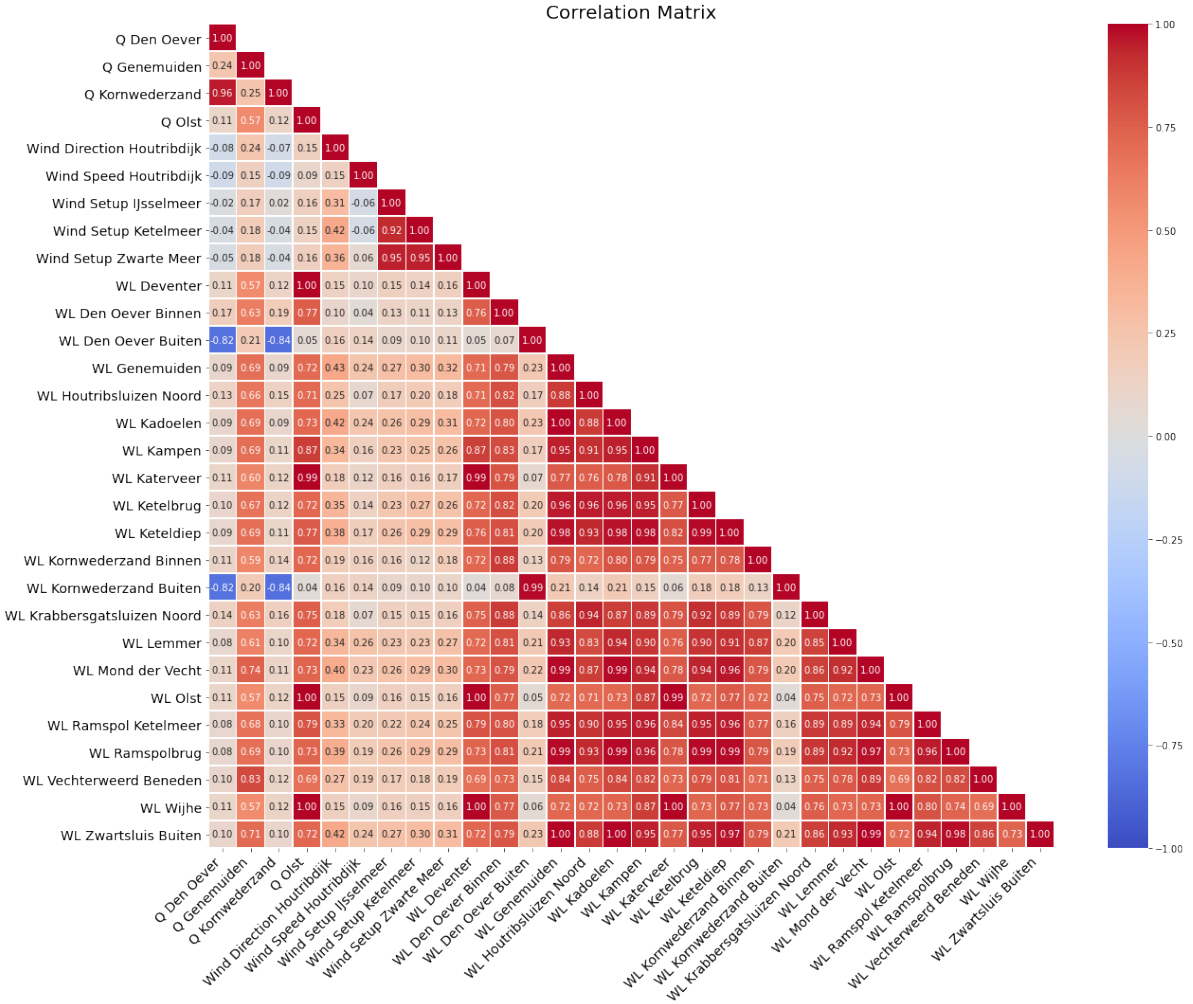

Figure 3.7: Cross-correlation matrix between all relevant variables in the IJsselmeer and the IJssel- and Vecht Delta.

3.4.2. With the Critical Water Levels at the Ramspol Barrier

The analysis of the cross-correlations between the critical water levels of +0.20m NAP, +0.40m NAP and +0.50m NAP at the Ramspol Barrier and the various other variables in the water system provides insights into the drivers of high water events and thus potential closures of the barrier. The findings are summarized as follows:

- Higher water levels at the Ramspol Barrier show a weaker relation with the discharges of the IJssel (Q_{olst}) and the Zwarte Water ($Q_{Genemuiden}$), suggesting that higher discharges directly influence lower water levels, whereas other factors dominate during high water conditions.
- Higher water levels at the barrier show a stronger positive correlation with the wind setup over the IJsselmeer, Ketelmeer, and Zwarte Meer. Across all observations, the correlation is quite weak, ranging from 0.2 to 0.25. However, for water levels exceeding 0.50m NAP, this correlation significantly increases to 0.90. This indicates that the wind setup strongly influences high water levels at the Ramspol Barrier.

- Lastly, as seen in Figure 3.9, for increasing water level thresholds, the cross-correlation with the drainage discharge through the Afsluitdijk (Q_{korn} and $Q_{denoever}$), shifts from positive to increasingly negative values. This pattern indicates that when the water level at the barrier exceeds 0.50m NAP, the drainage capacity of the IJsselmeer reduces. The reduction could be explained through the strong positive relationship between the Ramspol Barrier water levels and the Wadden Sea water levels ($WL_{korn,buiten}$ and $WL_{denoever,buiten}$). Elevated Wadden Sea water levels hinder the drainage process, increasing water levels at the IJsselmeer and thus high water conditions at the barrier.

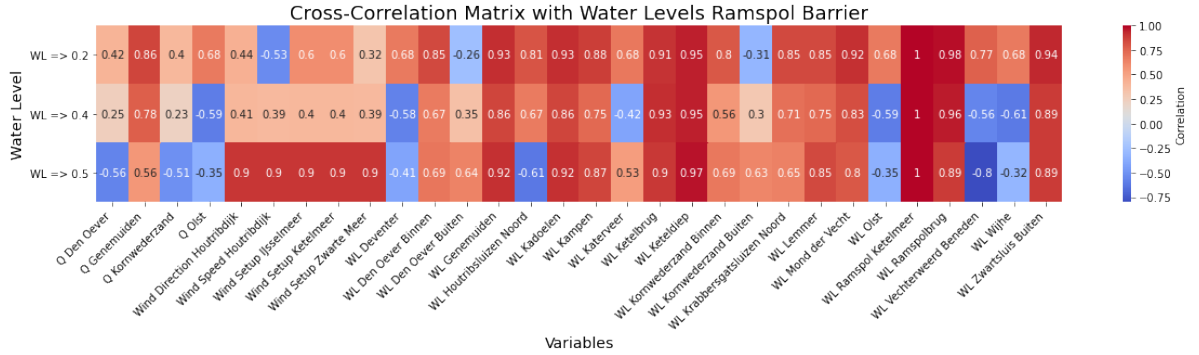

Figure 3.8: Cross-correlation matrix between all relevant variables in the water system with the critical water levels at the Ramspol Barrier.

3.4.3. Physical Lags in the System

The physical lags in the system are the delays between the forcing variables, such as the wind and discharge, and the system's response at a different location and time. It is assumed that when variables are strongly and consistently cross-correlated, such as a river's discharge and its water levels, the lag estimated during the cross-correlation analysis corresponds to the physical lag between the two variables.

The first analysed delay is related to the development of a wind-driven setup over the IJsselmeer, Ketelmeer and Zwarte Meer. This does not develop instantaneously but evolves gradually over time to the theoretical value for the setup, calculated by Equation 3.3. However, when the wind speed or its direction changes, the magnitude and direction of the setup also shift. The lag is determined through the cross-correlation analysis described in subsection 3.2.2
The setup's development time is expressed in minutes and represents the time difference between the peak of the theoretical wind setup and the observed water level peak at specific locations. The delays are shown in Table 3.3. It shows a propagation across the three lakes: at the Ketelbrug, the delay is 10 minutes, at the Ramspol Barrier, it increases by an additional 50 minutes, and at Kadoelen, there are 30 more minutes.

Table 3.3: The delays in the development of the wind-driven setup.

Variable and Location	Delay in Minutes
Water Level Ketelbrug	10
Water Level Ramspol Barrier	60
Water Level Kadoelen	90

The second type of physical lag in the system involves the discharge propagation along the IJssel and Zwarte Water. The discharge is measured at a single measurement station along both rivers: at Olst for the IJssel and at Genemuiden for the Zwarte Water. However, discharge waves move in space. Upstream locations witness discharges earlier in time, resulting in negative delays, while downstream measurement stations experience peaks later, resulting in positive lags. This propagation, expressed in minutes, is shown in Table 3.4 for the IJssel and in Table 3.5 for the Zwarte Water.

Table 3.4: Delays in the propagation of the discharge of the IJssel to the observed discharge at Olst.

Variable and Location	Delay in Minutes
Water Level Keteldiep	330
Water Level Kampen	250
Water Level Katerveer	200
Water Level Wijhe	130
Water Level Olst	0
Water Level Deventer	-260

Table 3.5: Delays in the propagation of the discharge of the Vecht/Zwarte Water to the observed discharge at Genemuiden.

Variable and Location	Delay in Minutes
Water Level Kadoelen	0
Water Level Genemuiden	0
Water Level Zwartsluis Buiten	-20
Water Level Mond der Vecht	-60
Water Level Vechterweerd Beneden	-100

3.5. Analysis of Critical Water Levels at the Ramspol Barrier

In the current operation procedure of the Ramspol Barrier, three critical water levels have been established: +0.20m NAP, +0.40m NAP, and +0.50m NAP. These correspond to the activation of the operation team, the obstruction of shipping traffic, and the closure of the barrier, respectively section 2.3. Analysing the frequency and duration at which these water levels are exceeded helps to assess the pressure and hindrance caused by the barrier's operation.

Since January 2012, the water level at the Ramspol Barrier has been estimated to have exceeded +0.20 m NAP for 2178 hours, +0.40m NAP for 610.5 hours and +0.50 m NAP for 335 hours. During this period, the passage of ships was disrupted about nine times without the deployment of the barrier, and the operation team was activated about 51 times without an actual closure. Additionally, significant annual variations in the number of occurrences and duration of certain water levels have been observed. The number and duration of critical water levels are illustrated in Figure 3.9.

It is important to note that these figures only account for high water conditions. Additional hindrances to the operational team and shipping industry arise during routine tests, maintenance and inspection. However, these closures are scheduled and can thus be anticipated.

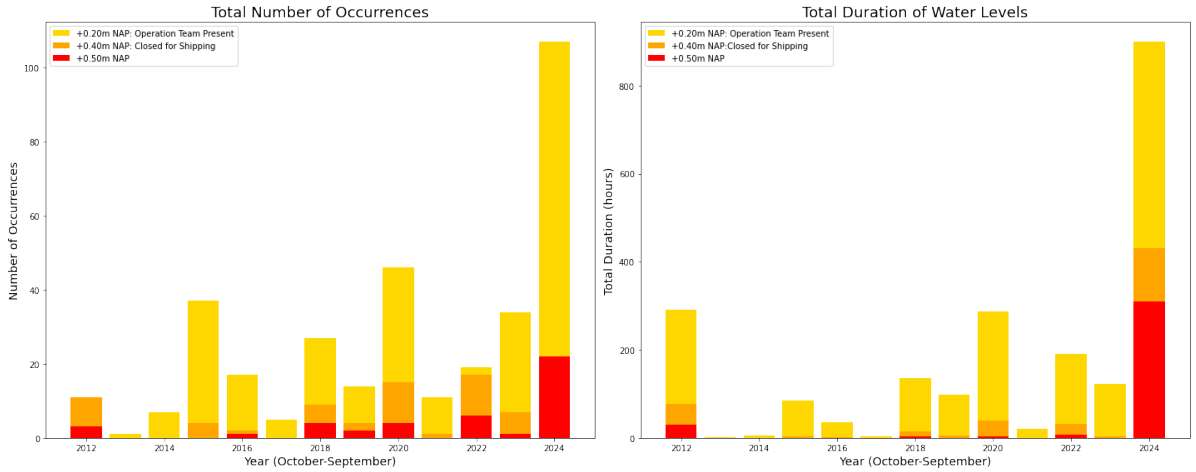

Figure 3.9: Frequency (left) and duration (right) of critical water levels (+0.20m NAP, +0.40m NAP, and +0.50m NAP) at the Ramspol Barriers since 2012.

Building on the insights from subsection 3.4.2 and section 3.5, it can be concluded that as water levels at the Ramspol Barrier rise, they become increasingly influenced by wind setup and less dependent on discharge from the Zwarte Water and IJssel. Additionally, the duration and frequency of critical water levels—+0.20m NAP, +0.40m NAP, and +0.50m NAP—vary significantly over the years but have reached extreme levels in recent years, particularly in 2024. These findings provide valuable insights into the system's behaviour under extreme conditions, informing both the hydraulic model and the need for improvements in operational procedures.

4

Hydraulic Model

As discussed in chapter 2, the closure of the Ramspol Barrier depends on the water level and the direction of water flow at its location. Both are continuously monitored, which currently plays a significant role in the barrier's closure procedure. In addition to real-time monitoring, hydrodynamic models could predict water levels and flow throughout the system. These models rely on weather forecasts and initial and boundary conditions to anticipate closures and estimate the effects of a closure or non-closure under different weather scenarios.

Currently, several models with varying complexity are in use, such as the WAQUA model. However, complexity limits the ability to easily explore or run specific scenarios due to the run time and requirements. A simpler reservoir model, similar to the DEZY model developed for the Noordzeekanaal and the IJsselmeer, has been developed to address this, which will be introduced starting in section 4.1. This model has also been developed to gain further insights into the system's workings. The model's validity will be discussed later in this chapter.

4.1. Conceptual Model

As mentioned in the introduction of this chapter, a simplified reservoir model has been developed to reduce computation time and sensitivity to boundary and initial conditions. The hydraulic model will support the operational optimisation of the barrier, which aims to minimise the pressure on the operation team and the hindrance for vessels, while still complying with the current flood safety regulations. For this goal, the model should be able to allow for extensive runs for varying weather scenarios and operation of the Ramspol Barrier (closure/non-closure, timing of closure, duration of closure, etc.), and predict water levels at critical locations throughout the system and the water flow direction at the barrier.

For this purpose, the water system comprising the IJsselmeer and the Vecht and IJssel Delta is schematised as a series of three rectangular basins with two inlets and two outlets. The largest basin represents the IJsselmeer, transitioning into the Ketelmeer at the Ketelbrug. The Ketelmeer is connected on its eastern side to the third basin, the Zwarte Meer. The Zwarte Water and Vecht rivers discharge into the east end of the Zwarte Meer, while the IJssel discharges into the east end of the Ketelmeer. The two outflows, the Stevin- and Lorentz drain sluices located in Den Oever and Kornwederzand, discharge water from the IJsselmeer through the Afsluitdijk into the Wadden Sea. The connection between the Ketelmeer and Zwarte Meer can be sealed off by inflating the Ramspol Barrier. This schematisation of the system is shown in Figure 4.1.

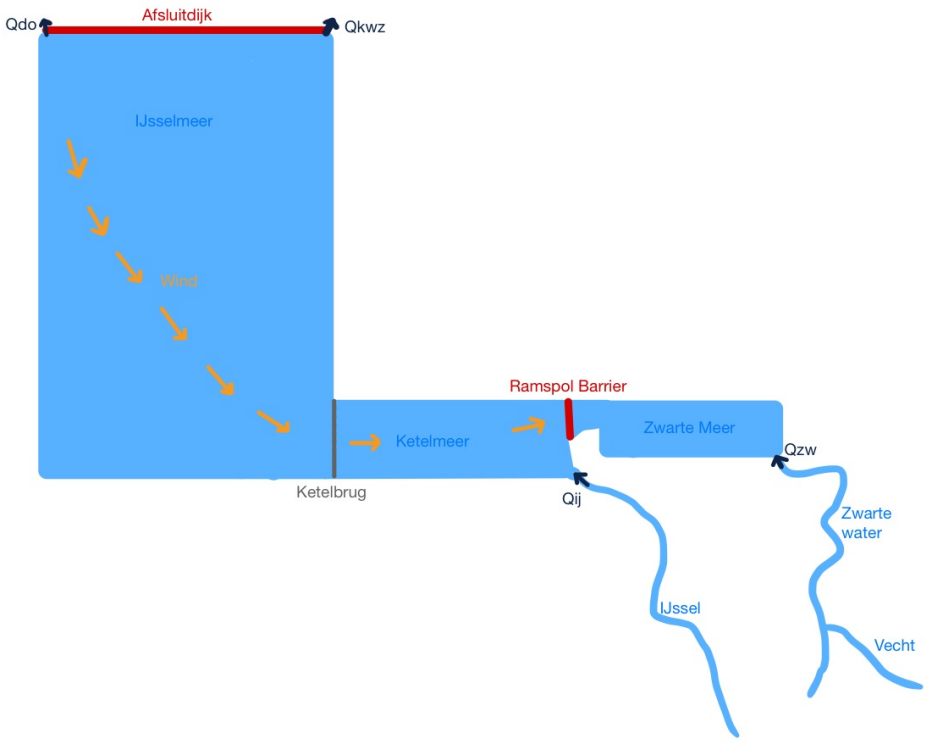

Figure 4.1: Overview of the simplified water system.

4.1.1. Inputs and Outputs

As previously mentioned, the model aims to predict water levels across the system and the flow direction and behaviour of the Ramspol Barrier under various weather and operational scenarios. This allows for informed decisions on restricting navigation and/or closing the barrier. To calculate these, the following processes are included: for the IJsselmeer, Ketelmeer, and Zwarte Meer, the water levels are calculated over time based on the initial water level, wind setup, and the incoming and outgoing discharges. For the IJssel, Zwarte Water and Vecht, the water levels are calculated with a developed empirical equation based on the downstream water level and the discharge. These processes are further explained in subsection 4.1.2 and subsection 4.1.3. The locations of the used measurement stations are shown in Figure 3.2, and an overview of the used variables is provided in Table 3.1.

As inputs, the layout of the water system and drainage locks at the Afsluitdijk, discharges, initial water levels, and wind speed and direction are required. An overview of the specific inputs, outputs and included processes is given in Table 4.1.

For the development of the model, the period between January 1, 2013 and October 20, 2024, has been selected. Part of this data is used for calibration, and the rest for validation.

Table 4.1: Overview of the input variables, included processes, and output variables of the conceptual model.

	Variables and Processes	Variables
Inputs	Initial Water Levels	WL_{kb}, $WL_{kadoelen}$, WL_{rp}
	Discharges IJssel and Zwarte Water	Q_{olst} and $Q_{genemuiden}$
	Wind Speed and Direction	u_{10} and ϕ
	Operation Ramspol Barrier	open or closed
	Surface Areas IJsselmeer, Ketelmeer and Zwarte Meer	A_{ij}, A_{km}, A_{zm}
	Fetches and Average Depths	F, $WL_{ij,avg}$, $WL_{km,avg}$, $WL_{zm,avg}$
	Precipitation and Evaporation	P and E
Processes	Wind Setup	IJsselmeer, Ketelmeer, and Zwarte Meer
	Inflow and Outflow	IJsselmeer, Ketelmeer, and Zwarte Meer
	Q,WL-Relation	IJssel, Zwarte Water and Vecht
Outputs	Flow direction Ramspol Barrier	Q_{rp}
	Water levels	Zwarte Water: $WL_{genemuiden}$, $WL_{zwartsluis}$, $WL_{monddervecht}$ Vecht: $WL_{vechterweerd}$ IJssel: WL_{kampen}, $WL_{katerveer}$, WL_{wijhe}, WL_{olst}, $WL_{deventer}$ Zwarte Meer: $WL_{kadoelen}$ Ketelmeer: WL_{rp} and WL_{kb}

4.1.2. Water Levels of the IJsselmeer, Ketelmeer, and Zwarte Meer

The water levels on the IJsselmeer, Ketelmeer, and Zwarte Meer are assumed to be influenced by the previous water level, changes in wind setup, and variations in the lake volume. The closure of the Ramspol Barrier significantly influences the volume balances and, thus, the water levels in the Zwarte Meer and Ketelmeer. These processes are further explained in the following sections.

The model focuses on four measurement locations on the lakes: Ketelbrug, Ramspol Ketelmeer side, Ramspolbrug, and Kadoelen. The water levels for these locations are described by Equation 4.1 and Equation 4.2 for the Ketelbrug, Equation 4.3 and Equation 4.4 for the Ramspol Barrier, and Equation 4.5. Flow from the Zwarte Meer and Ketelmeer towards the IJsselmeer is assumed positive, and the model takes a 10-minute time step.

$$WL_{kbij,i} = WL_{kbij,i-1} + \Delta h_{V,i} + \Delta h_{s,i} = WL_{kbij,i-1} + \frac{Q_{kb,i} - Q_{do,i} - Q_{kwz,i}}{A_{ij}} \cdot \Delta t + \frac{S_{ij,i} - S_{ij,i-1}}{\tau_{ij}} \cdot \Delta t \quad (4.1)$$

$$WL_{kbkm,i} = WL_{kbkm,i-1} + \Delta h_{V,i} + \Delta h_{s,i} = WL_{kbkm,i-1} + \frac{Q_{rp,i} + Q_{olst,i} - Q_{kb,i}}{A_{km}} \cdot \Delta t - \frac{S_{km,i} - S_{km,i-1}}{\tau_{km}} \cdot \Delta t \quad (4.2)$$

$$WL_{rpkm,i} = WL_{rpkm,i-1} + \Delta h_{V,i} + \Delta h_{s,i} = WL_{rp,i-1} + \frac{Q_{rp,i} + Q_{olst,i} - Q_{kb,i}}{A_{km}} \cdot \Delta t + \frac{S_{km,i} - S_{km,i-1}}{\tau_{km}} \cdot \Delta t \quad (4.3)$$

$$WL_{rpzm,i} = WL_{rpzm,i-1} + \Delta h_{V,i} + \Delta h_{s,i} = WL_{rpzm,i-1} + + \frac{Q_{genemuiden,i} - Q_{rp,i}}{A_{zm}} \cdot \Delta t - \frac{S_{zm,i} - S_{zm,i-1}}{\tau_{zm}} \cdot \Delta t \quad (4.4)$$

$$WL_{kadoelen,i} = WL_{kadoelen,i-1} + \Delta h_{V,i} + \Delta h_{s,i} = WL_{kadoelen,i-1} + \frac{Q_{genemuiden,i} - Q_{rp,i}}{A_{zm}} \cdot \Delta t + \frac{S_{zm,i} - S_{zm,i-1}}{\tau_{zm}} \cdot \Delta t \quad (4.5)$$

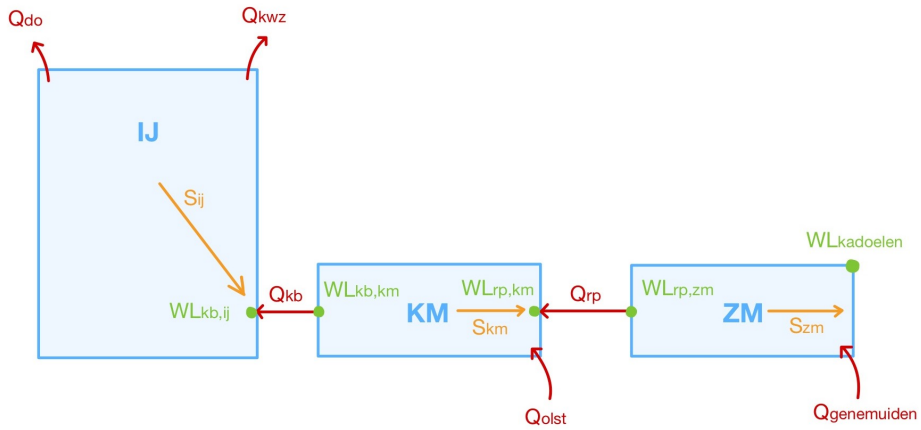

Figure 4.2: Overview of the in- and outflow of the IJsselmeer, Ketelmeer, and Zwarte Meer.

Wind Setup

When wind blows across water bodies, friction between the wind and the water generates waves and wind setup, which can significantly impact local water levels. In cases with a large fetch in combination with the same wind direction, wind setup can develop over considerable distances and become substantial. However, in the model, the fetches and thus the wind setup over the rivers, the Zwarte Water, Vecht, and IJssel, are negligible and therefore not considered. Conversely, the wind setup over larger water bodies in the system, such as the IJsselmeer, Ketelmeer and Zwarte Meer, is accounted for. The wind setup in lakes can be calculated using Equation 4.6.

$$S_{wind,i} = \frac{0.5\kappa \cdot F \cdot u_{10,i}^2}{g \cdot d} \cdot \cos\phi_i \tag{4.6}$$

In which κ is a frictional constant, $u_{10,i}$ is the wind speed at time step i in [m/s], F the fetch in [m], g the gravitational constant in $[\frac{m}{s^2}]$, d the average lake depth along the fetch in [m], and ϕ_i the wind angle at time step i in degrees. It was decided that $\kappa = 3.4 \cdot 10^{-6}$ [-] for the IJsselmeer by (Deltacommissie, 1961).

This equation assumes a rectangular basin with uniform depth and closed boundaries. Since these assumptions do not fully apply to the IJsselmeer, Ketelmeer and Zwarte Meer, some simplifications to the water system have been made in the model. Each of the three lakes is considered to be rectangular with closed boundaries. Within these basins, setup is expected on one end and an equal setdown at the opposite end, following a linear trend in between.

Due to the interconnected nature of the IJsselmeer, Ketelmeer and Zwarte Meer, a wind-induced setup in one lake propagates into the next, driving water movement between the basins. However, the processes, are inherently accounted for in the inflow and outflow of the lakes, represented by Q_{kb} and Q_{rp}, as described in Equation 4.1.2.

In addition, fetches and the averaged water depth have been estimated. The fetch has been measured at five-degree intervals using Google Earth. For the IJsselmeer, fetch measurements were taken from the Ketelbrug; for the Ketelmeer, from the Ramspol Barrier; and for the Zwarte Meer from the outlet of the Zwarte Water. An overview of the average depths and fetches is provided in Appendix B.

The wind setup calculated using Equation 4.6 is the theoretically possible wind setup when the wind speed and direction remain constant long enough for the system to reach a stationary situation. However, the wind, inflow, and outflow into the system constantly vary. This means that the system will move towards the calculated setup but does not directly reach this situation, resulting in a physical lag that needs to be accounted for in the model.
This is done by introducing an inertia factor, τ, when estimating the change in water level based on the theoretical setup and the previous water level. These physical lags have been set to 10 minutes for the IJsselmeer, 50 minutes for the Ketelmeer, and 30 minutes for the Zwarte Meer (see subsection 3.4.3). The inertia factor depends on the lake size since larger lakes need more water movement to reach the

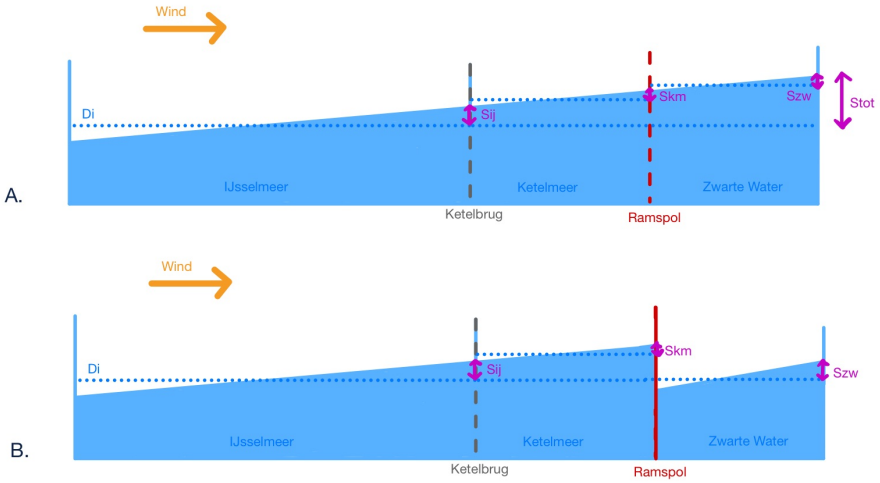

Figure 4.3: Calculation of the wind-driven set-up over the IJsselmeer, Ketelmeer, and Zwarte Meer in case of non-closure (a) and in case of closure (b).

equilibrium wind setup, S. These values are calibrated in section 4.2. The change in water level due to the wind setup development between time step i-1 and i can be calculated by Equation 4.7.

$$\delta h_{s,i} = \frac{S_i - S_{i-1}}{\tau} \cdot \Delta t \tag{4.7}$$

Volume Changes

In addition to the effect of the wind setup over the IJsselmeer, Ketelmeer and Zwarte Meer, the lake's water level is influenced by the volume changes, in other words, the inflow and outflow in the water system. The principle is as follows: if the incoming discharge exceeds the outgoing discharge, the total volume of water in the system increases, causing a water level rise. Conversely, if the outflow exceeds the inflow, the water level drops. This relation is illustrated in Figure 4.4.

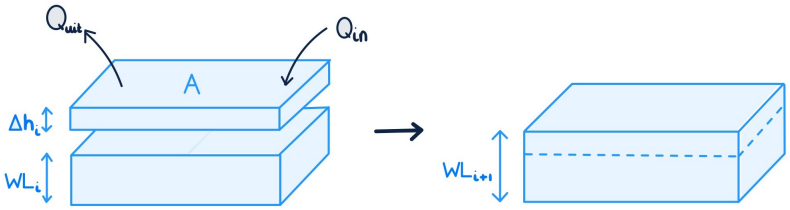

Figure 4.4: Change in water level due to inflow and outflow.

The volume change rates of the IJsselmeer, Ketelmeer, and Zwarte Meer is described by Equation 4.8, Equation 4.9, and Equation 4.10 respectively. In these equations, V indicates the lake's volume, t, the time, and Q, the discharges.

$$\frac{\delta V_{ij}}{\delta t} = Q_{kb} - Q_{do} - Qkwz \tag{4.8}$$

$$\frac{\delta V_{km}}{\delta t} = Q_{rp} + Q_{olst} - Qkb \tag{4.9}$$

$$\frac{\delta V_{zm}}{\delta t} = Q_{genemuiden} - Q_{rp} \tag{4.10}$$

Dividing these volume changes with the cross-sectional area of the lake, results in the water level change over a period. This is described by Equation 4.11 for the IJsselmeer, Equation 4.12 for the Ketelmeer, and Equation 4.13 for the Zwarte Meer.

$$\Delta h_{V,ij} = \frac{Q_{kb} - Q_{kwz} - Q_{do}}{A_{ij}} \cdot \Delta t \tag{4.11}$$

$$\Delta h_{V,km} = \frac{Q_{rp} + Q_{olst} - Q_{kb}}{A_{km}} \cdot \Delta t \tag{4.12}$$

$$\Delta h_{V,zm} = \frac{Q_{genemuiden} - Q_{km,zm}}{A_{zm}} \cdot \Delta t \tag{4.13}$$

The drainage capacity of the IJsselmeer, consisting of Q_{do} and Q_{kwz}, the water flow between lakes, Q_{kb} and Q_{rp}, and the integration of the closure of the Ramspol Barrier are further described in the following sections.

Drainage Capacity Afsluitdijk: Q_{do} and Q_{kwz}
The drainage discharge through the Stevin- and Lorentz Locks in Den Oever and Kornwederzand is crucial for assessing the inflow and outflow of the considered water system. The total drainage capacity is dependent on the inner and outer water levels, the configuration of the locks and the number of opened locks. This flow is described by Equation 4.14, which combines Bernoulli's principle and weir flow. The weir equation is used because the drainage process functions similarly to a free-flowing weir: water flows from the IJsselmeer to the Wadden Sea due to a hydraulic head difference, with the lock doors regulating the outflow. This assumption holds as long as the discharge remains free-flowing.

Draining only occurs when the IJsselmeer water level is lower than that of the Wadden Sea. The Stevinsluizen at Den Oever have three groups of five locks with a width of 12 metres, and the Lorentz Locks at Kornwederzand have two similar groups. The bottom of the locks is located at -4.65m NAP and the ceiling at +2.5m NAP (van Vossen et al., 2010).

$$Q_{spui} = c_{spui} \cdot B \cdot H \cdot \sqrt{2g \cdot \Delta WL} \tag{4.14}$$

Where:

- Q_{spui} is the drainage discharge in m^3/s,
- ΔWL is the water level difference between the IJsselmeer and Wadden Sea in m,
- B is the total flow width in m,
- H is the water depth at the opening in m,
- c_{spui} is a correction coefficient accounting for friction.

During the calibration of the parameter c_{spui}, it is assumed that drainage does not occur when the water level is below the target levels: -0.30 m NAP in summer and -0.40 m NAP in winter. During the process it became clear that additional factors influence the drainage capacity: such as summer droughts, partial lock openings, and other operational variables. Therefore, the winter conditions were used for model calibration, as they better reflect the potential drainage. This resulted in a friction coefficient c_{spui} of 0.65 for Kornwederzand and 0.59 for Den Oever.

Discharges Between Lakes: Q_{kb} and Q_{rp}
Within the system, water exchanges between the Zwarte Meer, Ketelmeer, and IJsselmeer occur. Quantification of these discharges helps to estimate the change in volume of a lake and the associated change in water level. Additionally, the flow direction between the Ketelmeer and Zwarte Meer plays a significant role, as it is tied to one of the closure criteria: flow from the Ketelmeer to the Zwarte Meer.

In the model, the discharge between the IJsselmeer and Ketelmeer, Q_{kb}, and the discharge between the Ketelmeer and Zwartemeer, Q_{rp}, are described by Equation 4.15 and Equation 4.16. Similarly to Q_{spui}, this combines Bernoulli's principle and weir flow. In these equations, flow is considered positive when it moves from the Zwarte Meer to the Ketelmeer, and from the Ketelmeer towards the IJsselmeer. The coefficients $alpha_{kb}$ and $alpha_{rp}$ will be calibrated (section 4.2).

$$Q_{kb;i} = \alpha_{kb} \cdot \sqrt{2g \cdot (WL_{kb,km;i-1} - WL_{kb,ij;i-1})} \tag{4.15}$$

$$Q_{rp;i} = \alpha_{rp} \cdot \sqrt{2g \cdot (WL_{rp,zm;i-1} - WL_{rp,km;i-1})} \tag{4.16}$$

Closure of the Ramspol Barrier
When closed, the Ramspol Barrier separates the Ketelmeer from the Zwarte Meer, setting $Q_{kb} = 0$. In reality, the barrier gradually inflates or deflates (Figure 4.5), indicating that the flow also changes over time. However, in the model, this process is highly simplified: the barrier is either fully open or fully closed. It is assumed to be fully closed, half an hour after meeting its closure criteria and to be fully opened two hours after meeting its opening criteria.

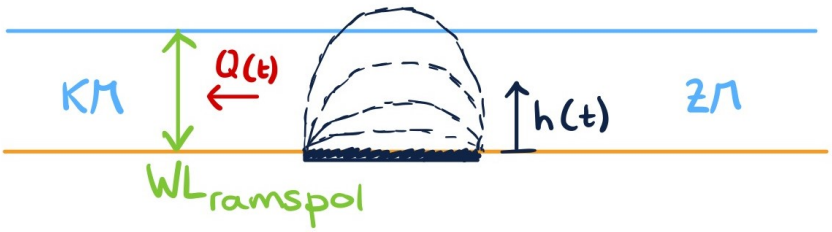

Figure 4.5: Inflation of the Ramspol Barrier.

4.1.3. Water Levels on the Zwarte Water, Vecht, and the IJssel

Water levels on the rivers as described in subsection 3.4.1 depend both on the downstream water level and the discharge. The effect of discharge and water level on the water level differs along rivers: more influence of discharge upstream and more influence of lake water level further downstream. This dependency can be described by Equation 4.17, similarly to (van den Brink & de Goederen, 2017).

Outlet water level is $WL_{kadoelen}$ for the water levels along the Zwarte Water and Vecht, and WL_{rpkm} for water levels along the IJssel. Discharge measured at Q_{olst} for the IJssel, and $Q_{genemuiden}$ for the Zwarte Water and Vecht. Delays in water flow as described in subsection 3.4.3 are taken into account. Constants a, b, and c need calibration for each location individually.

$$WL_{upstream} = a \cdot WL_{outlet} + b \cdot (Q_{river} - c) \tag{4.17}$$

Table 4.2: Overview of the locations on the IJssel and Zwarte Water where the water level is calculated and their calculation variables.

River	Location	a	b	c
IJssel	Kampen	$4.83e^{-1}$	$9.77e^{-4}$	$4.08e^{+2}$
	Katerveer	$5.86e^{-3}$	$3.43e^{-3}$	$2.17e^{+2}$
	Wijhe	$-1.05e^{-1}$	$5.26e^{-3}$	$7.62e^{+1}$
	Olst	$-1.72e^{-2}$	$5.57e^{-3}$	$-2.82e^{+1}$
	Deventer	$2.26e^{-1}$	5.68^{-3}	$-2.06e^{+2}$
Zwarte Water	Genemuiden	$8.36e^{-1}$	$7.43e^{-5}$	$-6.26e^{+2}$
	Zwartsluis	$8.46e^{-1}$	$2.38e^{-4}$	$-1.78e^{+2}$
	Mond der Vecht	$8.76e^{-1}$	$7.39e^{-4}$	$-2.74e^{+1}$
	Vechterweerd Beneden	1.39^{0}	$2.94e^{-3}$	$-1.02e^{+2}$

4.2. Model Calibration

The model calibration is carried out in three stages. First, the flow within the system, Q_{kb} and Q_{rp}, are calibrated with constants α_{kb} and α_{rp}. Subsequently, the peaks are incorporated by calibrating the wind setup in the system with constant α_{ij} for the IJsselmeer, α_{km} for the Ketelmeer, and α_{zm}. Lastly, the water levels along the IJssel, Zwarte Water, and Vecht are calibrated with constants a, b, and c for each measurement station. For calibration, the total mean squared error between the modeled and observed values at Ketelbrug, Ramspol Barrier (Ketelmeer), Ramspolbrug, and Kadoelen is minimised.

For the first part, the data between October 2015 and March 2016 is used since this is a longer time series without peaks exceeding +0.40 m NAP. This implies that the observed water levels, used for calibration, are less susceptible to the wind setup and more to the inflow, circulation, and outflow of the system. This is especially useful for the calibration of α_{kb} and α_{rp}, which resulted in α_{kb} = 1169.52 and α_{rp} = 251.06.

The second step focuses on the calibration of the wind setup with τ_{ij}, τ_{km} and τ_{zm}, which determines the behaviour of peaks in terms of duration, peak height and development time. This is done using 48 hours of data from past closures and near-closures: all 17 events with water levels exceeding +0.40m NAP between January 2012 and September 2024 (section 3.5. The calibration resulted in τ_{ij} = 1155.26, τ_{km} = 11639.31, and τ_{zm} = 251.06).

The final step calibrates the water levels along the IJssel, Zwarte Water, and Vecht. The coefficients c_1, c_2, and c_3 in Equation 4.17 for WL_{gen}, WL_{zs}, $WL_{vechtmond}$ along the Zwarte Water, $WL_{vechterweerd}$ along the Vecht, and WL_{kampen}, $WL_{katerveer}$, WL_{wijhe}, WL_{olst}, $WL_{deventer}$ along the IJssel are calibrated. The model calculates the downstream water levels, WL_{rpkm} for the IJssel and $WL_{kadoelen}$ for the Zwarte Water and Vecht, and uses those in combination with the observed discharges and water levels for the calibration.

An overview of the calibrated constants is given in Table 4.3 for the IJsselmeer, Ketelmeer and Zwarte Meer, and in Table 4.2 for the IJssel and Zwarte Water. All calibrations are visualised in Appendix C.

Table 4.3: Overview of the calibrated constants for the IJsselmeer, Ketelmeer and Zwarte Meer.

Coefficient	Value	Unit	Used for Variable
α_{kb}	1169.52	m^2	Q_{kb}
α_{rp}	251.06	m^2	Q_{rp}
τ_{ij}	1155.26	s	s_{ij}
τ_{km}	11639.31	s	s_{km}
τ_{zm}	251.06	s	s_{zm}

4.3. Model Validation

The model is validated using historical closure events, specifically focusing on the closure of December 6, 2024. This closure is selected because 2024 is the only year with available water level data on both the Ketelmeer and Zwarte Meer sides of the Ramspol Barrier. These data are essential for assessing the model's accuracy in capturing water levels at the Ketelmeer side of the Ramspol Barrier during closures, since this is not included in the calibration.

Key aspects of the validation include the timing, height, duration and development speed of water level peaks. Some overestimations of lower water levels are considered acceptable, as the primary objective is to achieve accurate water level predictions during and just before the operation of the Ramspol Barrier. If the timing of peaks is consistently off across all calibration and validation cases, a bias correction may be applied.

As mentioned, the closure of December 6, 2024, was analysed. During which, the water level rose to +0.40m NAP around 08:00, blocking vessels from passing, and around 08:00, the closure was initiated (Rijkswaterstaat, 2024b). In the model run, the water level exceeded +0.40m NAP around 07:10, and both closure criteria were met around 07:30. Consequently, the model triggered closure at this time. By 11:20, the water level on the Zwarte Meer side of the barrier had risen above that on the Ketelmeer side, prompting the initiation of the opening procedure. This sequence is visualised in Figure 4.6.

Several key observations emerge from the validation results:

- It does capture the maximum peak heights and closure timing correctly at the Ketelbrug, Ramspol Barrier and Kadoelen.
- The water level at the Ketelmeer side of the Ramspol Barrier rises and falls too quickly (left middle graph), leading to an earlier peak duration than observations. However, calibration results (Appendix C) indicate that peak development speeds vary, mainly due to differences in τ_{km}, the wind setup response time. This variability makes it challenging to accurately capture all peak development speeds using a single parameter.
- A similar inaccuracy is observed in the water level rise at the Ketelbrug (left upper graph), which is influenced by τ_{ij}.
- The decrease in water level on the Zwarte Meer side of the Ramspol Barrier is too slow in the model, whereas at Kadoelen, it aligns well with observations. This discrepancy may be attributed to hydrodynamic processes occurring when the Ramspol Barrier opens. The significant water level difference between the two sides of the barrier results in a rapid outflow, locally accelerating the decline in water level. However, the model simplifies this as an equal decline in water level over the Zwarte Meer.
- The model overestimates lower water levels, which is acceptable given that the primary goal is the capture peaks correctly.

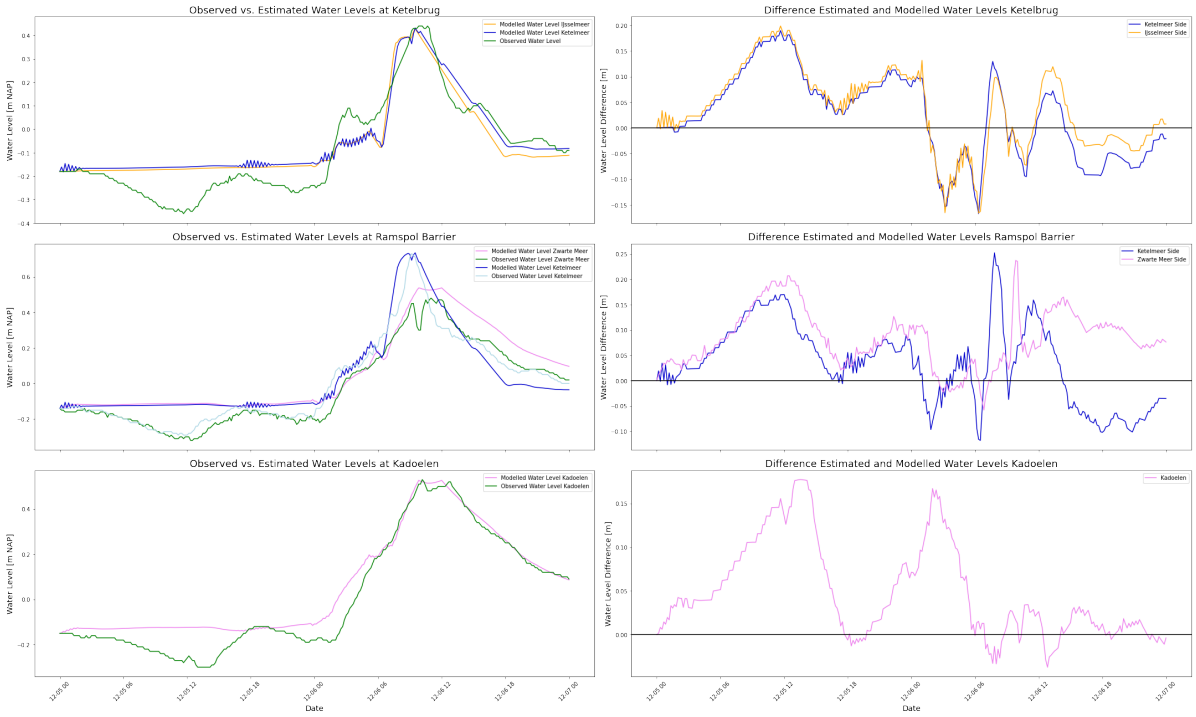

Figure 4.6: Validation results of the water levels at Ketelbrug, Ramspol Ketelmeer, Ramspolbrug and Kadoelen.

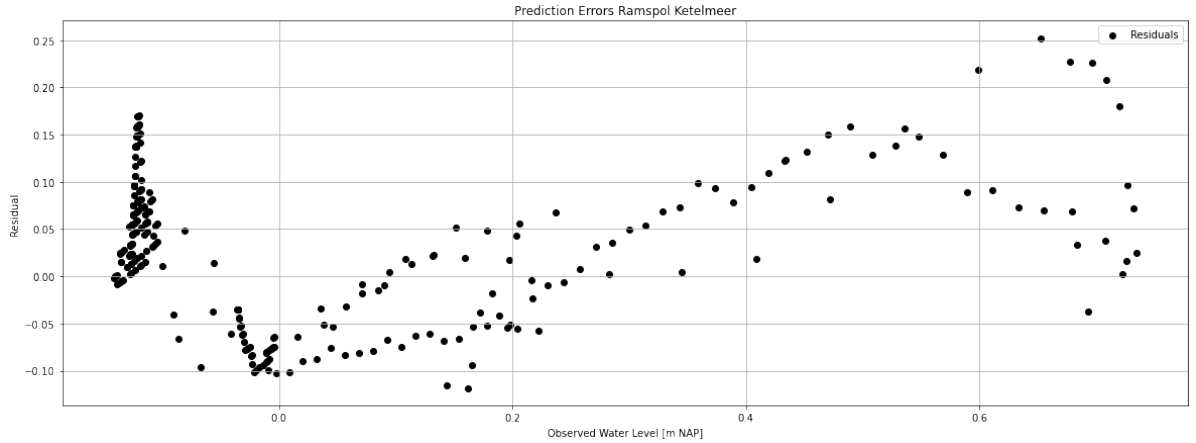

Figure 4.7: Error analysis of water level Ramspol Barrier Ketelmeer.

The errors in peak timing, development speed, and differences between observed and modeled water levels appear randomly distributed (Appendix C, Figure 4.6, and Figure C.26). This suggests that systematic bias correction is not applicable at this stage.

While the model exhibits some inaccuracies, particularly in the timing of peaks and the development speed of water level changes, it remains suitable for use in operational improvements (**??**). However, these limitations should be considered when interpreting results.

5

Improving Operational Scenarios

Effective water management is essential for guaranteeing flood safety in the water system. The current operation procedure of the Ramspol Barrier is believed to be suboptimal, potentially leading to inefficiencies that impact the operation team, the shipping industry and the system's flood safety. In section 5.1, these are examined in detail, and potential improvements are suggested.

Subsequently, the developed hydraulic model simulates various operational scenarios to evaluate these improvements. While the primary objective is to enhance the operational procedure's efficiency, these simulations also provide insights into the system's response to barrier closures and its sensitivity to varying discharge levels and wind setups. The modelled scenarios and their respective outcomes are analysed in section 5.2. Finally, a summary of these findings is presented in section 5.3.

5.1. Potential Improvements

To improve the performance of the Ramspol Barrier and enhance flood protection while minimising operational disruptions, it is essential to analyse various scenarios and refine the underlying water model. By improving predictive capabilities and understanding critical thresholds, the system can be managed more effectively, ensuring both safety and efficiency.

5.1.1. Implementing Forecasts to Improve Planning

Improving the ability to predict when critical water levels (+0.20 m NAP, +0.40 m NAP, and +0.50 m NAP) and closure and opening criteria will be reached can significantly benefit both operational teams and the shipping industry. Implementing 24-hour or 48-hour forecasts would provide more accurate planning capabilities, allowing operational teams to be on-site when needed while reducing unnecessary disruptions and allowing the shipping industry to adjust their schedule to limit the waiting time for a closed barrier. One way to demonstrate this would be to simulate past closure events, extracting the exact moments when thresholds were exceeded and evaluating the timing of opening and closing decisions.

5.1.2. Scenarios Requiring Further Analysis

Despite the Ramspol Barrier's effective protection of its hinterland during heavy storm closures, there are a couple of scenarios where there is hesitation if the current operation procedure optimally balances flood safety and operational efficiency.

- **Closures due to minor exceedances of +0.50m NAP**: In some cases, the Ramspol Barrier closes while the water level slightly surpasses +0.50m NAP before receding, as seen on March 12, 2020 and February 17, 2022. It remains unclear whether closure in these scenarios effectively reduces water levels on the Zwarte Meer or whether a more refined decision-making approach could allow the barrier to remain open without compromising flood safety. Conversely, on November 26, 2023, closure criteria were met, but the operational team decided not to close the barrier. It is interesting to see if this decision was justified.

- **Navigation Blockade without Closing**: Several instances, including March 14, 2019, April 5, 2021, and January 24, 2024, have shown water levels peaking or fluctuating between +0.40 m NAP and +0.50 m NAP. This fluctuation results in a blockade for vessels without triggering a full closure. Developing criteria for when to impose or lift such blockades would help minimise unnecessary disruptions while maintaining flood protection.
- **Initial Water Levels above +0.50m NAP:** When the Ketelmeer water level is already above +0.50 m NAP, the direction of flow at the Ramspol Barrier becomes the dominant closure criterion. This can be problematic, as it may lead to a closure and thus additional water accumulation behind the barrier for an extended period, exacerbating flood risks. Additionally, fluctuating discharge directions do not always correlate with immediate or significant water level increases in the Zwarte Meer, raising questions about whether current procedures are sufficiently robust.
- **Subsequent Peaks**: Storm systems frequently result in multiple peaks, sometimes occurring so closely together that the barrier may still be reopening from a previous closure, or the accumulated water has not fully drained. This was observed on February 17-18, 2022, and January 3-4, 2018. Given that stormy weather can persist over extended periods, it is important to evaluate how closure procedures should adapt to these recurring peaks.

5.1.3. Sensitivity of the System to Wind Setup and Discharge Variability

Analysis of the system's sensitivity to wind setup and discharge variability improves the understanding of the system under storm conditions and can thus help improve the barrier's operational effectiveness.

The first occurs when high water levels on the Wadden Sea limit drainage through the Afsluitdijk, causing water levels in the IJsselmeer, Ketelmeer, and Zwarte Meer to rise. In this situation, the Ramspol Barrier's closure criteria may be met by relatively small wind setups or discharge peaks. This raises the question: How sensitive is the system to mild wind setup peaks under different initial water levels when no closure takes place?

The second scenario unfolds when the Ramspol Barrier is closed, leading to the accumulation of discharge from the Zwarte Water behind it. Varying discharges result in different rates at which the water levels in the Zwarte Meer rise and how quickly they reach the reopening threshold, where water levels in the Zwarte Meer exceed those in the Ketelmeer. Additionally, are there discharge conditions under which the Zwarte Meer's water levels would remain lower if the barrier were left open?

5.2. Improvement of Scenarios

The scenarios described above will be analysed, and potential changes to the operational procedure will be tested. These analyses will be guided by three key criteria: ensuring and, where possible, reducing flood risk (which translates to lower water levels), minimising blockades for the shipping industry when safety permits, and alleviating pressure on the operational team by improving predictions of when critical water levels are reached and, if possible, reducing the frequency of closures.

To achieve this, the developed hydraulic model will be run for the scenarios outlined in section 5.1, incorporating uncertainty in discharge and wind setup, both important input variables. Monte Carlo simulations are used to account for uncertainty, applying a ±20 per cent variation to wind setup due to the turbulent nature of the wind speed and direction. The same ±20 per cent variation is applied to the discharge of the Zwarte Water, which is heavily influenced by local precipitation, a variable that fluctuates considerably over time and space. In contrast, the discharge of the IJssel is assigned a smaller uncertainty of ±5% per cent, as it is primarily driven by the discharge of the Rhine, making it more predictable. These uncertainties are implemented by adjusting all predicted values of discharge or wind setup by a randomly sampled percentage within the defined uncertainty range. A total of 1000 simulations will be conducted, generating 95 per cent confidence bands for the predictions.

No formal optimisation framework will be applied, as this would require assigning weights and quantifying optimisation criteria, which is beyond the scope of this analysis. Ultimately, defining acceptable water levels or balancing operational disruptions against flood protection is a policy decision. Instead, the scenarios will be assessed by comparing water levels, flow direction at the Ramspol Barrier, the closure and opening timing, closure duration, the developed wind setup in combination with

the theoretical predictions, and the rate of water level rise and decline. Based on these findings, recommendations will be made to refine the closure procedure for each scenario.

In subsection 5.2.1 to subsection 5.2.9, each scenario is described, potential improvements are discussed, results are presented, and interpretations and recommendations are given.

5.2.1. Normal Closure

This scenario explores whether forecasts made for 24 or 48 hours can provide accurate insights into if and when thresholds are reached. During storm conditions, the operational team is activated when water levels reach +0.20 m NAP, while vessel passage over the barrier is blocked at +0.40 m NAP. Closure occurs when the water level reaches +0.50 m NAP, combined with an inland stream direction. The barrier is reopened once the water level on the Zwarte Meer side exceeds that on the Ketelmeer side.

The analysis incorporates initial water levels, forecasts for the discharge of the IJssel and Zwarte Water, and wind speed and direction, including the associated uncertainty in these forecasts.

Observations from the storm event on February 18, 2022 were used as a reference case (second peak and green lines in Figure 5.1). During this event the Ramspol barrier was closed at 21:00 on 18 February, while vessel passage was blocked earlier, at 19:40 (Rijkswaterstaat, 2022). The water level at the Zwarte Meer starts decreasing from around 04:30 onwards on 19 February, corresponding to the reopening of the Barrier. As shown in the bottom two graphs of Figure 5.1, the observed water level at Ramspolbrug (Zwarte Meer side) exhibited a slight increase after closure, while the water level at Kadoelen plateaued.

To evaluate the forecasting capabilities of the hydraulic model, it was run for the same peak event. The model predicted a sharp spike in water levels at the Ramspol Barrier shortly after the wind increased, leading to a water level of +0.20 m NAP at 18:00. The navigation blockade threshold (+0.40 m NAP) was reached around 18:30, earlier than observed, while the closure threshold (+0.50 m NAP combined with inland stream direction) was met around 18:40, also preceding the actual event. The model indicated that the reopening condition, where the water level on the Zwarte Meer side exceeded that on the Ketelmeer side, occurred around 04:00. This may have resulted in a later predicted opening than what was observed in reality.

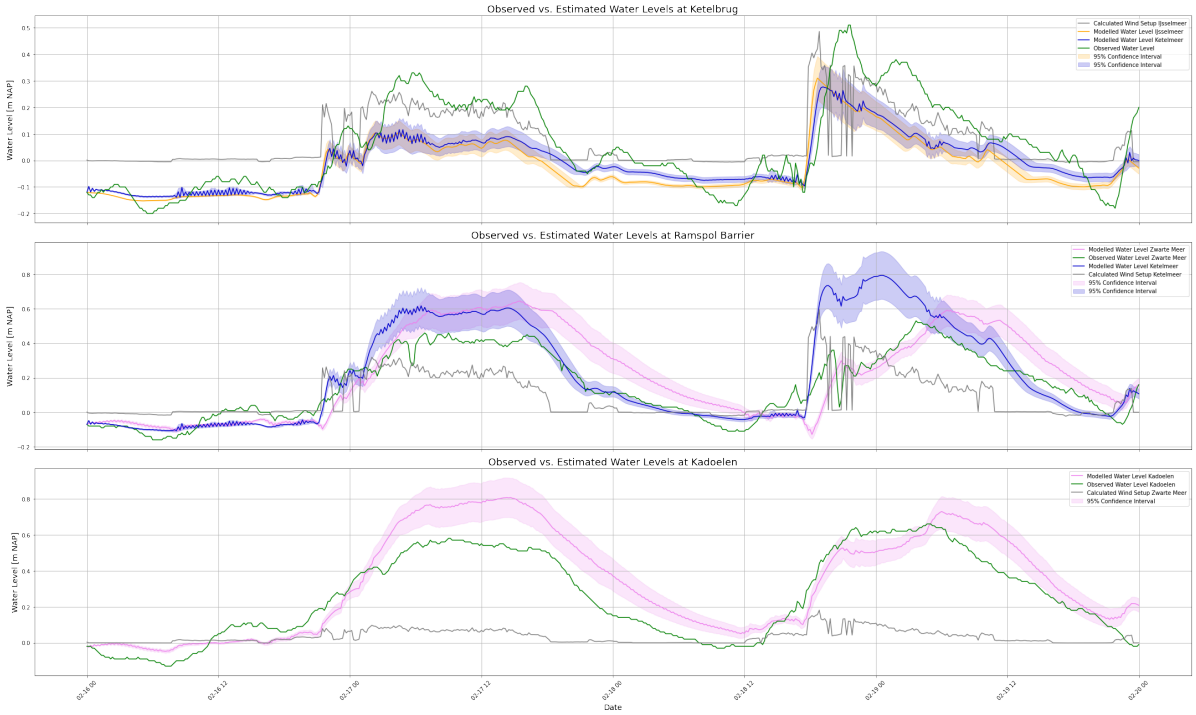

Figure 5.1: Modelled Water Levels at the Ketelbrug, Ramspol Barrier and Kadoelen during the closure of February 18, 2022.

While the model effectively extracts the timing of navigation blockade, closure, and reopening, these events occur earlier than in reality. This can be attributed to the sharp rise in water level after the theoretical wind setup (grey lines) spike. In contrast, water levels at the Zwarte Meer (represented by pink lines) align more closely with observations, accurately capturing the second peak, the water accumulation during closure, and a similar decreasing speed when reopening. However, the model predicts higher water peaks and later drops in both peaks, the closure event and the preceding one.

5.2.2. Maintenance and Test Closures

In addition to operational storm closures, the barrier is occasionally closed for maintenance or testing purposes. These test closures are planned well in advance, allowing both the shipping industry and the operations team to adjust their schedules accordingly. Unlike emergency storm closures, there is no sudden activation, instead, the process is carried out to assess the barrier's performance under milder conditions.

For this analysis, the test closure of October 3, 2023, was examined. Water levels during this event differed significantly from those observed during storm-induced closures, as no extreme peaks occurred. The closure began at approximately 07:00 and was fully in place by 08:00. Based on the assumption that the barrier remains closed for two hours, it was likely fully reopened around 13:00. However, the exact reopening time is of lesser relevance in this case, as the primary focus is on understanding the effects on the water levels of a test closure rather than the correctness its operational timing.

A simulation was conducted for the period between October 2, 12:00, and October 4, 12:00. The results indicate that water levels on the Zwarte Meer side of the barrier are slightly lower with the closure than in non-closure conditions, as illustrated with the black and pink lines in Figure 5.2. However, in this particular case, the differences between closure and non-closure scenarios were minimal, suggesting that test closures under calm conditions have a limited impact on overall water levels in the system.

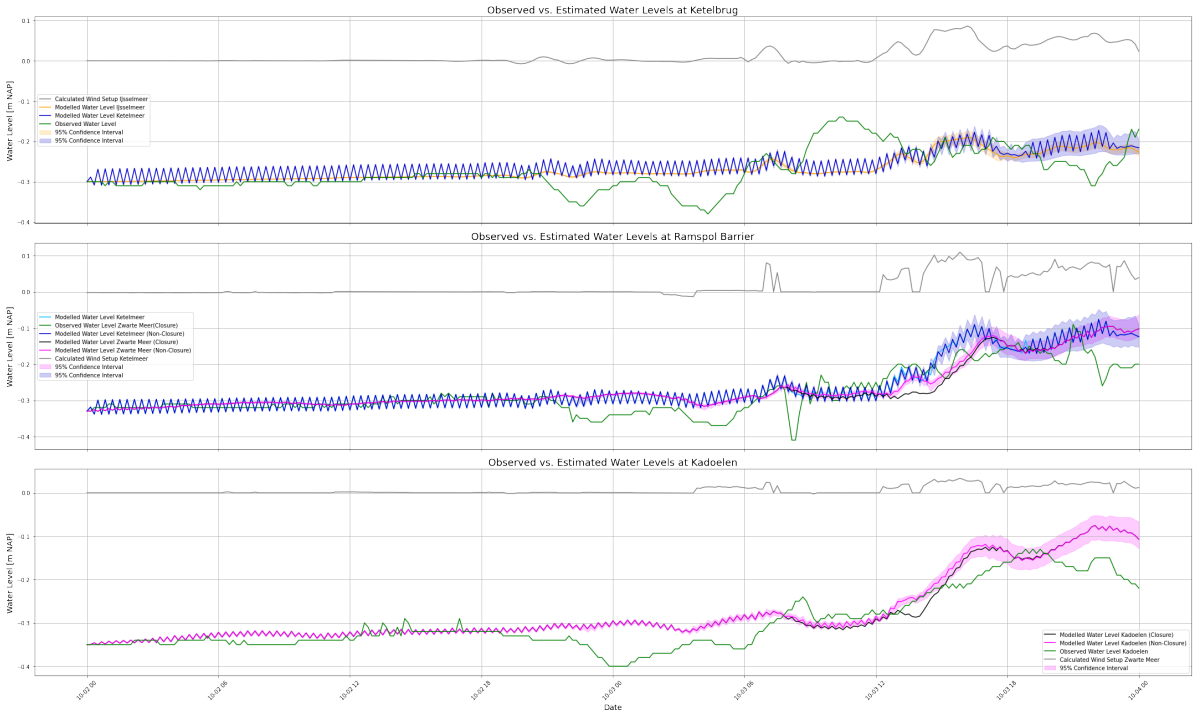

Figure 5.2: Modelled Water Levels at the Ketelbrug, Ramspol Barrier and Kadoelen during the test closure of October 3, 2023.

5.2.3. Closures at the Ramspol Barrier with Water Level Peaks Slightly Above +0.50 m NAP

The effectiveness of Ramspol Barrier's operation procedure in optimising flood safety around the Zwarte Meer when water levels peak just above the closing criteria of +0.50m NAP is unclear. Although water levels in the Zwarte Meer are initially lower during closures, since wind setup is obstructed from pushing water into the lake, this intervention allows for discharge accumulation in the lake and introduces operational risks. Given these complexities, the question arises: when is it appropriate to close the barrier when the closure criteria are just met, and when would maintaining an open status be more advantageous for flood safety and system operation?

One approach to addressing this question involves running two simultaneous simulations: one with the barrier closure and one without. Both simulations would incorporate predictive uncertainty in wind setup, volume changes, water levels, and flow directions. The closure scenario would follow established protocols, reopening when water levels in the Zwarte Meer exceed those in the Ketelmeer. The peak water levels observed in both scenarios would then be compared to assess the impact of the closure.

Alternatively, a more nuanced approach could focus on analysing the underlying drivers of water level peaks, such as wind setup and discharges in the system. As described in Figure 4.1.2, wind setup is a gradual process, and the model accounts for this by calculating the theoretical wind setup and the developed wind setup over time. By considering the predicted wind speed and direction, along with their associated uncertainty, the model can evaluate whether there is room for the wind setup to further develop. Additionally, the model can incorporate predicted discharge values and their uncertainties to estimate the potential for large volume increases in the lakes.

To evaluate these methods, a case study of the closure event on March 12, 2020, will be considered. This scenario will include three distinct cases: the actual closure, in which wind and water levels peaked and then receded rapidly; a modified closure, where the wind peak plateaus for an additional 5 hours; and a further modified closure, where wind speeds increase over the following 5 hours. These cases will be analysed in the following subsections.

Decreasing Wind: the Actual Closure of March 12, 2020

The analysis of the March 12, 2020, closure scenario, was conducted for both the closure and non-closure cases. The closure procedure was initiated around 04:40, when the water level reached +0.20 m NAP, triggering the activation of the operational team. By 06:00, a blockade was imposed on the shipping industry, and the closure criteria were met by 08:00. The Ramspol Barrier was closed in the closure scenario, and the reopening criteria were met around 11:40, prompting the barrier to reopen. These scenarios are illustrated in Figure D.13.

Comparing the peak water levels between the closure and non-closure simulations reveals the following: at the Ramspolbrug, the water level peaked at 0.59 m NAP in the non-closure scenario and at 0.53 m NAP in the closure scenario; similarly, at Kadoelen, the water level reached 0.71 m NAP without closure and 0.64 m NAP with closure. The non-closure scenario thus resulted in higher water levels compared to the closure scenario.

Further examination of the potential for wind setup and volume changes in the lakes shows that, as depicted in Figure D.15, the wind setup on the IJsselmeer had reached its maximum potential at the time of the closure and began to decline sharply thereafter. In terms of volume, the water level could have risen by an additional 0.0002 m. For the Ketelmeer, predictions indicated that the wind setup could have developed by another 5 cm, with an additional 1 cm rise due to volume change. On the Zwarte Meer, the wind setup had already plateaued, leaving room for a 6 cm increase in water level due to volume changes. However, this potential was rapidly declining over time.

Stagnation of the Wind

In this scenario, the wind setup following the closure of March 12, 2020, was modified such that it plateaued after the closure. Specifically, at the Ketelmeer, the wind setup was maintained at 0.17 m, and at the IJsselmeer, it was set to 0.15 m between 09:00 and 14:00. The remaining parameters of the scenario, including discharges and the activation of the operation procedure, were unchanged. The water level still activated the operation team around 04:40, navigation was blocked by 06:00, and the

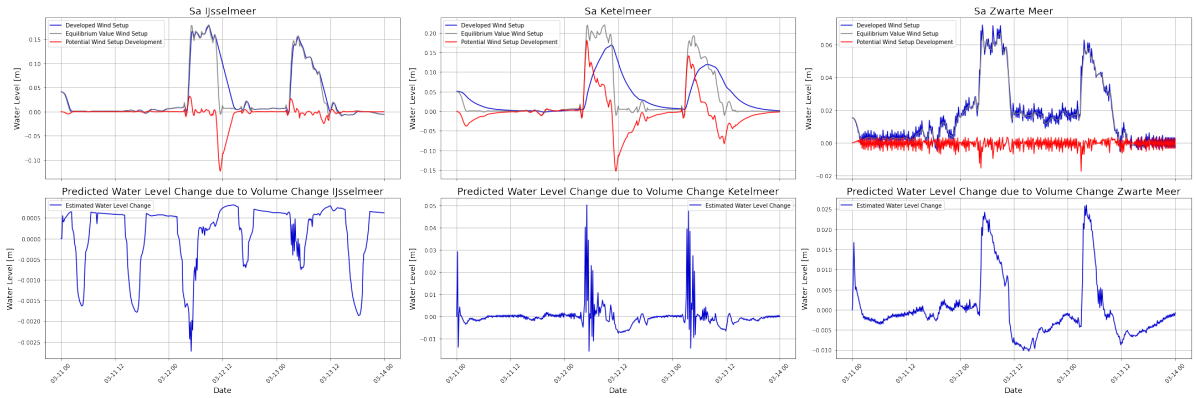

Figure 5.3: Wind setup development potential and predicted volume changes for March 12, 2020 using the non-closure simulation and a decreasing wind after closure.

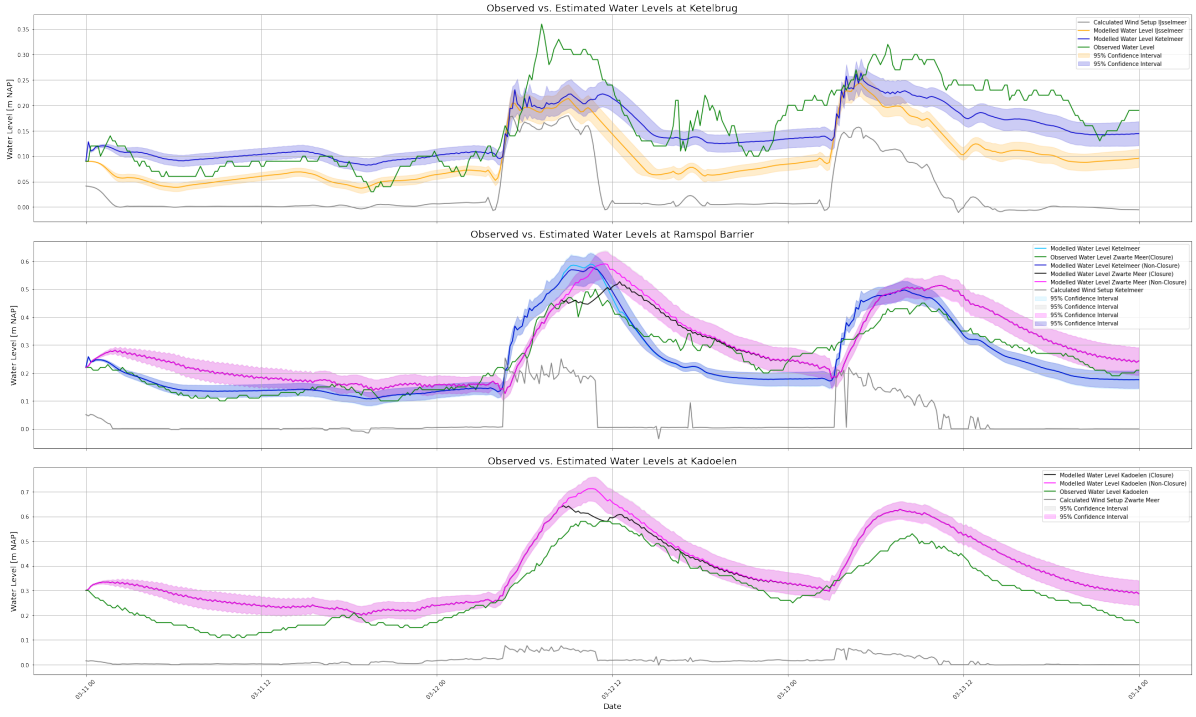

Figure 5.4: Modelled Water Levels at the Ketelbrug, Ramspol Barrier and Kadoelen during the closure (black lines) and non-closure (pink lines) on March 12, 2020.

closure criteria were met by 08:00. The Ramspol Barrier was then closed in the closure simulation and remained closed until the reopening criteria were met at approximately 14:00.

Comparing the peak water levels between the closure and non-closure simulations reveals that the water level at the Ramspolbrug peaked at 0.64 m NAP in both the non-closure and closure scenarios. At Kadoelen, the water level reached 0.72 m NAP without closure and 0.73 m NAP with closure. In this case, the water levels were nearly identical between the two simulations at the Ramspolbrug and slightly higher at Kadoelen in the closure scenario.

An analysis of the potential for wind setup and volume changes in the lakes shows, as illustrated in Figure D.20, that on the IJsselmeer, the wind setup had already plateaued at the time of the closure, and thus, during the extended wind peak, it remained stable before sharply declining. In terms of volume, the water level could have risen by an average of 0.0005 m every 10 minutes. For the Ketelmeer, the predicted wind setup could have developed by another 5 cm before plateauing, with an additional 1 cm rise due to volume changes. On the Zwarte Meer, the wind setup had already plateaued, and there was potential for a 0.01 m increase in water level every 10 minutes due to volume changes, although this potential rapidly reduces over time.

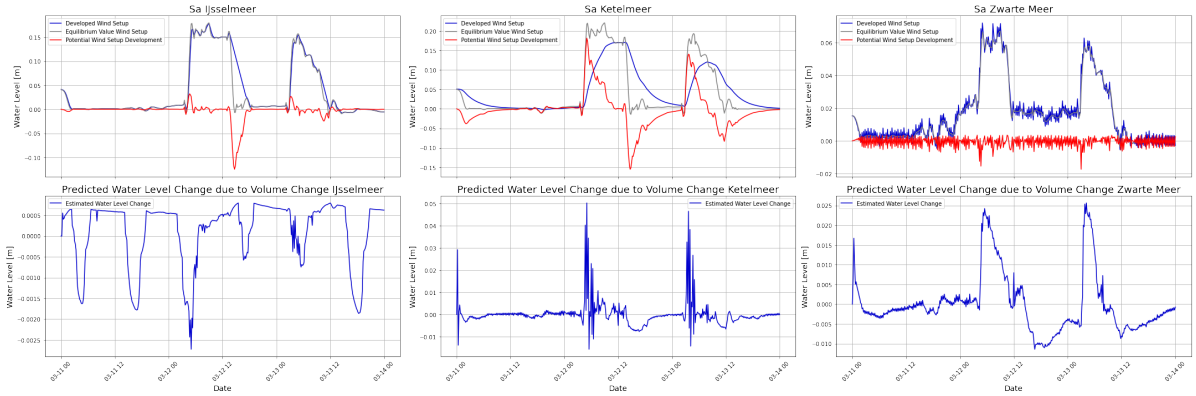

Figure 5.5: Wind setup development potential and predicted volume changes for March 12, 2020 using the non-closure simulation and a constant wind after closure.

Increasing Wind after Closure

In this scenario, the wind setup following the closure of March 12, 2020, is adjusted such that the wind setup increases after closure, reaching 0.25 m at the Ketelmeer and 0.22 m at the IJsselmeer between 09:00 and 14:00. The other parameters of the scenario remain unchanged: the discharges, the activation of the operational team around 04:40, the blockade of navigation around 06:00, and the closure criteria being met around 08:00. In the closure simulation, the Ramspol Barrier is closed and the reopening criteria are met around 15:10.

Comparing the peak water levels between the closure and non-closure simulations, the water level at the Ramspolbrug peaked at 0.79 m NAP in the non-closure scenario and 0.67 m NAP in the closure scenario. At Kadoelen, the water level reached 0.87 m NAP without closure and 0.75 m NAP with closure. In this case, the non-closure scenario resulted in significantly higher water levels compared to the closure scenario.

Analysis of the potential for wind setup and volume changes in the lakes shows, as illustrated in Figure D.20, that on both the Ketelmeer and the IJsselmeer, the wind setup had more potential for further increase due to the increasing theoretical wind setup, which had not yet reached equilibrium at the time of the closure. This increasing wind setup led to higher volume-related water level changes in the Ketelmeer and Zwarte Meer, as opposed to the declining water level changes observed in the decreasing and stagnating wind scenarios.

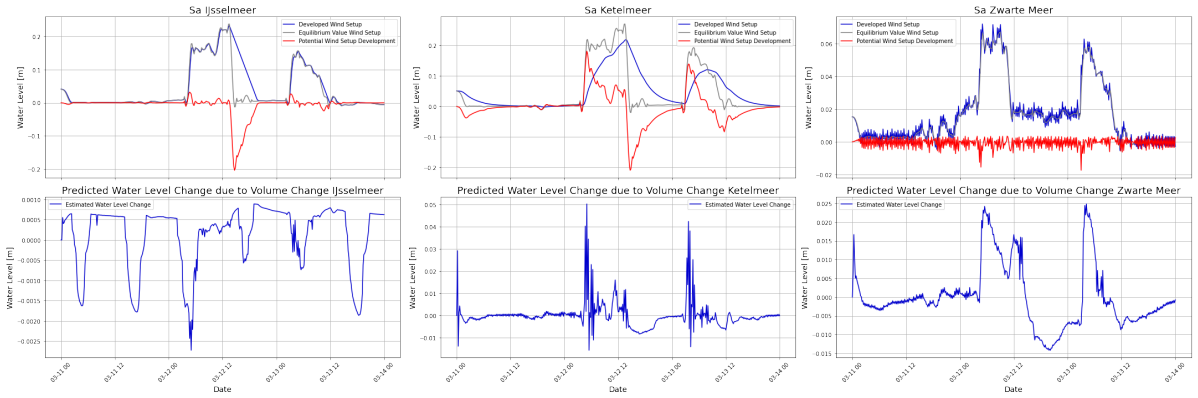

Figure 5.6: Wind setup development potential and predicted volume changes for March 12, 2020 using the non-closure simulation and a increasing wind after closure.

Recommendations

The analysis of the three closure scenarios, decreasing wind, stagnation of wind, and increasing wind, does not account for all possible scenarios, but they do provide insights into peak water levels during both closure and non-closure and into whether wind setup and volumes have the potential to further increase. Based on these analyses, the following could potentially be recommended:

- Lower peak water level without closure: if the peak water level without closure is lower than with closure, the barrier should remain open, as closing it would not provide any additional protection and may cause unnecessary disruption.
- No potential for wind setup to further develop: In scenarios where there is no further potential for wind setup development, it is advisable to keep the barrier open, as additional setup would not contribute to an increase in water levels.
- Limited potential for wind setup and lake volume increase: If the potential for wind setup and volume increase is limited, both closure and non-closure simulations should be run. In such cases, the decision to close should depend on whether the water levels from the non-closure scenario remain within acceptable limits for flood safety.
- Wind setup (and thus water level) still has development potential: If there is still potential for significant wind setup development and its associated impact on water levels, it is recommended to close the barrier, as this can help mitigate further water level increases.
- Significantly higher water levels without closure: In cases where water levels without closure are significantly higher than with closure, it is advisable to close the barrier to prevent unnecessary high water levels.

5.2.4. Overruled Scenario

On November 23, 2023, it was determined that closure of the Ramspol Barrier was not necessary, as it was expected to have minimal impact on flood safety around the Zwarte Meer. The observed scenario was a small, short-lived peak, and given that the closure and operation procedure requires a minimum of four hours, closing the barrier could have resulted in unnecessary water storage, potentially leading to higher water levels rather than mitigating them.

To evaluate the impact of this decision, model simulations were conducted for both closure and non-closure scenarios, analysing the resulting water levels at Ramspolbrug and Kadoelen. Water levels reached +0.40 m NAP around 12:40 and peaked at +0.50 m NAP around 13:20, with the closure criteria being met at 14:30. In the closure case, this triggered the closure of the Ramspol Barrier and reopening conditions were met at 19:10.

The results, illustrated in Figure D.9, show that while the closure scenario initially led to lower water levels compared to the non-closure case, this difference diminished as the storm receded. In the non-closure scenario, water levels naturally declined, whereas in the closure case, restricted outflow led to accumulation, ultimately resulting in similar or slightly higher water levels at Ramspolbrug and

Kadoelen. Peak water levels were 0.67 m NAP at Kadoelen without closure and 0.68 m NAP with closure, while at Ramspolbrug, the maximum water level reached 0.63 m NAP without closure and 0.64 m NAP with closure.

These findings suggest that the decision not to close the Ramspol Barrier was justified, as it avoided unnecessary water retention while maintaining flood safety. Given the minimal differences in peak water levels, either decision would probably have had a negligible impact on the overall risk of flooding.

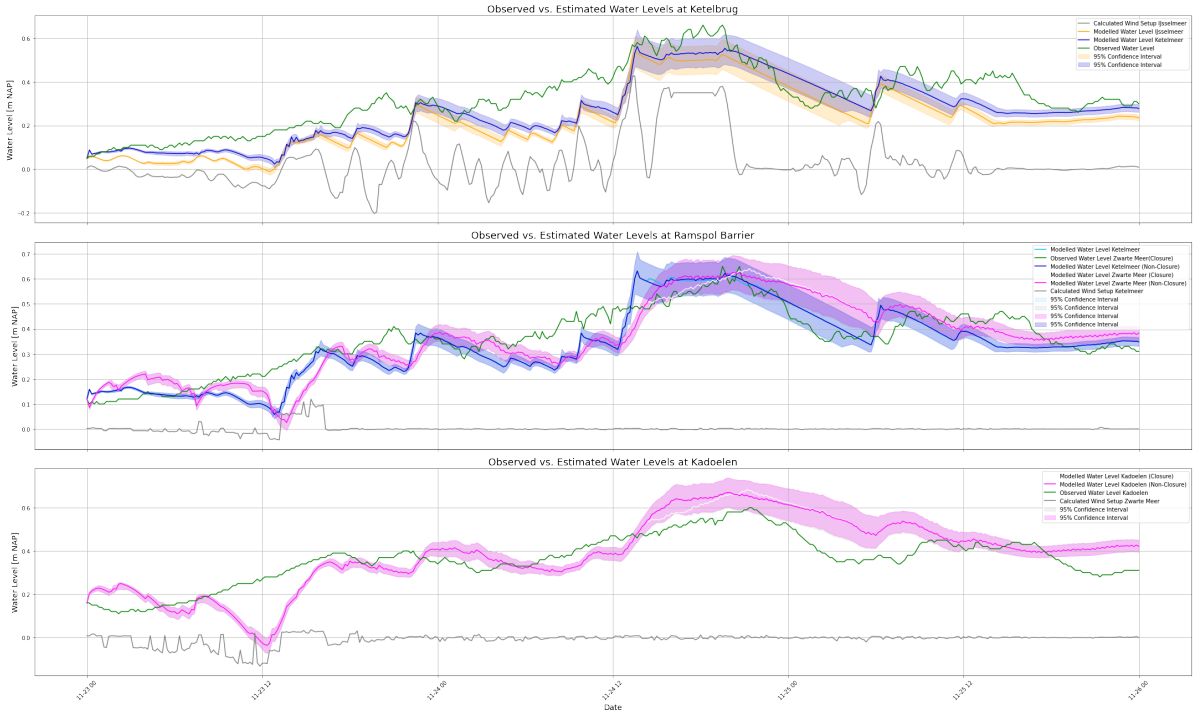

Figure 5.7: Modelled Water Levels at the Ketelbrug, Ramspol Barrier and Kadoelen during the overruled closure of the Ramspol Barrier on November 23, 2023, for both the closure and non-closure scenario.

5.2.5. Peaking Between +0.40m NAP and +0.50m NAP

Several times, including March 14, 2019, April 5, 2021, and January 24, 2024, water levels reached +0.40 m NAP but remained below +0.50 m NAP, leading to navigation blockages without closure of the Ramspol Barrier. This has caused frustration within the shipping industry, raising the question of whether such blockades are necessary and how to determine when they should be implemented.

The approach to evaluating this situation follows the method outlined in subsection 5.2.3. Predictions are used to assess the likelihood of water levels exceeding +0.50 m NAP, while the key drivers of water level changes—wind setup and volume variations—are analysed to determine the potential for further increases.

Similar to the scenario with peaks just above +0.50m, this analysis considered three different cases: an observed peak between +0.40m and +0.50 m NAP on February 23, 2024; a modified scenario where the wind peak plateaus for an additional four hours; and a further modified scenario where the wind peak continues over the following four hours. These cases will be analysed in the following subsections.

Decreasing Winds: the Case Study of February 23, 2024

This scenario examines the water level dynamics of February 23, 2024, focusing on the impact of decreasing winds. In the model simulation, the operation procedure was initiated at 21:10 on February 22, when the water level reached +0.20 m NAP, followed by the navigation blockade at 22:10 on February 2022, both slightly earlier than observed. The water level at the Ramspol Barrier and Zwarte Meer continued to rise steadily before reaching a plateau, after which it gradually declined. This is visualised in Figure D.28.

An analysis of wind setup potential and volume changes in the lakes, shown in Figure D.30, indicates that by the time the water levels at Ketelmeer and Zwarte Meer peaked around 01:00, the wind setup at both the IJsselmeer and Zwarte Meer had already stabilised at equilibrium. At the Ketelmeer, however, there was still potential for a further increase of approximately 4 cm. Nevertheless, immediately afterward, the wind setup began to diminish, leading to an overall decline in water levels across the system.

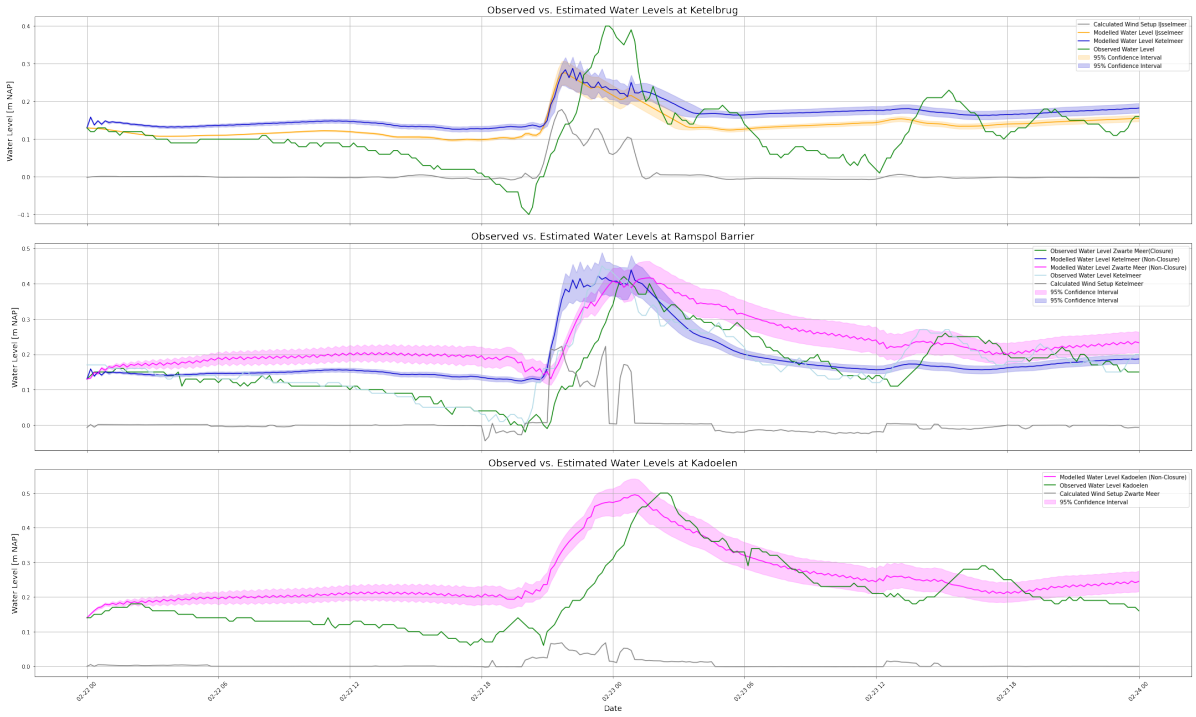

Figure 5.8: Modelled Water Levels at the Ketelbrug, Ramspol Barrier and Kadoelen on February 23, 2024, used for evaluating whether a navigation blockade is necessary.

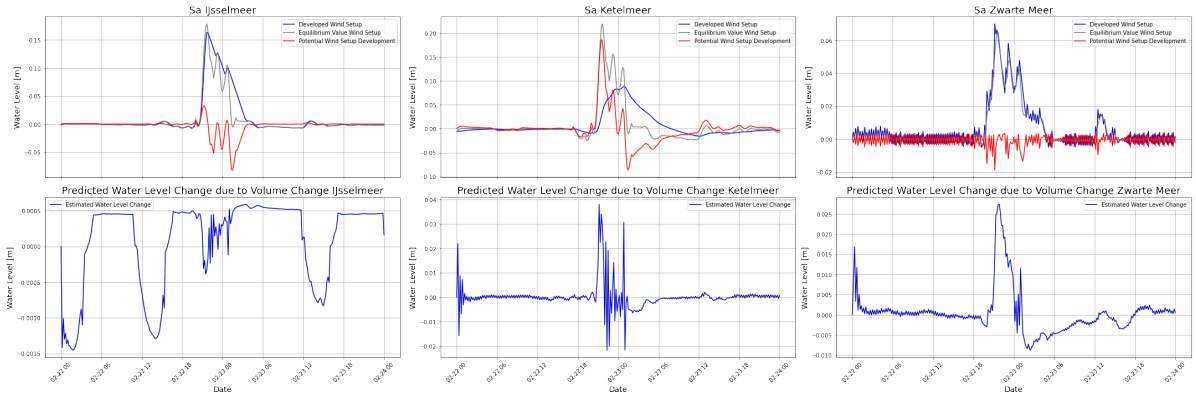

Figure 5.9: Wind setup development potential and predicted volume changes for February 23, 2024, during a decreasing wind to evaluate whether a navigation blockade is necessary.

Stagnation of the Winds

In this scenario, the wind setup following the February 23, 2024, peak is adjusted to remain stagnant rather than decreasing. After reaching its observed peak, the wind setup stabilises at 0.15 metres in the Ketelmeer and 0.10 metres in the IJsselmeer between 00:00 and 04:00. All other parameters remain unchanged, including the discharges, the activation of the operational team at 21:10 on February 22, and the navigation blockade at 22:10.

The model simulations indicate that under these conditions, the water level at the Ketelmeer and Zwarte

Meer continues to rise, reaching +0.50 m NAP at approximately 03:30 and peaking at +0.51 m NAP shortly thereafter.

As observed in the decreasing wind case, the wind setups across all three lakes had already reached their equilibrium values before beginning to subside, leaving no potential for further wind-driven water level increases. This is illustrated in Figure D.40. However, lake volumes continue to increase slightly over time, contributing to a gradual rise in water levels.

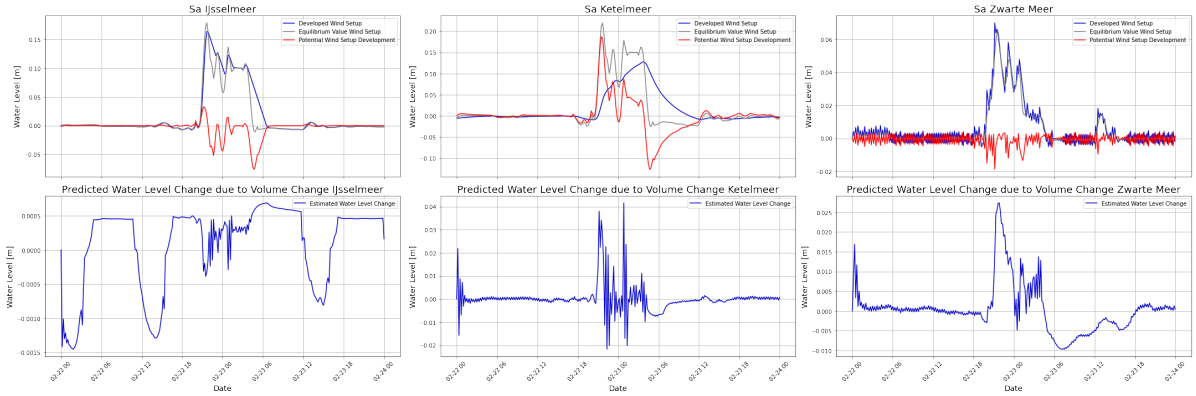

Figure 5.10: Wind setup development potential and predicted volume changes for February 23, 2024, during a stagnating wind to evaluate whether a navigation blockade is necessary.

Increasing Winds

In this scenario, the wind setup following the February 23, 2024 peak is adjusted to continue increasing rather than stabilising or decreasing. The wind setup reaches 0.20 m in the Ketelmeer and 0.15 m in the IJsselmeer between 00:00 and 04:00, while all other parameters remain unchanged, including the discharges, the activation of the operational team at 21:10 on February 22, and the navigation blockade at 22:10 on February 22.

Model simulations indicate that under these conditions, the water level in the Ketelmeer and Zwarte Meer steadily rises, reaching the closure criteria at approximately 01:30 and peaking at 0.61 m NAP around 04:00. The increase in wind setup directly contributes to this additional rise in water levels.

Analysis of wind setup potential and volume changes in the lakes, as shown in Figure D.40, reveals that in the Ketelmeer, the developed wind setup remains below its theoretical maximum, indicating further potential for wind-driven increases in water levels. However, in both the IJsselmeer and Ketelmeer, the developed wind setup matches the theoretical wind setup, suggesting no further increase beyond this point. In the Zwarte Meer, without a closure, the water level can rise by approximately 1.4 centimetres per 10 minutes, driven by the discharge of the Zwarte Water and the wind-induced flow from the Ketelmeer toward the Zwarte Meer.

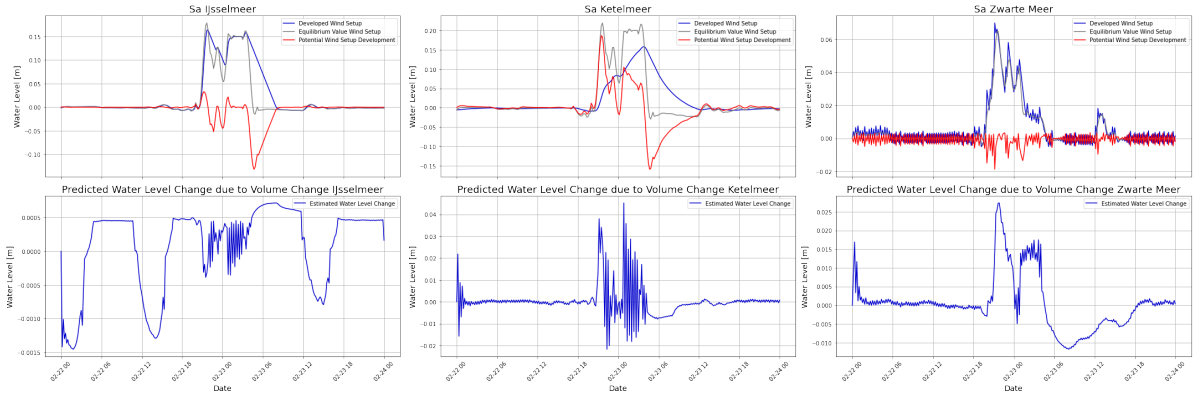

Figure 5.11: Wind setup development potential and predicted volume changes for February 23, 2024, during an increasing wind to evaluate whether a navigation blockade is necessary.

Recommendations
Although not covering all possibilities, based on these three scenarios, the following points can be taken into account to determine if a navigation blockade is necessary:

- If the prediction and its uncertainty show no further water level increase towards closure criteria and/or if no further wind setup development is possible and no significant predicted discharge peaks could contribute to water level increase, then the navigation blockade could be lifted.
- If model predictions indicate that water levels will continue to rise toward closure criteria, and if the wind setup still has the potential to develop further, allowing for additional water level increases, then the navigation blockade should remain in place.

5.2.6. Initial Water Level at the Ramspol Barrier is larger than +0.50 m NAP

When the initial water level exceeds +0.50m NAP, the direction of water flow at the Ramspol Barrier becomes the dominant criterion for triggering a closure. This raises concerns, as minor, short-lived fluctuations could prompt a closure, particularly when high discharges are present on the Zwarte Meer. Such closures may result in water accumulation, posing potential safety risks.

This analysis aims to establish a framework for assessing whether a closure is necessary in situations where flow direction dominates the decision-making process. Implementing a strict discharge or flow velocity threshold before initiating closure may not be advisable, as instantaneous discharge values can match those modelled during peak events, leading to unnecessary closures.

A potential method to refine the closure decision is to evaluate whether there is a net flow towards the Zwarte Meer for 30 to 60 minutes before closure. This approach accounts for short-lived flow fluctuations and prevents premature closures based on short-lived changes. An alternative method is determining whether a sustained flow towards the Zwarte Meer persists for at least a predefined duration before triggering closure.

To test the effectiveness of these methods, simulations were conducted under varying wind conditions, keeping the initial lake water levels at +0.50 m NAP and maintaining consistent discharges from the IJssel and Zwarte Water. The discharge data from February 16–17, 2024, was used as a reference for all cases (and chosen randomly).

The first simulation, with a wind setup of 0.10 m at the IJsselmeer for two hours, showed no sustained negative flow with closure, while in the non-closure case, negative flow persisted for 10 minutes. Maximum water levels reached 0.68 m at Ramspolbrug and Kadoelen with closure, compared to 0.59 m and 0.58 m, respectively, without closure, suggesting no significant advantage in closing, as shown in Figure D.53.

In a subsequent simulation, a peak height of 0.15 meters at the IJsselmeer for a duration of 2 hours was considered, representing a higher and longer peak than the previous scenario. The time-averaged discharge with closure is negative for 50 minutes, while without closure, it is negative for 30 minutes, as visualized in Figure D.56. The minimal discharge recorded is $-420 m^3/s$. The maximum water levels at Ramspolbrug are 0.65 meters without closure and 0.69 meters with closure, while at Kadoelen, the levels are 0.64 meters without closure and 0.69 meters with closure. As in the previous case, the simulation results indicate that closure leads to higher water levels, suggesting that closing the barrier does not provide a clear advantage in terms of reducing water levels.

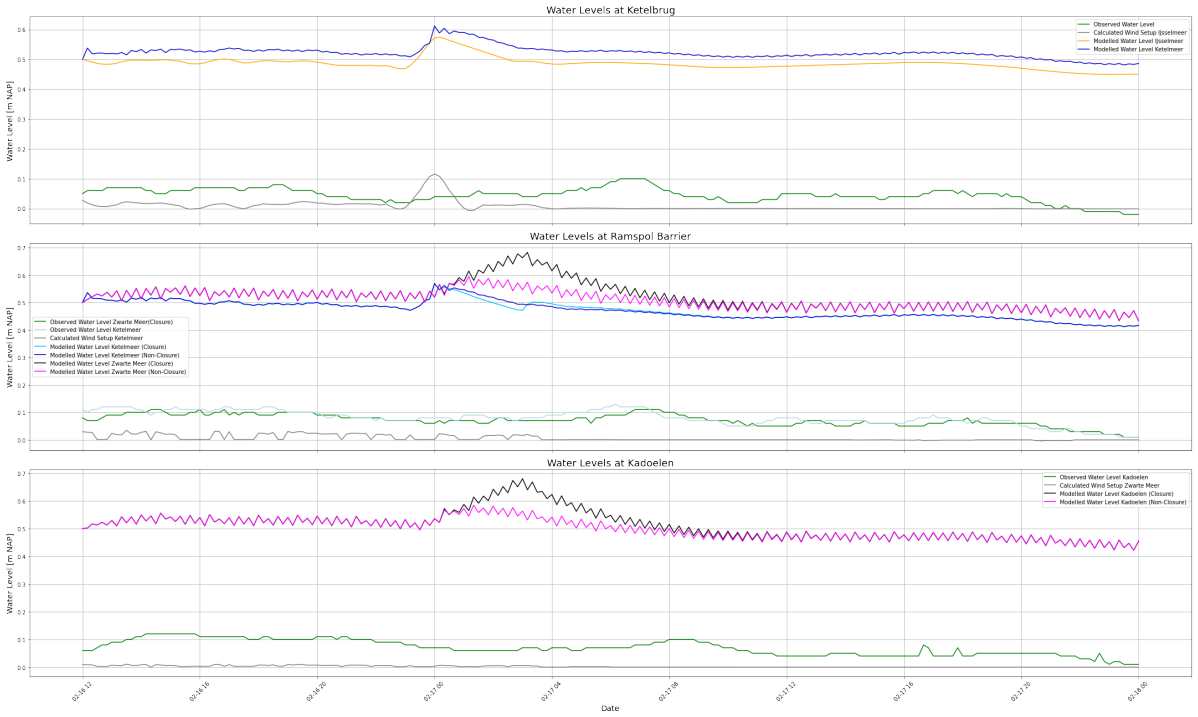

Figure 5.12: Modelled Water Levels at the Ketelbrug, Ramspol Barrier and Kadoelen during the simulation of an initial water level of +0.50m NAP and a wind setup 'peak' on the IJsselmeer of 0.10 metres for closure and non-closure case.

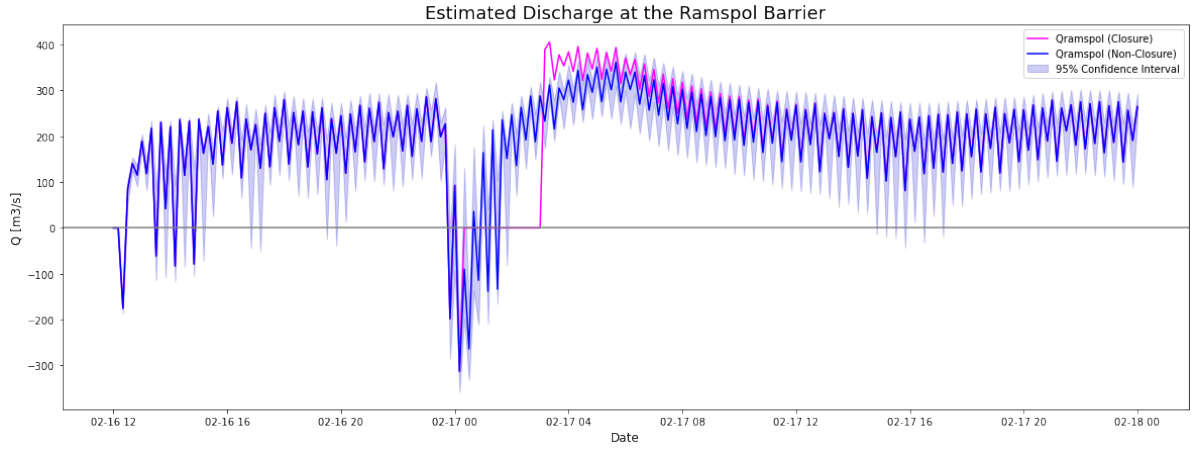

Figure 5.13: Modelled discharge at the Ramspol Barrier for a wind peak of 15 centimetres for two hours

A simulation was conducted with a peak height of 0.25 meters at the IJsselmeer, lasting for 3 hours, representing a more substantial and prolonged peak compared to the previous scenarios. The time-averaged discharge with closure remains negative for 40 minutes, while in the non-closure case, the negative discharge persists for 110 minutes, as shown in Figure D.58. The minimal discharge during this period is $-500 m^3/s$. The maximum water levels observed at Ramspolbrug are 0.76 meters without closure and 0.77 meters with closure, while at Kadoelen, the levels are 0.75 meters without closure and 0.74 meters with closure. These findings suggest that, in this instance, there is no significant advantage to closing the barrier, as the water level variation between the two cases is negligible.

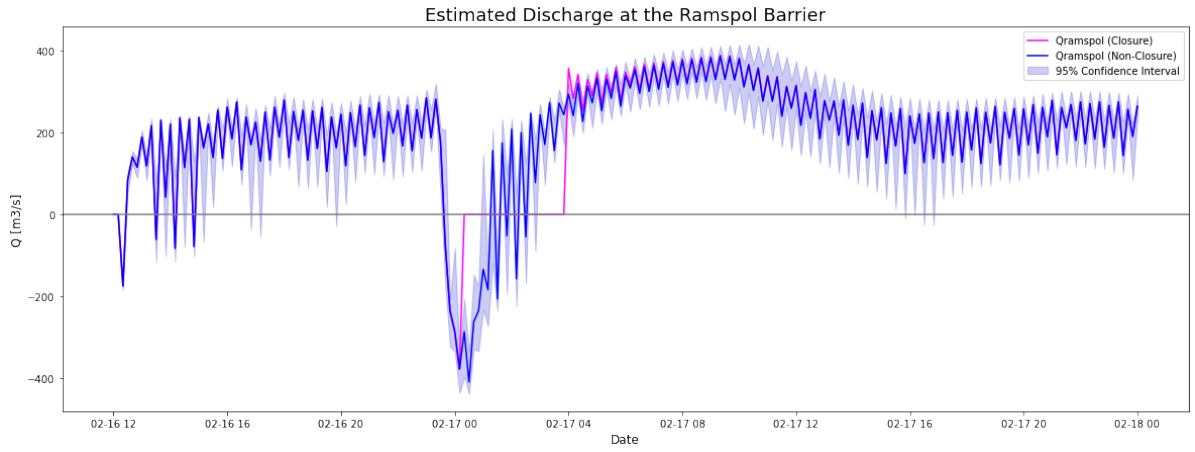

Figure 5.14: Modelled discharge at the Ramspol Barrier during a wind peak of 25 centimetres for 3 hours.

These findings suggest that closure becomes justified when the time-averaged discharge at the Ramspol Barrier shows a negative flow for at least 60 minutes and reaches -500 m^3/s. While based on a limited set of simulations, this approach offers a potential framework for improving closure decisions and reducing unnecessary interruptions while maintaining flood safety. Further testing is required to refine these criteria and validate their effectiveness.

5.2.7. Multiple Peaks

This scenario examines cases where two distinct peaks in water levels, each leading to a closure of the Ramspol Barrier, occur within a single day. Such events have been observed at least twice in the past: on January 3 and 4, 2018, and on February 17 and 18, 2022. These occurrences are typically linked to prolonged weather depressions, which can sustain storm conditions over an extended period, leading to either multiple storm peaks or consecutive storm events. In these cases, a temporary weakening of the storm triggers the opening of the Ramspol Barrier but is followed by a second peak, potentially triggering a second closure.

During such events, the wind setup initially forces water from the IJsselmeer into the Ketelmeer, raising water levels and triggering closure criteria. Once the barrier is closed, water levels on the IJsselmeer side initially drop relative to those in the Ketelmeer. The question then arises: how can the timing between consecutive peaks influence closure strategy? If peaks occur in quick succession, should the barrier remain closed to prevent excessive fluctuations? Conversely, if the time between peaks is long enough, should each peak be treated as an independent event, with the barrier reopening in between? In intermediate cases, where the second peak follows shortly after the first reopening, does the water level have sufficient time to recede, or would it be safer to change the timing of closure or not close at all?

To investigate these dynamics, the storm event of February 17 and 18, 2022, was selected for analysis. This period included two consecutive closures, making it an ideal case study. Data from February 16 to 19, 2022, was used, with modifications applied to explore different timing scenarios.

Using the model, three variations of this multiple-peak scenario were analysed: the original scenario of February 17 and 18, 2022, where peaks were sufficiently separated in time to be considered separate closures; A modified scenario in which the second peak occurs while water levels are still receding from the first closure, potentially delaying full recovery; and A further modified scenario where the second peak coincides with the reopening of the Ramspol Barrier.

Two Separate Peaks

In this scenario, the observed closures on February 17 and 18, 2022, are analysed. The events followed a straightforward sequence: the Ramspol Barrier closed in response to the first peak, reopened fully after the water had receded, allowed accumulated water on the Zwarte Meer to flow out completely, and subsequently closed again when the second peak met the closure criteria. This resulted in two independent closures.

To assess the necessity and impact of these closures, simulations were conducted for both closure events, as well as for a non-closure scenario. By including a scenario without closure, it becomes possible to evaluate whether closing the barrier was the most effective strategy for flood safety within the system. The outcomes are visualised in Figure 5.15.

For the first closure, model simulations indicate that the operation team was activated at approximately 22:10 on February 16, with vessel passage through the Ramspol Barrier restricted from 02:10 on February 17. The closure criteria were met around 03:30 on February 17, prompting the full closure of the barrier. Water levels on the Zwarte Meer exceeded those on the Ketelmeer starting from 14:40 on February 17, leading to the reopening of the barrier.

The simulation results show that during this closure, peak water levels reached 0.69 m NAP at the Ramspolbrug and 0.84 m NAP at Kadoelen. In the non-closure scenario, peak water levels were 0.65 m NAP at the Ramspolbrug and 0.84 m NAP at Kadoelen. This suggests that, in this instance, keeping the barrier open might have been a more favourable strategy for flood safety, as explored further in subsection 5.2.3.

For the second closure, the operation team was activated at 18:10 on February 18, and vessel passage restrictions were imposed at 18:30 on February 18. The closure criteria were met soon after, at 18:40 on February 18, resulting in the full closure of the barrier. The barrier was reopened when water levels on the Zwarte Meer once again exceeded those on the Ketelmeer, which occurred at 06:40 on February 19.

During this second closure, peak water levels reached 0.60 m NAP at the Ramspolbrug and 0.73 m NAP at Kadoelen. In contrast, the non-closure scenario resulted in significantly higher peak water levels: 0.99 m NAP at the Ramspolbrug and 0.60 m NAP at Kadoelen. In this case, the decision to close the barrier was clearly beneficial for flood safety, as it prevented a substantially higher peak water level.

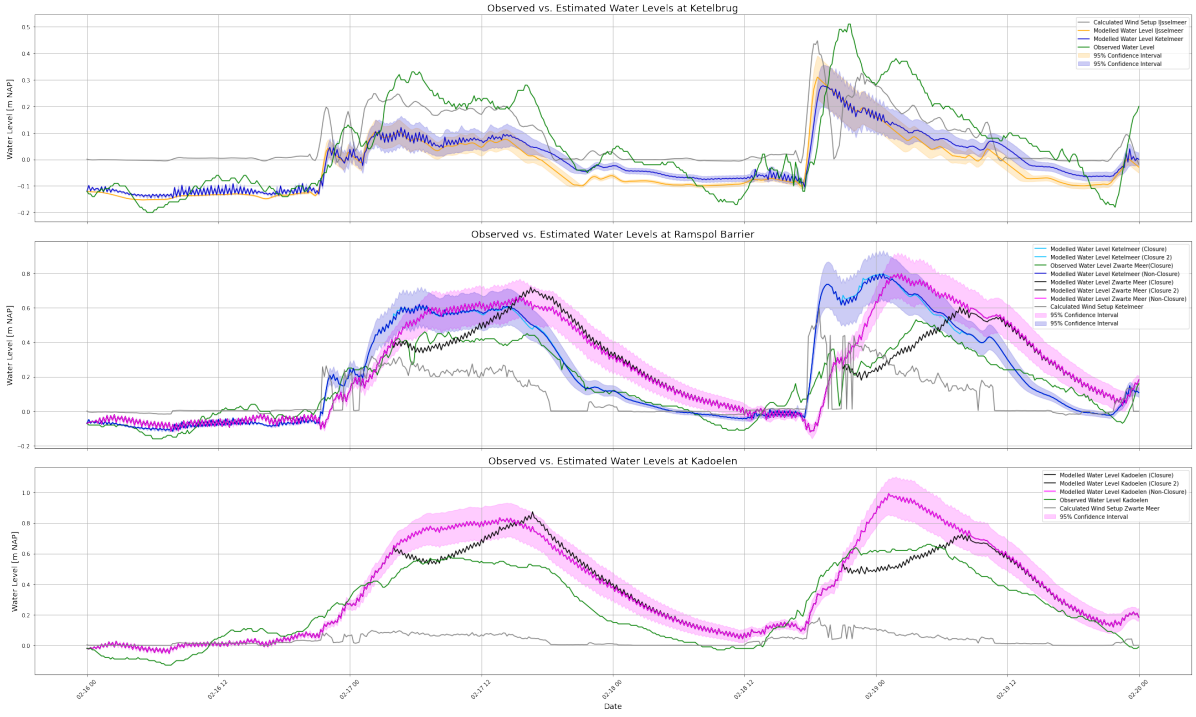

Figure 5.15: Modelled Water Levels at the Ketelbrug, Ramspol Barrier and Kadoelen during the closures of February 17 and 18, 2022.

Second Peak Hits when Water Levels are still Receding from First Closure

In this scenario, the first peak on February 17, 2022, remains unchanged, while the second peak on February 18 is shifted back in time. Instead of occurring in the afternoon and continuing into the following day, it now begins at midnight. This means that by the time the second peak arrives, the barrier has already reopened, and water levels on the Zwarte Meer are receding. However, due to accumulated discharge, the water level here remains higher than in the Ketelmeer.

The first closure remains the same, with the operation team being activated around 22:10 on February 16, vessels being blocked from passing the Ramspol Barrier at 02:10 on February 17, and the closure criteria being met at 03:30. The water level on the Zwarte Meer dropped below that of the Ketelmeer at 14:40, triggering the reopening of the barrier.

With the second peak now occurring earlier, the standard operational procedure is followed. Water levels on the Zwarte Meer rise again, reaching +0.40 m NAP at 23:10 on February 17, and the closure criteria are met at 23:20. The barrier remains shut until 06:10 on February 18, when opening conditions are met. Similar to the scenario with two separate closures, the peak water levels during the closure are lower than in the non-closure scenario: 0.85 m NAP compared to 0.88 m at the Ramspolbrug, and 1.04 m compared to 1.11 m at Kadoelen. This is visualised in Figure 5.16.

To assess whether adjusting the closure timing could further reduce water levels, an alternative scenario was tested where the second closure was initiated 30 minutes earlier. While this led to slightly higher initial water levels at the Zwarte Meer, it also prevented additional wind setups from entering the system. As a result, the barrier remained closed for a longer period, with reopening delayed until 10:30 on February 18. However, this led to lower peak water levels: 0.74 m NAP at Ramspolbrug and 0.87 m at Kadoelen. This highlights a challenge: earlier closures can improve flood protection but also extend the closure duration, increasing the operational burden and disrupting shipping for longer.

Prolonged and later closures were not considered since these would have resulted in continued water accumulation and additional flow into the Zwarte Meer due to the wind setup of the second peak.

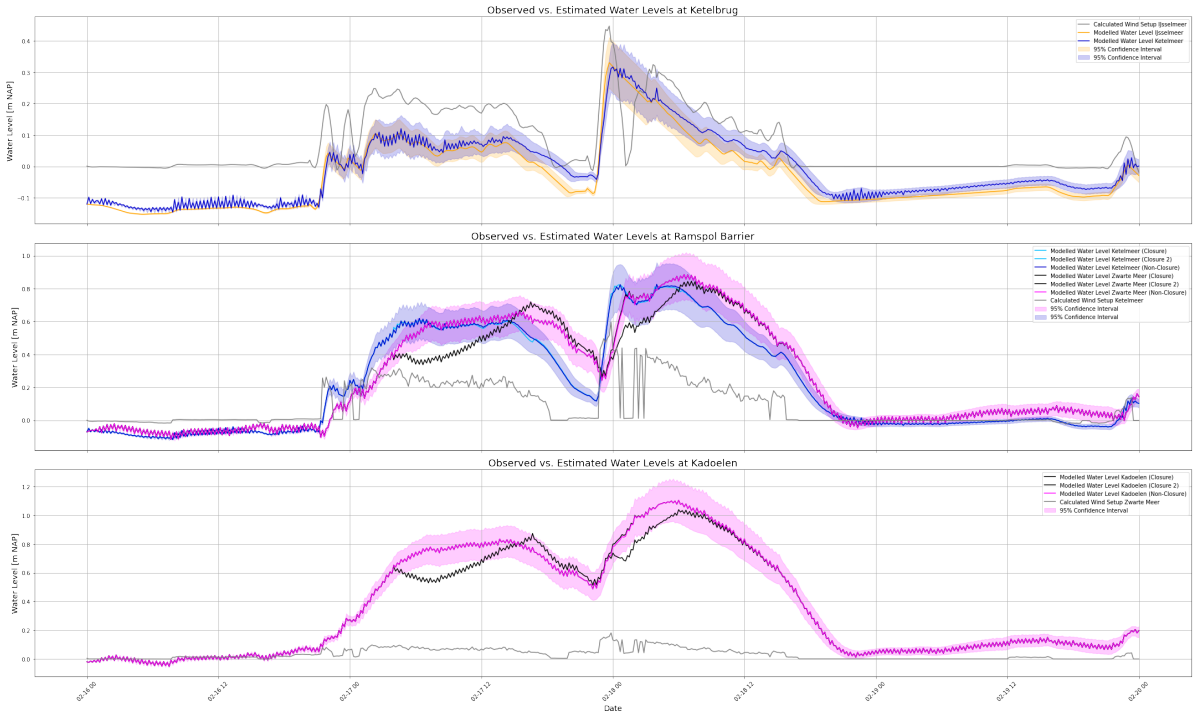

Figure 5.16: Modelled Water Levels at the Ketelbrug, Ramspol Barrier and Kadoelen during the adjusted closures of February 17 and 18, 2022, where the water level on the Zwarte Meer is still receding from the first closure.

Second Peak Hits when the Ramspol Barrier is still Opening from First Closure

In this scenario, the second peak arrives while the Ramspol Barrier is still in the process of opening after the first closure. Since the barrier has not fully reopened yet, it cannot immediately close again when the new peak meets closure criteria. This case examines the impact of a late second closure compared to an elongated closure where the barrier remains shut.

The first peak follows the same timeline as before, with opening criteria met at 14:40 on February 17 and the barrier fully opened by 17:40. The second peak is shifted back in time to approximately 16:00, meaning it arrives while the barrier is still in the process of opening. The key question is whether a delayed second closure or an extended closure leads to better flood management. To assess this, the hydraulic model is used to assess both scenarios.

In the first scenario, a late closure is applied. As soon as the barrier fully opens at 17:40, a new closure is immediately initiated. During the brief period when the barrier is open, some water is able to flow out before the second peak hits. As shown in Figure 5.17, both the late closure and non-closure scenarios result in a peak water level of 0.94 m NAP at Ramspolbrug. At Kadoelen, the second closure scenario reaches 1.18 m NAP, while the non-closure scenario reaches 1.16 m. However, for most of the duration, water levels remain lower in the late closure case.

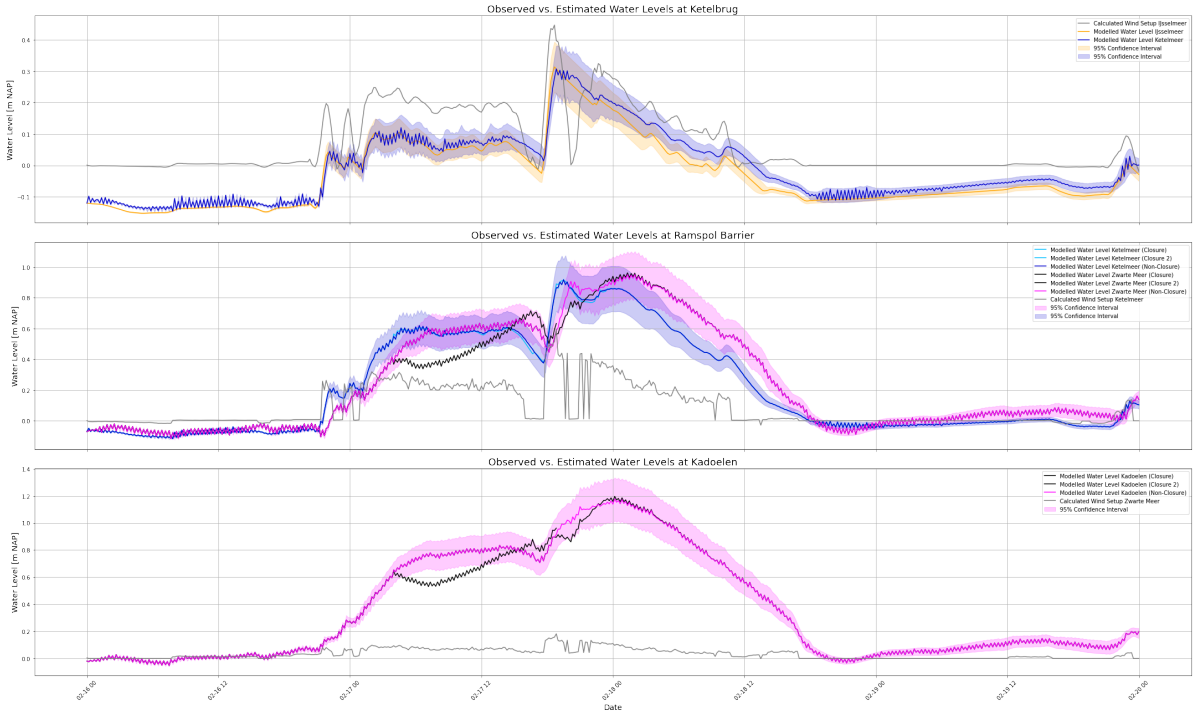

Figure 5.17: Modelled Water Levels at the Ketelbrug, Ramspol Barrier and Kadoelen during the adjusted closures of February 17 and 18, 2022, where the second peak hits during the opening procedure of the first closure and then directly closed.

In the second scenario, an elongated closure is implemented. Anticipating the second peak, the barrier remains closed instead of reopening. The opening criteria for the second peak are then met at 20:00 on February 17. As illustrated in Figure 5.18, water levels on the Zwarte Meer steadily rise throughout the extended closure. At Ramspolbrug, the peak water level reaches 0.98 m NAP, while at Kadoelen, it peaks at 1.23 m. This approach not only results in a prolonged closure, increasing pressure on the operation team and the shipping industry, but also leads to higher water levels on the Zwarte Meer, ultimately compromising flood safety.

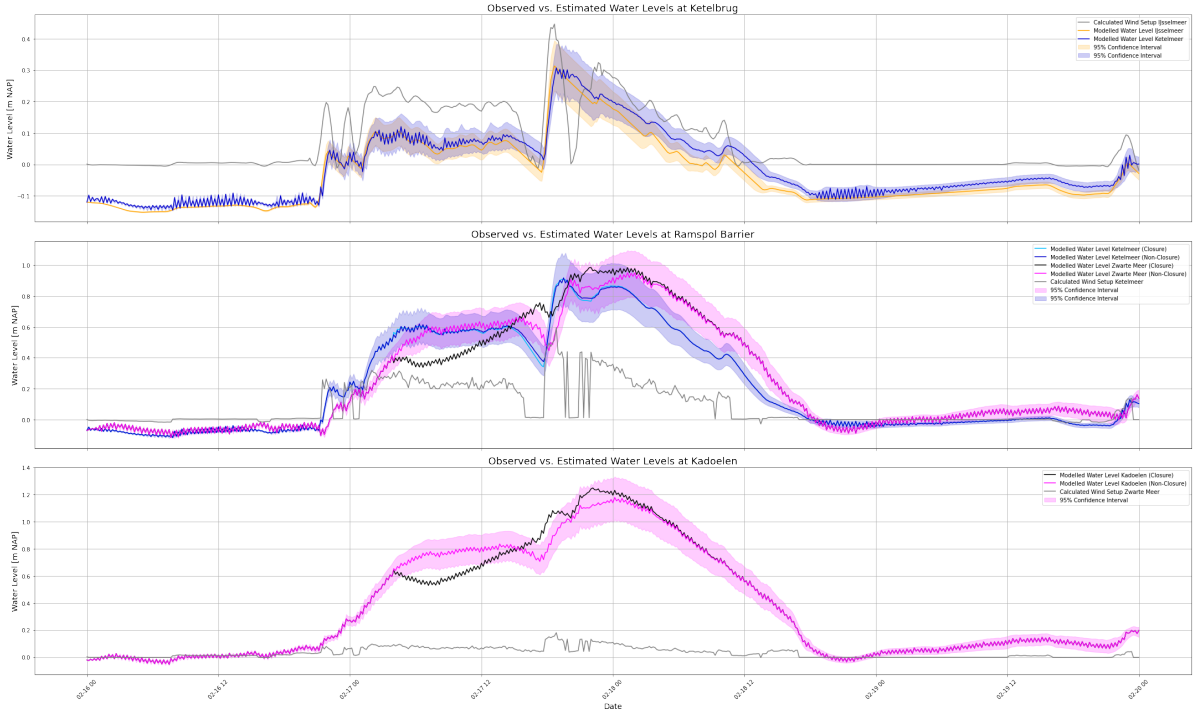

Figure 5.18: Modelled Water Levels at the Ketelbrug, Ramspol Barrier and Kadoelen during the adjusted closures of February 17 and 18, 2022, where the Ramspol Barrier is closed during both peaks.

Recommendations

In general, when peaks occur closer together, water levels remain elevated due to insufficient recovery time, leading to higher initial water levels on the Zwarte Meer and additional inflow during the second peak.

When the water level has fully recovered near the Ramspol Barrier before the second peak arrives, following the standard closure procedure is the most effective approach. This ensures that the system operates as intended without unnecessary delays or complications.

For cases where the second peak arrives before full recovery, implementing an earlier closure could help reduce water levels on the Zwarte Meer during the closure period. However, this presents a trade-off: while earlier closures improve flood safety, they also increase operational demands and disrupt shipping by extending closure durations. A balance must be struck between minimising water levels and maintaining manageable closure times.

If the second peak arrives while the barrier is still opening from the first closure, the decision between a late closure and no closure depends on the peak's characteristics. A late closure allows some drainage before the barrier shuts again, potentially mitigating extreme water levels. On the other hand, choosing not to close could be an option if the second peak does not pose a significant flood risk.

Finally, prolonged closures should be avoided whenever possible, as they not only extend navigation restrictions but also result in higher water levels in the Zwarte Meer, which ultimately compromises flood safety. However, since earlier closures have demonstrated potential in reducing peak water levels in scenarios where a second peak occurs before the water levels have fully recovered, an earlier but longer closure spanning both peaks could be considered.

5.2.8. Sensitivity to Varying Q_{zw} during Closures

This scenario explores the effect of varying discharges of the Zwarte Water (Q_{zw}) on the operation procedure and the water levels throughout the system during and after the closure of the Ramspol Barrier. It specifically evaluates how fast water levels rise in the Zwarte Meer following the closure, considering varying discharge values from the Zwarte Water while keeping other parameters constant, such as the initial water level, wind conditions, discharges from the IJssel and the drainage discharge.

For this analysis, a period of prolonged storm closure was selected, specifically focusing on conditions observed on February 17, 2022. An extended closure allows for a more pronounced effect of the variation in varying discharges to be observed over time. Discharges from the Zwarte Water were incrementally adjusted in steps of 50 m^3/s, with values rising to a peak of 500 m^3/s.

All scenarios are run in parallel in the hydraulic model and the results are visualised in Figure 5.19. An overview of the peak water heights at Ramspolbrug and Kadoelen and the time when the opening criteria is met is shown in Table 5.1. As expected, the closure timing remained largely consistent across different discharge scenarios, since discharges have a minimal effect on storm closures compared to wind setup (subsection 3.4.2). However, larger differences between discharges emerged during and after the closure. For larger discharges, the opening criteria were met earlier than for smaller discharges, due to the increased volume accumulating in the system. This is consistent with the expectation that larger discharges result in a faster rate of water level rise. In terms of peak water level, higher discharges were also associated with larger peak water heights. This is because a larger volume of water accumulates behind the Ramspol Barrier, accelerating the rise in water levels. Lastly, the water level throughout the system remain higher after closure for large discharges. The bottom two graphs in Figure 5.19, clearly show that larger discharges need more time for the accumulated water to flow out. Similarly, the water levels on the IJsselmeer and Ketelmeer were higher by a few centimetres for the higher discharges. This is since the overall water volume is larger in the system in this case.

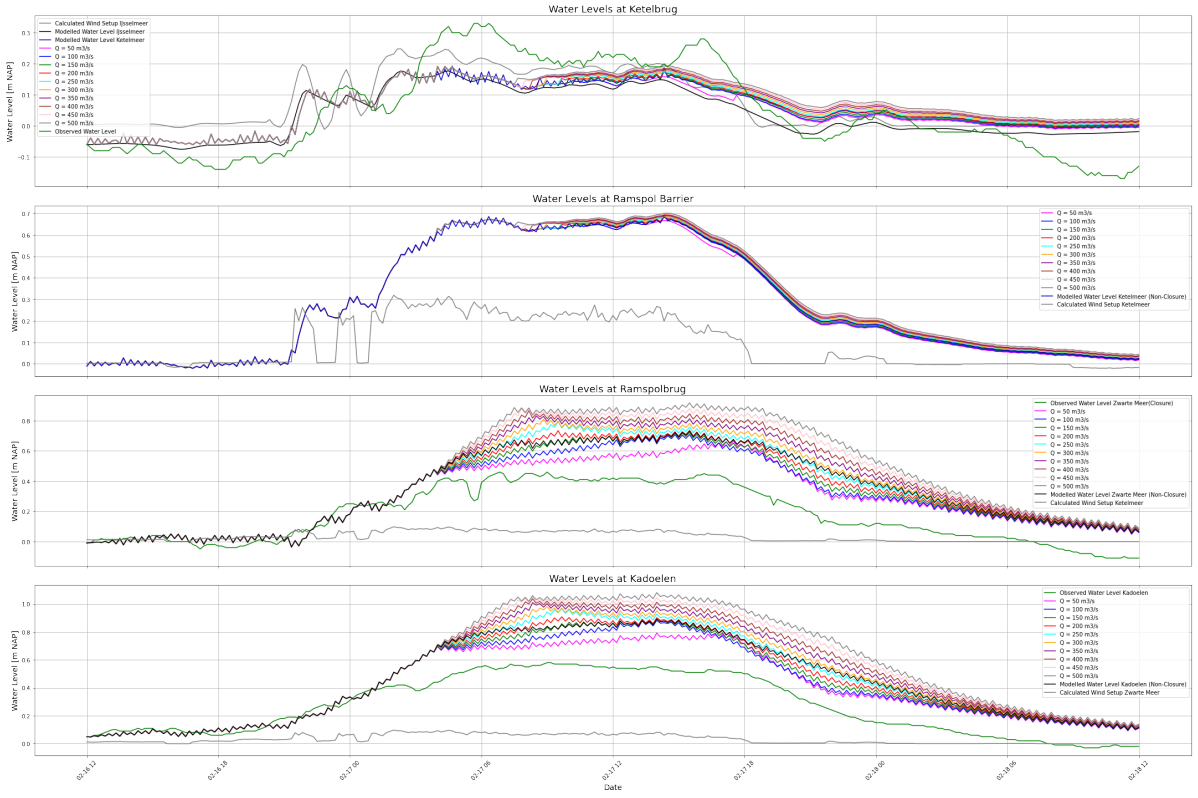

Figure 5.19: Modelled Water Levels at the Ketelbrug, Ramspol Barrier and Kadoelen for different discharges of the Zwarte Water during the closure of February 17, 2022.

Table 5.1: Overview of the maximum peak height during closure and closure duration for different discharges of the Zwarte Water for the scenario on 17 February 2022.

Discharge Zwarte Water	Peak Water Height Ramspolbrug [m NAP]	Peak Water Height Kadoelen [m NAP]	Opening Criteria Met
$50 m^3/s$	0.67	0.79	15:30, 17 February
$100 m^3/s$	0.71	0.88	11:30, 17 February
$150 m^3/s$	0.72	0.89	08:10, 17 February
$200 m^3/s$	0.74	0.91	07:30, 17 February
$250 m^3/s$	0.79	0.97	07:10, 17 February
$300 m^3/s$	0.81	0.98	06:50, 17 February
$350 m^3/s$	0.83	1.01	06:30, 17 February
$400 m^3/s$	0.87	1.04	06:10, 17 February
$450 m^3/s$	0.88	1.05	05:50, 17 February
$500 m^3/s$	0.92	1.08	05:30, 17 February

5.2.9. No Drainage Capacity over the Afsluitdijk in Combination with Mild Winds

in this scenario, drainage through the Afsluitdijk is entirely blocked while lake water levels are elevated, and winds remain relatively mild. This situation presents a significant challenge, as the absence of drainage capacity leads to immediate water level rises in the system, potentially to dangerously high water levels. The key objective of this analysis is to assess how quickly water levels increase under these conditions, how sensitive the system is to varying wind setups, and at what point critical thresholds and closure criteria are reached for these winds.

To explore these dynamics, a series of simulations were conducted in which the initial water level was systematically varied while keeping discharge from the IJssel and Zwarte Water constant. The chosen discharge values, based on observed conditions from February 16–18, 2024, reflect a mean flow of 778 m^3/s at Olst and 194 m^3/s at Genemuiden. By maintaining discharge rates consistent across all scenarios, the analysis isolates the effects of wind-induced water level changes, allowing for a direct comparison between different wind conditions and initial lake levels.

The wind setup was modelled for values ranging between 0.30 and 0.50 m, with wind speeds increasing gradually from 1 to 13 m/s over a defined period, allowing equilibrium wind setup to develop before decreasing again. A northwesterly wind direction was selected since it is frequently observed during storm conditions and allows for large fetches, leading to large wind setups.

For each of the scenarios, it is determined whether and when certain thresholds and closure criteria are met. An overview of the smallest peaks leading to a threshold is given in Table 5.2 and for an initial water level of +0.40m NAP visualised in Figure D.72.

The results highlight the system's sensitivity to wind setup, particularly under high initial water levels. When the starting water level is relatively low (+0.30 m NAP), no scenario led to the exceedance of closure criteria, as the moderate wind speeds considered were insufficient to induce a critical rise. In contrast, at an initial level of +0.50 m NAP, even the slightest breeze of 1 m/s resulted in closure thresholds being exceeded, demonstrating the system's vulnerability to wind when water levels are already elevated.

The influence of wind speed on the timing of threshold exceedance is particularly evident. For instance, with an initial water level of +0.40 m NAP, the closure criterion was met at 00:50 on February 17 under 11 m/s winds, whereas under 12 m/s winds, the same threshold was reached 30 minutes earlier.

Table 5.2: Overview of which wind conditions are required to reach certain steps in the operation procedure.

Initial Water Level	+0.40m NAP Exceeded	+0.50m NAP Exceeded	Closure Criteria Met
+0.30m NAP	With $u_{10} = 10 m/s$ at 01:00 on 17 February	n/a	n/a
+0.35m NAP	With $u_{10} = 7 m/s$ at 01:00 on 17 February	n/a	n/a
+0.40m NAP	Initial value, all scenarios.	With $u_{10} = 10 m/s$ at 01:00 on 17 February	With $u_{10} = 11 m/s$ at 00:50 on 17 February
+0.45m NAP	All scenarios	With $u_{10} = 7 m/s$ at 01:00 on 17 February	With $u_{10} = 8 m/s$ at 00:50 on 17 February
+0.50m NAP	All scenarios	All scenarios	With $u_{10} = 1 m/s$ at 00:10 on 17 February

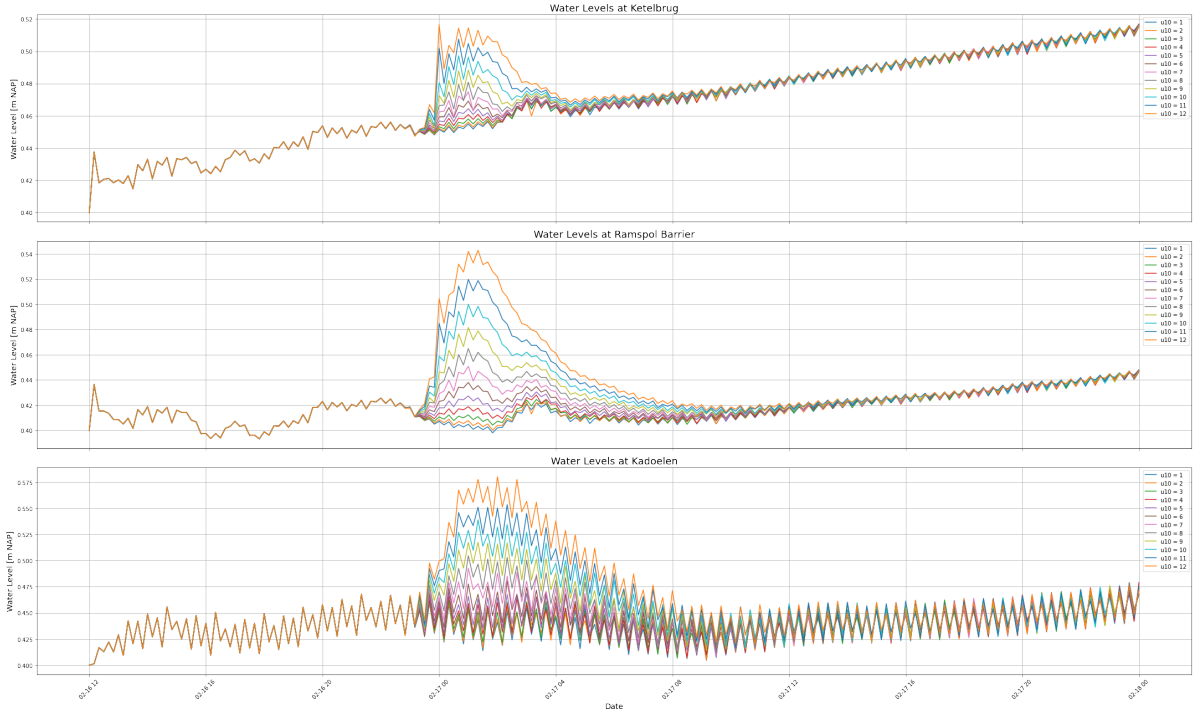

Figure 5.20: Modelled Water Levels at the Ketelbrug, Ramspol Barrier and Kadoelen for different wind speed scenarios with an initial water level of +0.40m NAP and no drainage over the Afsluitdijk.

5.3. Summary of Improved Scenarios

In Table 5.3 an overview is given of all considered scenarios, why they are interesting to consider, and what the key results are from the corresponding simulations in the hydraulic model.

Table 5.3: Overview of Scenarios.

Scenario	Why it is Interesting	Findings
Normal Closure	Evaluates the accuracy of 24-48h forecasts in predicting water levels and closure timing during storm conditions.	Possible, but the model shows deviations from observations.
Test Closure	Insights into how the system behaves under a test closure.	Little impact on water levels in the system.
Necessity Closures when the closure criteria are just exceeded	Examines whether closing the barrier at +0.50m NAP optimises flood safety or if keeping it open would be more beneficial.	Run parallel simulations (closure vs. non-closure) and consider the potential for further wind setup development. **Keep barrier open** if peak water levels are lower without closure and/or wind setup cannot further develop. **Close barrier** if significant wind setup development is still possible or if water levels without closure are significantly higher.
Overruled Closure of November 26, 2023	Examines what would have happened if the barrier closed on November 26, 2023.	Water levels at Ramspolbrug and Kadoelen would have been slightly higher during closure.
Necessity Navigation Blockades between +0.40m NAP and +0.50m NAP	Examines when blockades can safely be lifted between water levels of +0.40m NAP and +0.50 m NAP.	Lift blockade if no or minimal further water level increase is predicted, and no or minimal further development of the setup and discharge peaks are predicted. Maintain blockade if the water level increases towards the closure criteria predicted or the wind setup shows significant development potential.
Multiple Peaks	Focuses on the timing of consecutive peaks and how this influences the closure strategy.	For peaks in short succession, earlier closure may decrease peak water levels, but elongate closures. For second peaks during barrier opening, consider late or non-closure for the second peak or non-closure for the first peak, depending on peak characteristics. Avoid elongated closures over both peaks.
Initial water level Ketelmeer above +0.50m NAP	Assesses when a closure is necessary when initial water levels are higher than +0.50m NAP at the Ketelmeer.	The slightest breeze results in closure in this case; therefore, the framework proposed to decide if the closure is safer (needs refinement). Run parallel simulations: do not close when the predicted water level is lower in case of non-closure. Evaluate discharge predictions: closure when time-averaged discharge is negative for at least an hour or reaches -500 m^3/s
Sensitivity to Varying Q_{zw} during Closures	Insights in how the Ramspol Barrier's closure and the water levels in the system are impacted by varying discharges of the Zwarte Water.	Closure timing is minimally impacted by varying discharges. Higher discharges lead to faster water level rise at the Zwarte Meer during closure, earlier barrier openings and longer higher water levels throughout the system.
Sensitivity to Wind Setup when $Q_{spui} = 0$	Insights into the influence of mild winds in the case of no drainage on whether and when critical water levels at the Ramspol Barrier are met for varying wind speeds and initial water levels.	Higher wind speeds lead to earlier exceedance of critical water levels. Higher initial water levels need weaker winds to meet certain thresholds.

6

Discussion

This chapter evaluates the results of calibrating and validating the hydraulic model and the improvement scenarios. It also discusses the underlying assumptions and methods used in the analysis.

6.1. Discussion of the Hydraulic Model

The simplified reservoir model's primary objective was to predict water levels across the IJsselmeer and the IJssel and Vecht Delta and determine the flow direction at the Ramspol Barrier with sufficient accuracy. At the same time, the model needed to be computationally efficient, account for uncertainty in predictions, and remain accessible for users without prior Python knowledge.

The computational efficiency and user-friendliness of the model enable extensive scenario testing during the improvement phase. The model executes within one minute, including uncertainty predictions, making it significantly faster than more complex 1D or 2D models. It requires only initial water levels and forecasts for wind speed, wind direction, and the discharges of the IJssel, Genemuiden, and the drainage over the Afsluitdijk as inputs. Since the model automatically processes and runs as long as this data is formatted according to the structure of files obtained from (Rijkswaterstaat, 2024c), its usability is straightforward. The ease of implementing improvement scenarios is further discussed in section 6.2.

6.1.1. Accuracy of the Hydraulic Model

A key requirement for model robustness is the correct representation of peak water levels, including their timing, height, duration, and rate of development. While minor overestimations of lower water levels are considered acceptable, accuracy during and immediately preceding the operation of the Ramspol Barrier is of primary concern. As demonstrated in the error analysis of the model validation (subsection C.3.1), deviations between modelled and observed water levels show no systematic bias or trend. However, significant discrepancies remain, indicating that the model is imperfect.

As noted in section 4.3, the peaks used for calibration and validation exhibit distinct characteristics. For example, the January 12, 2012, peak (Figure C.1) features a relatively high initial water level of approximately +0.25m NAP, followed by a sharp increase to +0.48m NAP at the Ramspolbrug, before gradually decreasing. The model captures the gradual decline well but overestimates the peak development speed, placing the peak one hour too early and underestimating it by 8 cm. Conversely, the January 22, 2012 peak (Figure C.3) displays different behaviour: the model captures the peak development speed, decline, and height accurately for the Ramspol Barrier, Ramspolbrug, and Kadoelen, yet predicts the peak three hours too early. The December 6, 2024, closure event (Figure 4.6) also reveals discrepancies, with closure criteria being met two hours too early. The model overestimates peak development and decline speeds at the Ketelbrug and Ramspol Barrier but performs well at Kadoelen and slightly underestimates the response on the Zwarte Meer side of the Ramspol Barrier. This discrepancy may be attributed to hydrodynamic processes occurring when the barrier opens. In reality, a significant water level difference across the barrier leads to rapid outflow, accelerating local water level decline. However, the model assumes an equal decline across the Zwarte Meer, simplifying

this process. Despite these inaccuracies, the model correctly predicts the peak height at all locations and effectively captures the closure of the Ramspol Barrier, with a half-hour timing discrepancy at the barrier itself.

A common feature among these peaks is their immediate response to changes in the theoretical wind setup, highlighting a key model limitation. The wind setup is calculated using Equation 4.6, incorporating wind speed, direction, fetch, and depth. The theoretical values fluctuate significantly due to abrupt wind speed and direction changes. This leads to frequent sign changes in wind setup calculations during storms, necessitating model simplification by rounding wind direction to the nearest 15-degree increment. However, this approach can lead to over- or underestimation of wind setup, causing peaks to appear earlier, later, higher, lower, shorter, or longer than observed. This limitation likely contributes to some of the inaccuracies in peak prediction. Additionally, Equation 4.6 uses a cosine function to account for wind direction, resulting in maximum wind setup for northern and southern winds, while potentially underestimating it for westerly and easterly winds. The formula provides a more accurate estimation of wind setup in the IJsselmeer, as its north-south orientation aligns well with the formula's assumptions. However, the wind setup is underestimated for the Ketelmeer and Zwarte Meer, which are oriented west to east. This inaccuracy could be addressed by adjusting the wind direction to its angle relative to the perpendicular axis at each location.

Another issue is the development speed of wind setup, reflected in the calibrated parameters τ_{ij}, τ_{km}, and τ_{zm}, which were determined as $\tau_{ij} = 1155.26$, $\tau_{km} = 11639.31$, and $\tau_{zm} = 251.06$. These values suggest that wind setup on the IJsselmeer develops in approximately 20 minutes, on the Ketelmeer in 3 hours and 15 minutes, and on the Zwarte Meer in 4 minutes. Physically, this is impossible: the Ketelmeer, the smallest lake, requires the most time to develop a setup, while the IJsselmeer, 85 times larger, requires 97 times less time. In reality, larger lakes should exhibit greater inertia, requiring more time to reach equilibrium. This inaccuracy may explain the model's tendency to overestimate wind-driven setup and its development speed at the IJsselmeer while underestimating it at the Ketelmeer, leading to errors in peak height and timing. This suggests that the model and its calibration need refinement in how and how fast the wind setup is captured over the lakes.

6.1.2. Model Simplifications

In addition to the simplification of the wind direction in the calculation of the wind direction as explained in subsection 6.1.1, there are various simplifications made in the model, which have shortcomings that should be discussed. First, as a reservoir model, it assumes constant average water depth in all directions, neglecting bathymetry and using fetch measurements at 5-degree increments with interpolation. While incorporating these features could enhance wind setup accuracy, their influence on overall model performance is likely minimal, whereas their inclusion would significantly increase model complexity.

Additionally, certain hydrological processes are left out. Discharges between the IJsselmeer and Markermeer, contributions from locks and minor streams, and precipitation and evaporation are not explicitly modelled. While their impact on volume balances and water levels is relatively small, incorporating them would yield a more complete model.

The Ramspol Barrier closure process has also been simplified. In reality, closure occurs gradually over one hour, while reopening takes three hours. The model approximates this as an instantaneous closure 30 minutes after meeting closure criteria and an immediate opening two hours after meeting reopening criteria. This simplification likely reduces accuracy in simulating water flow between the Ketelmeer and Zwarte Meer, and thus, the volume-related water level changes in both lakes.

Finally, the flow between the IJsselmeer, Ketelmeer, and Zwarte Meer is modelled using a weir overflow equation based on water level differences. These discharge coefficients were calibrated using data from October 2015 to March 2016. While this calibration ensures no gradual outflow surplus or deficit, it results in larger deviations in water levels of about a metre in periods with varying discharges. Over short-term simulations, these effects remain negligible, but in long-term applications, variations in α_{rp} and α_{kb} could lead to systematic volume imbalances.

Lastly, the discharge of the Zwarte Water and IJssel, as well as the drainage discharge are now based on observations of the discharges or water levels. Including weather scenarios and upstream discharges, to calculate these discharges could improve the predictive nature of the model, but also increase its complexity.

Overall, the simplified reservoir model provides a fast and user-friendly approach to predicting water levels and flow direction in the IJsselmeer and IJssel-Vecht Delta. Its efficiency allows for extensive scenario testing, and despite simplifications in wind setup, bathymetry, and hydrological processes, it captures key trends in water level fluctuations and barrier closures. However, the model's limitations, particularly in wind setup development speed and peak timing accuracy, highlight areas where refinement is needed. A slightly more advanced 1D model could offer a better balance between accuracy, intuitiveness, adaptability, and computational efficiency. By incorporating spatial variations in water levels and flow velocities while remaining significantly faster and more accessible than full hydrodynamic models, such an approach could improve both predictive accuracy and practical usability for operational decision-making.

6.2. Discussion of the Improvements

Is the hydraulic model also easy to use in the improvement phase? As discussed in section 6.1, the model runs efficiently and enables quick predictions. During the improvement phase, it automatically evaluates both closure and non-closure scenarios based on predefined operational criteria. However, testing alternative closure strategies or assessing model sensitivity to varying discharges, as done in subsection 5.2.8 and subsection 5.2.9, still requires manual input modifications. This limits the model's usability in fully automated analyses. While integrating these variations into separate functions could improve flexibility, it would also increase model complexity, making it less accessible to all users.

The presented scenarios represent only a limited set of simulations illustrating practical challenges within the current operational procedure. Although many cases suggest potential improvements, a more accurate hydraulic model is needed to fully assess the consequences of deviating from existing procedures. Given the numerous scenario possibilities—varying initial water levels, discharges from the IJssel and Zwarte Water, wind speed and direction, and drainage capacity over the Afsluitdijk—a more automated optimisation model would be more suitable. However, this approach was deliberately avoided in favour of case-by-case conceptual analysis. An optimisation framework would require assigning weights to different criteria, which falls outside the scope of this study. Determining acceptable water levels or balancing operational efficiency against flood protection is a policy decision rather than a technical one. Nevertheless, such trade-offs should be considered when interpreting the scenario results or before developing an optimisation model. The case-by-case conceptual approach demonstrates that, for example, in multi-case scenarios, a trade-off exists between reducing water levels and operating the barrier, which impacts the shipping industry. These trade-offs must be carefully evaluated before making recommendations or pursuing optimisation-based improvements.

Although the model was used to assess how closure decisions influence water level rise and closure duration, additional methods were employed to gain insights into the role of wind setup and volume changes over time. While not essential for decision-making if predictions are sufficiently accurate, these insights provide valuable information on the underlying processes driving water level fluctuations.

To address prediction uncertainty, Monte Carlo simulations were incorporated, where wind speed, wind direction, and discharges from the IJssel and Zwarte Water were varied by ±20 per cent of the predicted values (based on past observations). The discharge of the IJssel has varied by ±5 per cent. However, uncertainty quantification could be further refined to provide probabilistic assessments, such as the likelihood of meeting closure criteria. Improving uncertainty analysis would enhance the robustness of operational decision-making.

7

Conclusion and Recommendations

This chapter concludes this thesis and gives recommendations for further research and applications.

7.1. Conclusion

The Ramspol Barrier is an integral component of the flood protection system for the Zwarte Meer and its hinterland. However, its current operational procedure faces several challenges that compromise flood safety, increase disruptions for the shipping industry, and significantly burden the operation team. The existing approach follows a fixed protocol: the operation team is activated when water levels exceed +0.20 m NAP, vessel passage is blocked at +0.40 m NAP, and the barrier closes at +0.50 m NAP if there is an inflow from the Ketelmeer toward the Zwarte Meer. This one-size-fits-all strategy has led to situations where the team is mobilised and shipping is disrupted without the barrier ultimately closing. Conversely, the barrier has sometimes been closed when, in retrospect, it was questioned if this was optimal for flood safety within the system.

This thesis, therefore, aimed to improve the Ramspol Barrier's operation procedure by balancing the pressure on the operation team, minimising vessel disruptions, and ensuring flood safety within the IJsselmeer, IJssel, and Vecht Delta water systems. To answer this, a system analysis and data analysis were performed to fully understand the system's dynamics. Additionally, a simplified reservoir model was developed to evaluate the effects of different operational strategies on vessel disruptions, operational workload, and water levels. The research questions guiding this study are addressed below.

1. What are the characteristics of the Ramspol Barrier water system, including its layout, meteorological and hydrological conditions, operation, and flood safety requirements?

The IJsselmeer and IJssel and Vecht Delta water system, in which the Ramspol Barrier operates, is fed by the precipitation-dependent Zwarte Water, which discharges into the Zwarte Meer, and the IJssel, which discharges into the Ketelmeer. Water is drained from the system through the Zwarte Meer, Ketelmeer, and IJsselmeer toward the Wadden Sea via the Stevin Locks in Den Oever and the Lorentz Locks in Kornwerderzand, but only when the water level in the IJsselmeer exceeds that of the Wadden Sea. The initial IJsselmeer water level governs the water levels within the system, wind setup over the IJsselmeer, Ketelmeer, and Zwarte Meer, the discharges from the IJssel, Vecht, and Zwarte Water, the drainage capacity through the Afsluitdijk, and local precipitation.

High-water scenarios in the system typically result from specific meteorological conditions: onshore winds from the North Sea drive precipitation and wind-induced water set up along the coast. High water levels at the Wadden Sea side of the Afsluitdijk can further restrict the drainage of the IJsselmeer. In addition, heavy regional precipitation increases the discharges of the Zwarte Water and IJssel, further elevating water levels. During these events, strong northwesterly winds generate a significant wind setup, pushing water through the funnel-shaped IJsselmeer, Ketelmeer, and Zwarte Meer, leading to a rapid rise in water levels at the Ramspol Barrier. When the water level reaches +0.50 m NAP with an inflow from the Ketelmeer, the barrier is closed to protect the Vecht Delta from flooding and

wind-induced surges. However, closure disrupts navigation and blocks the outflow from the Zwarte Meer to the Ketelmeer, delaying vessel movements and causing water accumulation in the Zwarte Meer.

A cross-correlation analysis of discharges and water levels within the IJsselmeer and IJssel and Vecht Delta water system, with the critical water levels of +0.20 m NAP, +0.40 m NAP, and +0.50 m NAP at the Ramspol Barrier, provided further insight into the primary drivers of water level peaks. The findings indicate that as water levels rise, the influence of IJssel and Zwarte Water discharge diminishes, while the correlation with wind setup intensifies, reaching a peak correlation of 0.90 at closure thresholds. Additionally, the analysis revealed that drainage discharge decreases significantly as system-wide water levels increase.

Further investigation into the frequency of critical water levels at the Ramspol Barrier highlights increasing pressure on the operation team and growing disruptions for the shipping industry. During the analysed period, ship passage was disrupted approximately nine times without the barrier being deployed, and the operation team was activated 51 times without an actual closure during storm conditions. Moreover, substantial variability in the frequency and duration of these critical water levels was observed, emphasizing the need for a more adaptive operational strategy.

2. How can the system be modelled and how will changes in operation procedures of the Ramspol Barrier affect water levels within the system?

A simplified reservoir model was developed to assess how changes in Ramspol Barrier operations affect water levels and compliance with flood safety regulations. The system was schematised as three interconnected basins (IJsselmeer, Ketelmeer, Zwarte Meer), with inflows from the IJssel and Zwarte Water and outflows via the Afsluitdijk sluices. The model accounts for wind-driven and volume-related water level changes and includes immediate closure of the Ramspol Barrier, setting the flow between Ketelmeer and Zwarte Meer to zero. It was calibrated and validated using peak events since 2012, showing variability in peak height, duration, and recession, which are not always accurately captured by the model. Despite its inaccuracies, it was proven to be computationally fast, adaptable to test scenarios, and intuitive to use.

Nine different scenarios were evaluated using the hydraulic model. Some tested the model's predictive capabilities (normal case), while others assessed the system's sensitivity to wind setups and discharges (closure with varying Zwarte Water discharges and sensitivity to wind peaks at high initial water levels). Additional scenarios addressed conditions not covered by current operational criteria (initial water levels above +0.50m NAP and multiple peaks) or past cases that caused operational uncertainties (blockade without closure, closures just exceeding the criteria, and the overruled closure of November 26, 2023).

The effects on the water level during the simulation of these scenarios are as follows:

- **Impact of test closures**: Since they are generally performed in mild conditions, they show little effect on water levels.
- **Peaks just above +0.50m NAP**: closures during receding or stagnating water levels, or when wind setup is already developed, lead to similar or higher water levels than non-closure scenarios. The simulation of the overruled closure on November 26, 2023, confirmed that water levels on the Ketelmeer would have been slightly higher than on the Zwarte Meer, justifying the closure decision.
- **Initial water level above +0.50m NAP**: When the initial water level exceeds +0.50 m NAP, even minor wind events trigger closure criteria. If the wind peak is not prolonged, closures can lead to higher water levels than non-closure scenarios.
- **Impact of Multiple Peaks**: The water levels in this case depend on the predicted peak timing and height. When peaks are close together, insufficient recovery time results in persistently high water levels. An earlier closure before a second peak can help lower Zwarte Meer levels, but extend operational disruptions. If a second peak arrives during reopening, the decision between a late closure or no closure depends on the peak. Prolonged closures should be avoided to prevent unnecessary navigation restrictions and increased water levels.

- **System Sensitivity to Wind at High Initial Water Levels**: at +0.30 m NAP, moderate winds do not exceed closure thresholds, while at +0.50 m NAP, even a 1 m/s breeze triggers closure criteria. Higher wind speeds lead to earlier exceedance of closure thresholds.
- **Effect of Zwarte Water Discharge on Closure**: discharge variations have minimal influence on closure timing but affect post-closure water levels. Higher discharges lead to faster water level rise, earlier reopening, and prolonged elevated water levels due to the increased water volume in the system.

3. How can the operation procedure of the Ramspol Barrier be improved?

Although the hydraulic model has flaws when predicting peaks and is based on a limited number of scenarios, its simulations for the nine scenarios show potential for implementing a scenario-based operation procedure. This procedure could minimise water levels in the system, the burden on the operation team, and blockades for the shipping industry. Additionally, it showed potential to quickly consider various scenarios, thus enabling the possibility of using them during the procedure.

Enhancing the ability to predict critical water levels (+0.20 m NAP, +0.40 m NAP, and +0.50 m NAP), as well as closure and opening criteria, can significantly benefit operational teams and the shipping industry. Implementing 24- to 48-hour forecasts would enhance planning by ensuring teams are on-site when needed, minimizing unnecessary disruptions, predicting the timing and likelihood of Ramspol Barrier closures, and enabling the shipping industry to adjust schedules to reduce waiting times.

In cases where the water level slightly exceeds +0.50m NAP, the following can be recommended:

- If closure does not reduce peak water levels or if wind setup has no further potential to develop, keeping the barrier open could prevent unnecessary disruption and high water levels.
- If significant wind setup is still possible or if water levels would be significantly higher without closure, closing the barrier could help mitigate rising water levels.

In cases where the water level fluctuates between +0.40 and +0.50 m NAP, creating a blockade for vessels but not a closure, the following can be recommended:

- If the prediction and its uncertainty show no further water level increase towards closure criteria and/or if no further wind setup development is possible and there are no significant predicted discharge peaks that could contribute to water level increase, then the navigation blockade could potentially be lifted.
- If model predictions indicate that water levels will continue to rise toward closure criteria, and if the wind setup still has the potential to develop further, allowing for additional water level increases, then the navigation blockade should remain in place.

When initial water levels at the Ramspol Barrier exceed +0.50m NAP, the flow direction becomes the dominant closure criterion, triggering closure by the slightest breeze or flow, sometimes unnecessarily. A more robust approach should base closure on sustained negative flow (-500 m^3/s for at least 60 minutes) rather than momentary fluctuations. Further testing is needed to refine these criteria.

When storm systems cause multiple peaks, closure procedures could be adjusted such that:

- If the second peak arrives before full recovery, earlier closure may reduce flooding but increases disruption.
- If the second peak arrives while reopening, a late closure may allow drainage, but no closure could be an option if the peak is not critical.
- Avoid prolonged closures when possible, as they disrupt navigation and can increase flood risks.

Applying the hydraulic model and scenario-based recommendations to historical high-water events between January 2012 and October 2024 revealed that in four of the 14 closures, keeping the barrier open would have resulted in lower water levels. Additionally, the blockade for the shipping industry could have been reduced or avoided, shortening the total disruption by approximately 280 minutes from the original 610.5 minutes when water levels exceeded +0.40 m NAP. This is illustrated in Figure 7.1.

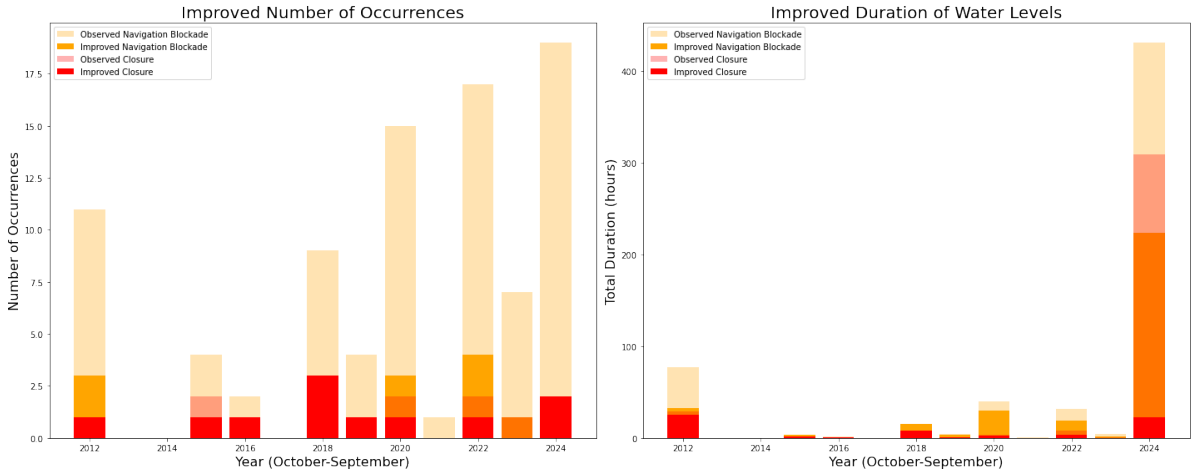

Figure 7.1: Frequency (left) and duration (right) of navigation blockades and closures at the Ramspol Barriers between January 2012 and October 2024 after application of the recommendations.

7.2. Recommendations

This thesis highlights the potential of scenario-based adjustments to operational procedures, combined with a computationally efficient model, to enhance decision-making during operations. However, while promising, these findings are insufficient grounds for immediate implementation. The case-by-case approach used in this study does not address all possible scenarios or balance the trade-offs between minimising vessel disruptions, easing the operational burden, and optimizing flood safety. To further explore the potential of scenario-based operation procedures, the following recommendations are proposed:

First, developing an optimization framework to evaluate scenarios could be the next step. This framework would automatically assess the trade-offs between reducing vessel hindrances and operational burdens and maintaining flood safety for each scenario. Such a system would not only identify the best course of action in a specific scenario but could also run numerous simulations to provide general improvements. However, creating this framework would require quantifying and weighting these factors, vessel disruptions, operational burden, and safety, which would require a comprehensive study.

Second, implementing a slightly more advanced 1D model during operations could provide a better balance between accuracy and practicality. While simple reservoir models allow for quick assessments, they often lack the spatial resolution needed to capture key dynamics, such as wind setup variations across the system. A 1D model, incorporating flow dynamics and spatial differences, would offer improved accuracy while remaining computationally efficient and intuitive for operational use. This approach would enhance decision-making without requiring the complexity and processing time of more detailed hydrodynamic models, making it a viable tool for refining closure strategies in real time.

If both the optimization framework and a computationally fast, accurate model are developed, their results could be structured into a decision-support flowchart for seamless implementation in operational procedures.

Lastly, the findings from scenario-based operation procedures indicate that one-size-fits-all solutions may not always improve flood safety and can place unnecessary strain on the operational team and the shipping industry. Given the rising frequency of closures (as shown in section 3.5), it would be valuable to explore whether scenario-based operation procedures could improve outcomes at other storm surge barriers. Researching this potential could reduce closure frequency by evaluating each storm event individually and determining whether closure is the most optimal response. This approach could help balance flood safety with operational efficiency and minimize disruptions for both the barrier operation and the shipping industry.

References

Deltacommissie. (1961). *Rapport deltacommissie* (Accessed: 2024-10-09). Rijkswaterstaat. https://open.rijkswaterstaat.nl/zoeken/@69428/rapport-deltacommissie/#highlight=deltacommissie

Google Maps. (2024). Google Maps. https://www.google.com/maps

Grevers, W., & Zwaneveld, P. (2011). Een kosteneffectiviteitsanalyse naar de toekomstige inrichting van de afsluitdijk. *Centraal Planbureau*. https://www.cpb.nl

Institute), K. (N. M. (2023). Windgegevens (1.0) [Accessed: 2024-11-05]. https://dataplatform.knmi.nl/dataset/access/windgegevens-1-0

Killick, R., Fearnhead, P., & Eckley, I. A. (2012). Optimal detection of changepoints with a linear computational cost. *Journal of the American Statistical Association*, *107*(500), 1590–1598. https://doi.org/10.1080/01621459.2012.737745

Pfaff-Wagenaar, M., De Gruiter, M., Alphanaar, K., & Boer, S. (2016, October). Impactanalyse ijsselvechtdelta; inventarisatie en systeembeschrijving (be)dreigende hoogwatersituaties. *Rijkswaterstaat*.

Rijksoverheid. (2015). Water act (waterwet). https://wetten.overheid.nl/BWBR0025458/2015-07-01#BijlageI

Rijksoverheid. (2024). Maatregelen tegen overstromingen [Accessed: 16-12-2024]. https://www.rijksoverheid.nl/onderwerpen/water/maatregelen-tegen-overstromingen

Rijkswaterstaat. (2022). Stormvloedkering ramspol gesloten op donderdag 17 februari 2022 rond 06:00 uur [Accessed: 2025-02-18]. https://www.rijkswaterstaat.nl/nieuws/archief/2022/02/stormvloedkering-ramspol-donderdagochtend-17-februari-rond-0600-uur-gesloten

Rijkswaterstaat. (2023, July). Operationeel watermanagement ijsselmeergebied.

Rijkswaterstaat. (2024a). Stormvloedkering ramspol [Accessed: 2024-09-18].

Rijkswaterstaat. (2024b). Stormvloedkering Ramspol sluit vrijdagochtend 6 december 2024 [Accessed: 2025-02-19]. https://www.rijkswaterstaat.nl/nieuws/archief/2024/12/stormvloedkering-ramspol-sluit-vrijdagochtend-6-december-2024#:~:text=Vanwege%20forse%20wind%20en%20hoog,uur%20tot%20in%20de%20namiddag.

Rijkswaterstaat. (2024c). Waterbeheer: Waterinfo [Accessed: 2024-10-09].

Rijkswaterstaat. (2024d, July). Normaal amsterdams peil (nap) [Accessed: 2024-09-29].

Rijkswaterstaat. (2024e, September). Ijsselmeer: Zoetwatervoorraad op peil - doelen en resultaten. https://www.rijkswaterstaat.nl/water/projectenoverzicht/ijsselmeer-zoetwatervoorraad-op-peil/doelen-en-resultaten

Slootjes, N., & van der Most, H. (2016). Achtergronden bij de normering van de primaire waterkeringen in nederland: Hoofdrapport. *Ministerie van Infrastructuur en Milieu, Directie Ruimte en Water*. https://www.helpdeskwater.nl

van Infrastructuur en Waterstaat, M. (n.d.). Norms and standards for flood defences. https://waterveiligheidsportaal.nl/nss/norm

van Vossen, B., Swinkels, C. M., Wichman, B. G. H. M., Dionisio Pires, L. M., & van Meurs, G. A. M. (2010). *Toekomst afsluitdijk: Antwoorden op vijf onderzoeksvragen* (Technical Report No. 1201757-000-GEO-0017) (Versie definitief, 5 maart 2010). Deltares. Delft, Netherlands.

van den Brink, H. W., & de Goederen, S. (2017). Recurrence intervals for the closure of the dutch maeslant surge barrier. *Ocean Science*, *13*, 691–701. https://doi.org/10.5194/os-13-691-2017

Vergouwe, R. (2014). *De veiligheid van nederland in kaart: Eindrapportage vnk* (Eindverslag No. HB2540621). Ministerie van Infrastructuur en Milieu.

A

Overview Measurements

A.1. Data Cleaning Method

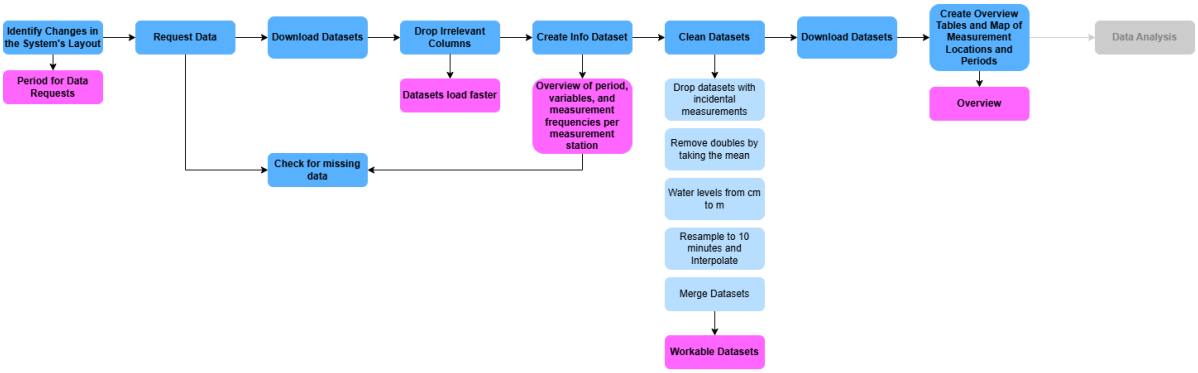

Figure A.1: Flowchart of the data acquisition.

A.2. Discharge

Table A.1: Overview of the possibly relevant measurement station for the discharge.

Measurement Station	Start Period	End Period	Frequency
Den Oever buiten	01-01-2012	31-12-2022	10 minutes
Kornwederzand buiten	01-01-2012	31-12-2022	10 minutes
Houtrib noord	01-01-1979 01-01-2012	31-12-1999 31-12-2022	1 day 10 minutes
Krabbersgat noord	01-01-1979 01-01-2012	31-12-1999 31-12-2022	1 day 10 minutes
Genemuiden/Genemuiden de Ketting	04-11-2009	01-01-2023	10 minutes
Meppelerdiep	01-11-2001 26-11-2013	25-11-2013 20-10-2024	1 hour 10 minutes
Olst	01-01-2024	20-10-2024	10 minutes

A.3. Wind Speed and Direction

Table A.2: Overview of the analysed measurement stations for the wind speed and direction, and their observation periods.

Measurement station	Start period	End period	Frequency
Houtribdijk	01-01-2006	20-10-2024	10 minutes
Marknesse	01-04-2003	20-10-2024	10 minutes
Stavoren	01-04-2003	20-10-2024	10 minutes
Vlieland	01-01-2004	20-10-2024	10 minutes

A.4. Water Level

Table A.3: Overview of the analysed water level measurement stations, and their observation periods.

Measurement Station	Start Period	End Period	Frequency
Den Oever binnen	07-07-1988	20-10-2024	10 minutes
Den Oever buiten	01-01-1989	20-10-2024	10 minutes
Deventer	01-01-1969	25-11-1996	1 day
	26-11-1996	25-11-2013	1 hour
	26-11-2013	20-10-2024	10 minutes
Genemuiden/Genemuiden de Ketting	04-11-2009	20-10-2024	10 minutes
Houtrib noord	05-02-1989	20-10-2024	10 minutes
Houtrib zuid	15-10-1992	20-10-2024	10 minutes
Kadoelen	01-01-1990	20-10-2024	10 minutes
Kampen/Kampen Bovenhaven	01-01-1969	31-12-1979	1 day
	01-01-1981	25-11-2013	1 hour
	26-11-2013	20-10-2024	10 minutes
Kamperhoek	01-01-2024	20-10-2024	10 minutes
Katerveer	01-01-1969	31-12-1980	1 day
	01-01-1981	25-11-2013	1 hour
	26-11-2013	20-10-2024	10 minutes
Keteldiep	01-01-1971	18-01-2008	1 day
	19-01-2008	20-10-2024	10 minutes
Ketelmeer west	20-03-2001	31-12-2023	10 minutes
Ketelmond	31-01-2020	31-12-2023	10 minutes
Kornwederzand binnen	01-01-1989	20-10-2024	10 minutes
Kornwederzand buiten	01-01-1989	20-10-2024	10 minutes
Krabbersgat noord	20-03-2001	20-10-2024	10 minutes
Krabbersgat zuid	13-10-1992	20-10-2024	10 minutes
Lemmer	01-01-1990	20-10-2024	10 minutes
Mond der Vecht	06-04-1995	20-10-2024	10 minutes
Olst	01-01-2024	20-10-2024	10 minutes
Ramspol Ketelmeer	01-01-2024	10-09-2024	10 minutes
Ramspolbrug	06-08-1990	20-10-2024	10 minutes
Spooldersluis binnen	01-01-1969	30-4-1994	1 day
	06-04-1995	15-11-2013	1 hour
	26-11-2013	20-10-2024	10 minutes
Vechterweerd beneden	01-01-1969	31-12-1986	1 day
	01-01-1989	25-11-2013	1 hour
	26-11-2013	20-10-2024	10 minutes
Wijhe	01-01-1969	04-07-2006	1 day
	05-07-2006	25-11-2013	1 hour
	26-11-2013	20-10-2024	10 minutes
Zwartsluis buiten	01-01-1969	31-12-1982	1 day
	01-01-1983	19-01-1984	1 hour
	20-01-1984	05-04-1995	1 day
	06-04-1995	25-11-2013	1 hour
	26-11-2013	20-10-2024	10 minutes

A.5. Water Flow Speed and Direction

Table A.4: Overview of the analysed measurement stations for the water flow velocity, and their observation periods.

Measurement station	Start period	End period	Frequency
Genemuiden	01-01-2024	20-10-2024	10 minutes
Ramspolkering	24-11-2023 21-12-2023 02-01-2024	27-11-2023 28-12-2023 04-01-2024	1 minute

A.6. Overview of Observed Trends in the Data

Excludes WL_{olst} and $WL_{rp,km}$ since it only contains the observations for 2024.

Table A.5: Overview of the observed, seasonal, and peak trends, and trend breaks for all variables.

Variable	Trend	Trend Summer	Trend Winter	Trend Nr. Peaks	Observed Trend Breaks
Q_{do}	None, p=0.59	None, p=0.76	None p=1.0	None, p=0.81	None
$Q_{Genemuiden}$	None, p=0.59	None, p=0.76	None, p=62	None, p=46	None
$Q_{Houtrib}$	None, p=0.39	None, p=0.24	None, p=0.14	None, p=0.48	None
Q_{Olst}	None, p=0.17	None, p=0.12	None, p=0.25	None, p=0.06	None
$Q_{Krabbersgat}$	None, p=0.88	None, p=0.24	None, p=0.41	None, p=0.19	None
Q_{kwz}	None, p=0.72	None, p=1.00	None, p=0.75	None, p=0.81	None
$WL_{Deventer}$	None, p=0.14	None, p=0.99	None, p=0.20	None, p=0.49	None
$WL_{do,binnen}$	Decreasing, p=0.01	None, p=0.70	None, p=0.38	None, p=0.20	None
$WL_{do,buiten}$	Increasing, p=0.00	None, p=0.03	Increasing, p=0.03	Increasing, p=0.00	None
$WL_{Genemuiden}$	None, p=0.69	None, p=0.052	None, p=0.08	None, p=0.61	None
$WL_{Houtrib,noord}$	Decreasing, p=0.00	None, p=0.76	None, p=0.38	None, p=0.12	None
$WL_{Kadoelen}$	Decreasing, p=0.00	None, p=0.13	None, p=0.08	Decreasing, p=0.00	None
WL_{Kampen}	Decreasing, p=0.00	None, p=0.11	None, p=0.15	None, p=0.13	None
$WL_{Katerveer}$	None, p=0.08	None, p=0.84	None, p=0.06	None, p=0.30	None
$WL_{Ketelbrug}$	None, p=0.45	None, p=0.07	None, p=0.12	None, p=0.87	None
$WL_{Keteldiep}$	Decreasing, p=0.00	None, p=0.56	Increasing, p=0.01	Increasing, p=0.00	None
$WL_{Krabbersgat,noord}$	None, p=1.00	None, p=0.10	Increasing, p=0.01	None, p=0.29	None
$WL_{kwz,binnen}$	None, p=0.99	None, p=0.76	None, p=0.57	None, p=0.31	None
$WL_{kwz,buiten}$	Increasing, p=0.00	Increasing, p=0.01	Increasing, p=0.02	None, p=0.27	None
WL_{Lemmer}	None, p=0.44	None, p=0.95	None, p=0.32	None, p=0.41	None
$WL_{MondderVecht}$	Decreasing, p=0.01	None, p=0.76	None, p=0.53	None, p=0.19	None
$WL_{Ramspolbrug}$	Decreasing, p=0.04	None, p=0.95	None, p=0.41	Decreasing, p=0.00	None
$WL_{Vechterweerd,beneden}$	None, p=0.23	None, p=0.21	None, p=0.41	None, p=0.85	None
WL_{Wijhe}	None, p=0.08	None, p=0.73	None, p=0.06	None, p=0.49	None
$WL_{Zwartsluis,buiten}$	None, p=0.82	None, p=0.33	Increasing, p=0.01	Increasing, p=0.02	
$WS_{Houtrib}$	Decreasing, p=0.01	None, p=0.82	None, p=0.26	None, p=0.18	

B

Overview of Fetches and Depths IJsselmeer, Ketelmeer, and Zwarte Meer

Table B.1: Overview of the average observed water levels of the IJsselmeer, Ketelmeer and Zwarte Meer in the summer and winter.

	IJsselmeer	**Ketelmeer**	**Zwarte Meer**
Average Summer Water Level [m NAP]	-0.18	-0.17	-0.17
Average Winter Water Level [m NAP]	-0.26	-0.24	-0.23

Table B.2: Overview of the fetches and average bottom depths of the IJsselmeer, Ketelmeer and Zwarte Meer at 5-degree increments.

Angle {[}∘{]}	F IJsselmeer {[}m{]}	F Ketelmeer {[}m{]}	F Zwarte Meer {[}m{]}	davg IJsselmeer {[}m NAP{]}	davg Ketelmeer {[}m NAP{]}	davg Zwarte Meer {[}m NAP{]}
0	1135	220	900	-4,5	-3,5	-3
5	980	230	815	-4,5	-3,5	-3
10	785	245	725	-4,5	-3,5	-3
15	720	255	680	-4,5	-3,5	-3
20	665	270	650	-4,5	-3,5	-3
25	630	295	650	-4,5	-3,5	-3
30	590	300	665	-4,5	-3,5	-3
35	310	340	600	-4,5	-3,5	-3
40	280	400	625	-4,5	-3,5	-3
45	280	450	625	-4,5	-3,5	-3
50	280	530	615	-4,5	-3,5	-3
55	300	735	600	-4,5	-3,5	-3
60	565	1030	590	-4,5	-3,5	-3
65	585	1790	600	-4,5	-3,5	-3
70	615	7060	615	-4,5	-3,5	-3
75	670	12000	600	-4,5	-3,5	-3
80	735	1145	485	-4,5	-3,5	-3
85	870	735	470	-4,5	-3,5	-3
90	13000	530	390	-4,5	-3,5	-3
95	10500	400	550	-4,5	-3,5	-3
100	6230	350	1065	-4,5	-3,5	-3
105	6070	295	1315	-4,5	-3,5	-3
110	6415	280	680	-4,5	-3,5	-3
115	7970	250	615	-4,5	-3,5	-3
120	5550	240	525	-4,5	-3,5	-3
125	4300	225	440	-4,5	-3,5	-3
130	3515	205	295	-4,5	-3,5	-3
135	3010	200	235	-4,5	-3,5	-3
140	2610	190	195	-4,5	-3,5	-3
145	2350	185	180	-4,5	-3,5	-3
150	2145	190	165	-4,5	-3,5	-3
155	1990	175	145	-4,5	-3,5	-3
160	1800	145	135	-4,5	-3,5	-3
165	1650	150	125	-4,5	-3,5	-3
170	1415	205	125	-4,5	-3,5	-3
175	1230	230	115	-4,5	-3,5	-3
180	1085	275	110	-4,5	-3,5	-3
185	980	545	105	-4,5	-3,5	-3
190	900	530	105	-4,5	-3,5	-3
195	830	570	105	-4,5	-3,5	-3
200	780	680	100	-4,5	-3,5	-3
205	730	2030	100	-4,5	-3,5	-3
210	730	1900	100	-4,5	-3,5	-3
215	690	730	100	-4,5	-3,5	-3
220	660	670	100	-4,5	-3,5	-3
225	340	750	170	-4,5	-3,5	-3
230	340	855	2130	-4,5	-3,5	-3
235	1450	980	2130	-4,5	-3,5	-3
240	1955	1110	3350	-4,5	-3,5	-3
245	2980	1260	3690	-4,5	-3,5	-3
250	12900	1970	7340	-4,5	-3,5	-3
255	12820	2100	12000	-4,5	-3,5	-3
260	12960	5940	7580	-4,5	-3,5	-3
265	13400	13070	4730	-4,5	-3,5	-3
270	14100	13300	3440	-4,5	-3,5	-3
275	14940	790	3080	-4,5	-3,5	-3
280	16120	480	2945	-4,5	-3,5	-3
285	17680	405	2845	-4,5	-3,5	-3
290	20275	350	2775	-4,5	-3,5	-3
295	25700	310	2735	-4,5	-3,5	-3
300	28316	285	2710	-4,5	-3,5	-3
305	43850	270	2710	-4,5	-3,5	-3
310	51200	250	2740	-4,5	-3,5	-3
315	53700	235	825	-4,5	-3,5	-3
320	53700	230	725	-4,5	-3,5	-3
325	53900	220	645	-4,5	-3,5	-3
330	5460	215	540	-4,5	-3,5	-3
335	3750	215	505	-4,5	-3,5	-3
340	2705	190	505	-4,5	-3,5	-3
345	1910	190	510	-4,5	-3,5	-3
350	1515	220	530	-4,5	-3,5	-3
355	1245	225	530	-4,5	-3,5	-3

C

Results of the Calibration and Validation of the Hydraulic Model

C.1. Calibration Results of τ_{ij}, τ_{km}, and τ_{zm}

2019: wind data not available, so not possible to correctly model peaks. Therefore, these closures are not used for the calibration.

Table C.1: Overview of the calibrated parameters for the wind setup per peak date.

Peak Date	τ_{ij}	τ_{km}	τ_{zm}
January 5, 2012	2472.60	19112.01	313.92
January 12, 2012	560.40	25583.02	312.66
January 22, 2012	6217.04	7722.21	288.21
March 31, 2015	371.03	62560.33	408.84
November 17, 2015	1265.40	13160.55	297.37
January 3, 2018	1618.27	10738.17	160.80
January 5, 2018	1732.84	10376.49	6146.79
January 18, 2018	478.50	489.64	297.49
March 11, 2019	N/A	N/A	N/A
March 14, 2019	N/A	N/A	N/A
February 23, 2020	352.70	4243.30	3793.92
March 12, 2020	1496.03	25940.85	1133.72
February 17, 2022	512.00	48739.36	297.07
February 18, 2022	3499.45	9766.01	300.81
January 15, 2023	418.58	10211.01	2339.38
December 21, 2023	402.62	707.90	300.65
January 24, 2024	9921.31	2071.16	951.84
January 26, 2024	279.34	31194.85	300.44
February 23, 2024	322.47	6511.14	296.53
Average	1155.26	11639.31	335.10

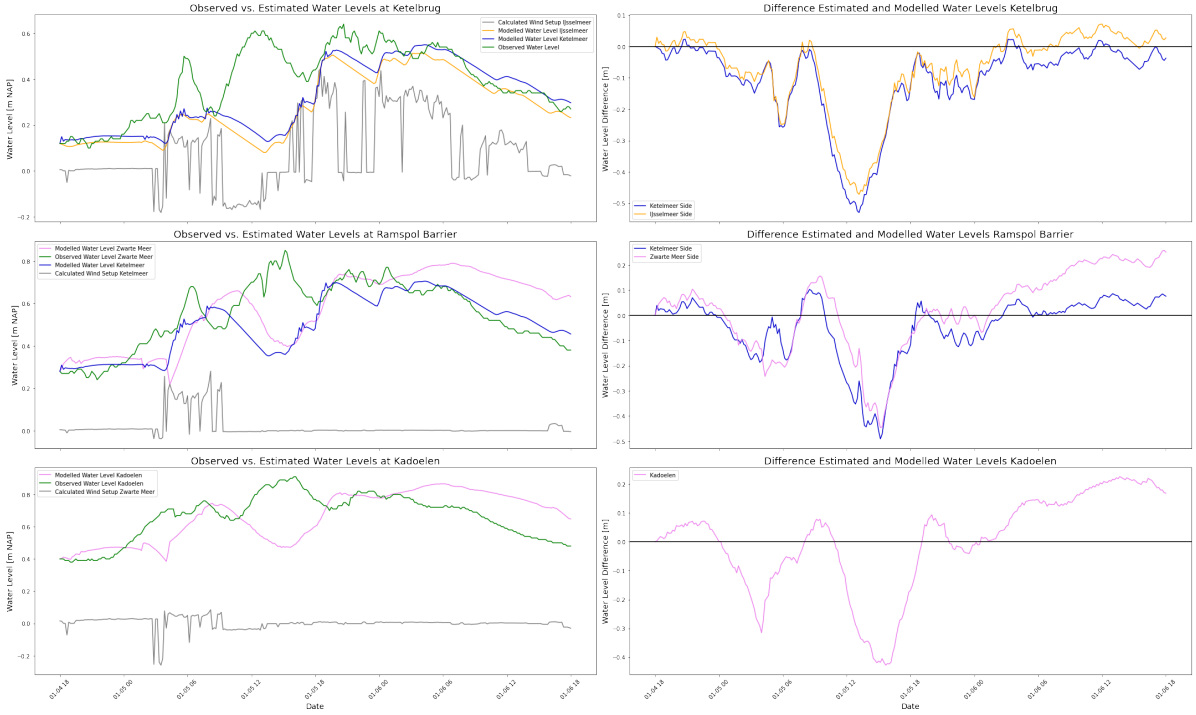

Figure C.1: Calibration results of the closure of January 5, 2012 with τ_{ij} = 2472.60, τ_{km} = 19112.01, and τ_{zm} = 313.92.

Figure C.2: Calibration results of the peak of January 12, 2012 with τ_{ij} = 560.40, τ_{km} = 25583.02, and τ_{zm} = 312.66.

Figure C.3: Calibration results of the peak of January 22, 2012 with $\tau_{ij} = 6217.04$, $\tau_{km} = 7722.21$, and $\tau_{zm} = 288.12$.

Figure C.4: Calibration results of the closure of March 15, 2015 with $\tau_{ij} = 371.03$, $\tau_{km} = 62560.33$, and $\tau_{zm} = 408.84$.

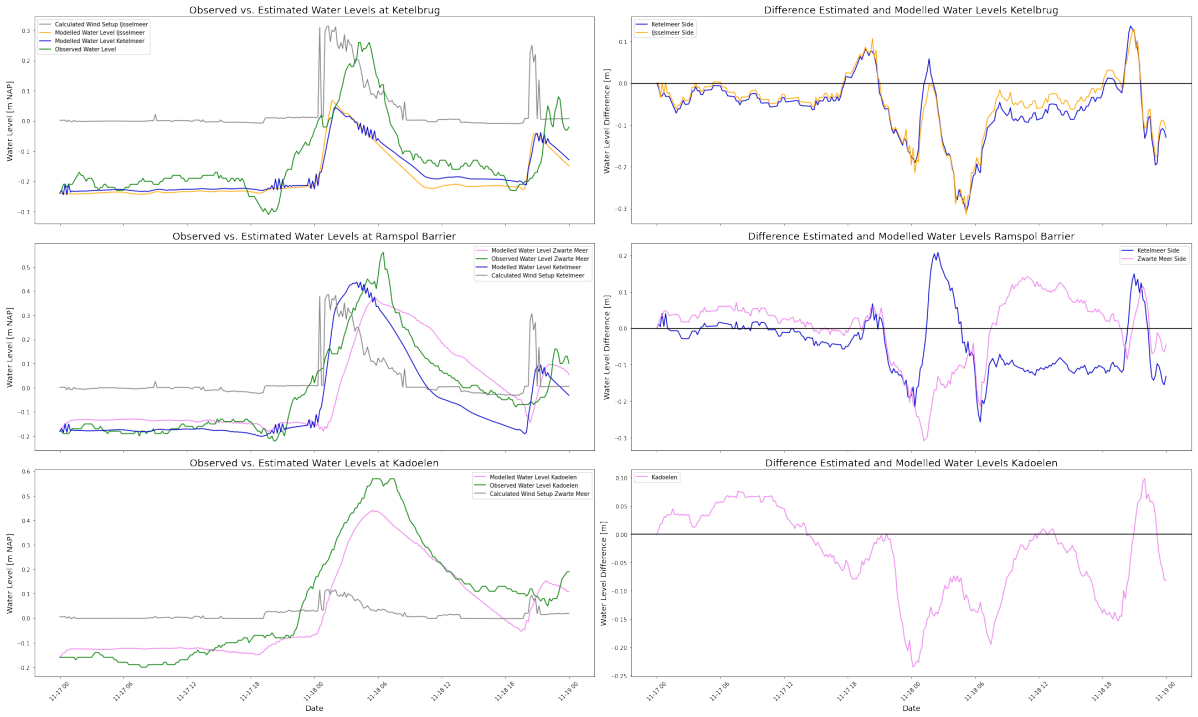

Figure C.5: Calibration results of the closure of November 17, 2015 with $\tau_{ij} = 1265.40$, $\tau_{km} = 13160.55$, and $\tau_{zm} = 297.37$.

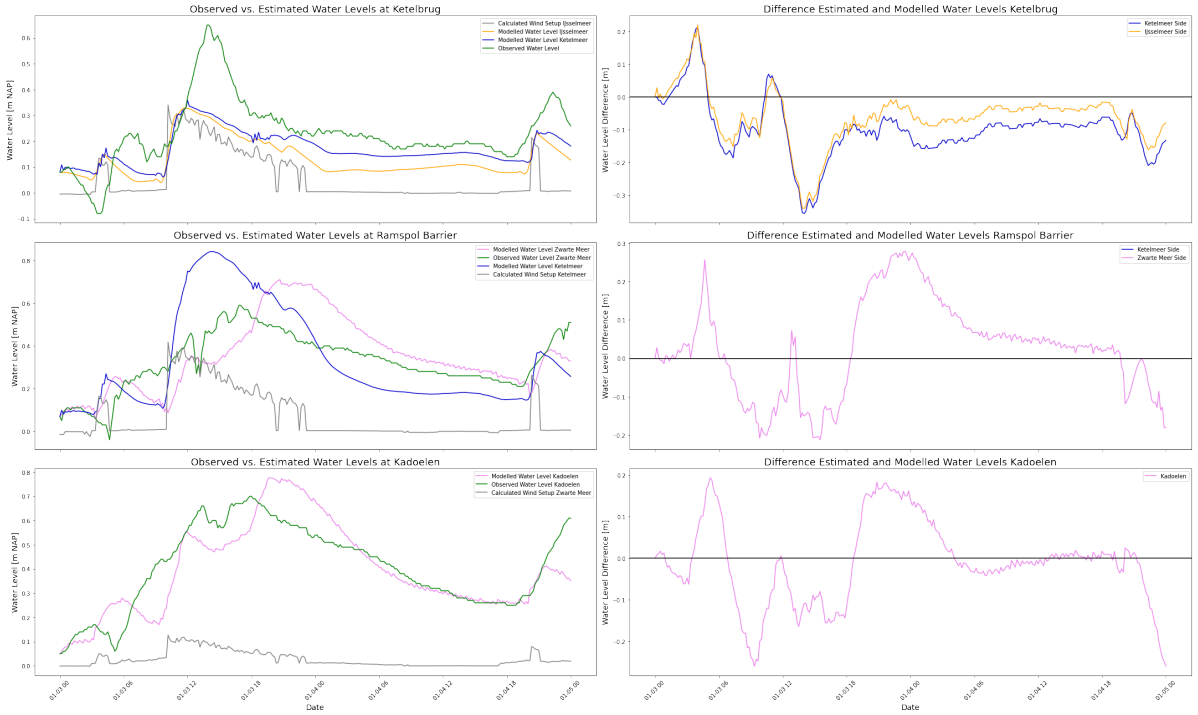

Figure C.6: Calibration results of the closure of January 3, 2018 with $\tau_{ij} = 1618.27$, $\tau_{km} = 10738.17$, and $\tau_{zm} = 160.80$.

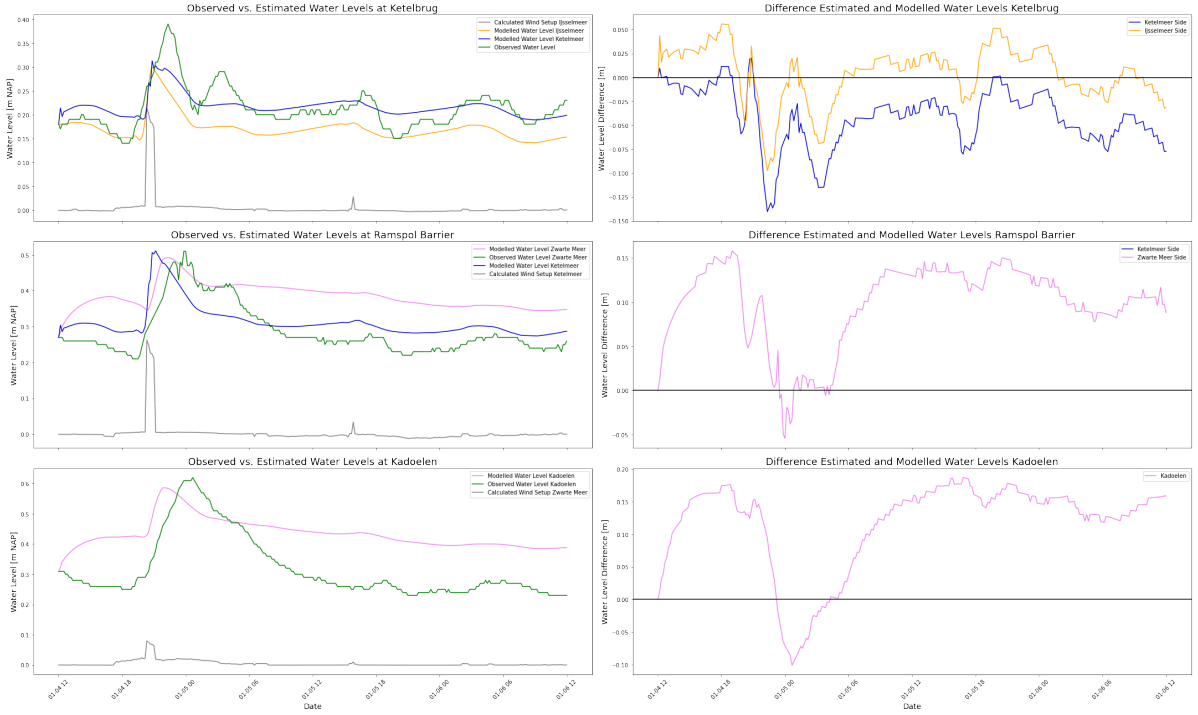

Figure C.7: Calibration results of the closure of January 5, 2018 with $\tau_{ij} = 1732.84$, $\tau_{km} = 10376.49$, and $\tau_{zm} = 6146.79$.

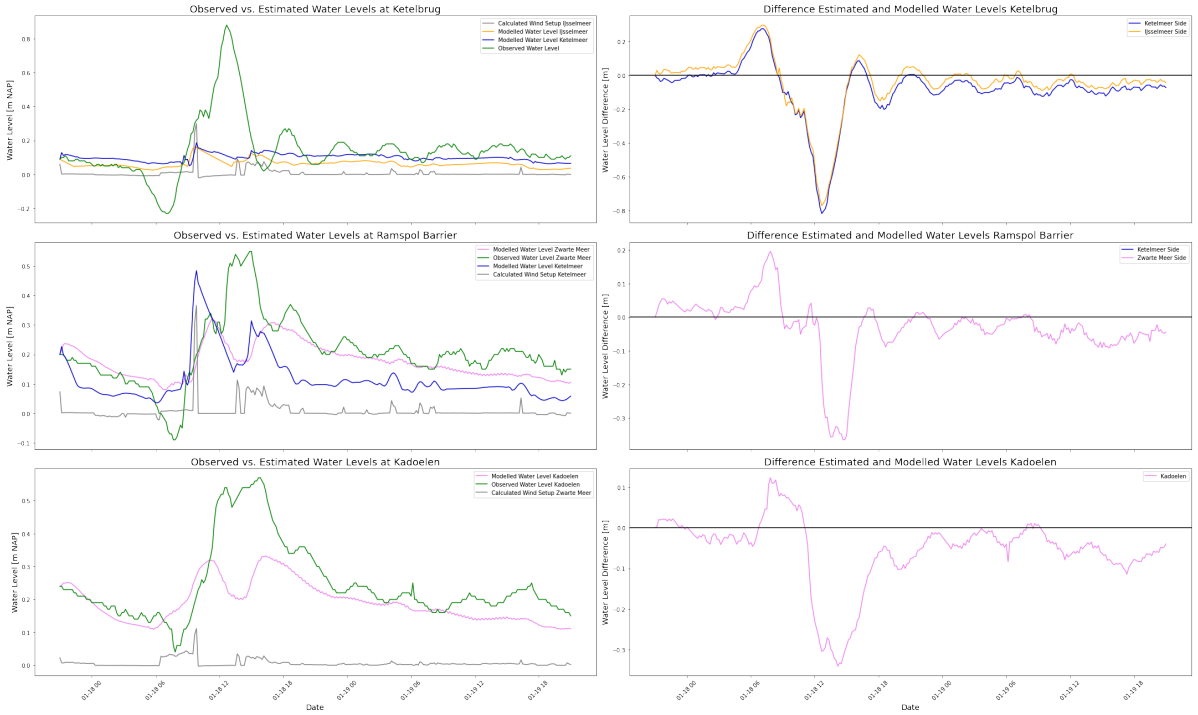

Figure C.8: Calibration results of the peak of January 18, 2018 with $\tau_{ij} = 478.50$, $\tau_{km} = 489.64$, and $\tau_{zm} = 297.49$.

Figure C.9: Calibration results of the closure of February 23, 2020 with $\tau_{ij} = 352.70$, $\tau_{km} = 4243.30$, and $\tau_{zm} = 3793.92$.

Figure C.10: Calibration results of the closure of March 12, 2020 with $\tau_{ij} = 1496.03$, $\tau_{km} = 25940.85$, and $\tau_{zm} = 1133.72$.

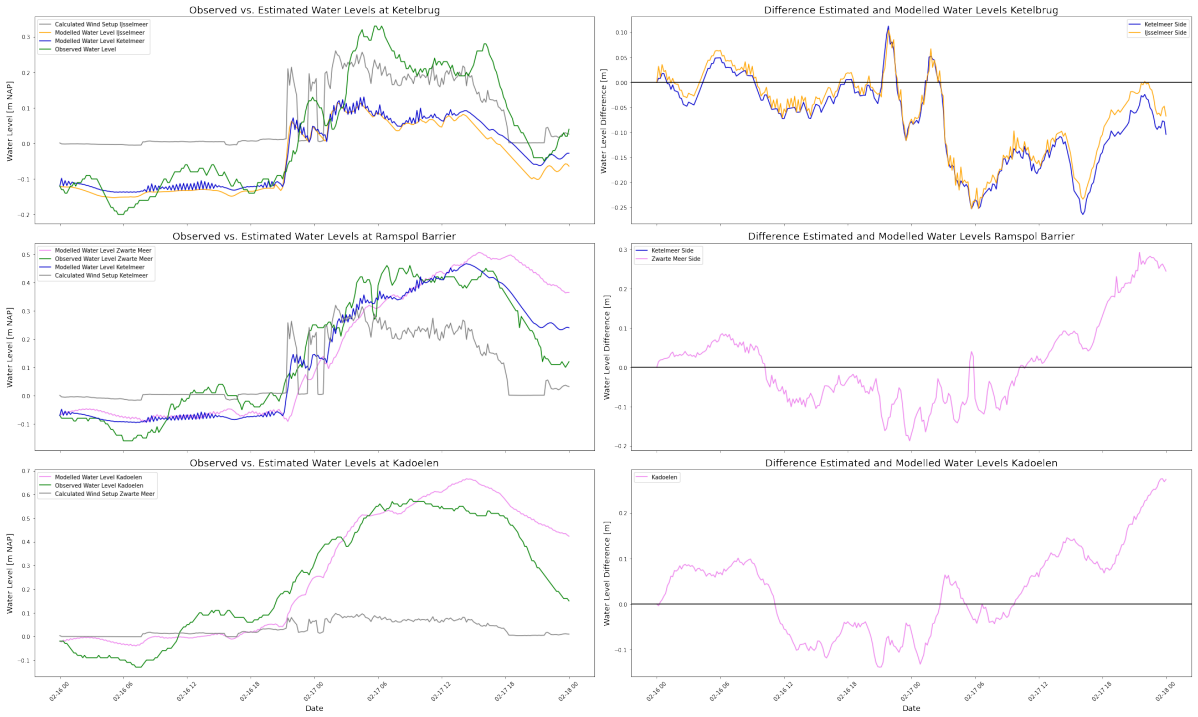

Figure C.11: Calibration results of the closure of February 17, 2022 with $\tau_{ij} = 512.00$, $\tau_{km} = 48739.36$, and $\tau_{zm} = 297.07$.

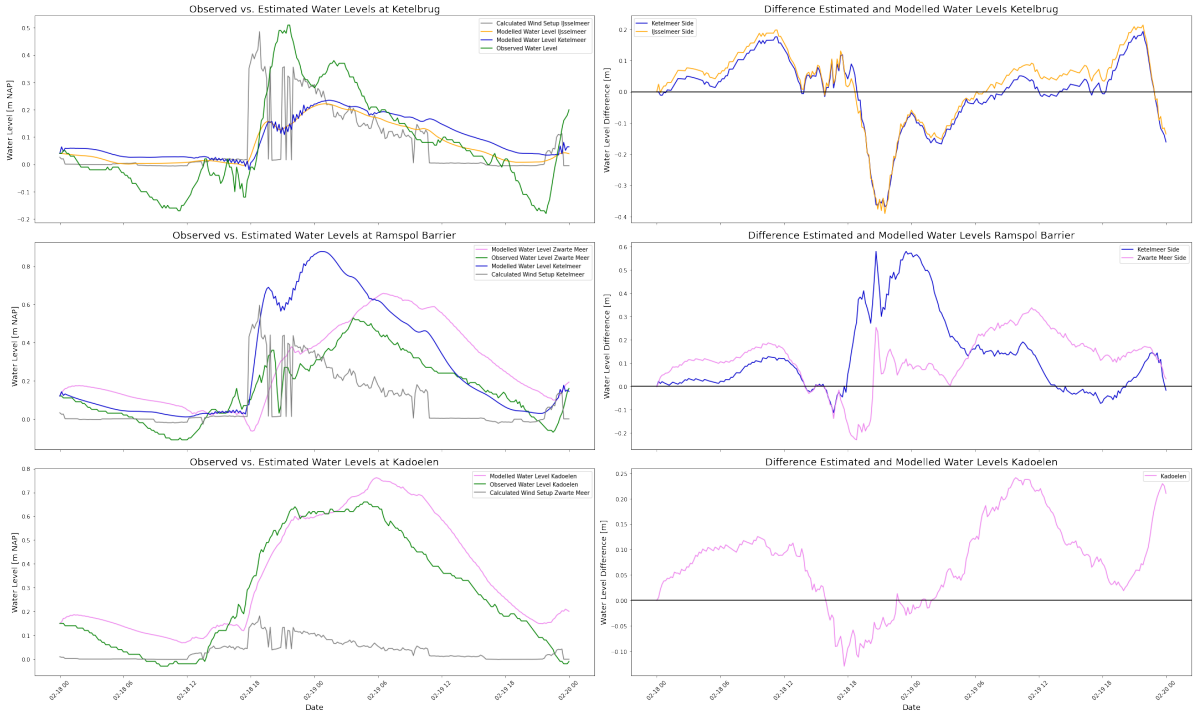

Figure C.12: Calibration results of the closure of February 18, 2022 with $\tau_{ij} = 3499.45$, $\tau_{km} = 9766.01$, and $\tau_{zm} = 300.81$.

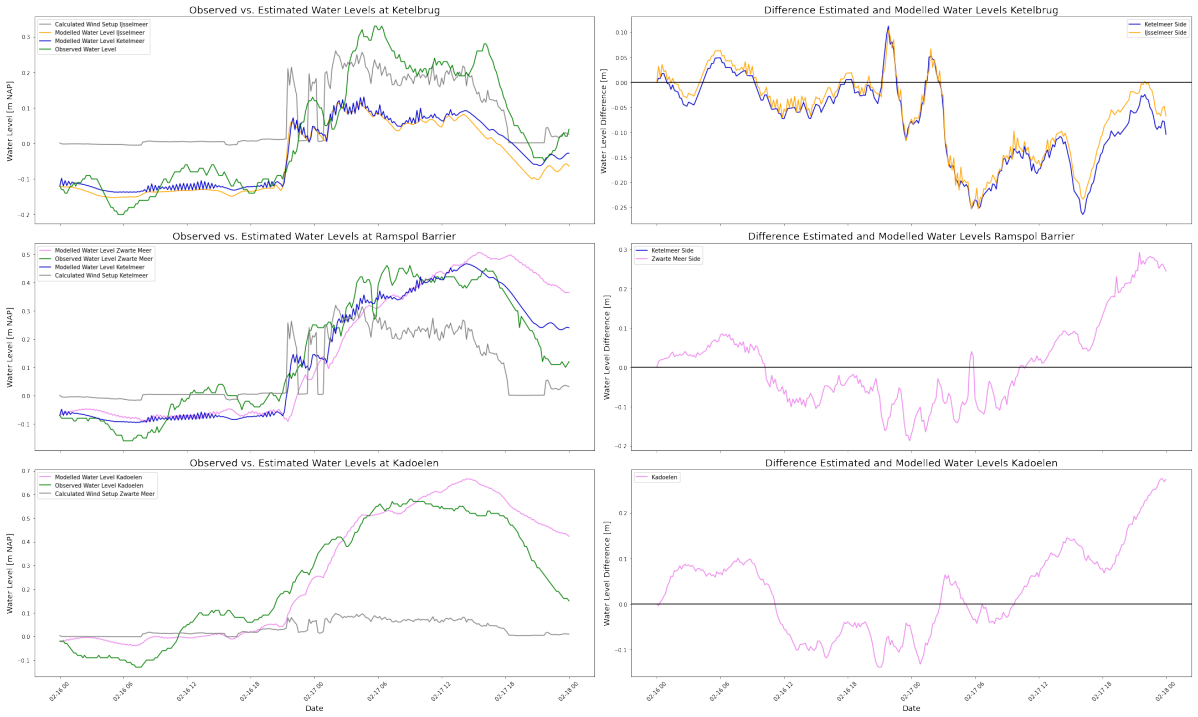

Figure C.13: Calibration results of the closure of February 17, 2022 with $\tau_{ij} = 512.00$, $\tau_{km} = 48739.36$, and $\tau_{zm} = 297.07$.

Figure C.14: Calibration results of the closure of January 15, 2023 with $\tau_{ij} = 418.58$, $\tau_{km} = 10211.01$, and $\tau_{zm} = 2339.38$.

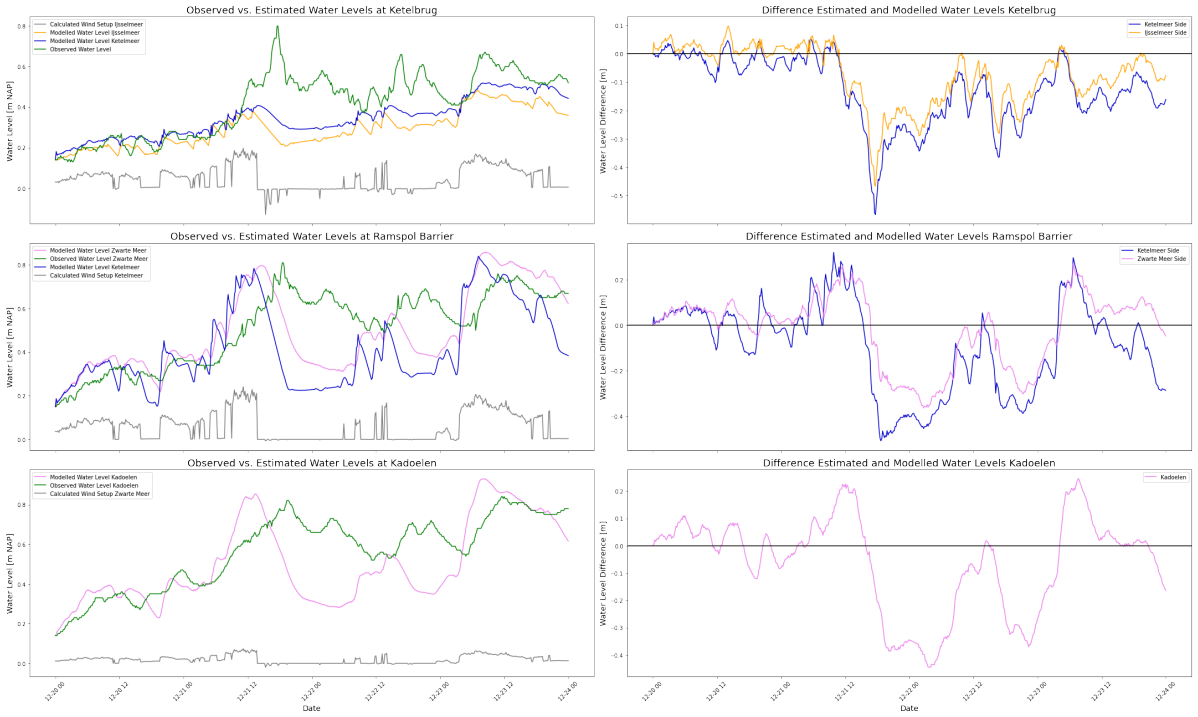

Figure C.15: Calibration results of the closure of December 21, 2023 with $\tau_{ij} = 402.62$, $\tau_{km} = 707.90$, and $\tau_{zm} = 300.65$.

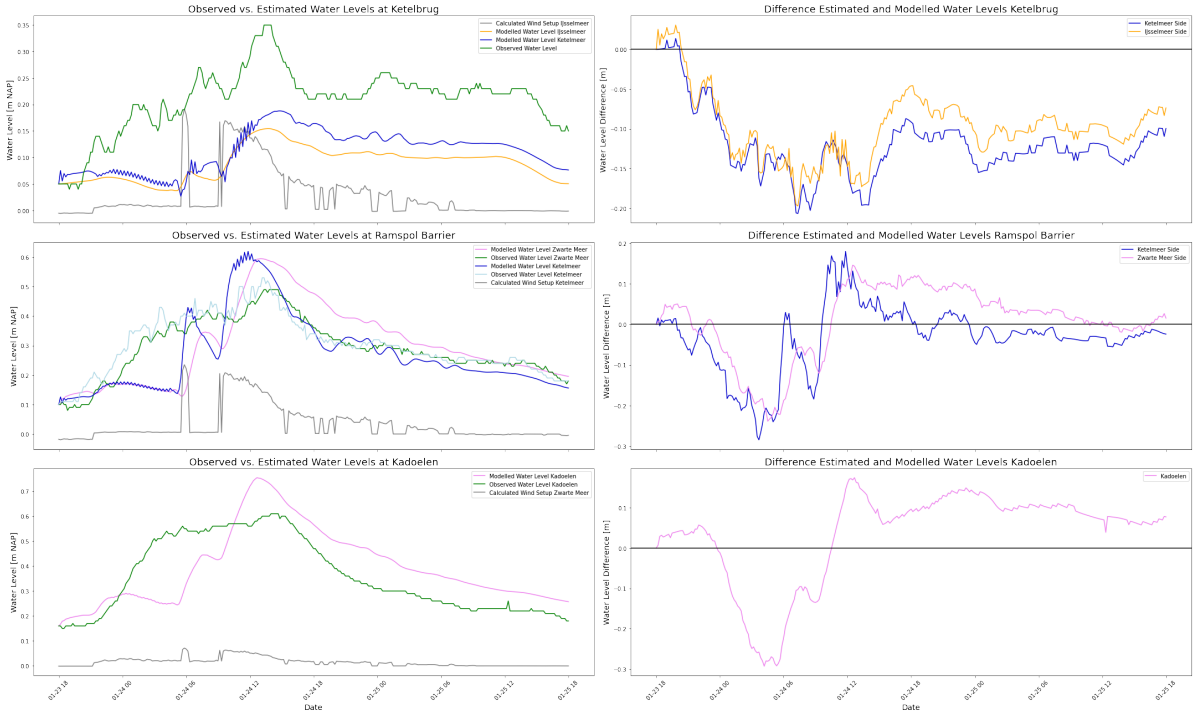

Figure C.16: Calibration results of the peak of January 24, 2024 with $\tau_{ij} = 9921.31$, $\tau_{km} = 2071.16$, and $\tau_{zm} = 951.84$.

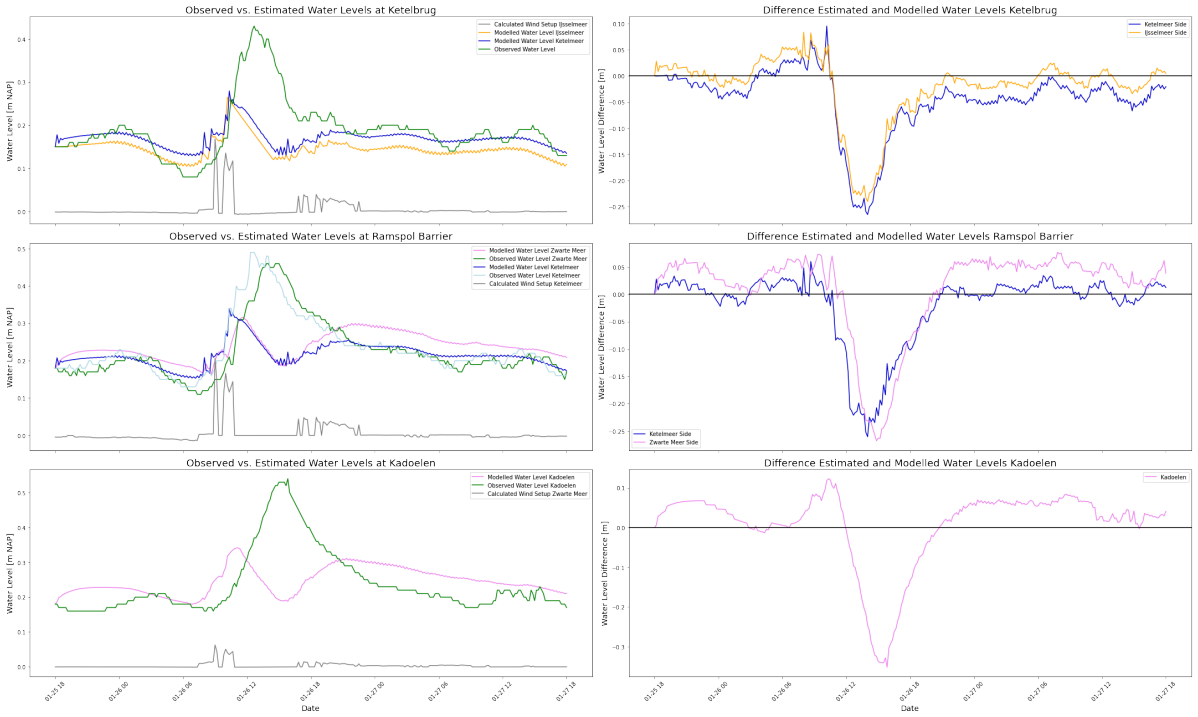

Figure C.17: Calibration results of the peak of January 26, 2024 with $\tau_{ij} = 279.34$, $\tau_{km} = 31194.85$, and $\tau_{zm} = 300.44$.

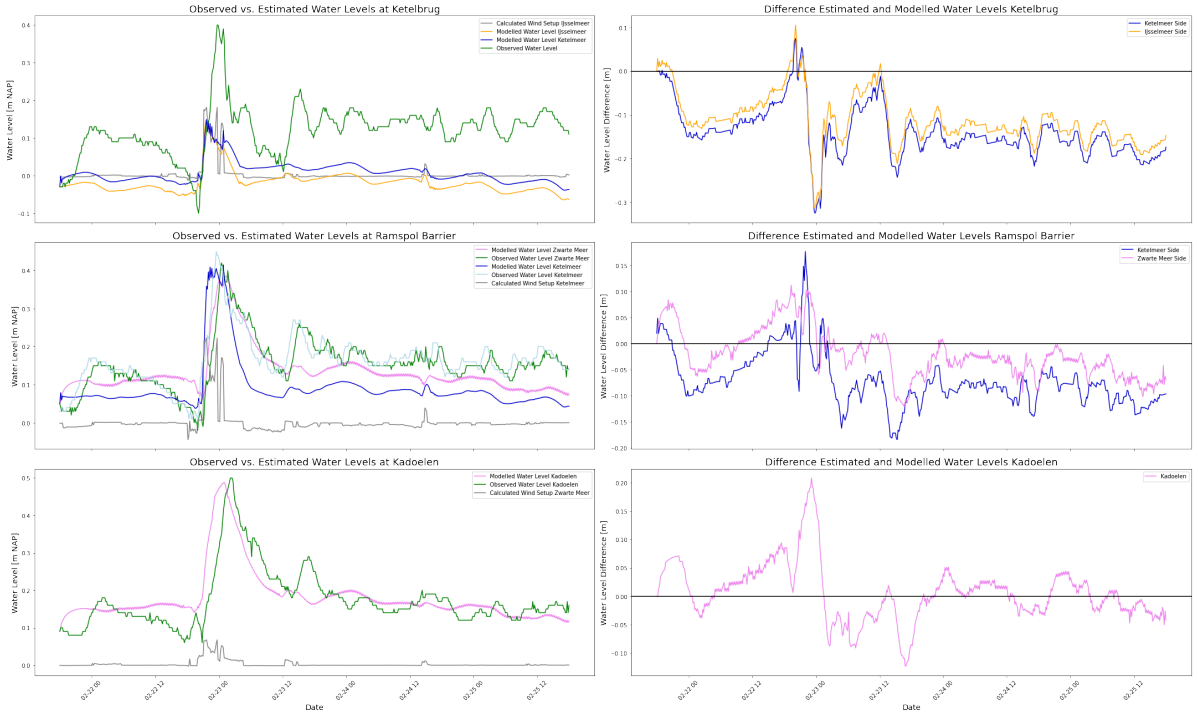

Figure C.18: Calibration results of the peak of February 23, 2024 with $\tau_{ij} = 322.47$, $\tau_{km} = 6511.14$, and $\tau_{zm} = 296.53$.

C.2. Calibration Results of a, b, and c

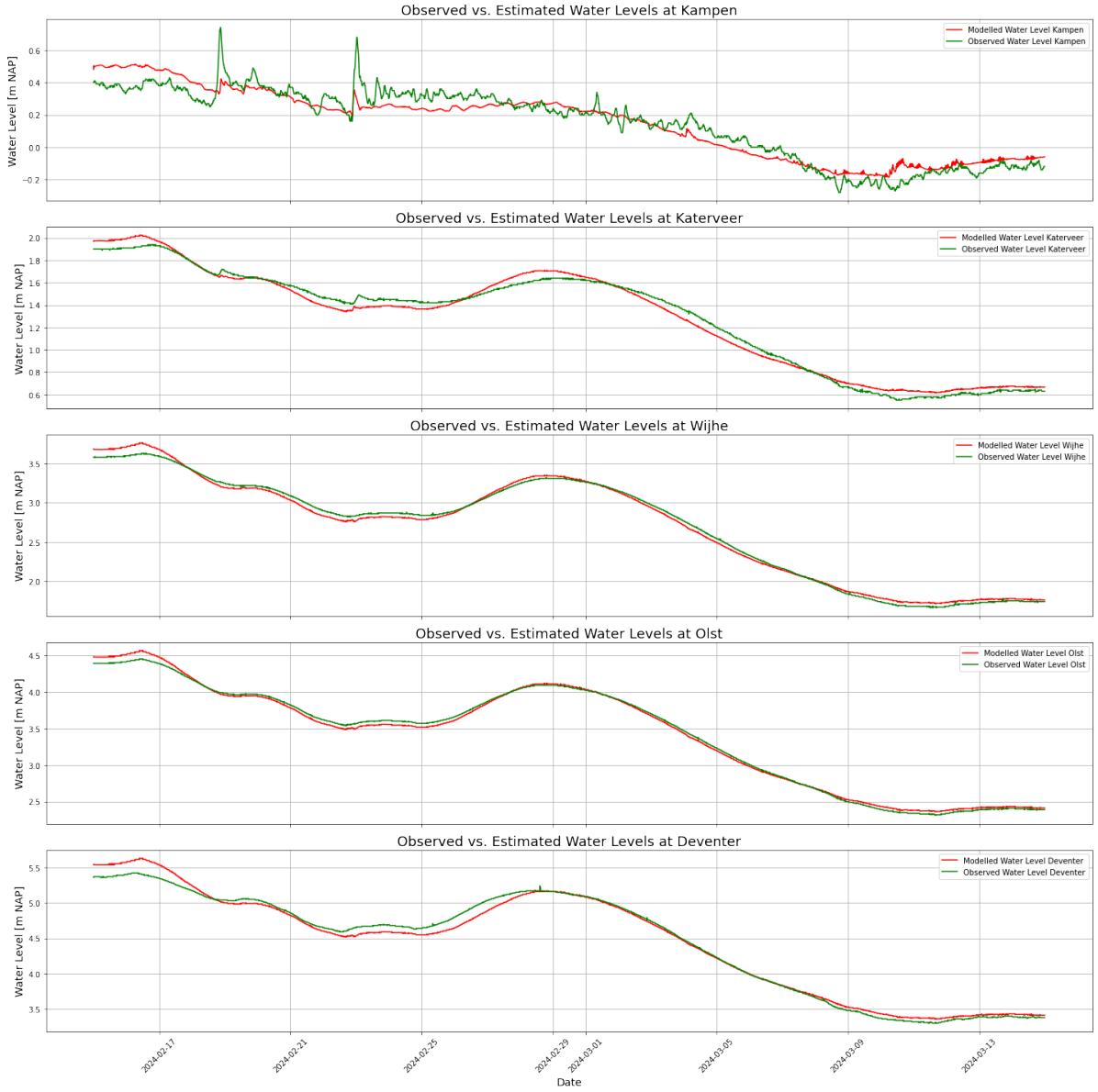

Figure C.19: Calibration results of a, b and c for Kampen, Katerveer, Wijhe, Olst, and Deventer along the IJssel.

Figure C.20: Calibration results of a, b and c for Genemuiden, Zwartsluis, Mond der Vecht, and Vechterweerd Beneden along the Zwarte Water and Vecht.

C.3. Validation Results

Scenario: closure on 6 December 2024 taken. Closure around 09:30 initiated, blocked for vessels (+0.40m NAP) from 08:00 onwards Rijkswaterstaat, 2024b. In the model, the water level exceeded +0.20m NAP around 05:00, +0.40m NAP around 07:10, and the closure criteria around 07:30.

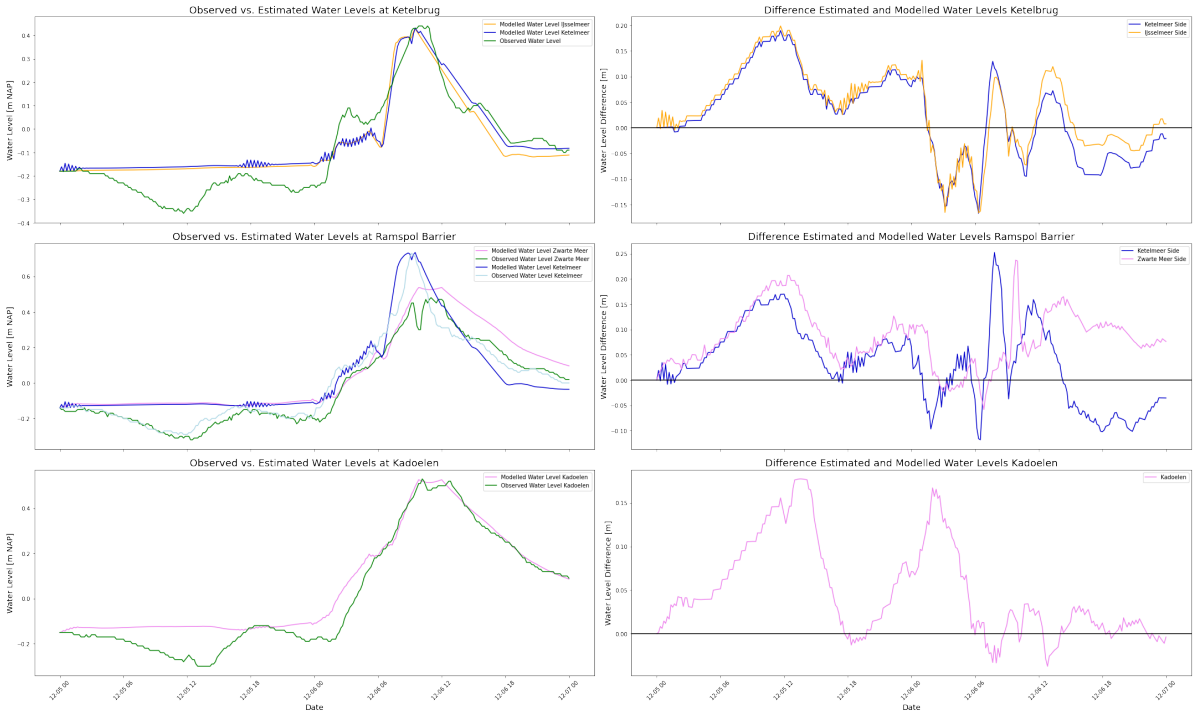

Figure C.21: Validation results of the water levels at Ketelbrug, Ramspol Ketelmeer, Ramspolbrug and Kadoelen.

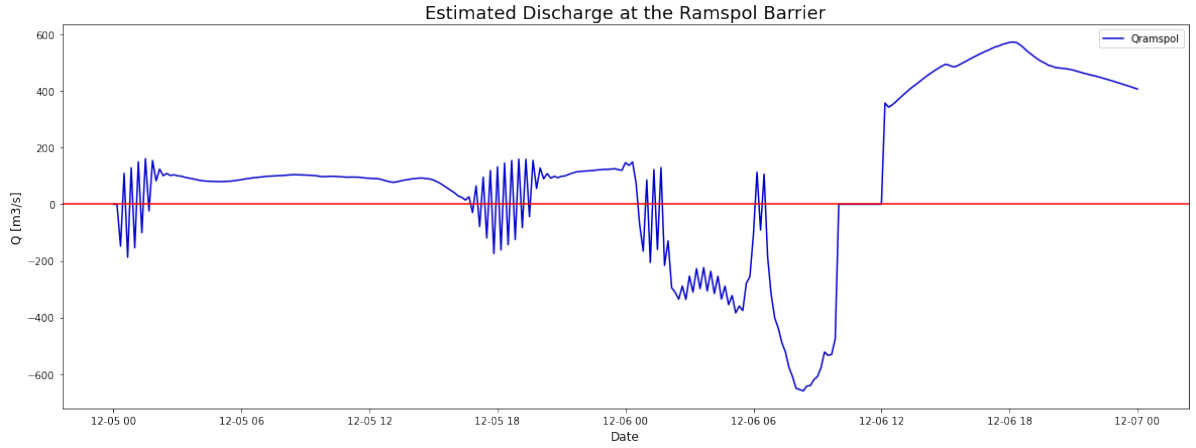

Figure C.22: Modelled Q_{rp} around the closure of December 6, 2024.

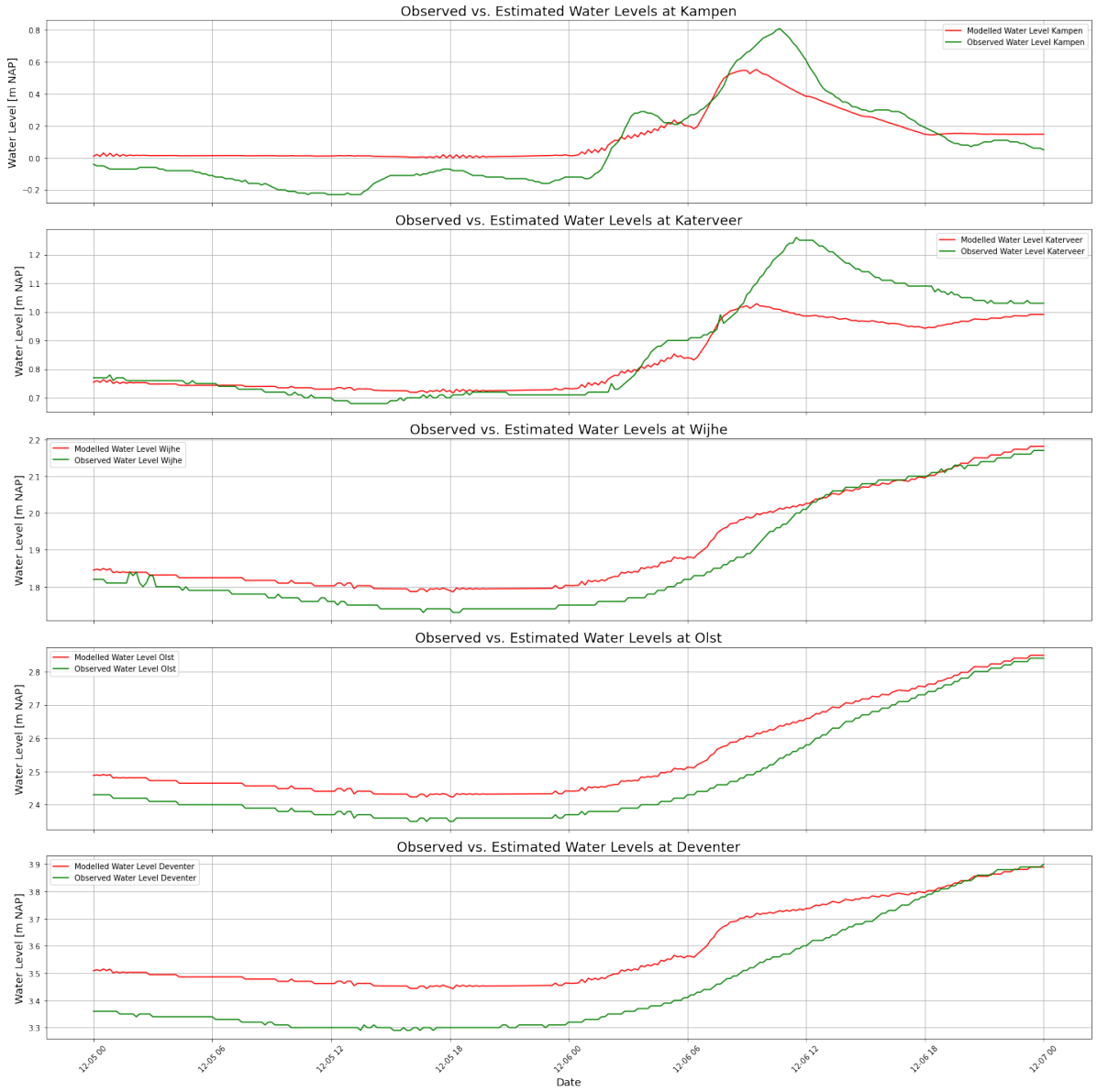

Figure C.23: Validation results of the water levels at Kampen, Katerveer, Wijhe, Olst and Deventer along the IJssel.

Figure C.24: Validation results of the water levels at Genemuiden, Zwartsluis, Mond der Vecht and Vechterweerd Beneden along the Zwarte Water and Vecht.

C.3.1. Error Analysis Results

Lakes

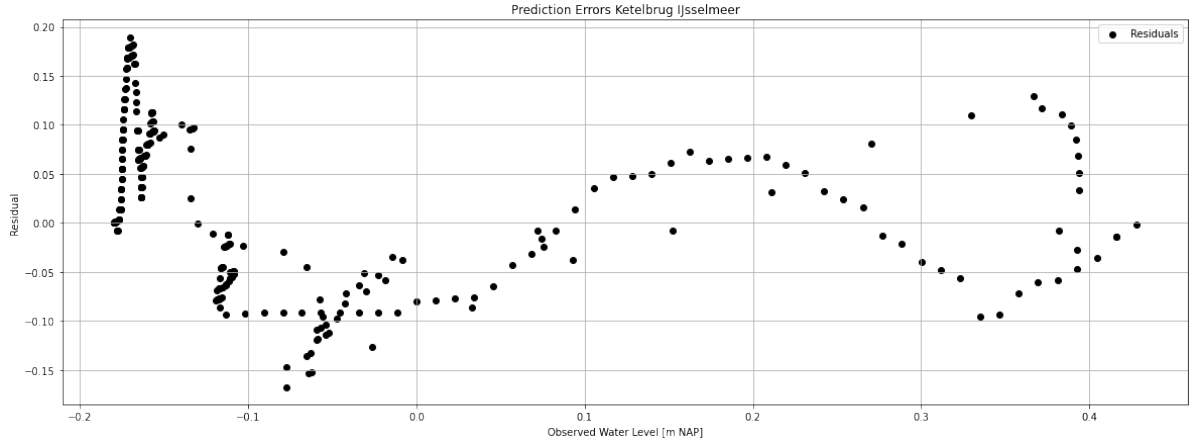

Figure C.25: Error analysis of water level Ketelbrug.

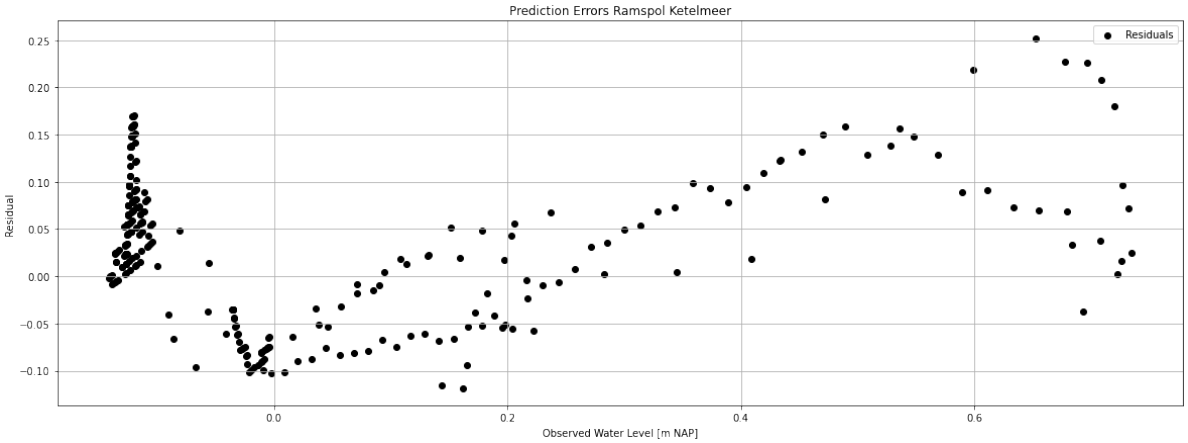

Figure C.26: Error analysis of water level Ramspol Barrier Ketelmeer.

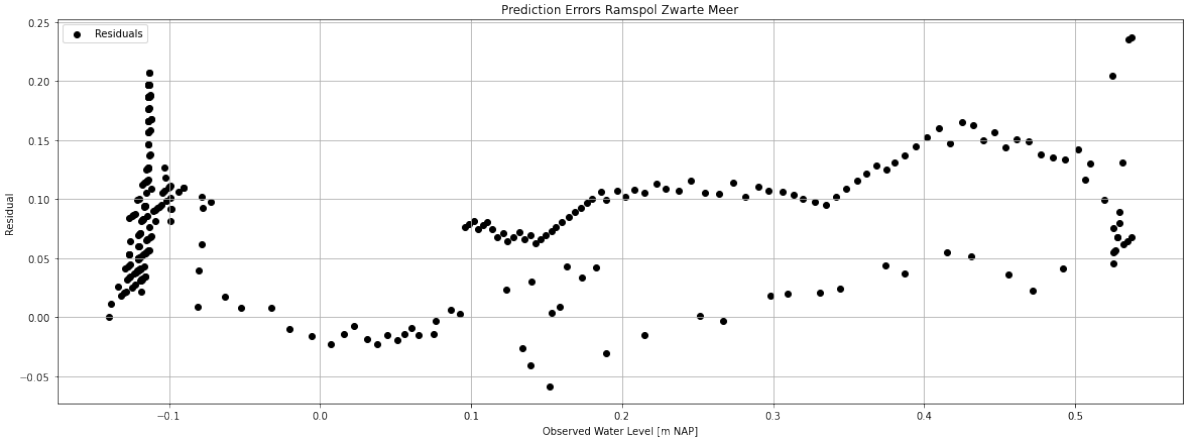

Figure C.27: Error analysis of water level Ramspolbrug.

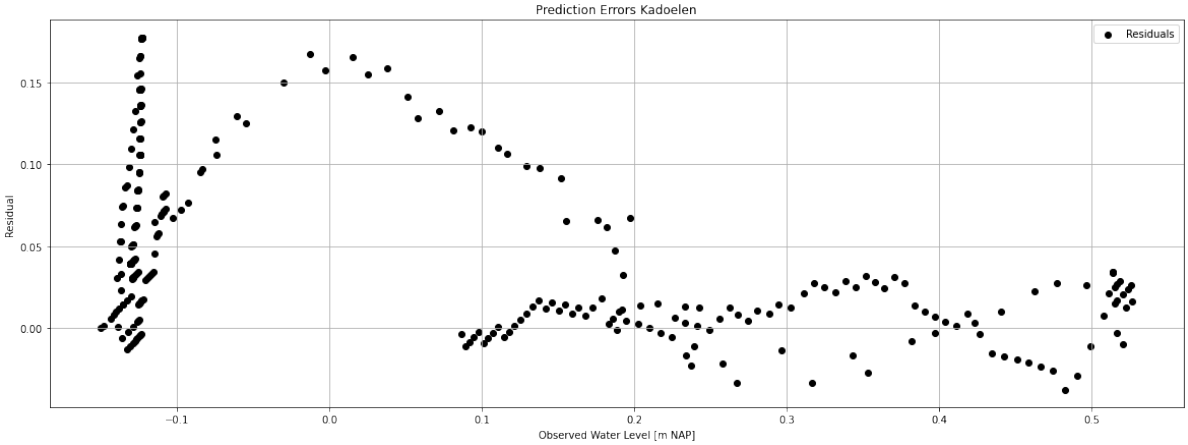

Figure C.28: Error analysis of water level Kadoelen.

IJssel

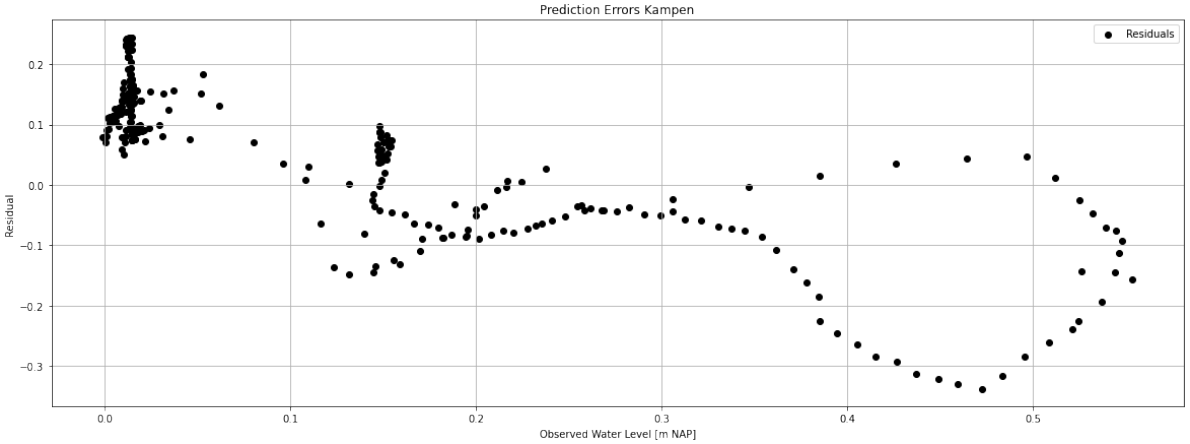

Figure C.29: Error analysis of water level Kampen.

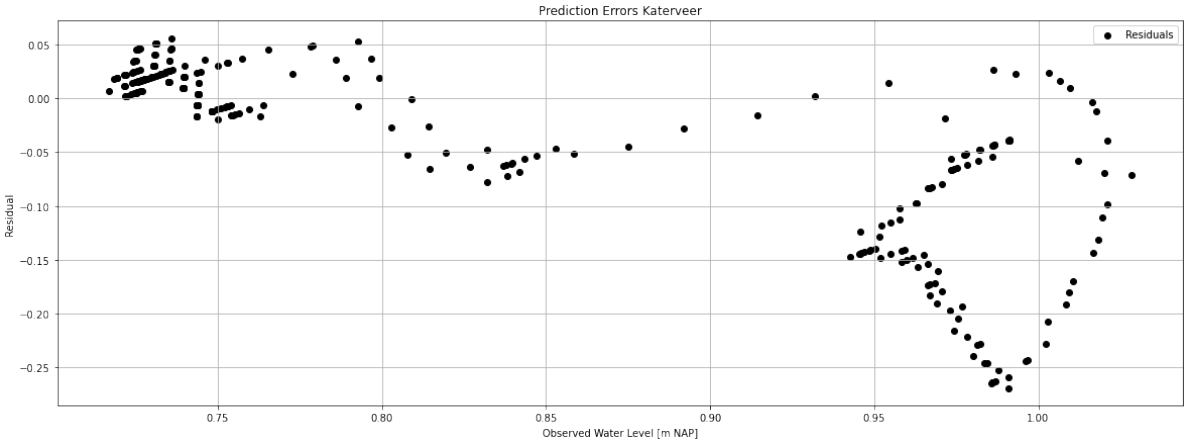

Figure C.30: Error analysis of water level Katerveer.

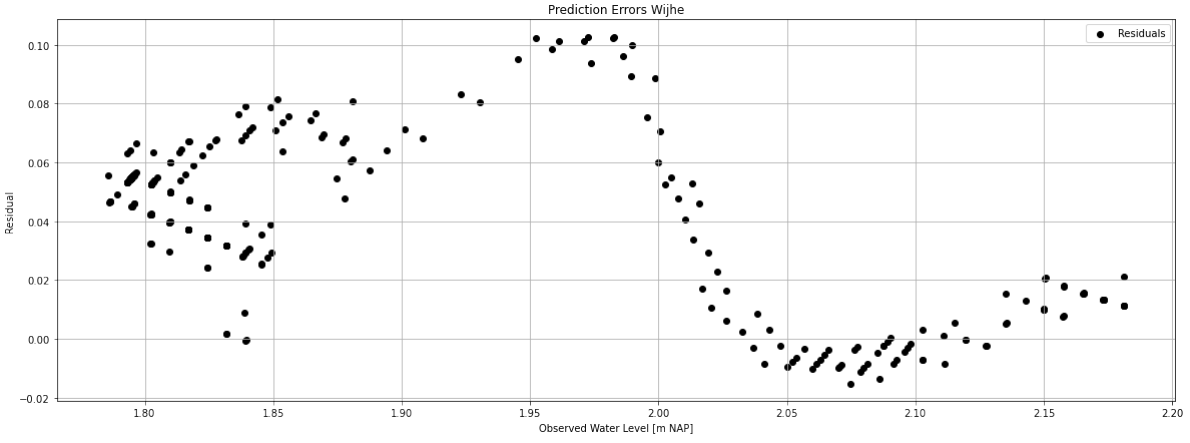

Figure C.31: Error analysis of water level Wijhe.

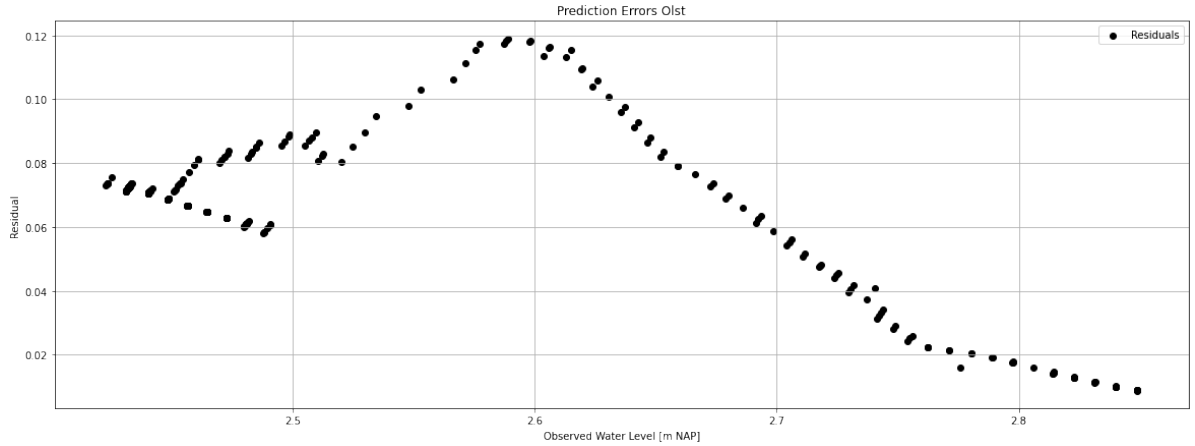

Figure C.32: Error analysis of water level Olst.

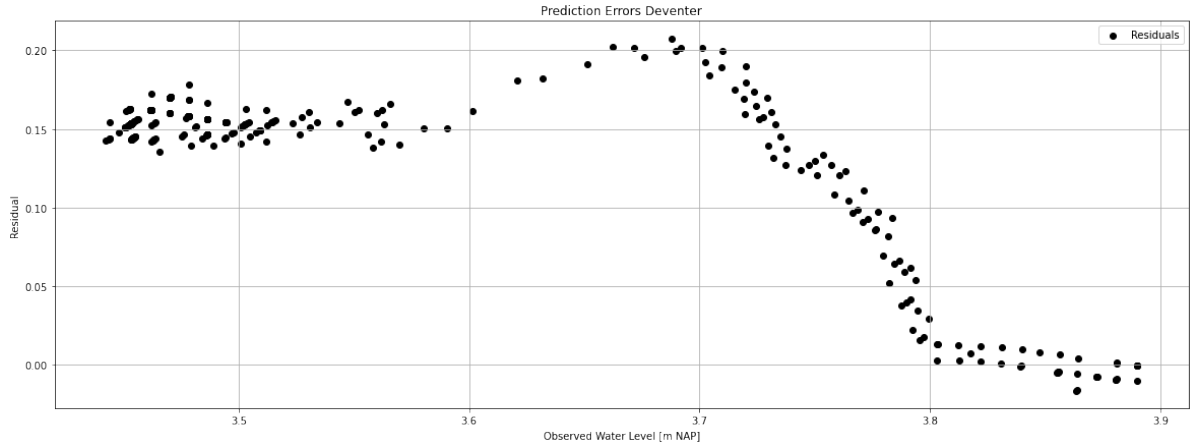

Figure C.33: Error analysis of water level Deventer.

Zwarte Water and Vecht

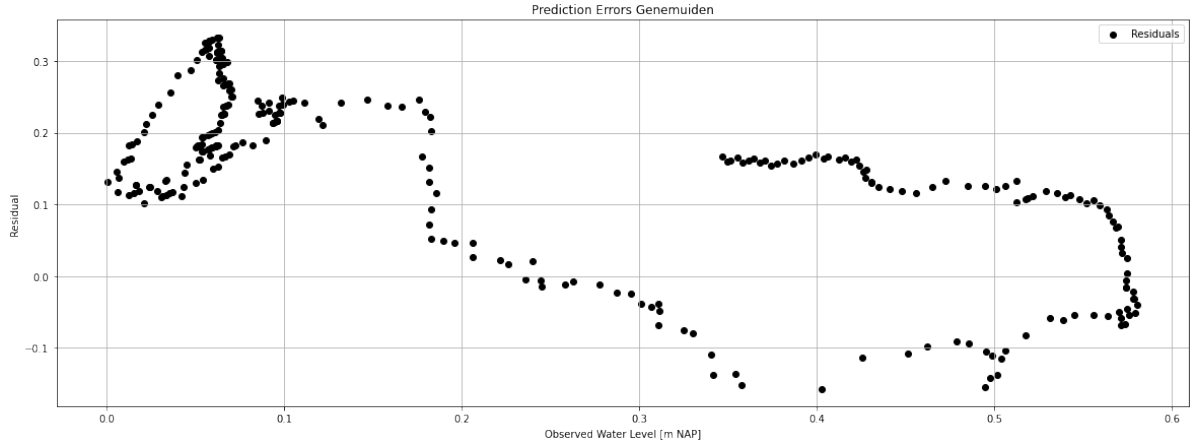

Figure C.34: Error analysis of water level Genemuiden.

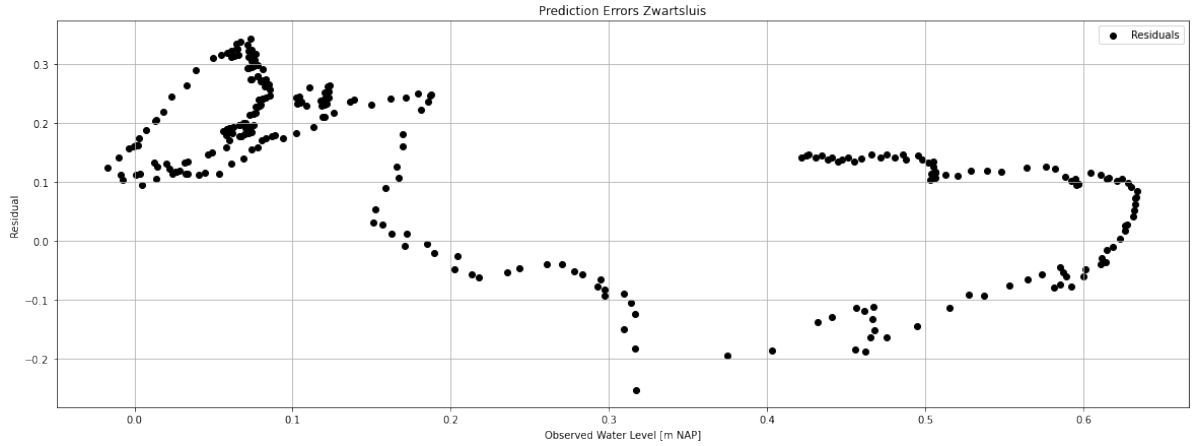

Figure C.35: Error analysis of water level Zwartsluis.

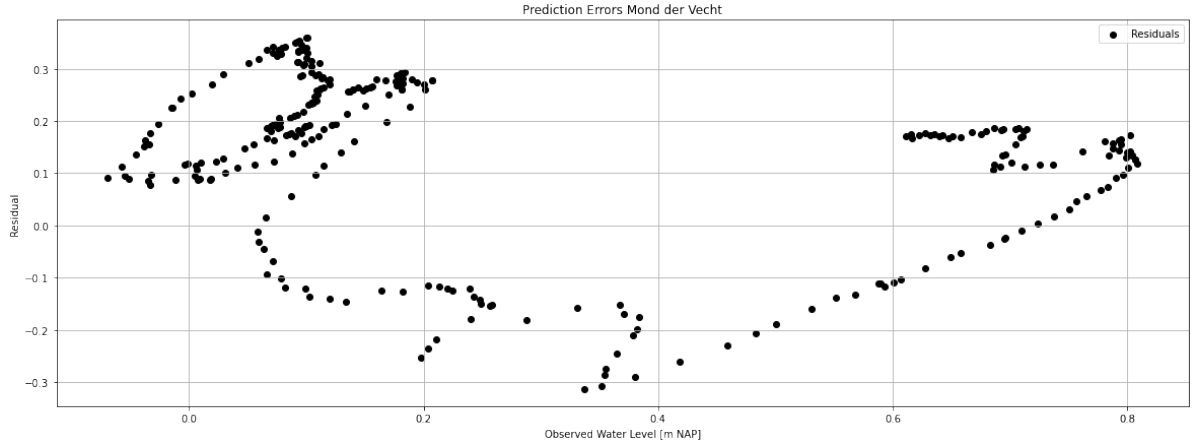

Figure C.36: Error analysis of water level Mond der Vecht.

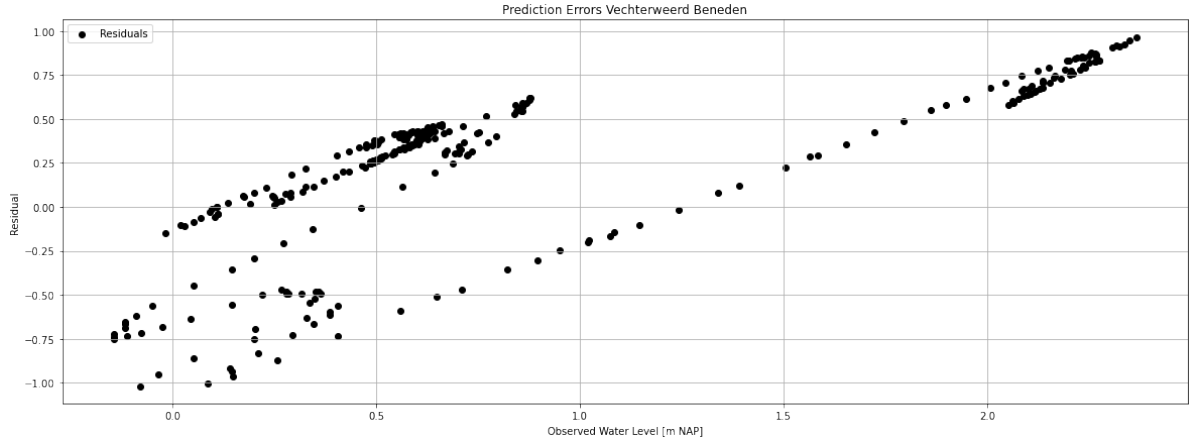

Figure C.37: Error analysis of water level Vechterweerd Beneden.

D

Results of Improvements Scenarios

D.1. Normal Closure: February 18, 2022

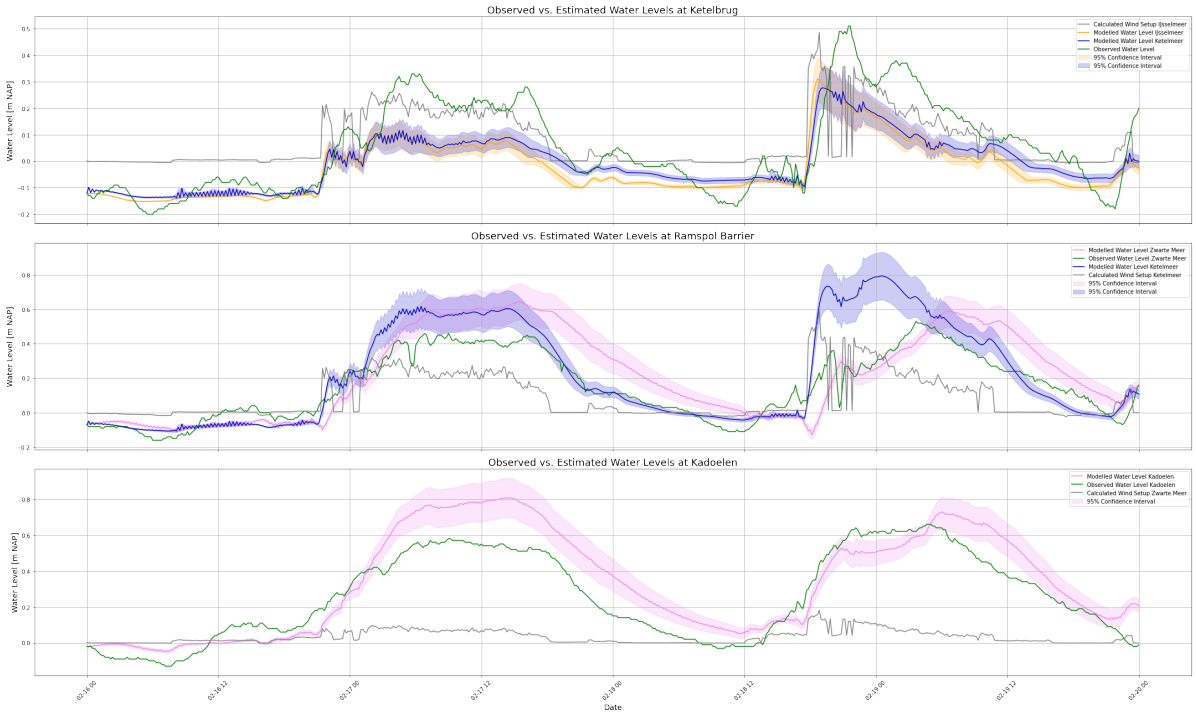

Figure D.1: Modelled Water Levels at the Ketelbrug, Ramspol Barrier and Kadoelen during the closure of February 18, 2022.

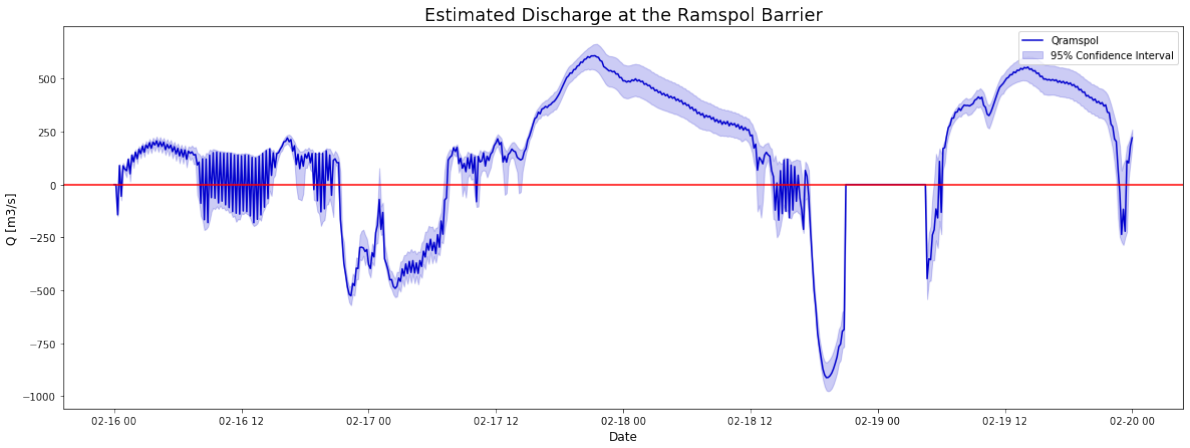

Figure D.2: Modelled discharge at the Ramspol Barrier during the closure of February 18, 2022.

Figure D.3: Modelled Water Levels at Kampen, Katerveer, Wijhe, Olst and Deventer along the IJssel during the closure of February 18, 2022.

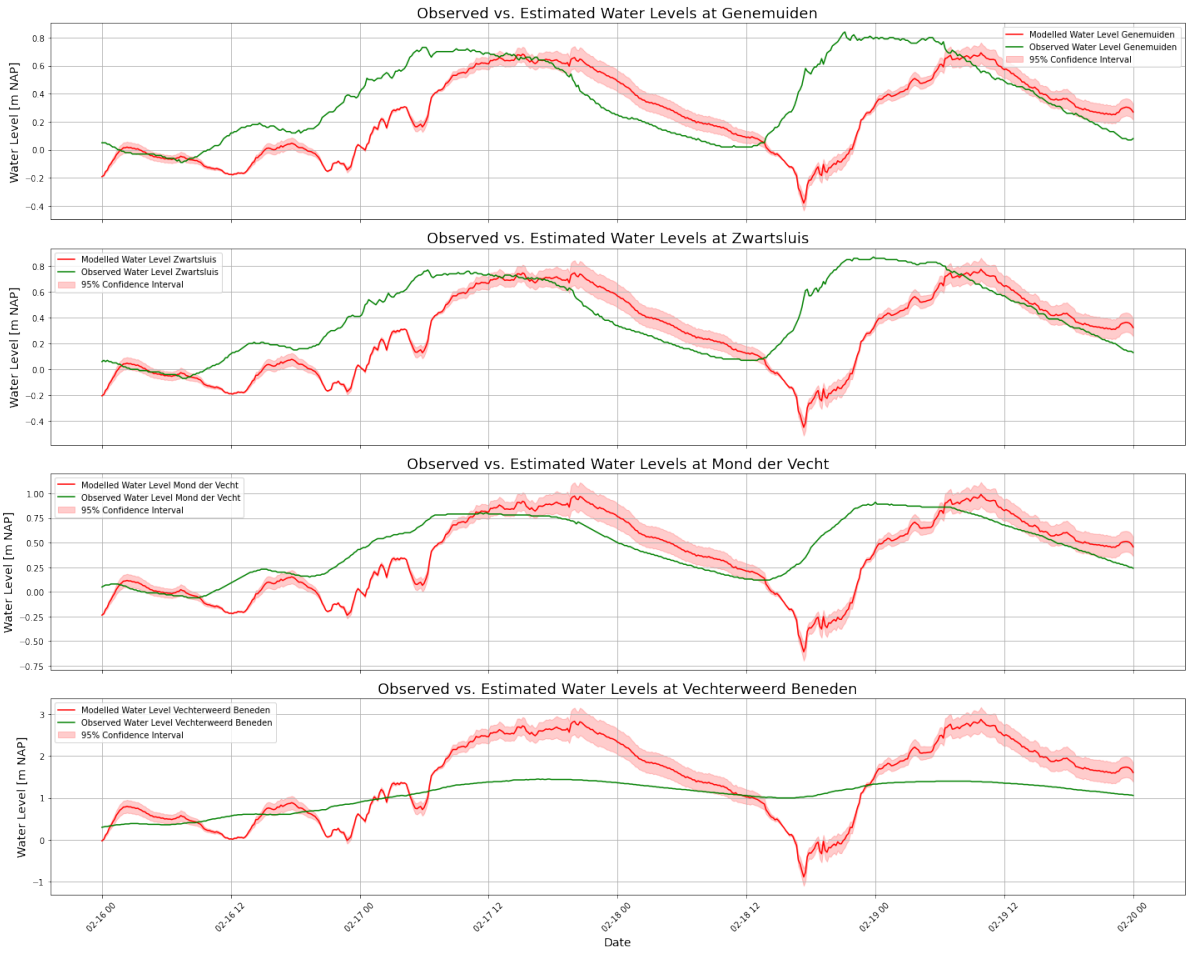

Figure D.4: Modelled Water Levels at Genemuiden, Zwartsluis, Mond der Vecht and Vechterweerd Beneden along the Zwarte Water and Vecht during the closure of February 18, 2022.

D.2. Test Closure: October 3, 2023

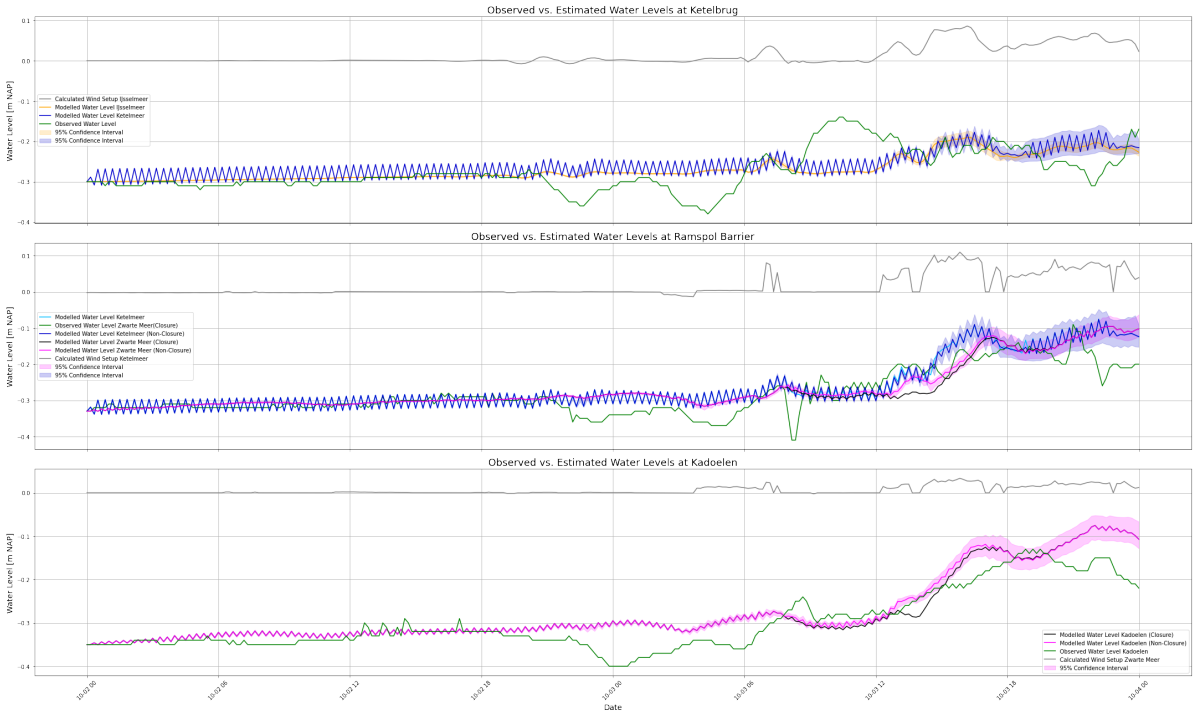

Figure D.5: Modelled Water Levels at the Ketelbrug, Ramspol Barrier and Kadoelen during the test closure of October 3, 2023.

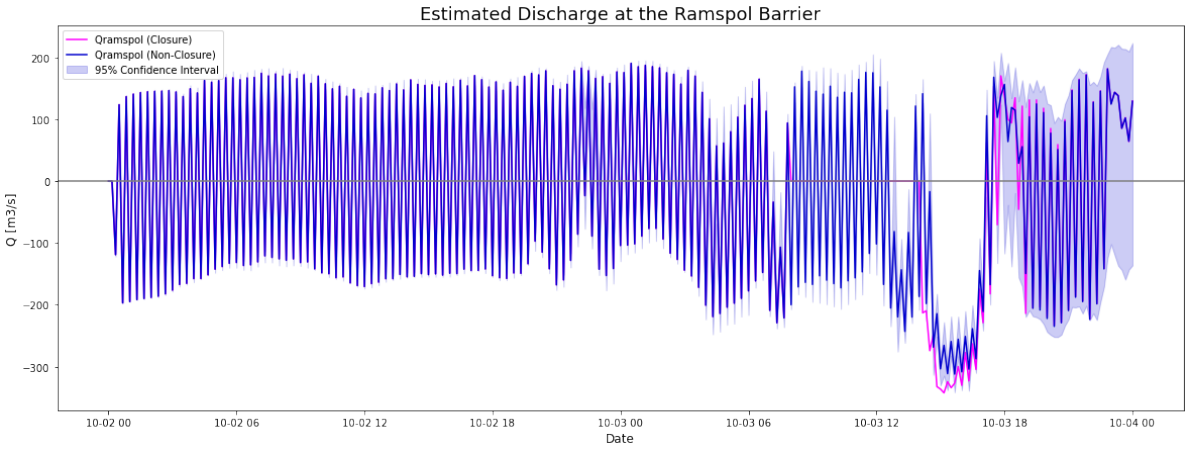

Figure D.6: Modelled discharge at the Ramspol Barrier during the test closure of October 3, 2023.

Figure D.7: Modelled Water Levels at Kampen, Katerveer, Wijhe, Olst and Deventer along the IJssel during the test closure of October 3, 2023.

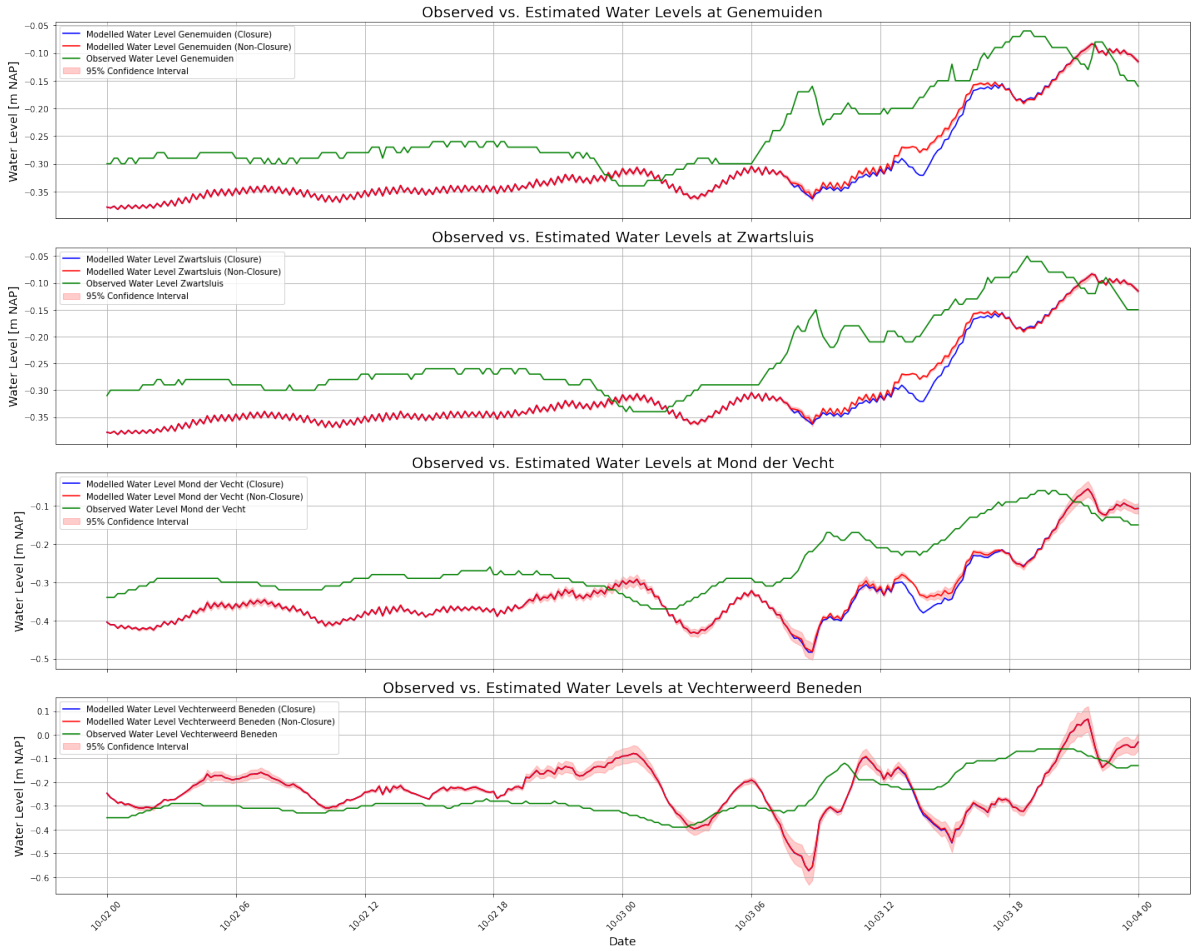

Figure D.8: Modelled Water Levels at Genemuiden, Zwartsluis, Mond der Vecht and Vechterweerd Beneden along the Zwarte Water and Vecht during the test closure of October 3, 2023.

D.3. Overruled Scenario: November 23, 2023

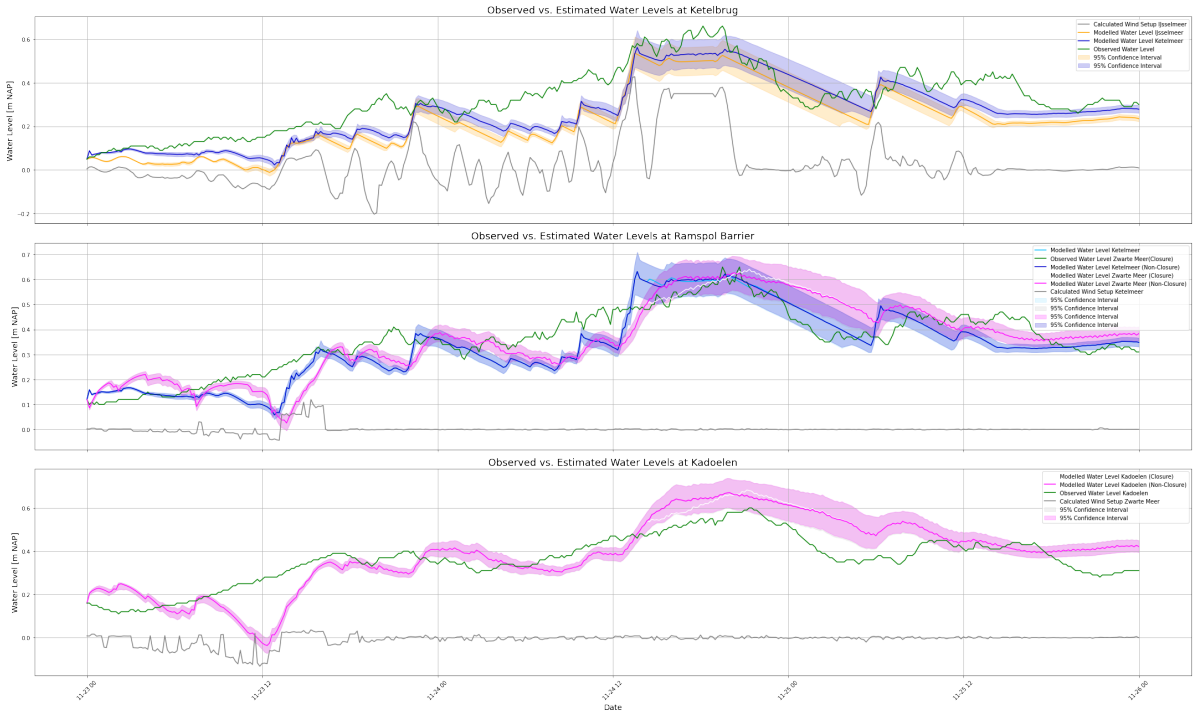

Figure D.9: Modelled Water Levels at the Ketelbrug, Ramspol Barrier and Kadoelen during the overruled closure of the Ramspol Barrier on November 23, 2023 for both the closure and non-closure scenario.

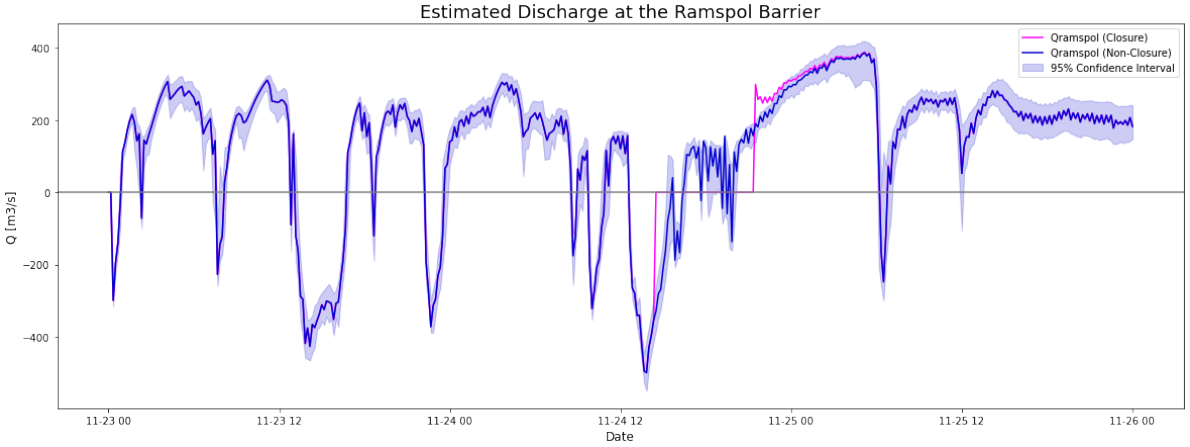

Figure D.10: Modelled discharge at the Ramspol Barrier during the overruled closure of the Ramspol Barrier on November 23, 2023 for both the closure and non-closure scenario.

Figure D.11: Modelled Water Levels at Kampen, Katerveer, Wijhe, Olst and Deventer along the IJssel during the overruled closure of the Ramspol Barrier on November 23, 2023 for both the closure and non-closure scenario.

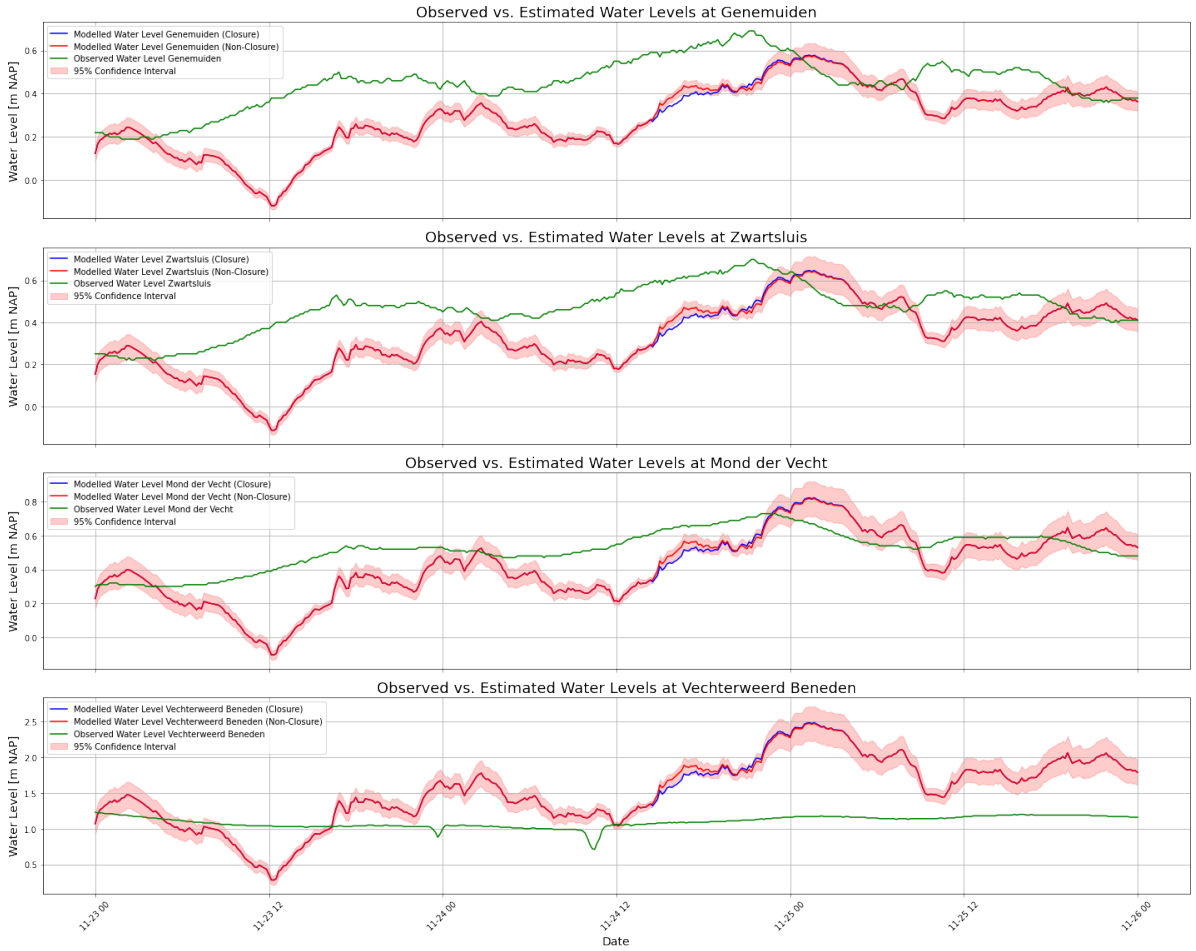

Figure D.12: Modelled Water Levels at Genemuiden, Zwartsluis, Mond der Vecht and Vechterweerd Beneden along the Zwarte Water and Vecht during the overruled closure of the Ramspol Barrier on November 23, 2023 for both the closure and non-closure scenario.

D.4. Closures at the Ramspol Barrier with Water Level Peaks Slightly Above +0.50 m NAP

D.4.1. Peaking

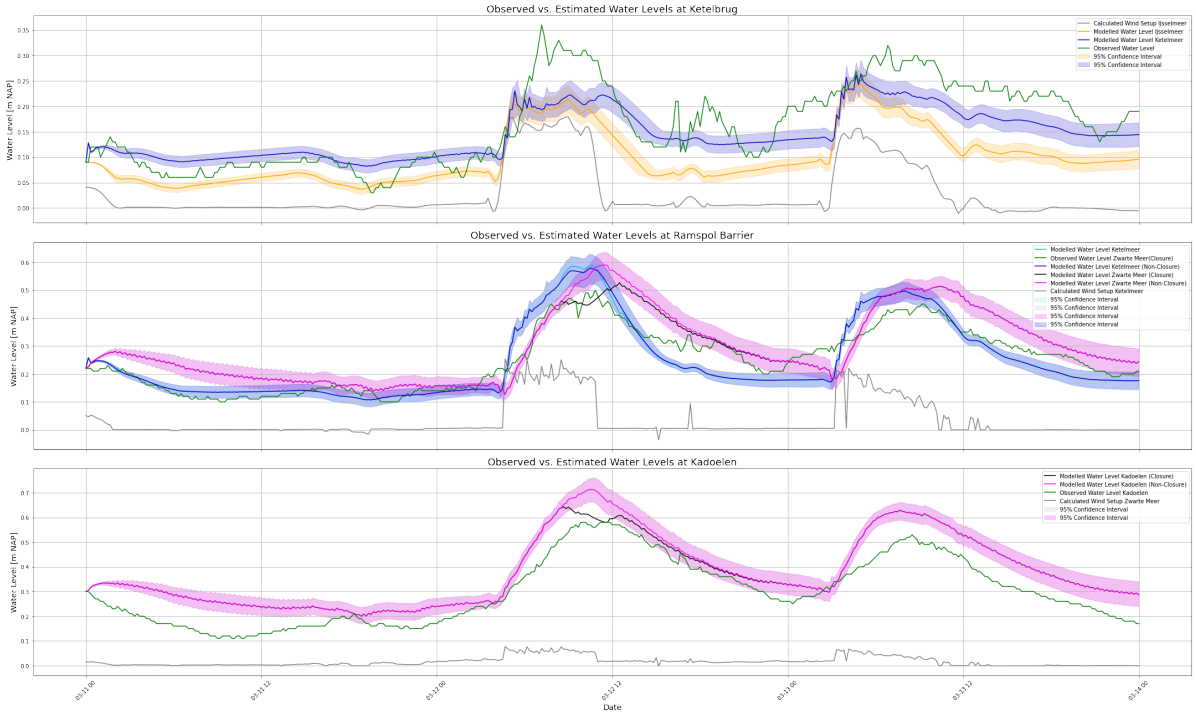

Figure D.13: Modelled Water Levels at the Ketelbrug, Ramspol Barrier and Kadoelen during the closure (black lines) and non-closure (pink lines) on March 12, 2020.

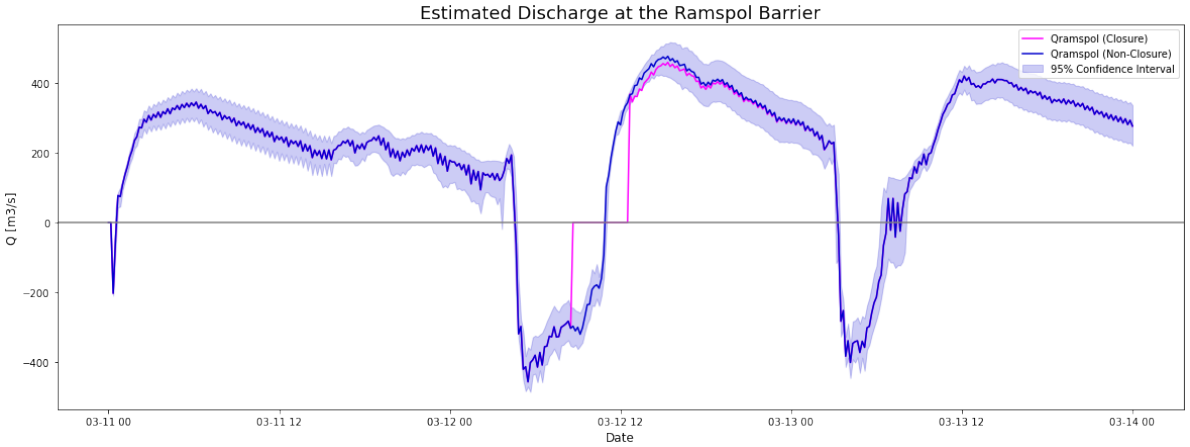

Figure D.14: Modelled discharge at the Ramspol Barrier for decreasing winds after closure.

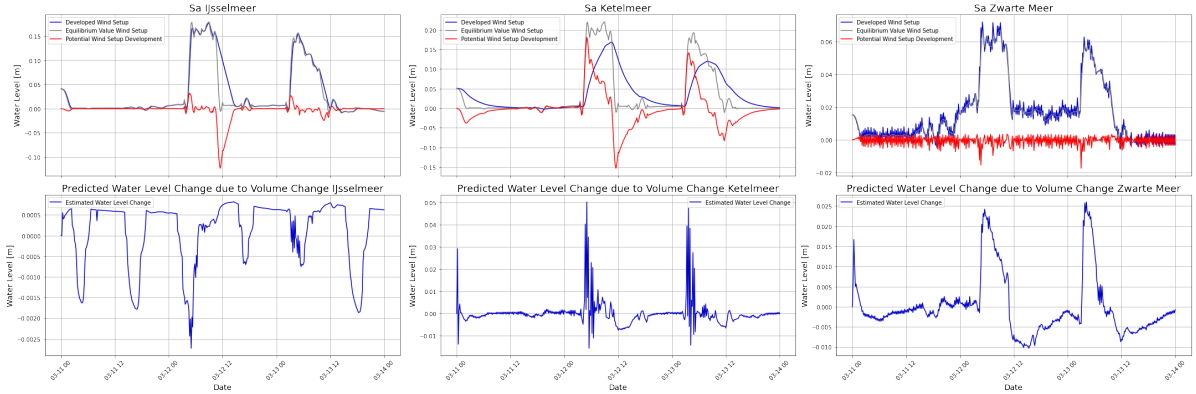

Figure D.15: Wind setup development potential and predicted volume changes for March 12, 2020 using the non-closure simulation and a decreasing wind after closure.

D.4.2. Fluctuating

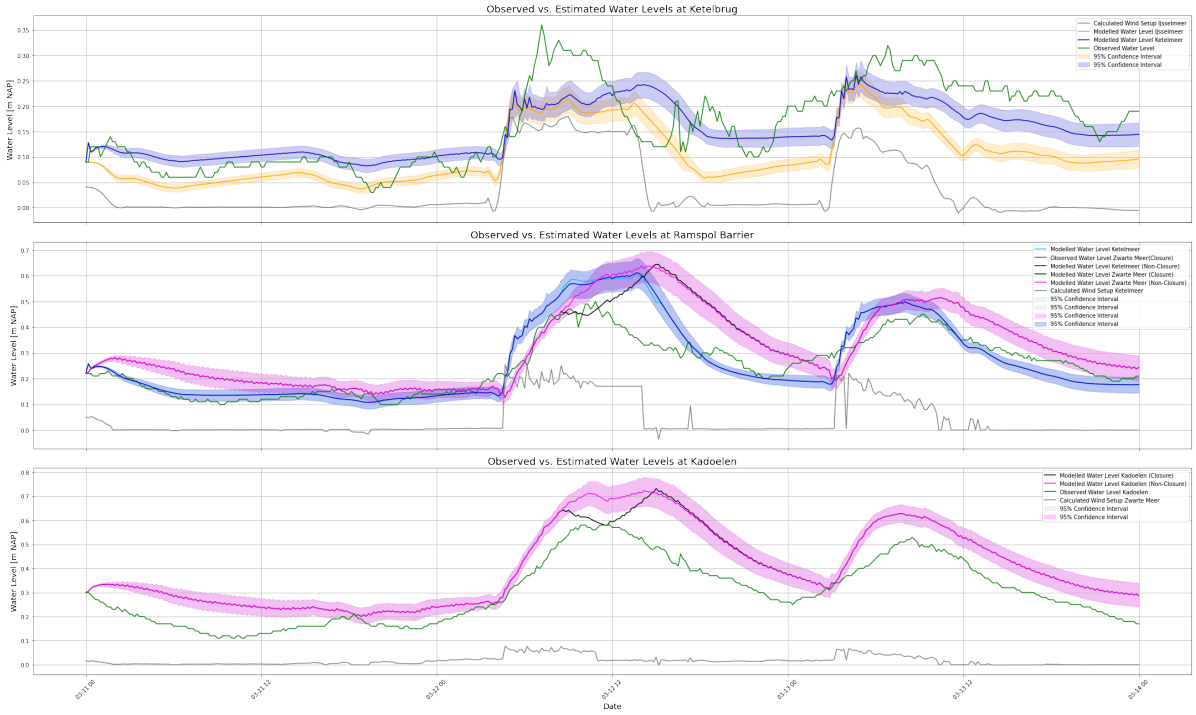

Figure D.18: Modelled Water Levels at the Ketelbrug, Ramspol Barrier and Kadoelen during the closure (black lines) and non-closure (pink lines) on March 12, 2020, for constant winds after closure.

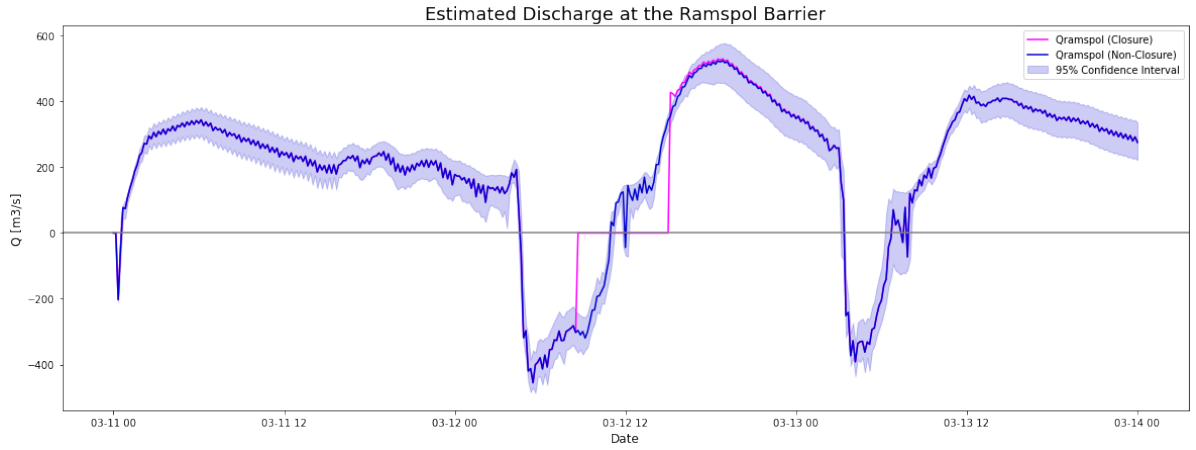

Figure D.19: Modelled discharge at the Ramspol Barrier for constant winds after closure.

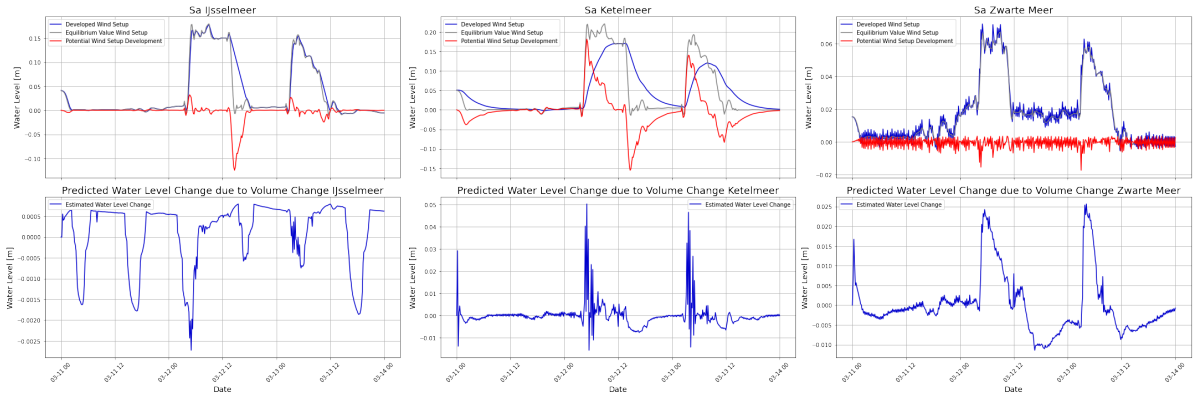

Figure D.20: Wind setup development potential and predicted volume changes for March 12, 2020 using the non-closure simulation and a constant wind after closure.

Figure D.21: Modelled Water Levels at Kampen, Katerveer, Wijhe, Olst and Deventer along the IJssel for constant winds after closure.

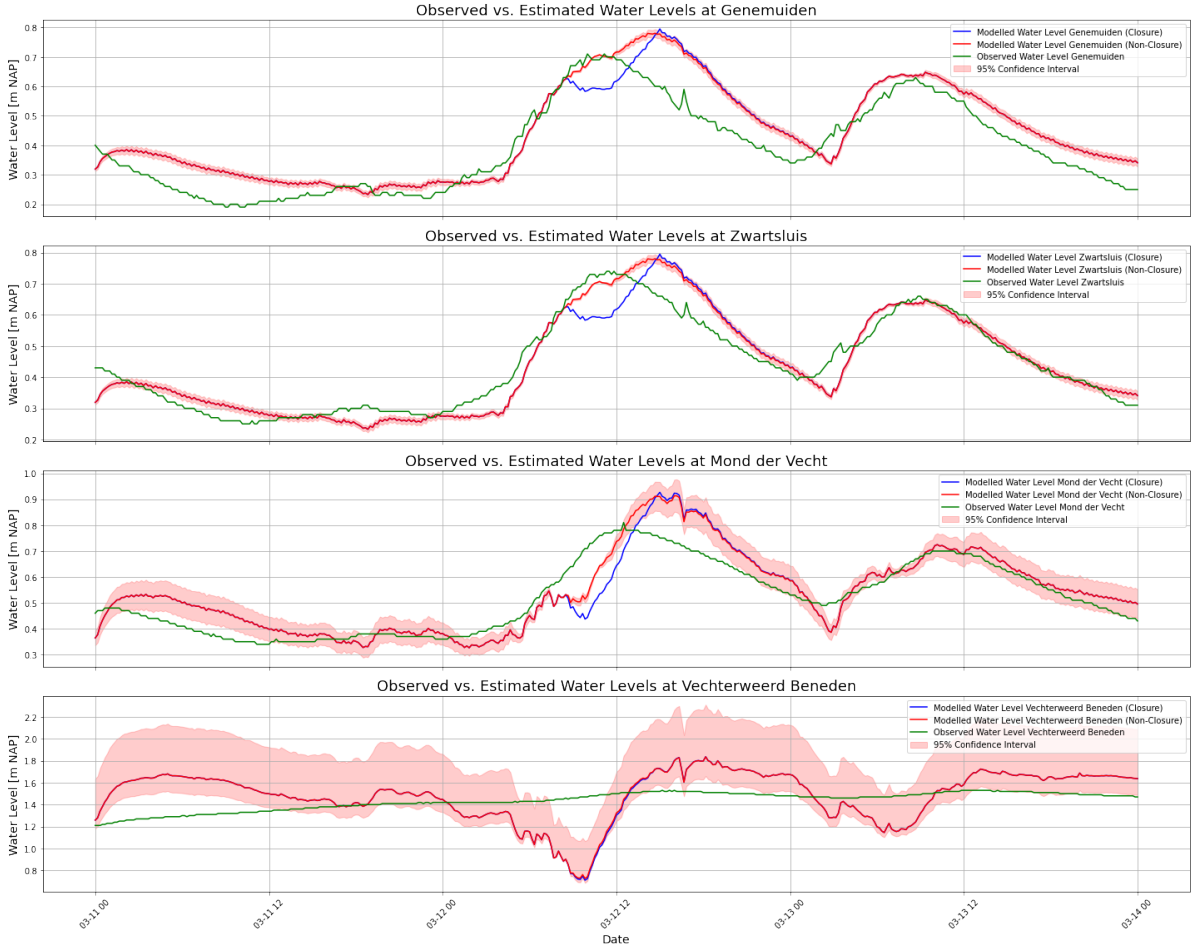

Figure D.22: Modelled Water Levels at Genemuiden, Zwartsluis, Mond der Vecht and Vechterweerd Beneden along the Zwarte Water and Vecht for constant winds after closure.

D.4.3. Increasing

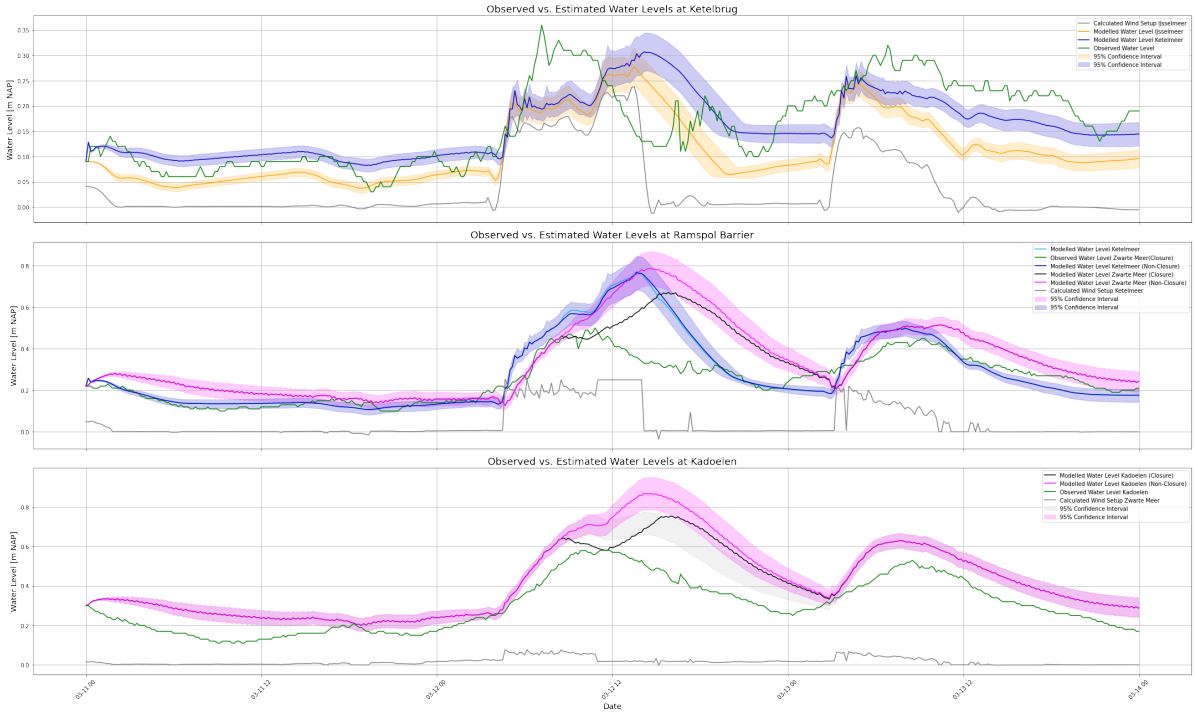

Figure D.23: Modelled Water Levels at the Ketelbrug, Ramspol Barrier and Kadoelen during the closure (black lines) and non-closure (pink lines) on March 12, 2020, for increasing winds after closure.

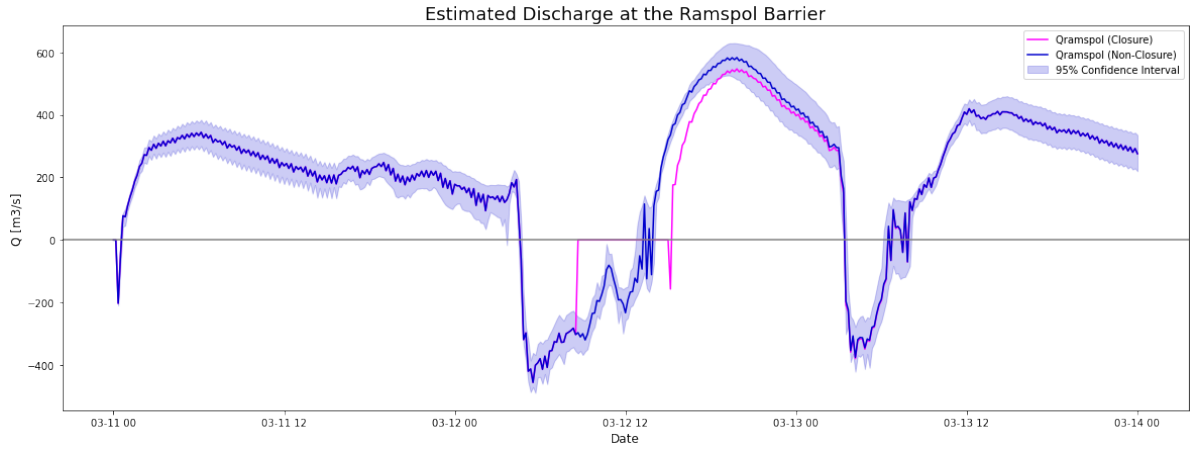

Figure D.24: Modelled discharge at the Ramspol Barrier for increasing winds after closure.

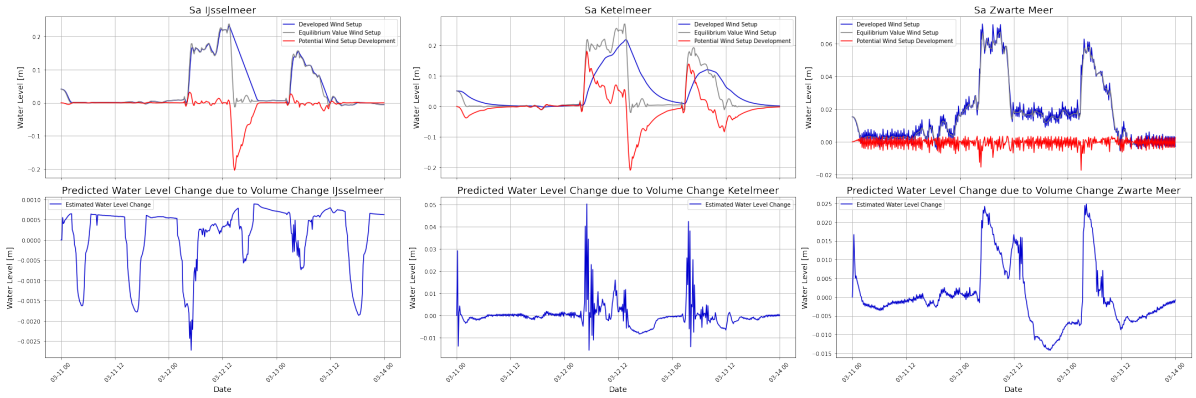

Figure D.25: Wind setup development potential and predicted volume changes for March 12, 2020 using the non-closure simulation and a increasing wind after closure.

Figure D.26: Modelled Water Levels at Kampen, Katerveer, Wijhe, Olst and Deventer along the IJssel for increasing winds after closure.

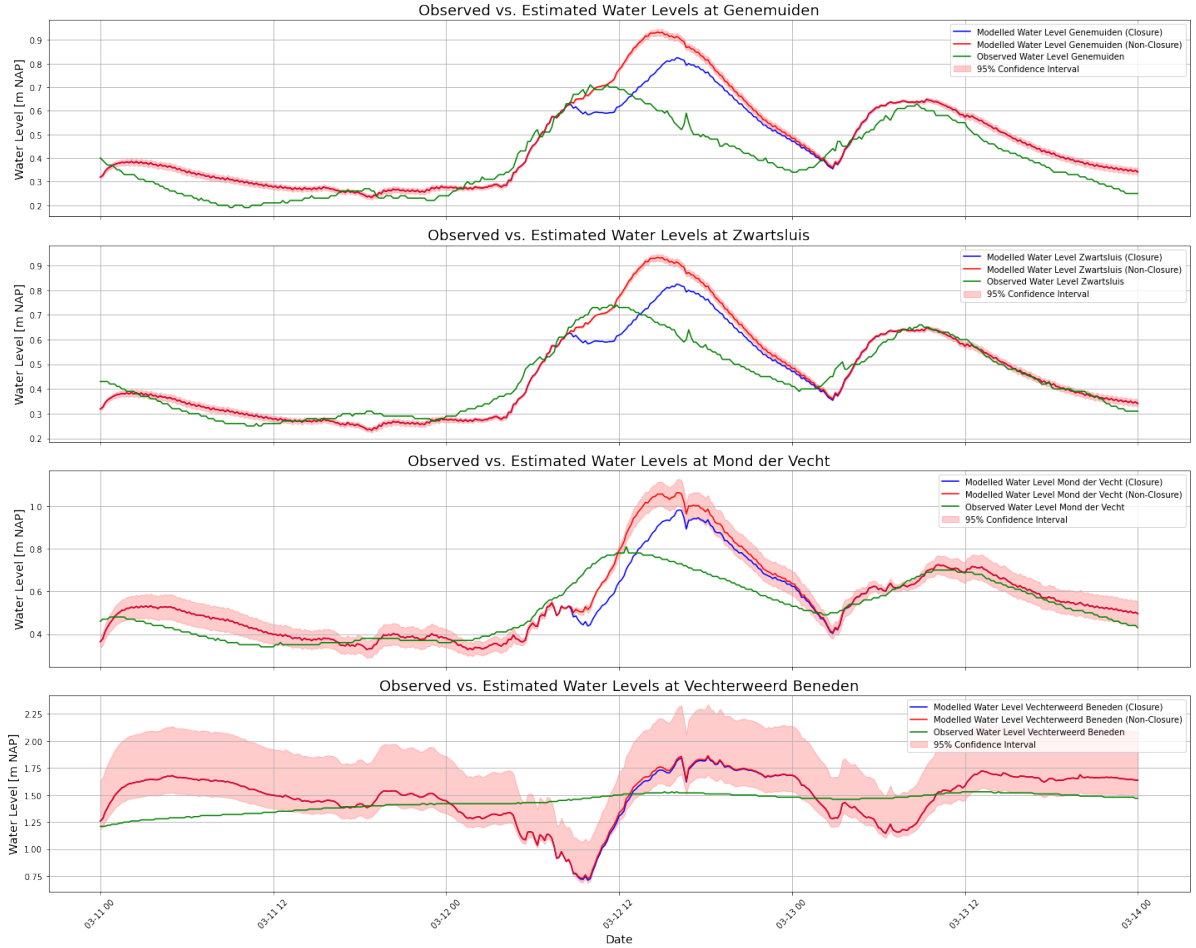

Figure D.27: Modelled Water Levels at Genemuiden, Zwartsluis, Mond der Vecht and Vechterweerd Beneden along the Zwarte Water and Vecht for increasing winds after closure.

D.5. Water Level Peaks at the Ramspol Barrier Between +0.40m and +0.50m NAP: No Closure, but Navigation Blocked

D.5.1. Peaking

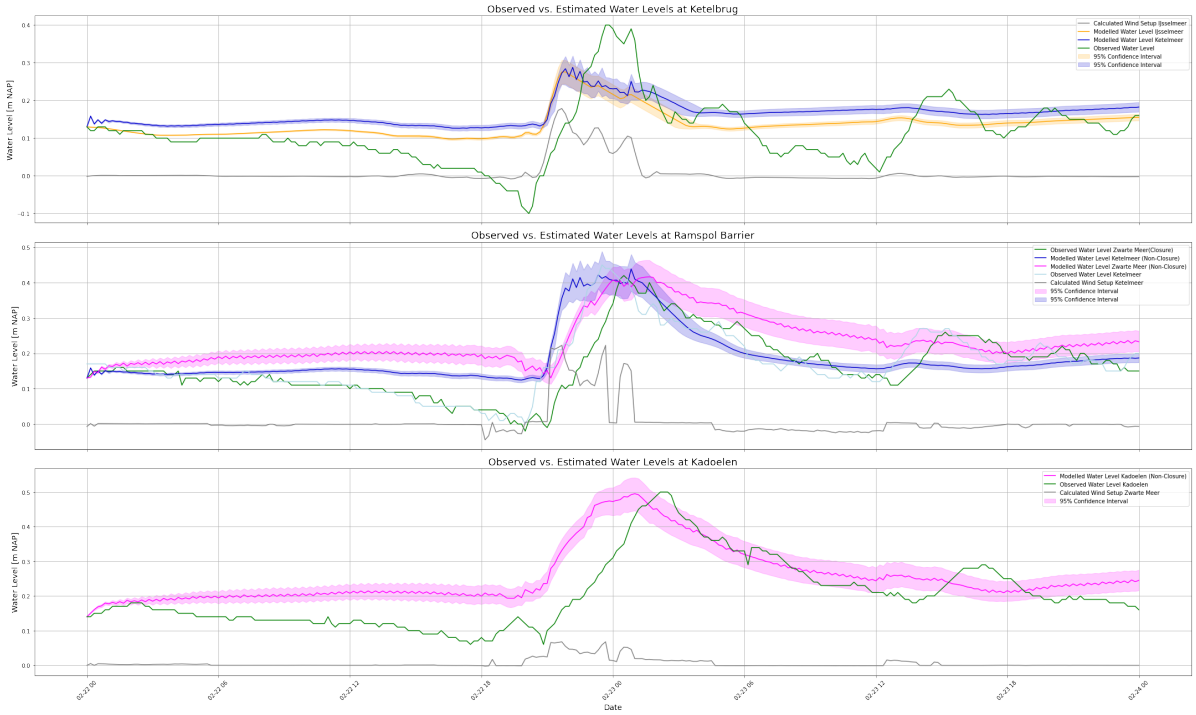

Figure D.28: Modelled Water Levels at the Ketelbrug, Ramspol Barrier and Kadoelen on February 23, 2024, used for evaluating whether a navigation blockade is necessary.

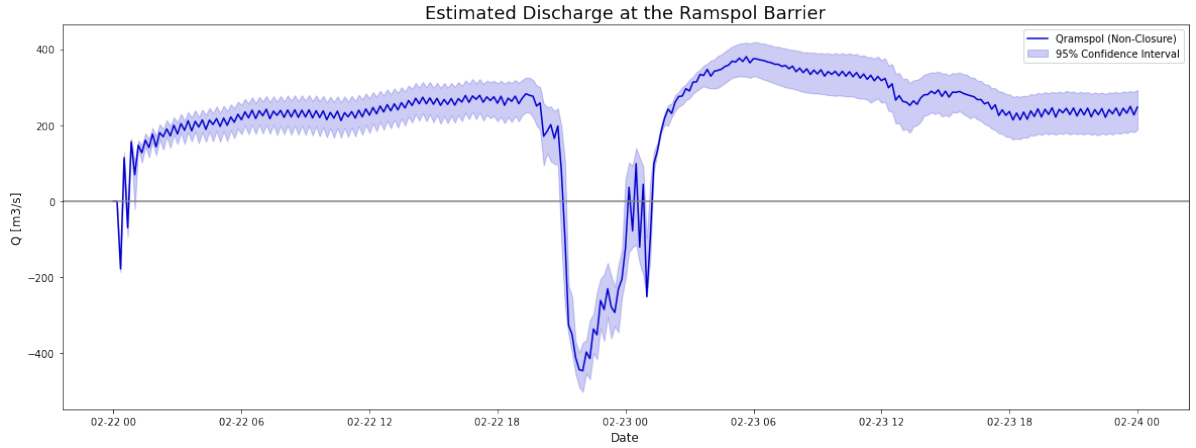

Figure D.29: Modelled discharge at the Ramspol Barrier for water levels between +0.40m and +0.50m NAP for decreasing winds.

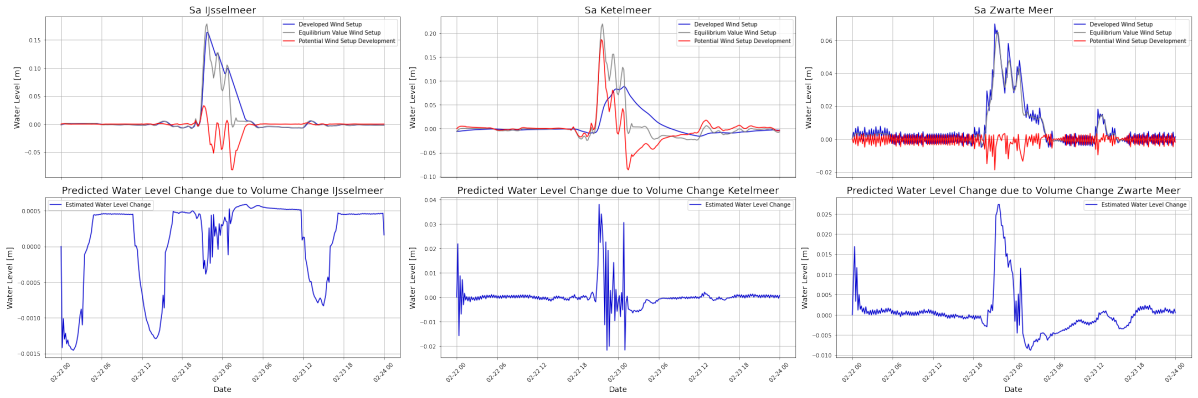

Figure D.30: Wind setup development potential and predicted volume changes for February 23, 2024, during a decreasing wind to evaluate whether a navigation blockade is necessary.

Figure D.31: Modelled Water Levels at Kampen, Katerveer, Wijhe, Olst and Deventer along the IJssel for water levels between +0.40m NAP and +0.50m NAP for decreasing winds.

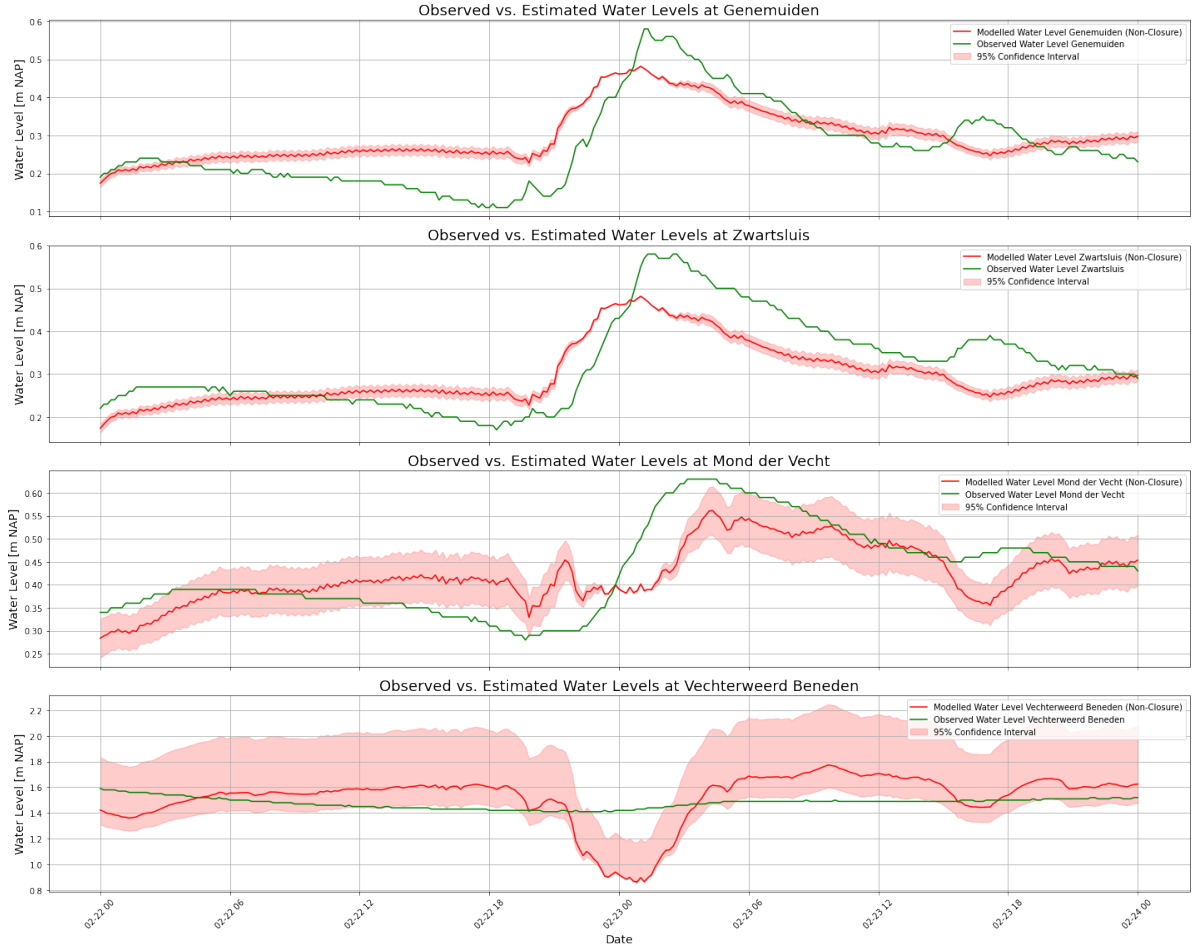

Figure D.32: Modelled Water Levels at Genemuiden, Zwartsluis, Mond der Vecht and Vechterweerd Beneden along the Zwarte Water and Vecht for water levels between +0.40m NAP and +0.50m NAP for decreasing winds.

D.5.2. Fluctuating

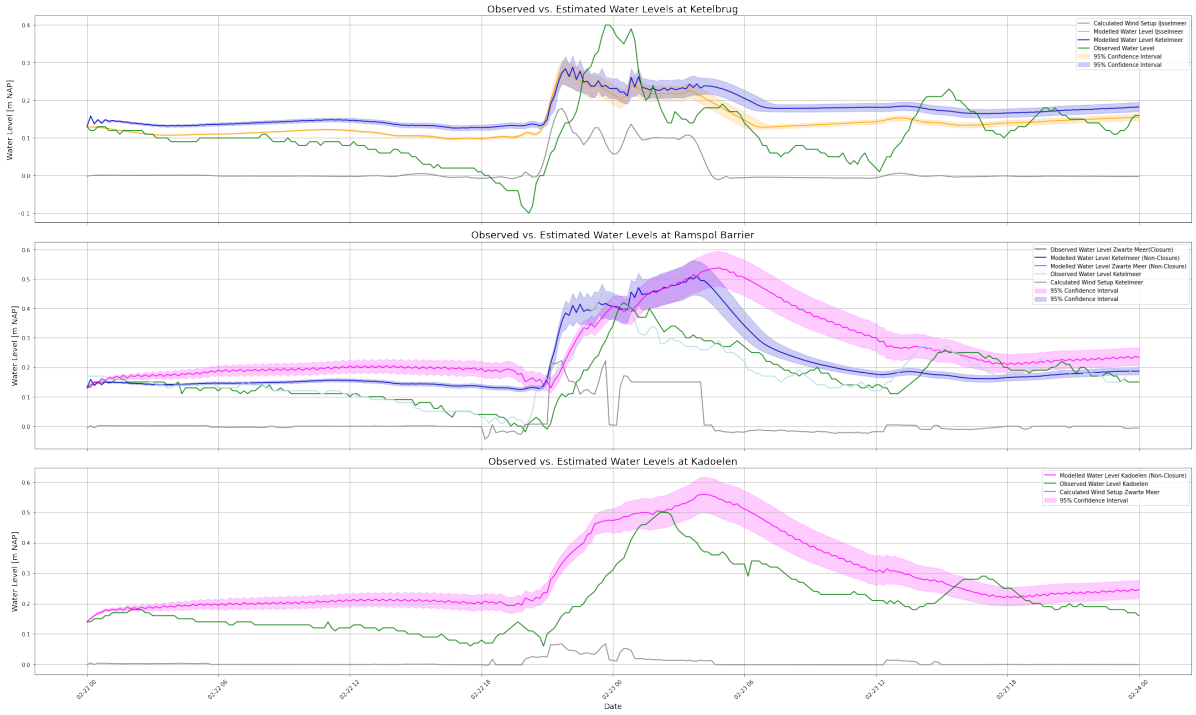

Figure D.33: Modelled Water Levels at the Ketelbrug, Ramspol Barrier and Kadoelen for water levels between +0.40m and +0.50m NAP for increasing winds.

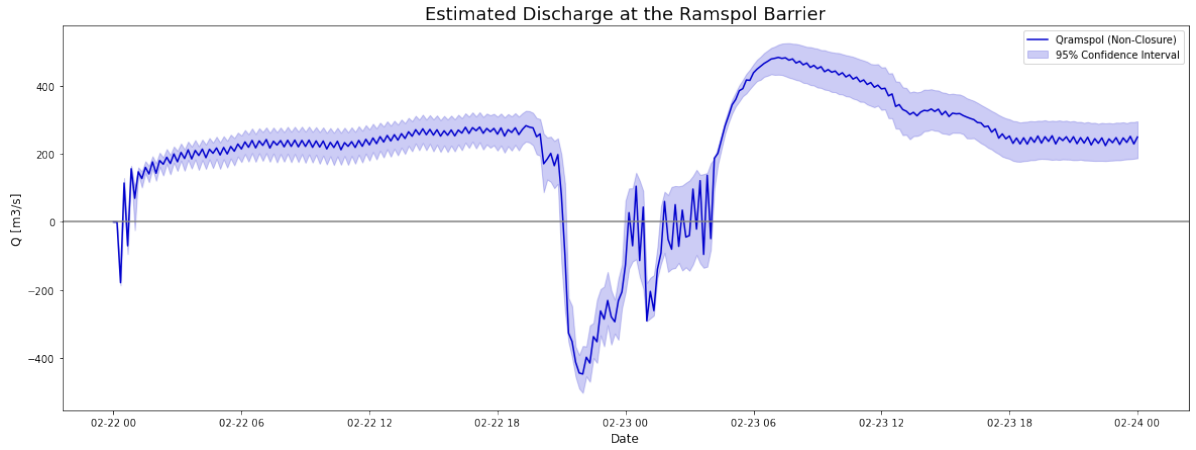

Figure D.34: Modelled discharge at the Ramspol Barrier for water levels between +0.40m and +0.50m NAP for increasing winds.

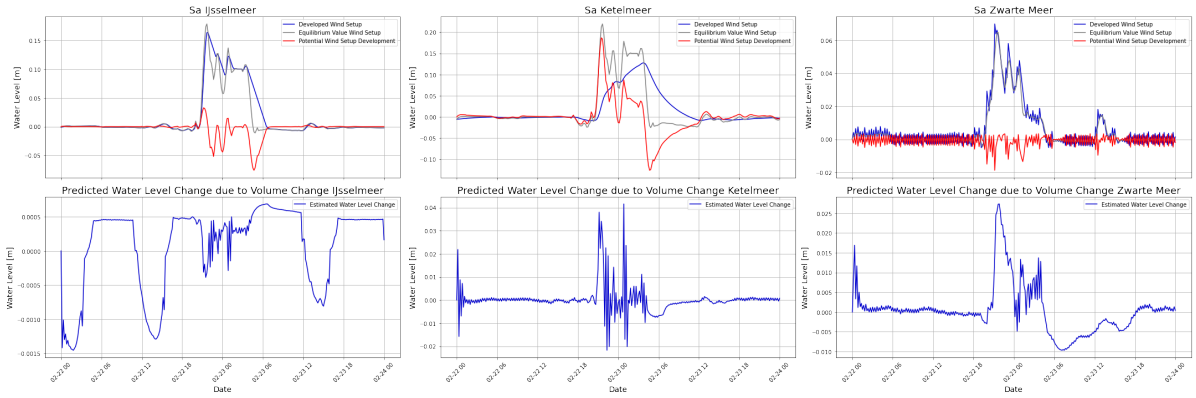

Figure D.35: Wind setup development potential and predicted volume changes for February 23, 2024, during a stagnating wind to evaluate whether a navigation blockade is necessary.

Figure D.36: Modelled Water Levels at Kampen, Katerveer, Wijhe, Olst and Deventer along the IJssel for water levels between +0.40m NAP and +0.50m NAP for stagnating winds.

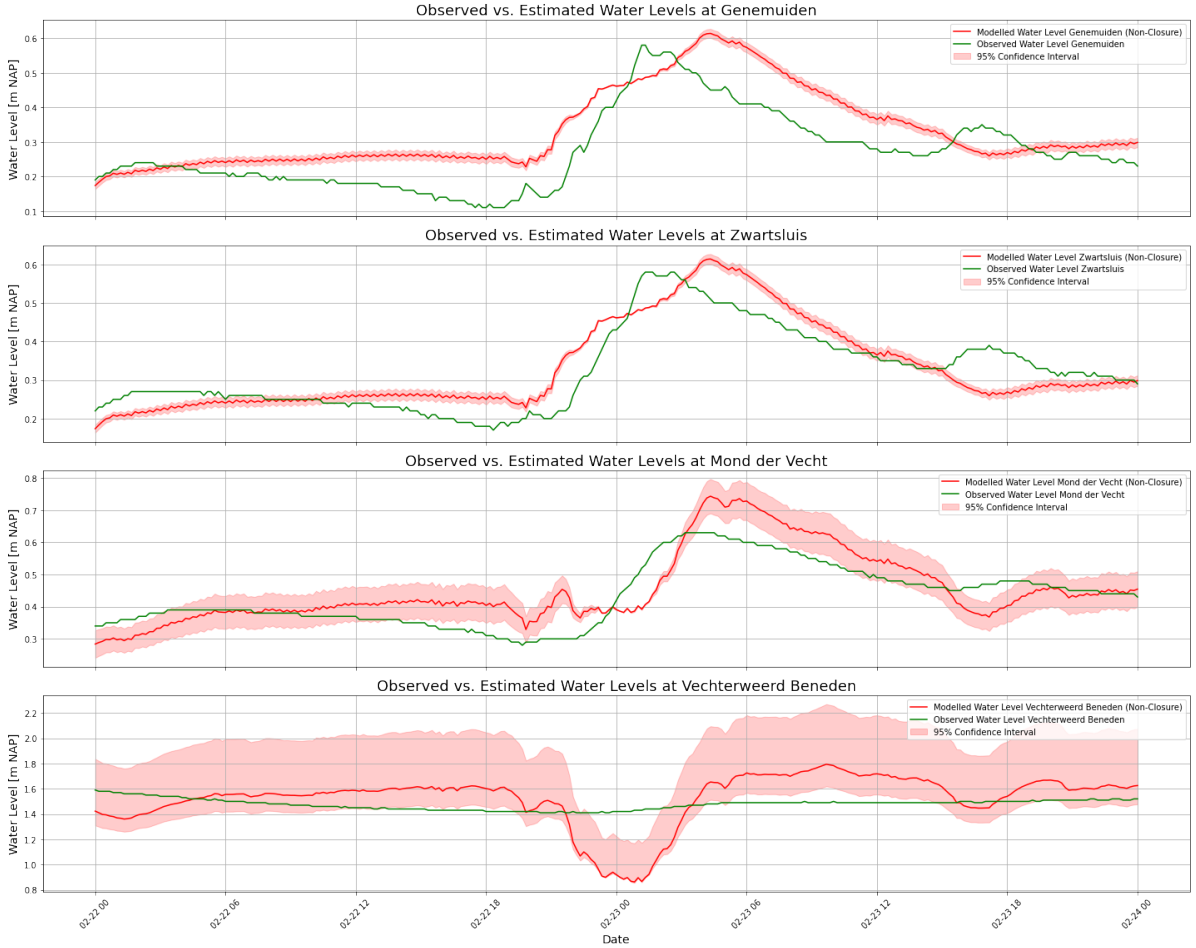

Figure D.37: Modelled Water Levels at Genemuiden, Zwartsluis, Mond der Vecht and Vechterweerd Beneden along the Zwarte Water and Vecht for water levels between +0.40m NAP and +0.50m NAP for stagnating winds.

D.5.3. Increasing

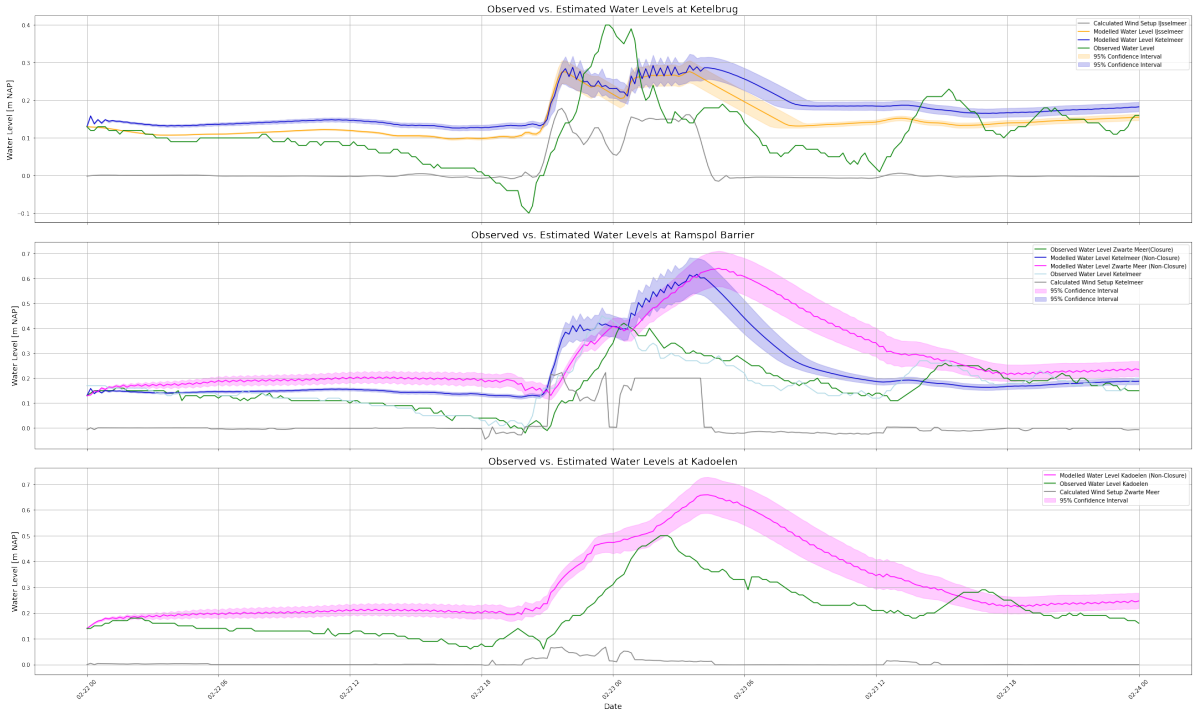

Figure D.38: Modelled Water Levels at the Ketelbrug, Ramspol Barrier and Kadoelen for water levels between +0.40m and +0.50m NAP for increasing winds.

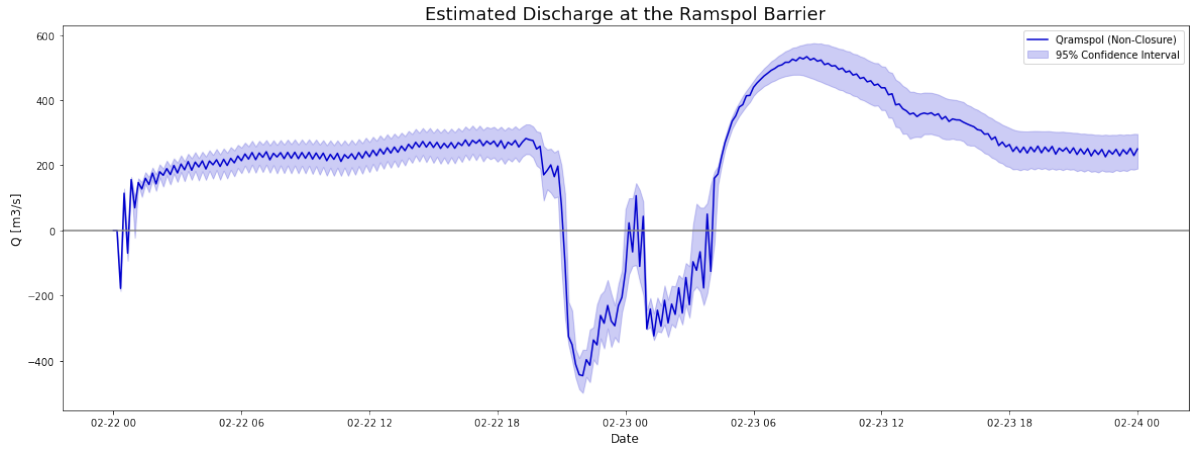

Figure D.39: Modelled discharge at the Ramspol Barrier for water levels between +0.40m and +0.50m NAP for increasing winds.

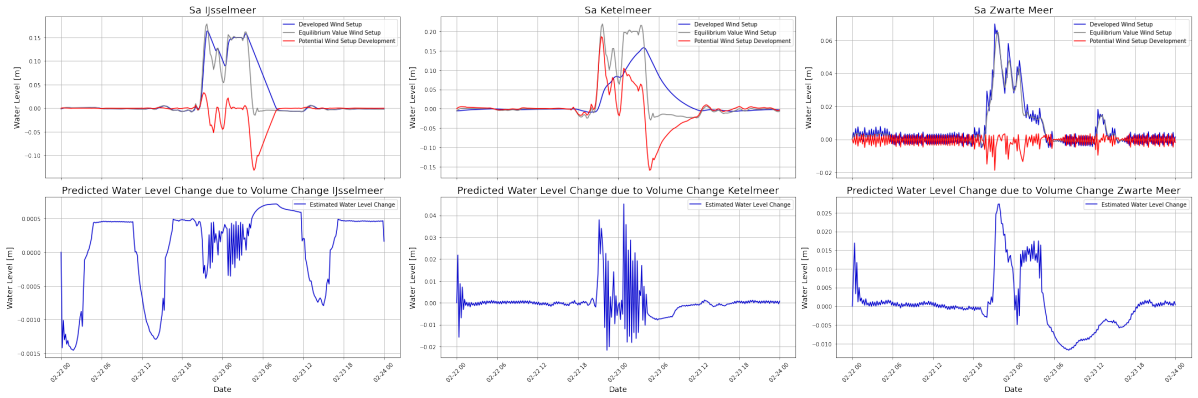

Figure D.40: Wind setup development potential and predicted volume changes for February 23, 2024, during an increasing wind to evaluate whether a navigation blockade is necessary.

Figure D.41: Modelled Water Levels at Kampen, Katerveer, Wijhe, Olst and Deventer along the IJssel for water levels between +0.40m NAP and +0.50m NAP for increasing winds.

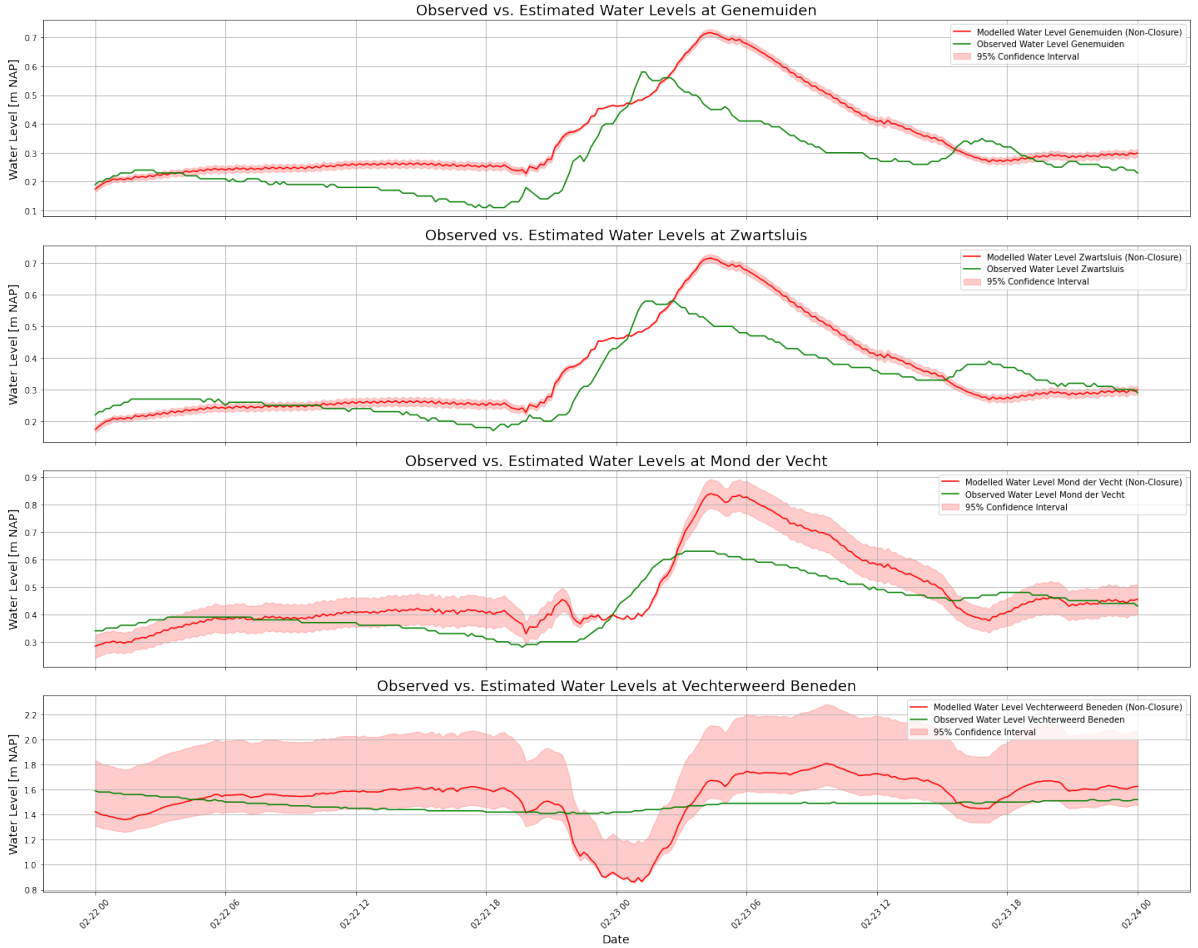

Figure D.42: Modelled Water Levels at Genemuiden, Zwartsluis, Mond der Vecht and Vechterweerd Beneden along the Zwarte Water and Vecht for water levels between +0.40m NAP and +0.50m NAP for increasing winds.

D.6. Subsequent Water Level Peaks and Closures

D.6.1. Second Peak when Water Levels are Recovered from First Closure

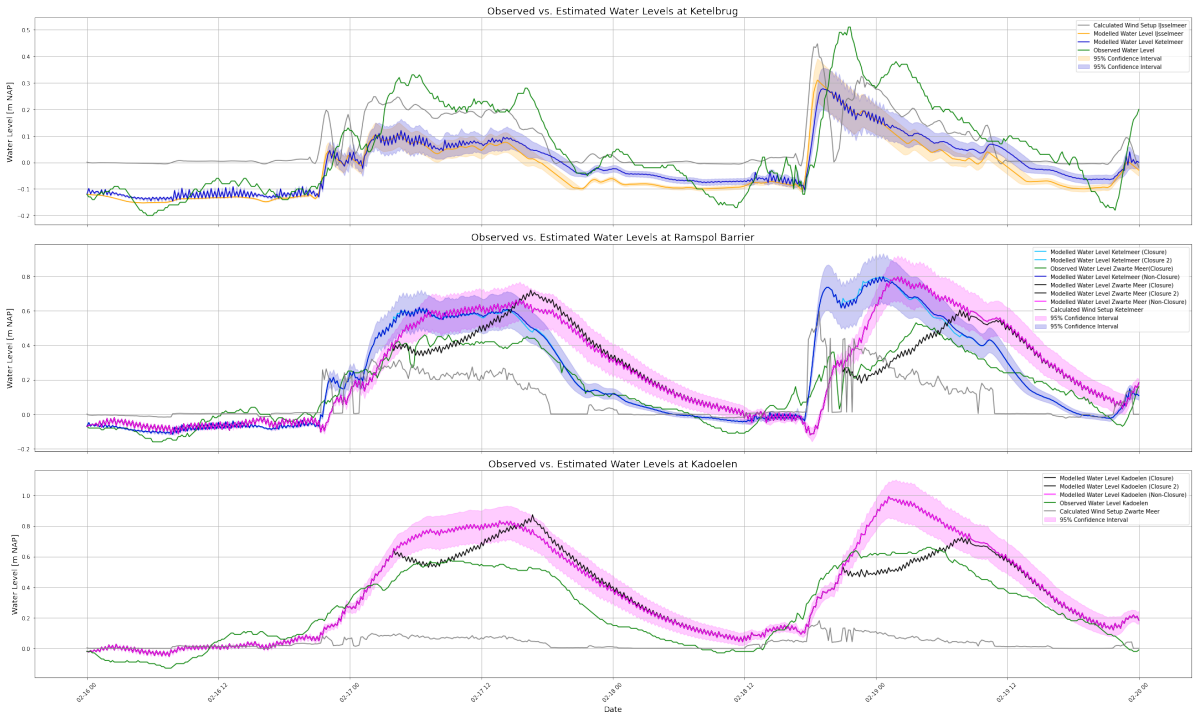

Figure D.43: Modelled Water Levels at the Ketelbrug, Ramspol Barrier and Kadoelen for two closures with the second peak hitting when the water levels in the system have recovered.

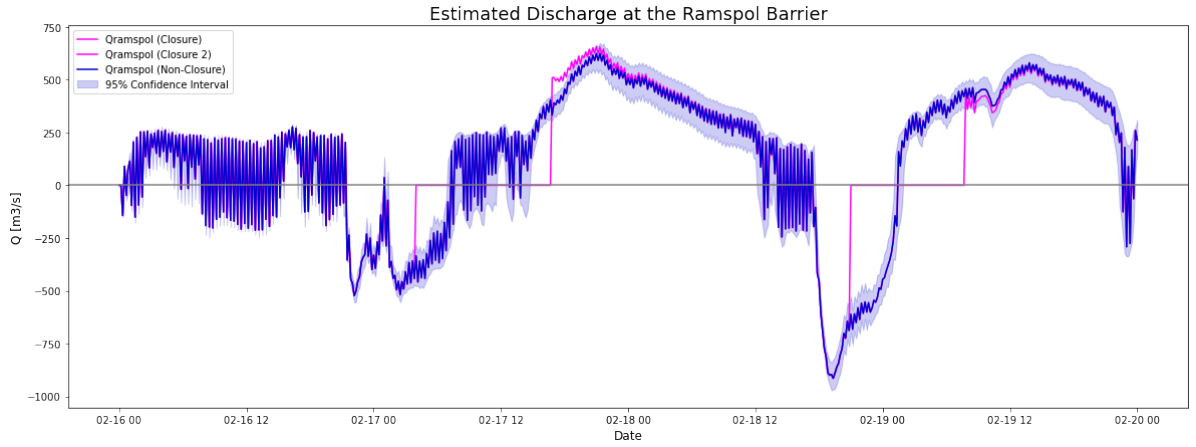

Figure D.44: Modelled discharge at the Ramspol Barrier for northwestern winds for two closures with the second peak hitting when the water levels in the system have recovered.

Figure D.45: Modelled Water Levels at Kampen, Katerveer, Wijhe, Olst and Deventer along the IJssel for two closures with the second peak hitting when the water levels in the system have recovered

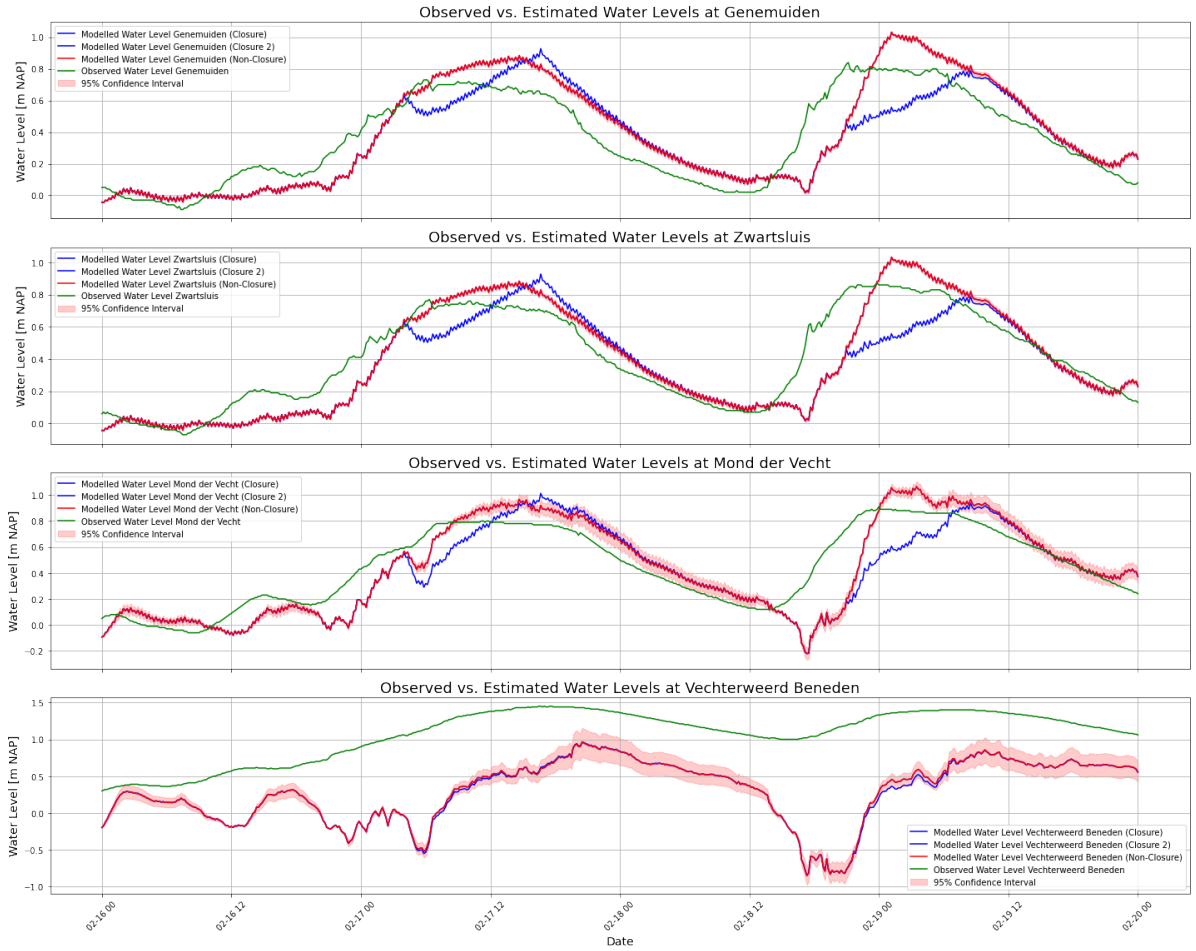

Figure D.46: Modelled Water Levels at Genemuiden, Zwartsluis, Mond der Vecht and Vechterweerd Beneden along the Zwarte Water and Vecht for two closures with the second peak hitting when the water levels in the system have recovered

D.6.2. Second Peak while Water Levels are still Recovering from First Closure

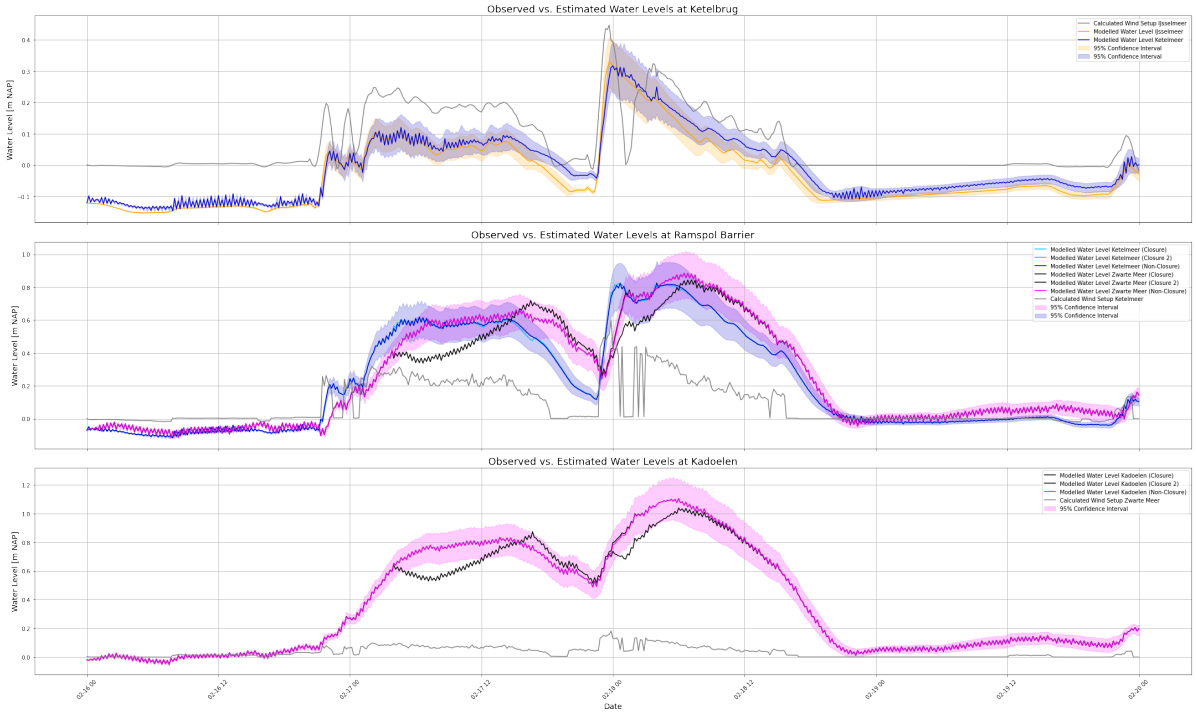

Figure D.47: Modelled Water Levels at the Ketelbrug, Ramspol Barrier and Kadoelen for two closures with the second peak hitting when the water levels in the system are still recovering.

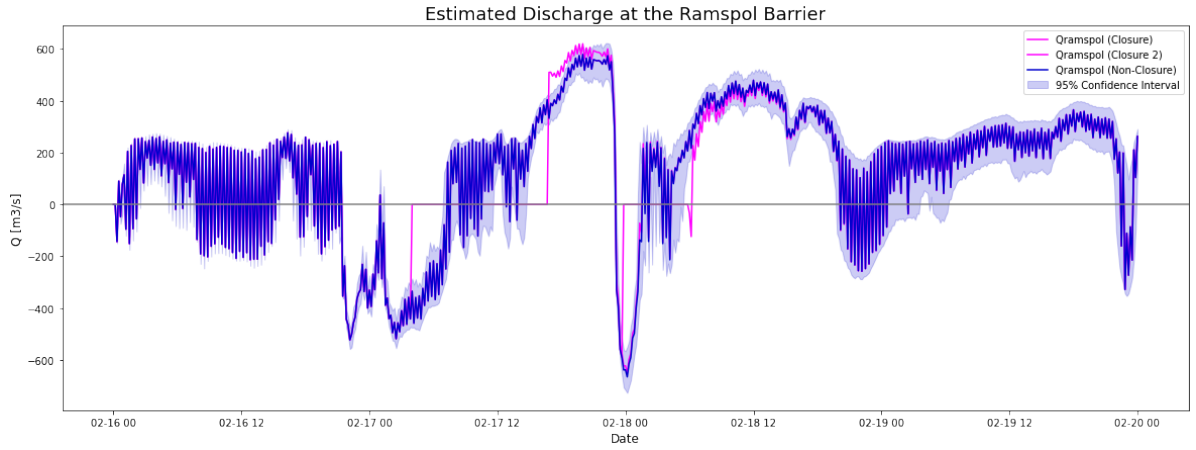

Figure D.48: Modelled discharge at the Ramspol Barrier for northwestern winds for two closures with the second peak hitting when the water levels in the system are still recovering.

Figure D.49: Modelled Water Levels at Kampen, Katerveer, Wijhe, Olst and Deventer along the IJssel for two closures with the second peak hitting when the water levels in the system are still recovering.

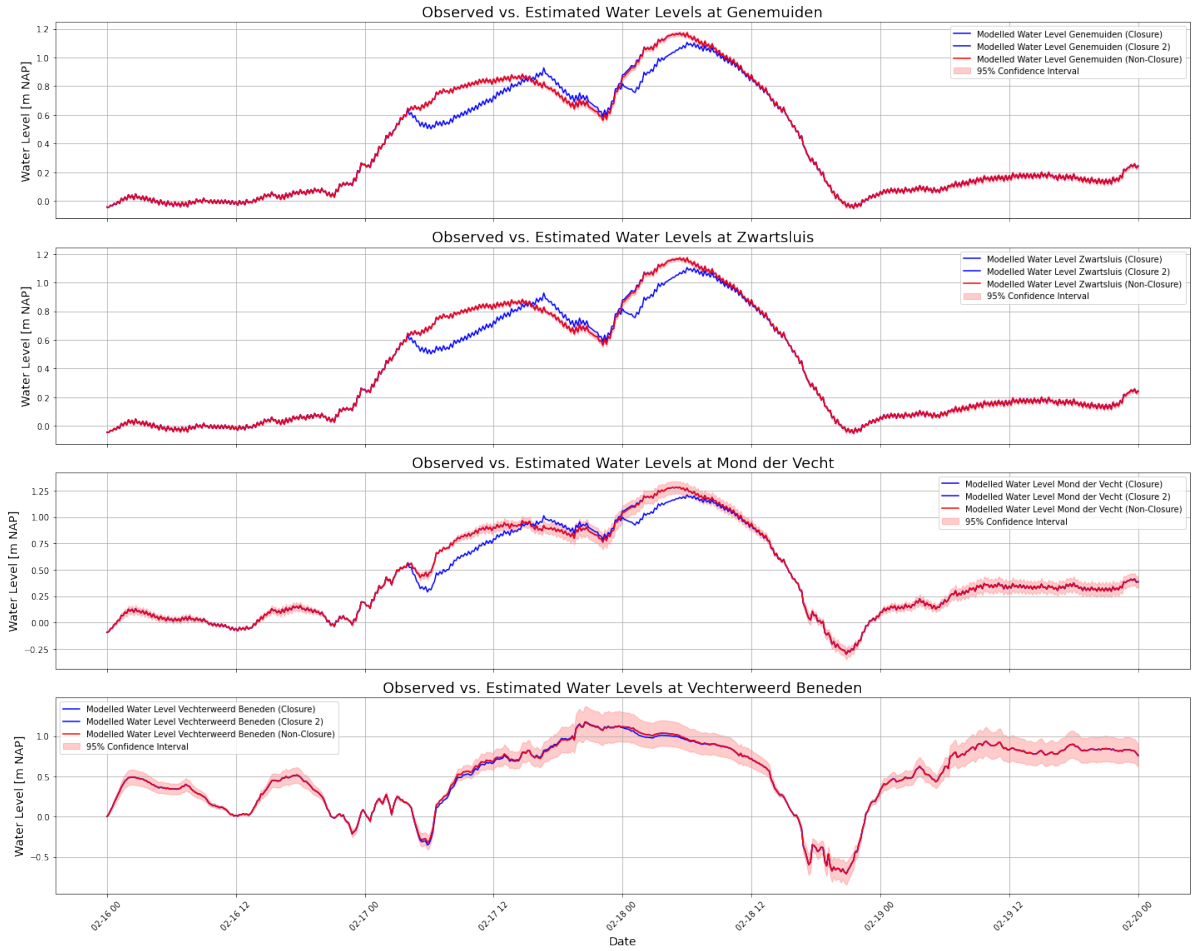

Figure D.50: Modelled Water Levels at Genemuiden, Zwartsluis, Mond der Vecht and Vechterweerd Beneden along the Zwarte Water and Vecht for two closures with the second peak hitting when the water levels in the system are still recovering.

D.6.3. Second Peak during Opening Procedure

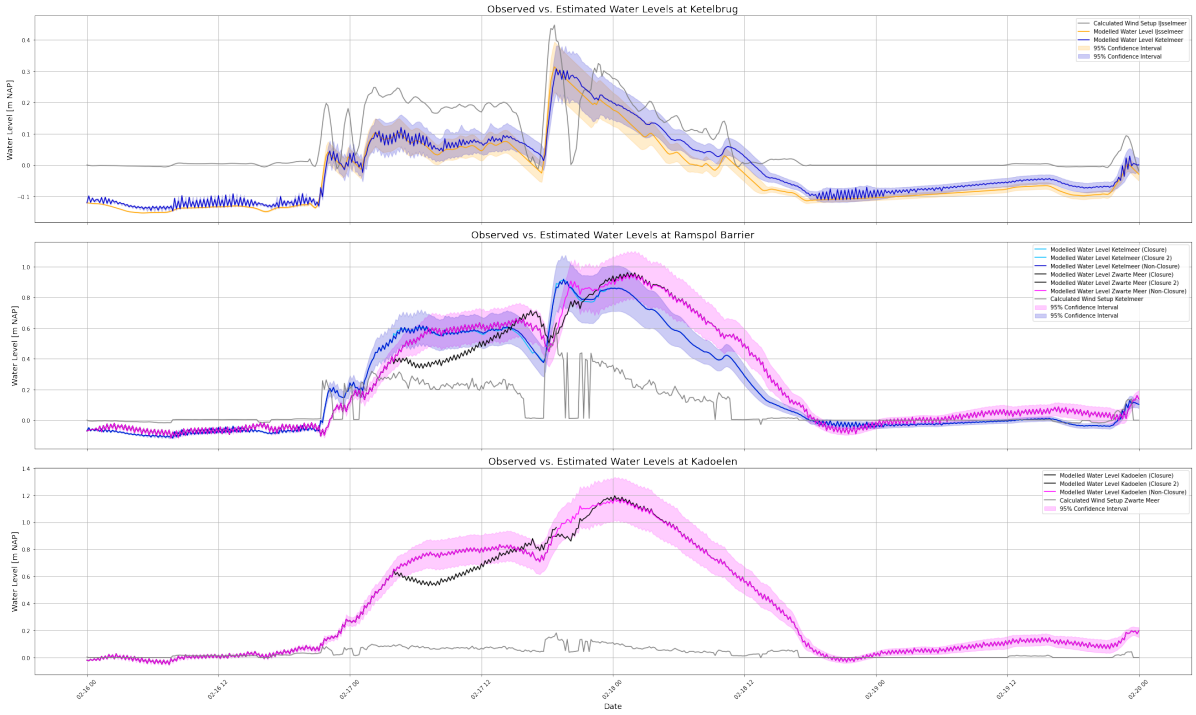

Figure D.51: Modelled Water Levels at the Ketelbrug, Ramspol Barrier and Kadoelen for two closures with the second peak hitting when the barrier is opening from the first peak.

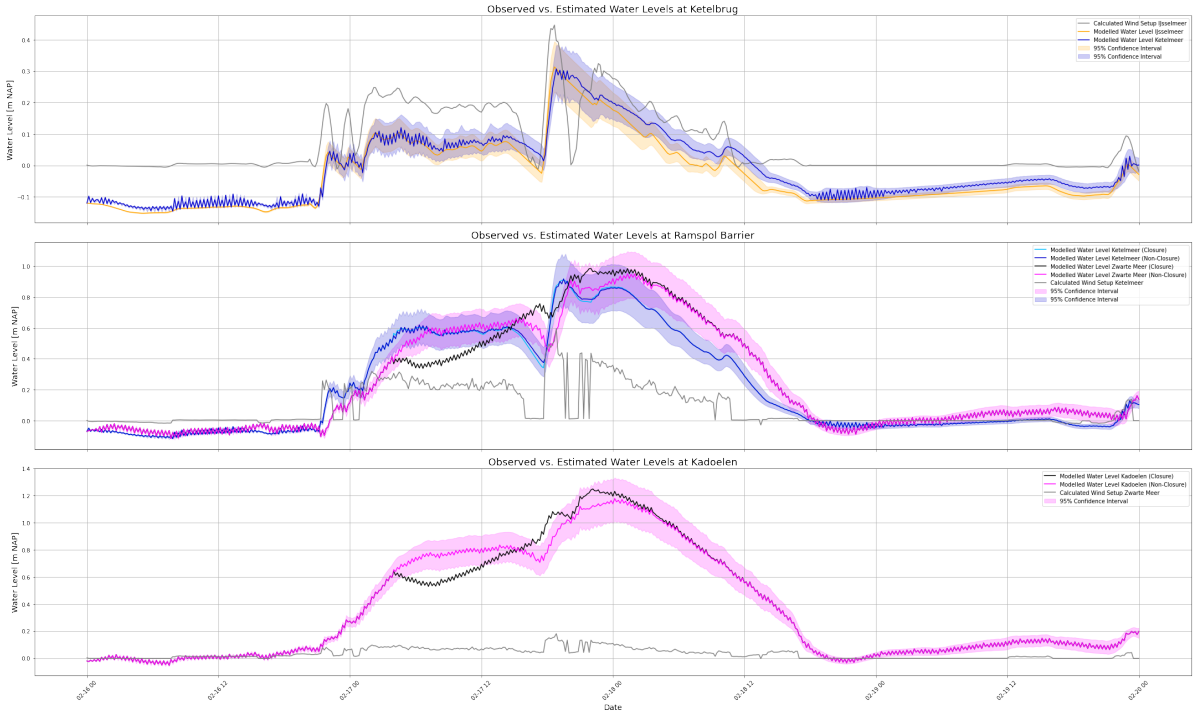

Figure D.52: Modelled Water Levels at the Ketelbrug, Ramspol Barrier and Kadoelen for northwestern winds for two peaks with an elongated closure.

D.7. Initial Water Level at the Ketelmeer above +0.50m NAP

Shorter Scenario

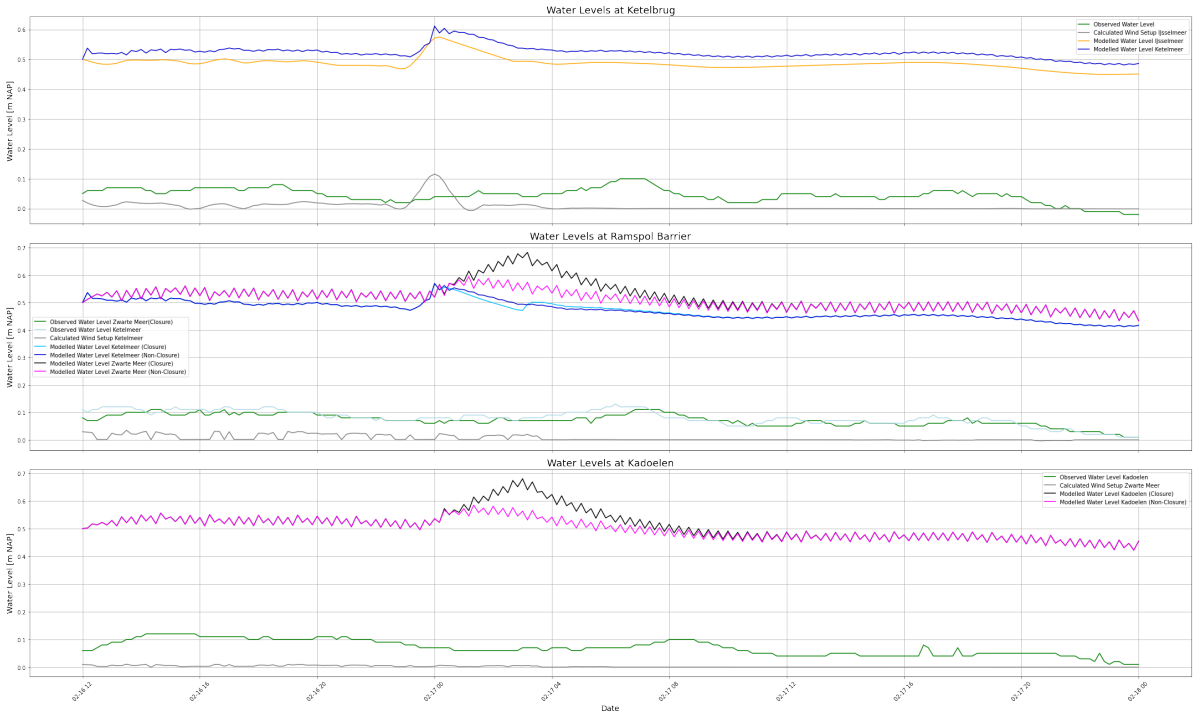

Figure D.53: Modelled Water Levels at the Ketelbrug, Ramspol Barrier and Kadoelen during the simulation of an initial water level of +0.50m NAP and a wind setup 'peak' on the IJsselmeer of 0.10 metres for closure and non-closure case.

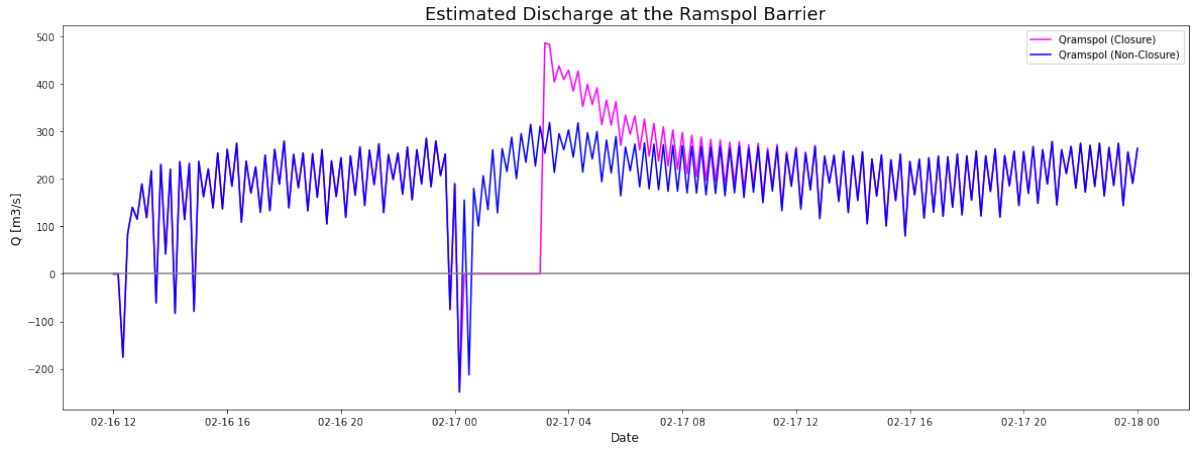

Figure D.54: Modelled discharge at the Ramspol Barrier for a wind peak of 10 centimetres for two hours

Longer Peak Scenario

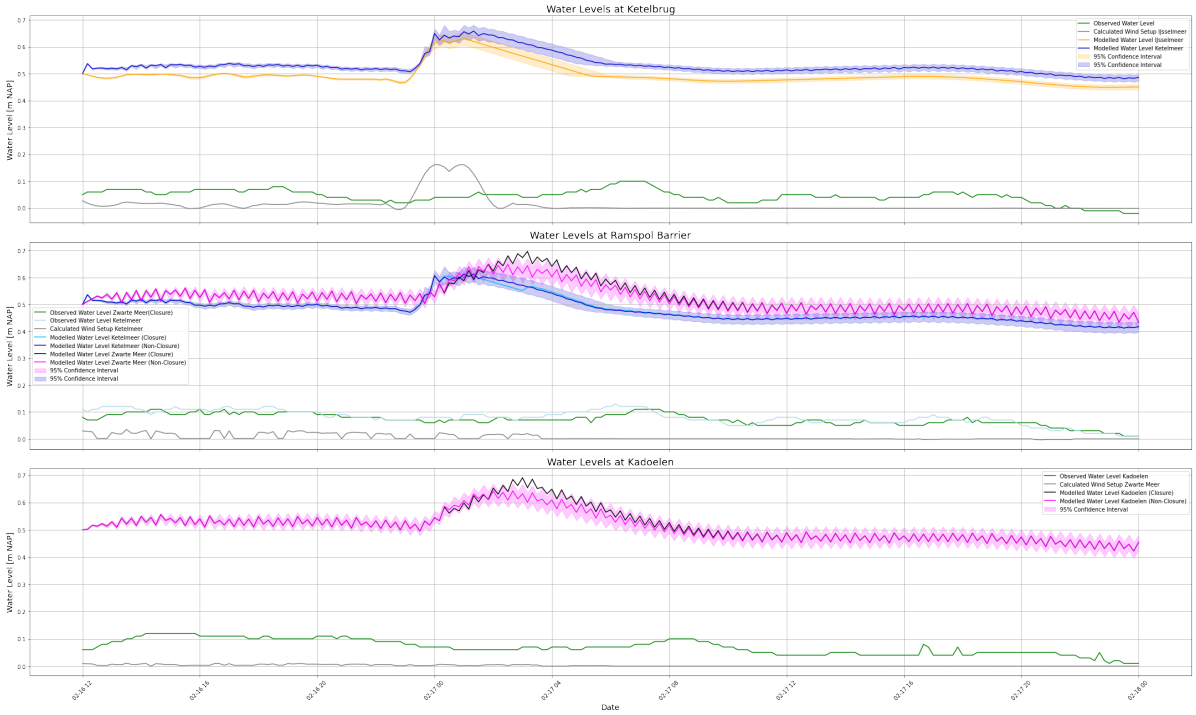

Figure D.55: Modelled Water Levels at the Ketelbrug, Ramspol Barrier and Kadoelen during the simulation of an initial water level of +0.50m NAP and a wind setup 'peak' on the IJsselmeer of 0.15 metres for two hours for closure and non-closure case.

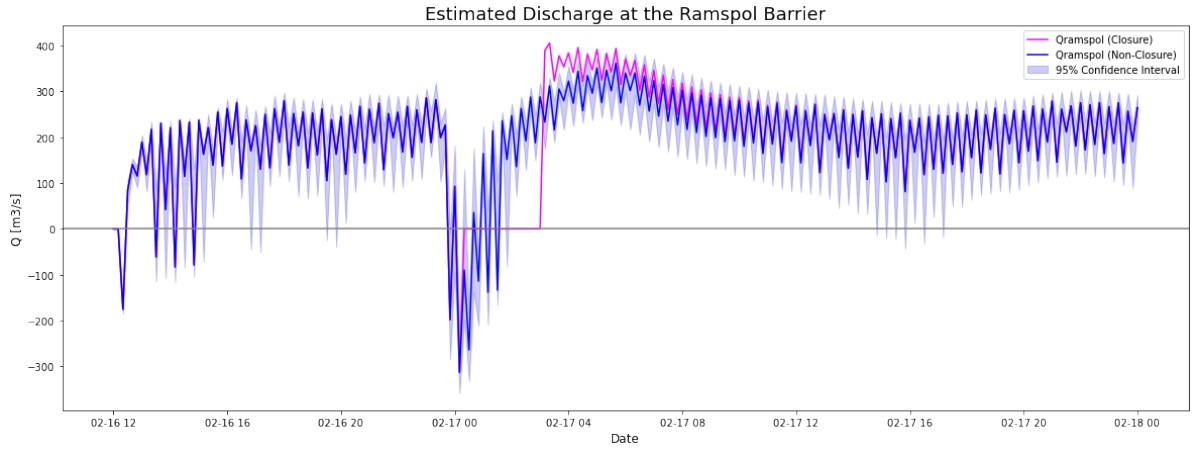

Figure D.56: Modelled discharge at the Ramspol Barrier for a wind peak of 15 centimetres for two hours

Middle Peak Scenario

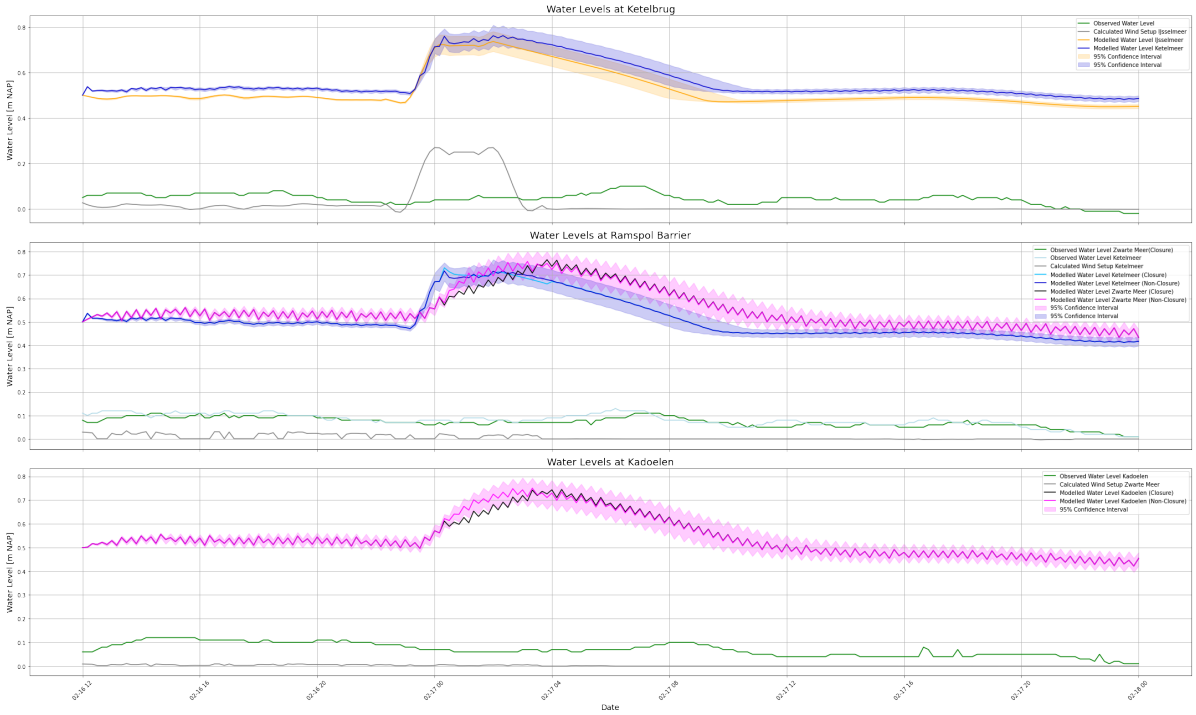

Figure D.57: Modelled Water Levels at the Ketelbrug, Ramspol Barrier and Kadoelen during the simulation of an initial water level of +0.50m NAP and a wind setup 'peak' on the IJsselmeer of 0.25 metres for three hours for closure and non-closure case.

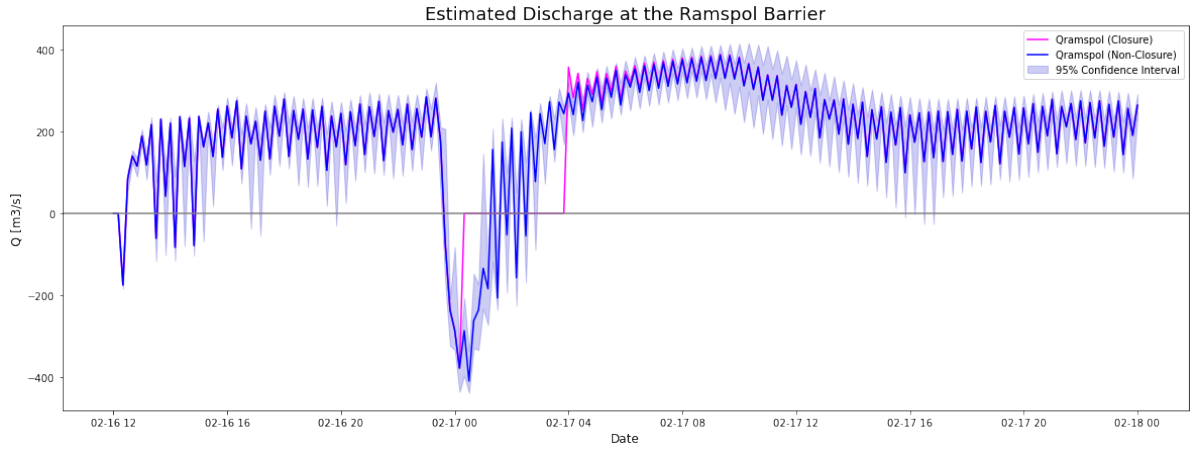

Figure D.58: Modelled discharge at the Ramspol Barrier during a wind peak of 25 centimetres for 3 hours.

Higher Peak Scenrio

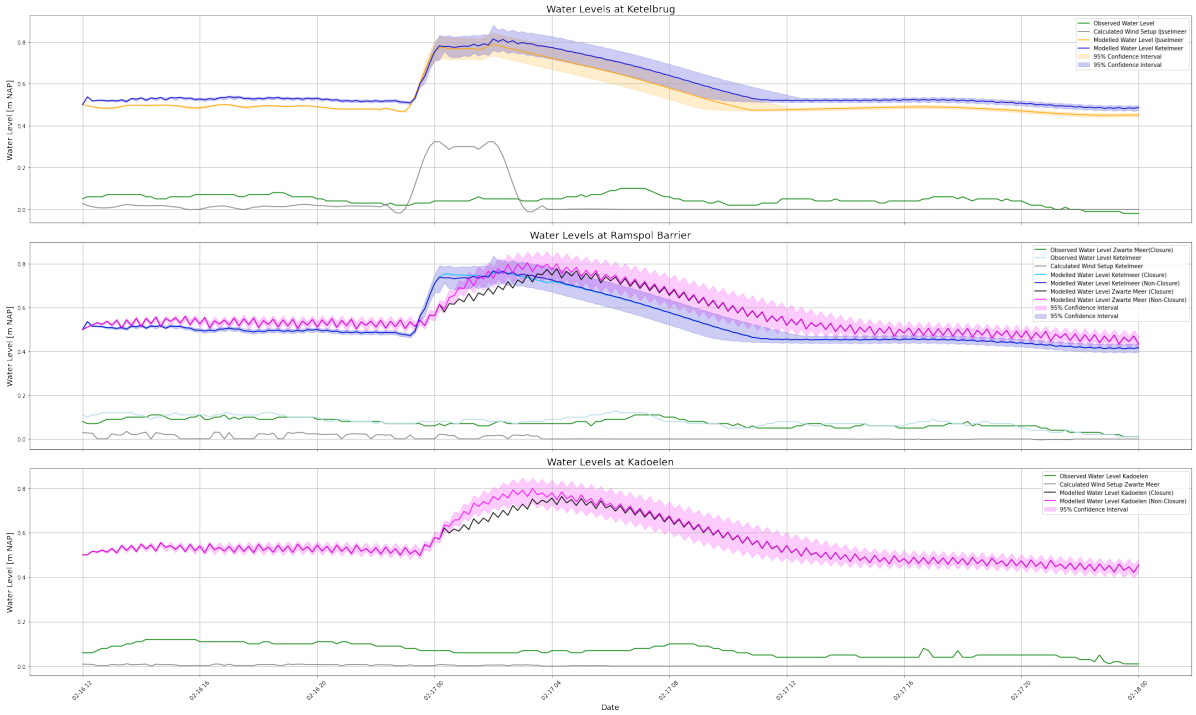

Figure D.59: Modelled Water Levels at the Ketelbrug, Ramspol Barrier and Kadoelen during the simulation of an initial water level of +0.50m NAP and a wind setup 'peak' on the IJsselmeer of 0.30 metres for three hours for closure and non-closure case.

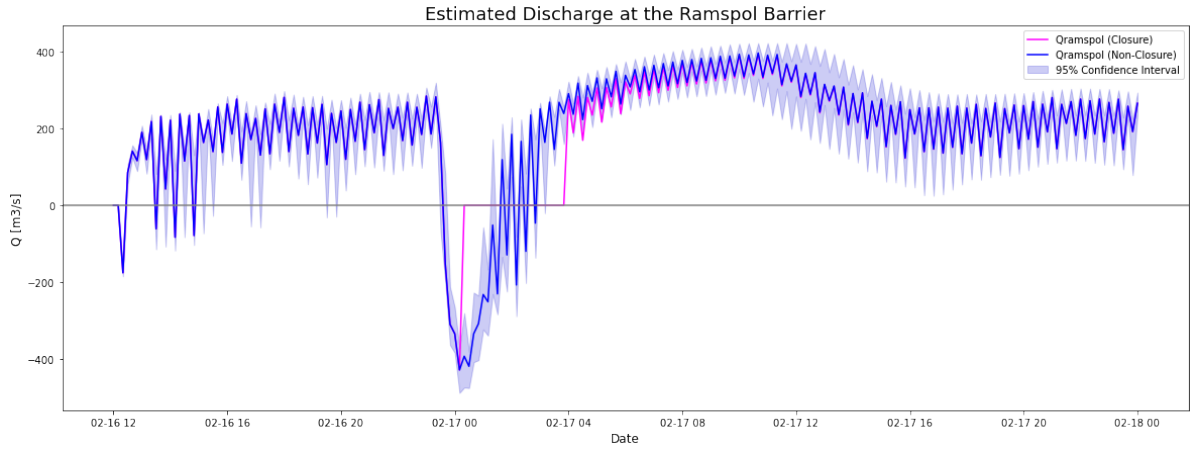

Figure D.60: Modelled discharge at the Ramspol Barrier during a wind peak of 30 centimetres for 3 hours.

D.8. Closures Combined with a large Q_{ZW}

Initial Water Level: +0.30m NAP

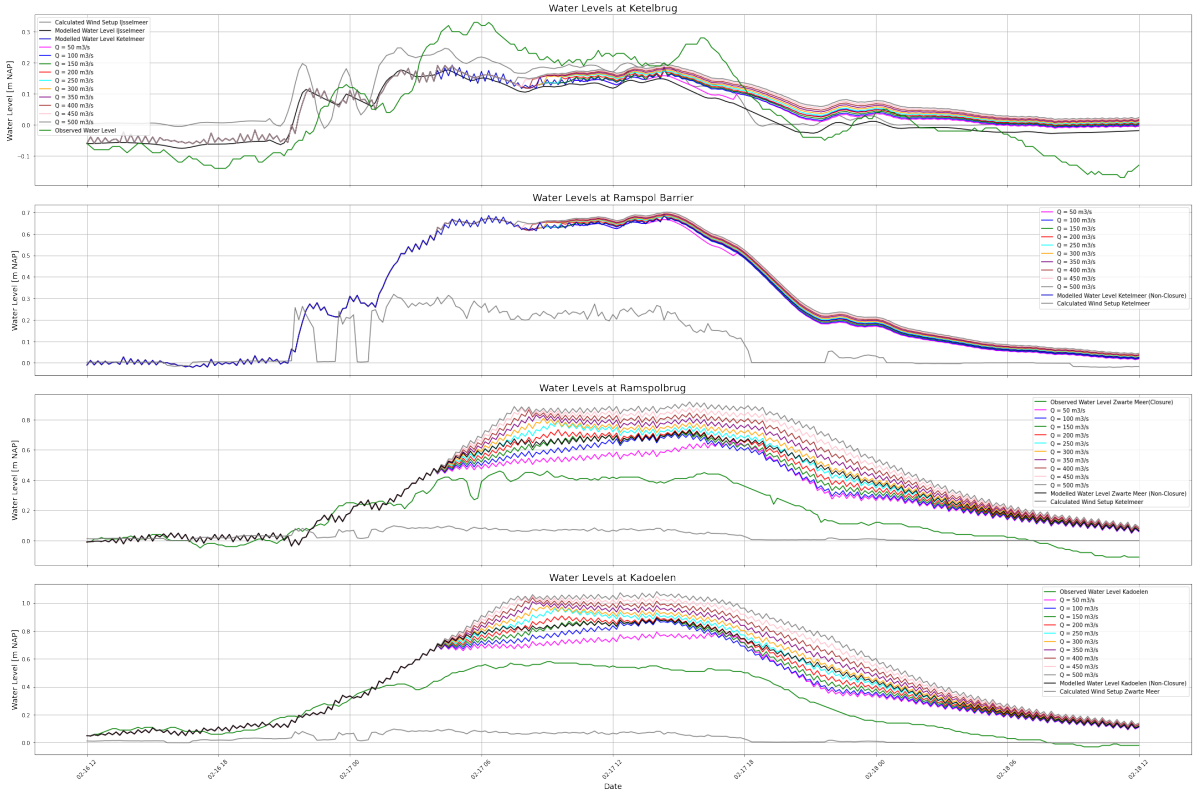

Figure D.61: Modelled Water Levels at the Ketelbrug, Ramspol Barrier and Kadoelen for varying Q_{zw} during closure.

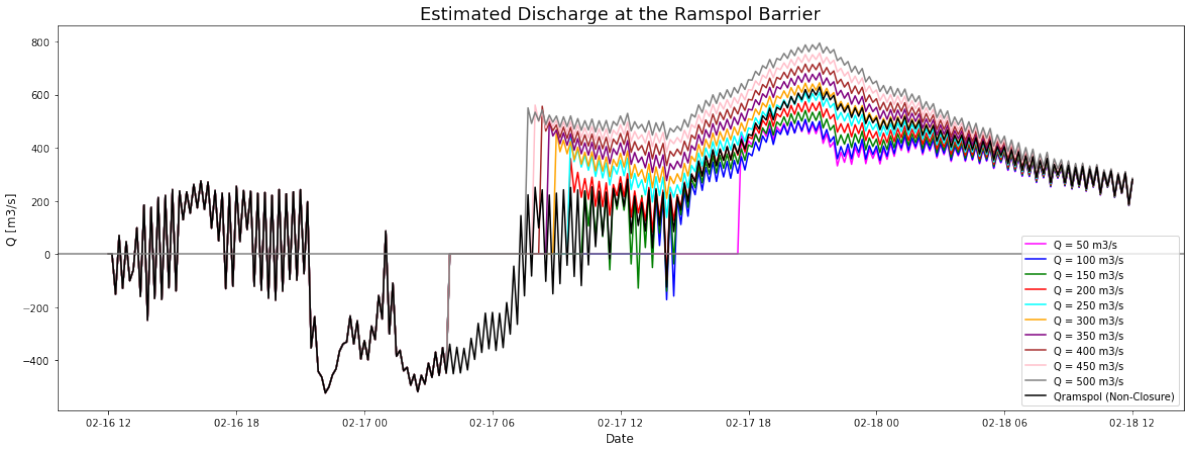

Figure D.62: Modelled discharge at the Ramspol Barrier for northwestern winds for varying Q_{zw} during closure.

Figure D.63: Modelled Water Levels at Kampen, Katerveer, Wijhe, Olst and Deventer along the IJssel for varying Q_{zw} during closure.

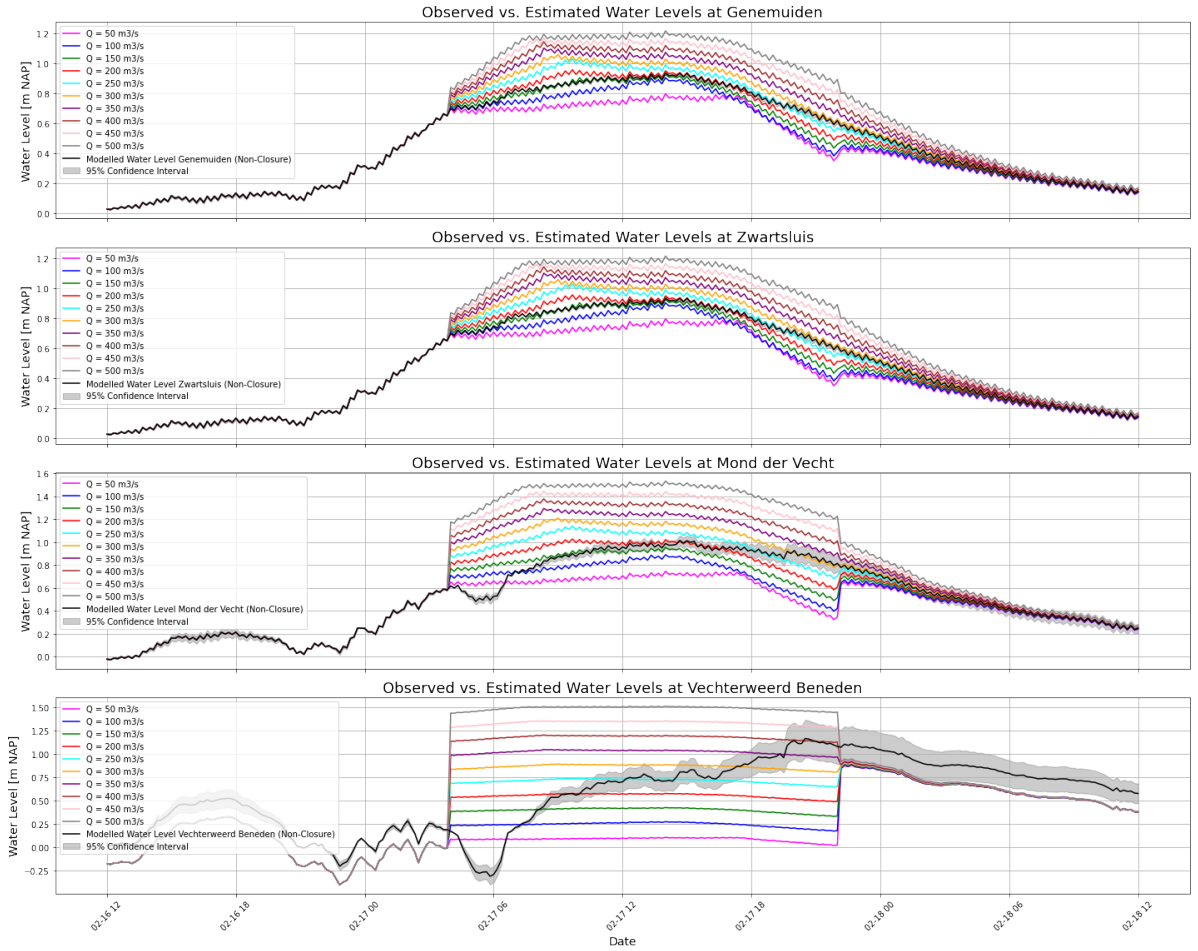

Figure D.64: Modelled Water Levels at Genemuiden, Zwartsluis, Mond der Vecht and Vechterweerd Beneden along the Zwarte Water and Vecht for varying Q_{zw} during closure.

D.9. No Drainage Capacity over the Afsluitdijk Combined with Wind Setup

Initial Water Level: +0.30m NAP

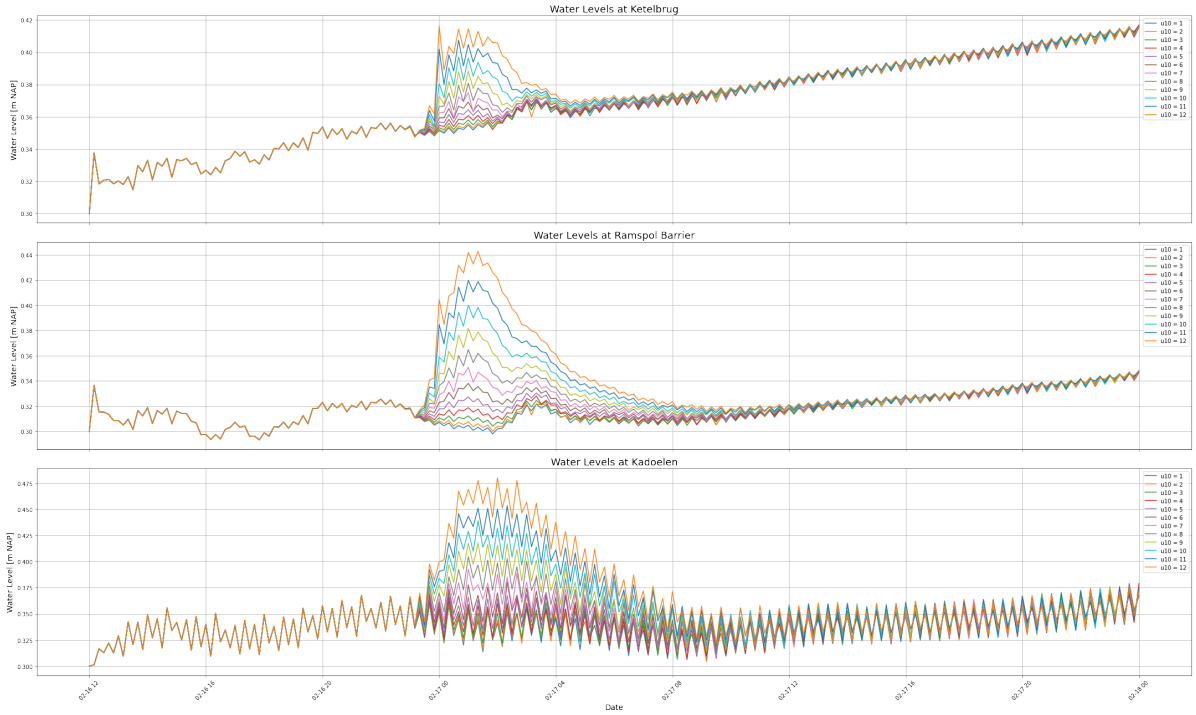

Figure D.65: Modelled Water Levels at the Ketelbrug, Ramspol Barrier and Kadoelen for northwestern winds with varying speed and an initial water level of +0.30m NAP.

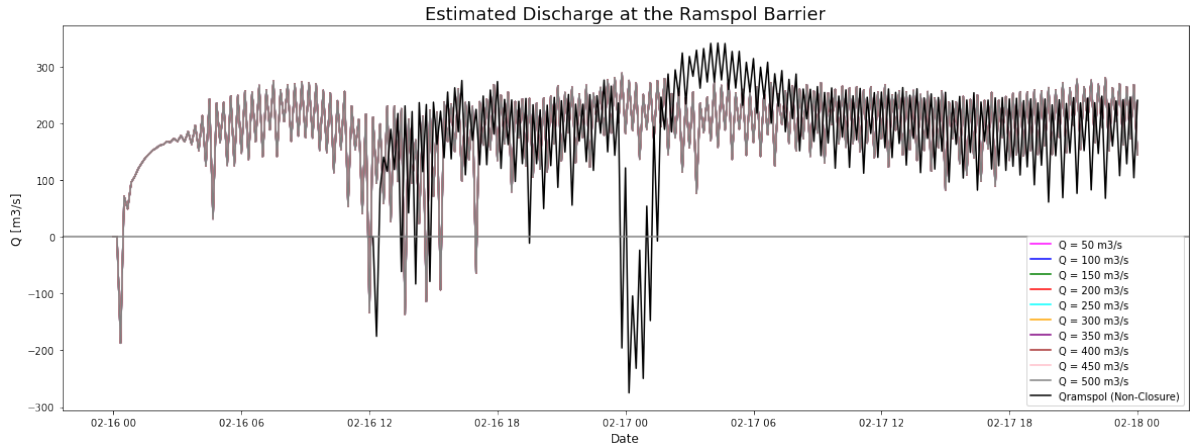

Figure D.66: Modelled discharge at the Ramspol Barrier for northwestern winds with varying speeds and an initial water level of +0.30m NAP.

Figure D.67: Modelled Water Levels at Kampen, Katerveer, Wijhe, Olst and Deventer along the IJssel for northwestern winds with varying speeds and an initial water level of +0.30m NAP.

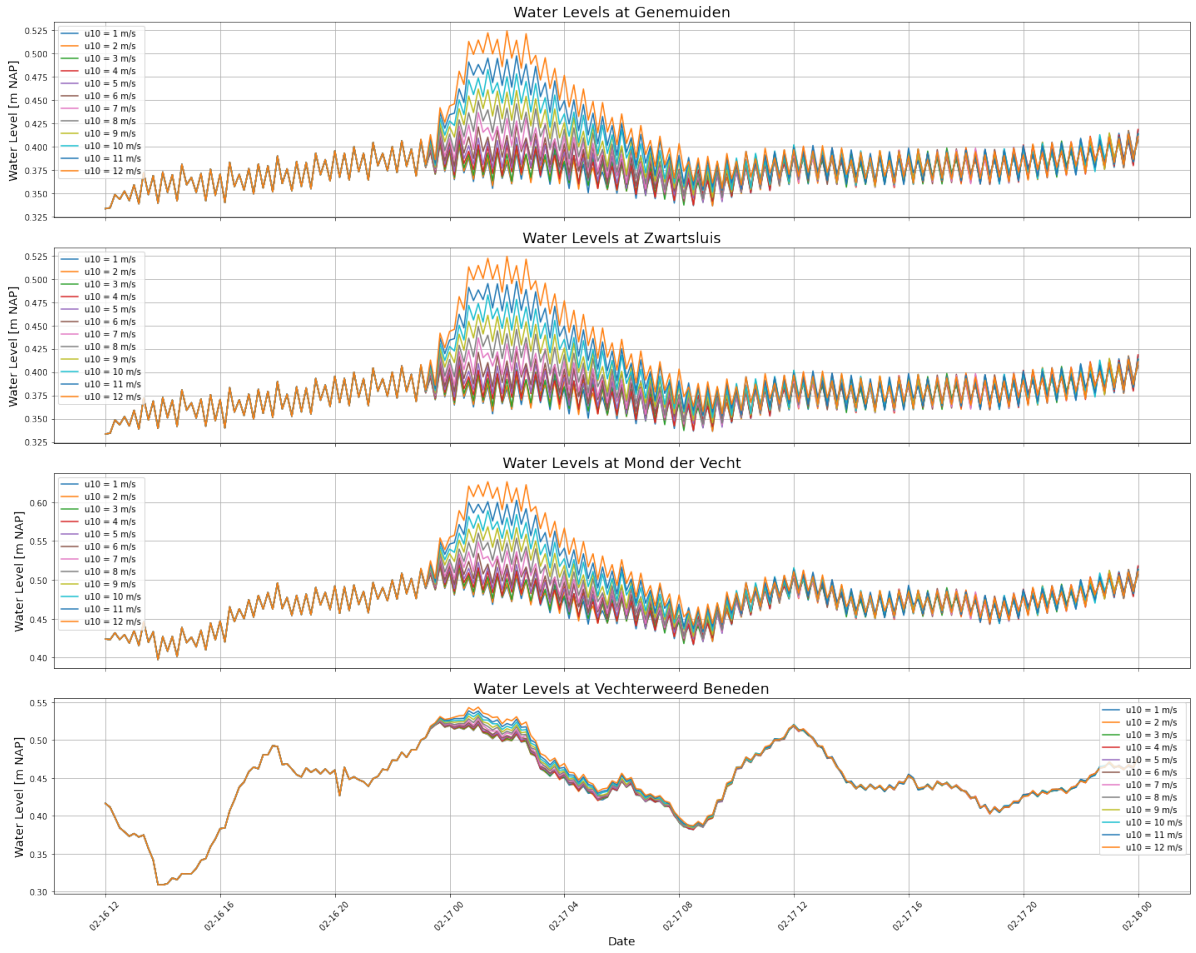

Figure D.68: Modelled Water Levels at Genemuiden, Zwartsluis, Mond der Vecht and Vechterweerd Beneden along the Zwarte Water and Vecht for northwestern winds with varying speed and an initial water level of +0.30m NAP.

Initial Water Level: +0.35m NAP

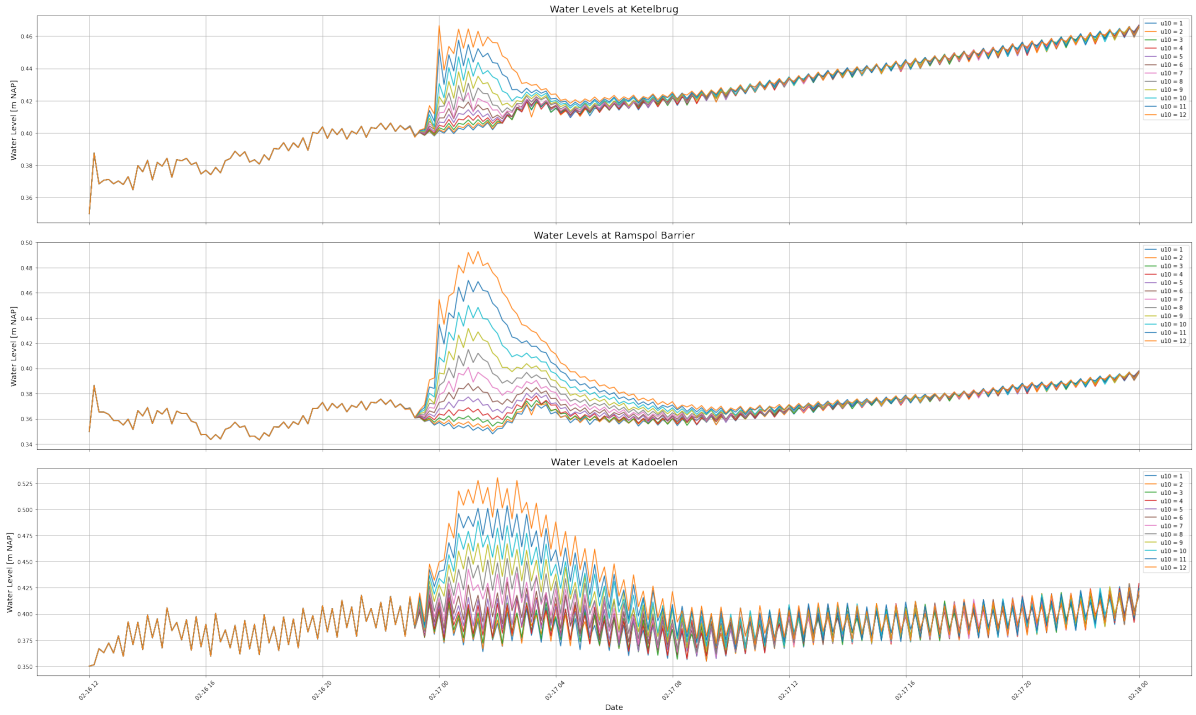

Figure D.69: Modelled Water Levels at the Ketelbrug, Ramspol Barrier and Kadoelen for northwestern winds with varying speed and an initial water level of +0.35m NAP.

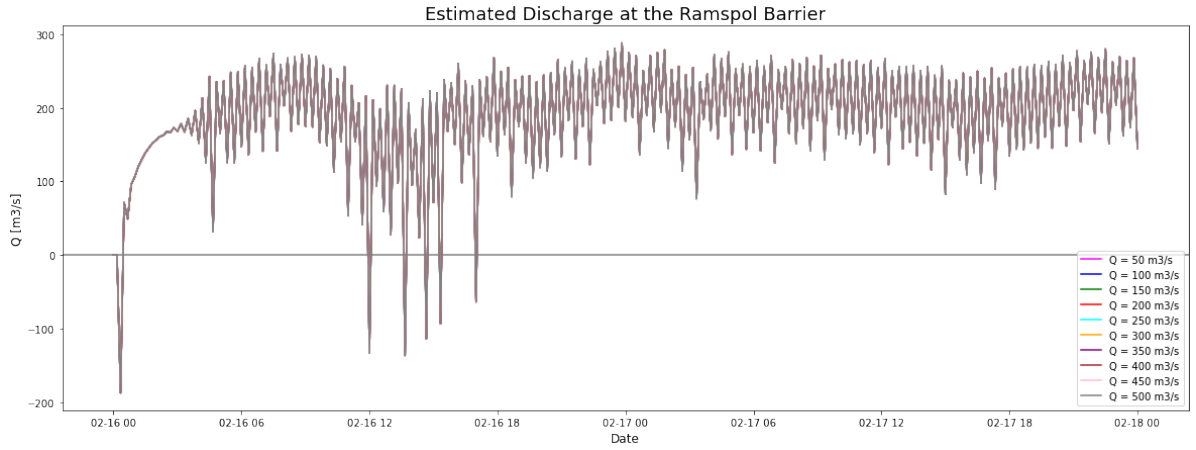

Figure D.70: Modelled discharge at the Ramspol Barrier for northwestern winds with varying speeds and an initial water level of +0.35m NAP.

Figure D.71: Modelled Water Levels at Kampen, Katerveer, Wijhe, Olst and Deventer along the IJssel for northwestern winds with varying speeds and an initial water level of +0.30m NAP.

Initial Water Level: +0.40m NAP

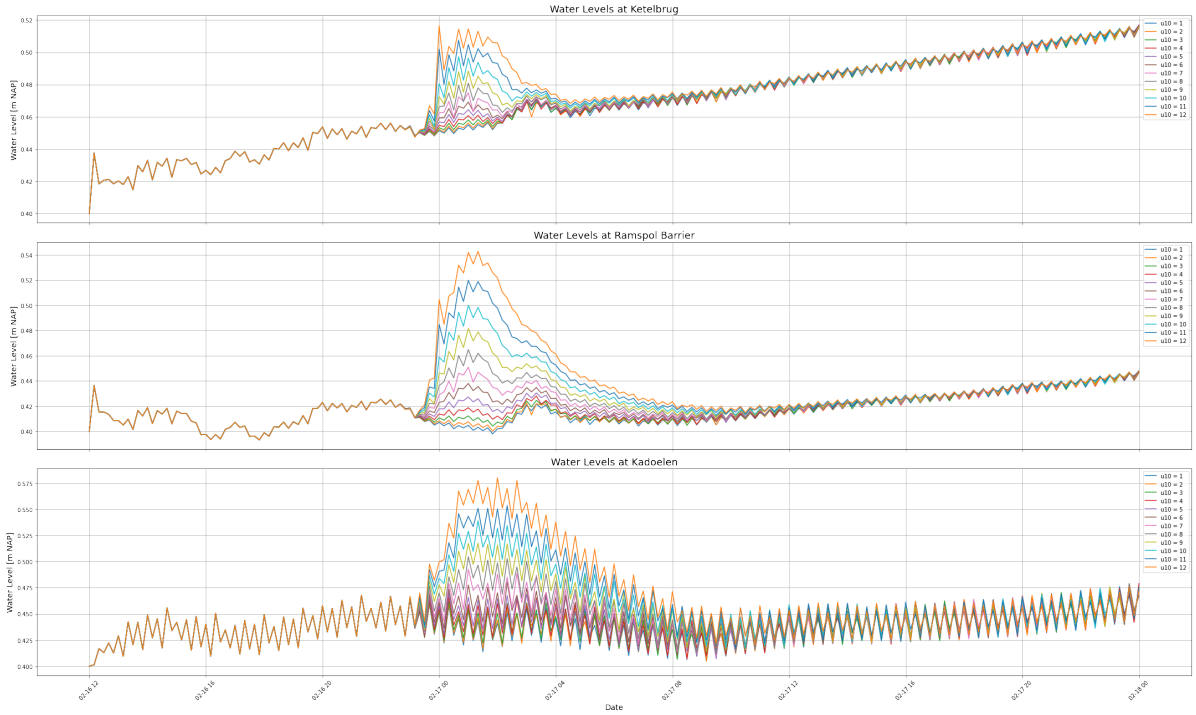

Figure D.72: Modelled Water Levels at the Ketelbrug, Ramspol Barrier and Kadoelen for northwestern winds with varying speed and an initial water level of +0.40m NAP.

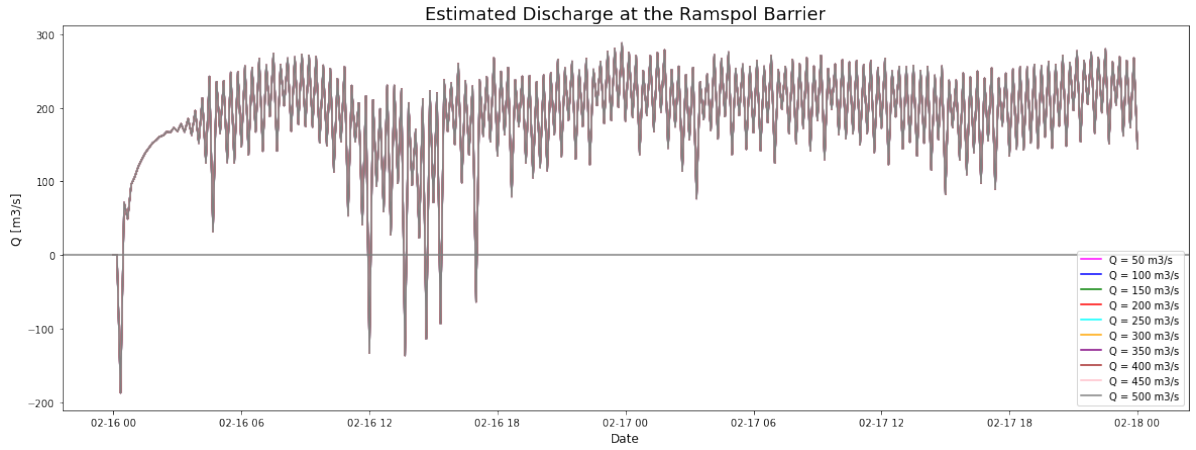

Figure D.73: Modelled discharge at the Ramspol Barrier for northwestern winds with varying speeds and an initial water level of +0.40m NAP.

Figure D.74: Modelled Water Levels at Kampen, Katerveer, Wijhe, Olst and Deventer along the IJssel for northwestern winds with varying speeds and an initial water level of +0.40m NAP.

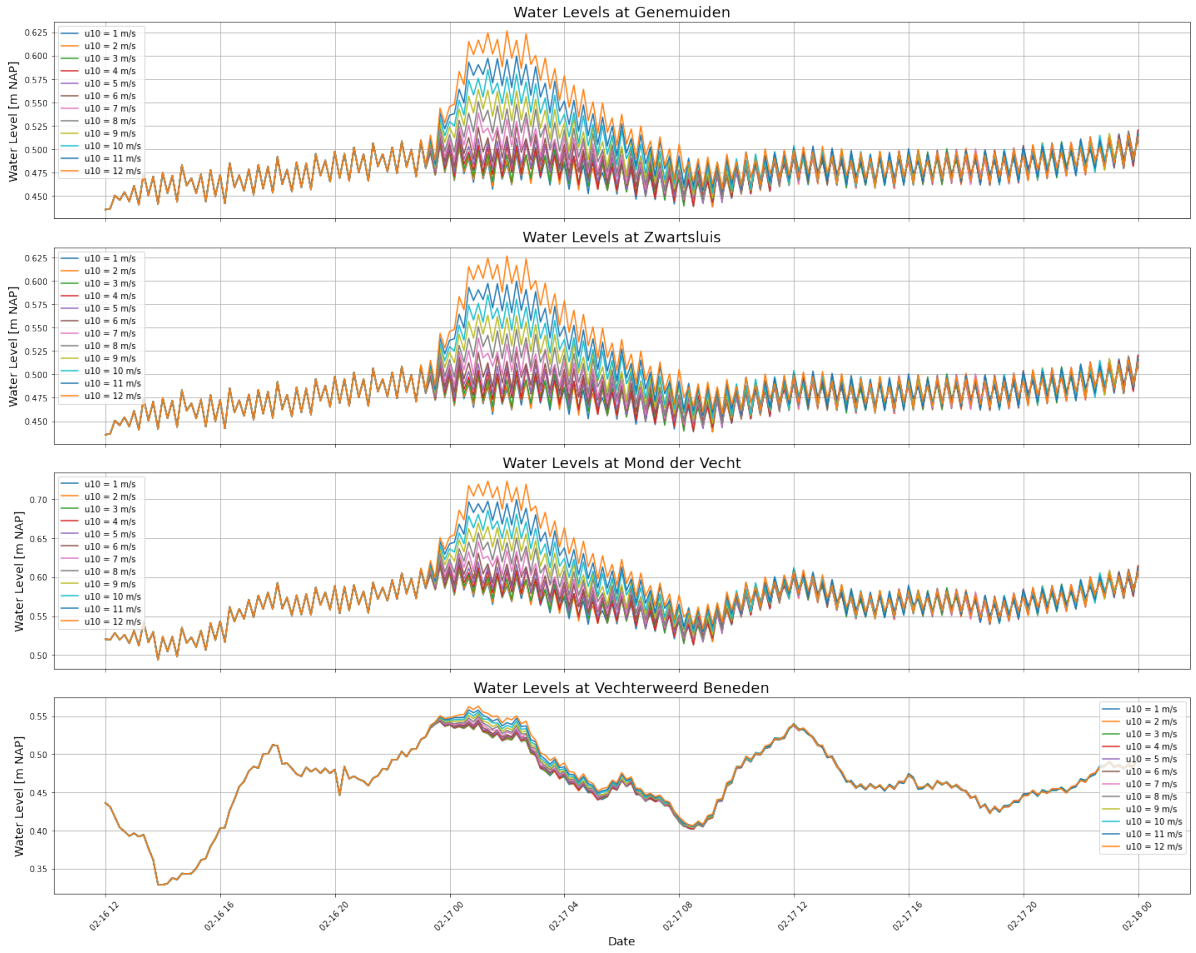

Figure D.75: Modelled Water Levels at Genemuiden, Zwartsluis, Mond der Vecht and Vechterweerd Beneden along the Zwarte Water and Vecht for northwestern winds with varying speed and an initial water level of +0.40m NAP.

Initial Water Level: +0.45m NAP

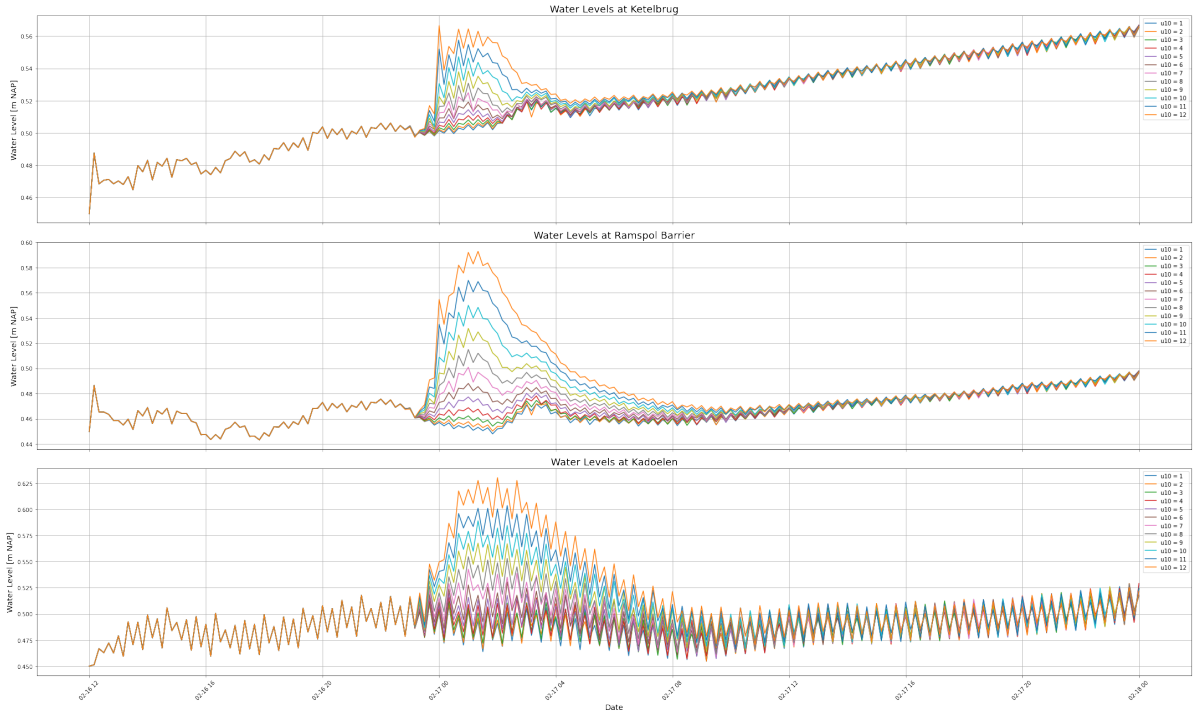

Figure D.76: Modelled Water Levels at the Ketelbrug, Ramspol Barrier and Kadoelen for northwestern winds with varying speed and an initial water level of +0.45m NAP.

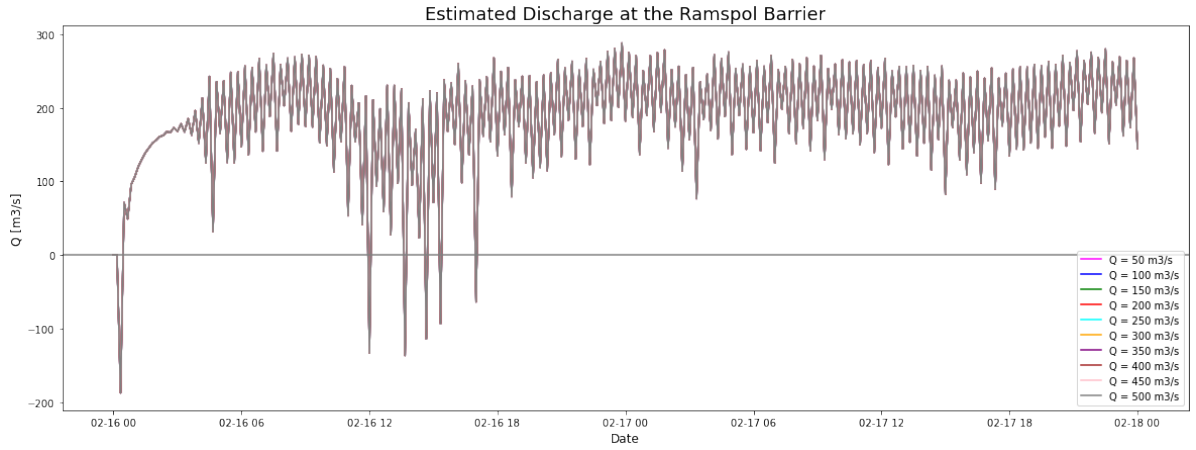

Figure D.77: Modelled discharge at the Ramspol Barrier for northwestern winds with varying speeds and an initial water level of +0.45m NAP.

Figure D.78: Modelled Water Levels at Kampen, Katerveer, Wijhe, Olst and Deventer along the IJssel for northwestern winds with varying speeds and an initial water level of +0.45m NAP.

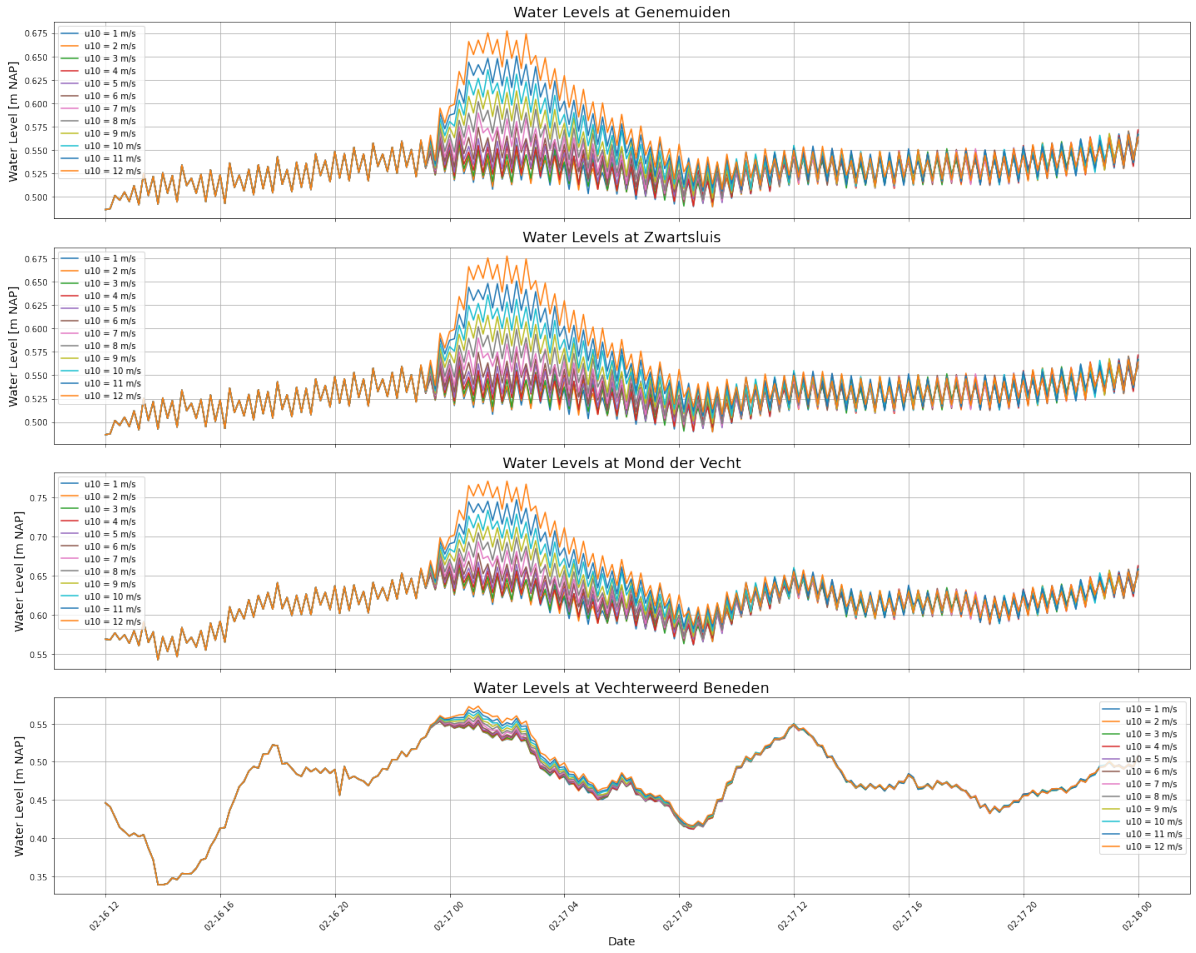

Figure D.79: Modelled Water Levels at Genemuiden, Zwartsluis, Mond der Vecht and Vechterweerd Beneden along the Zwarte Water and Vecht for northwestern winds with varying speed and an initial water level of +0.45m NAP.

Initial Water Level: +0.50m NAP

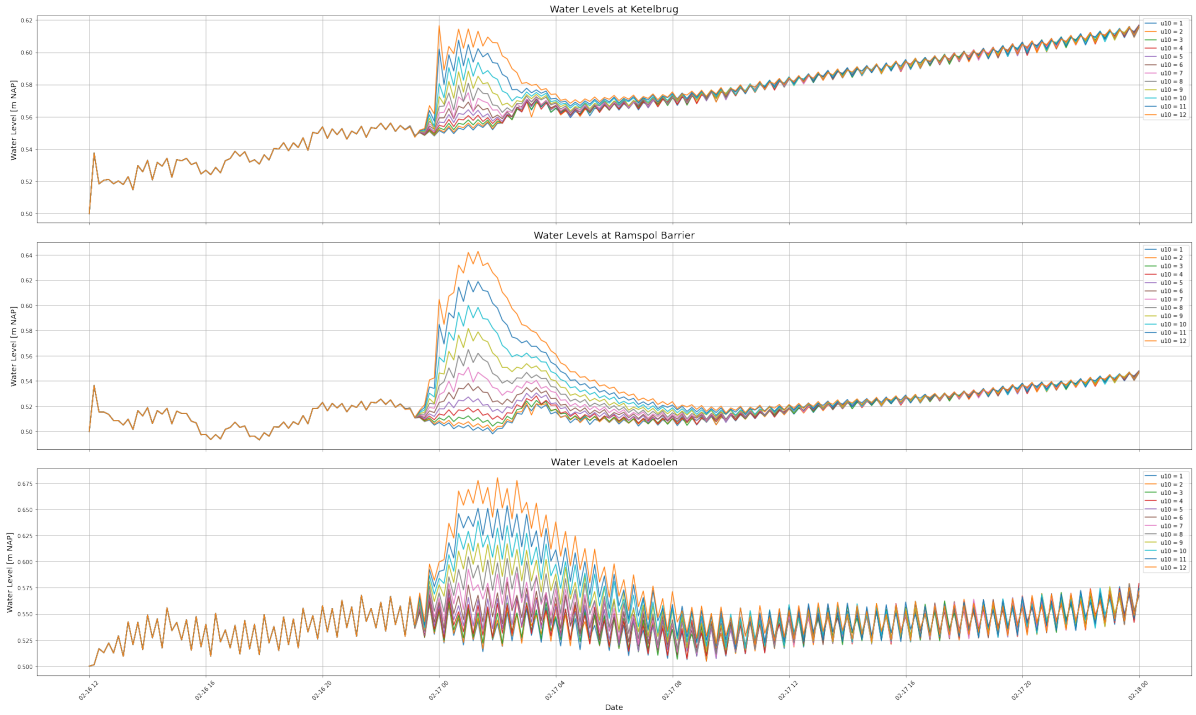

Figure D.80: Modelled Water Levels at the Ketelbrug, Ramspol Barrier and Kadoelen for northwestern winds with varying speed and an initial water level of +0.50m NAP.

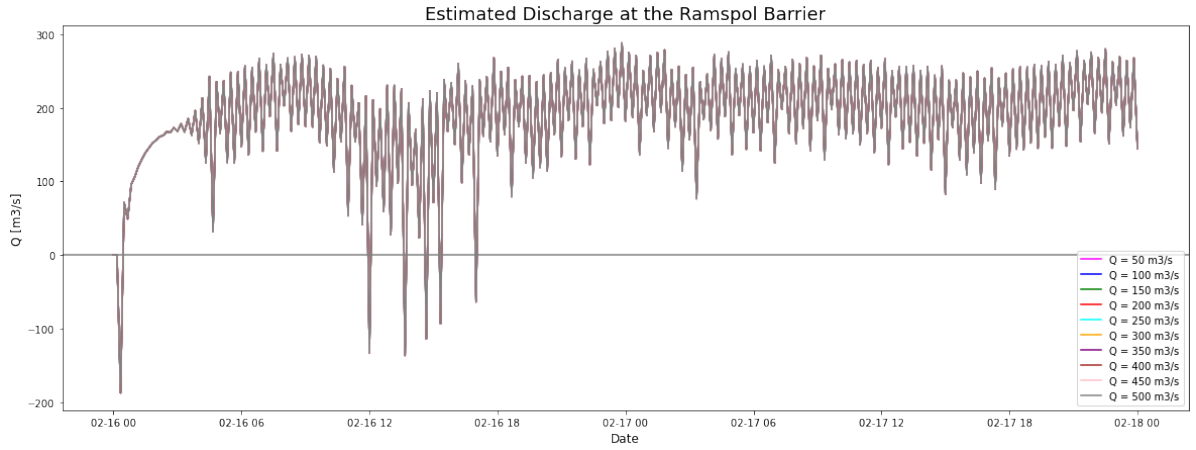

Figure D.81: Modelled discharge at the Ramspol Barrier for northwestern winds with varying speeds and an initial water level of +0.50m NAP.

Figure D.82: Modelled Water Levels at Kampen, Katerveer, Wijhe, Olst and Deventer along the IJssel for northwestern winds with varying speeds and an initial water level of +0.50m NAP.

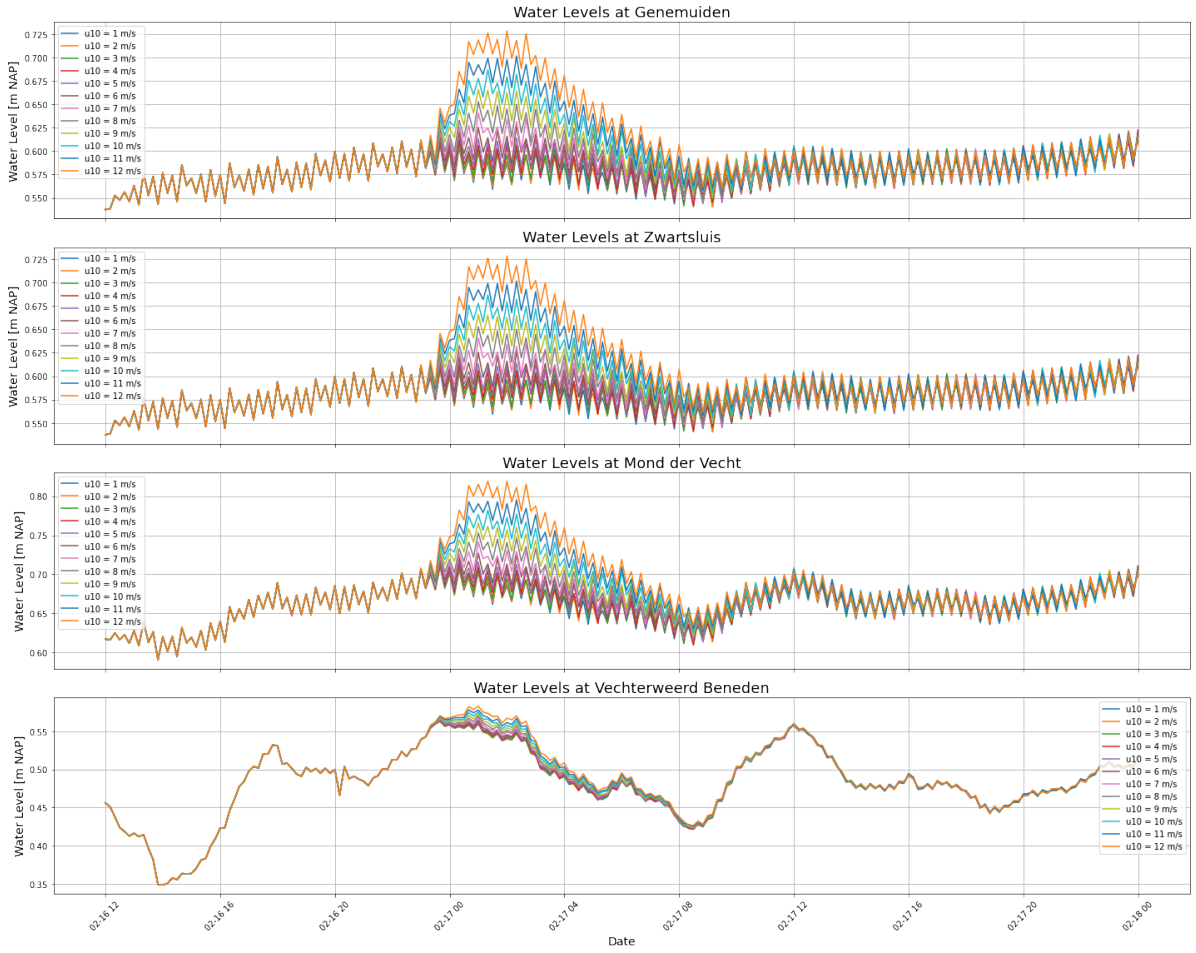

Figure D.83: Modelled Water Levels at Genemuiden, Zwartsluis, Mond der Vecht and Vechterweerd Beneden along the Zwarte Water and Vecht for northwestern winds with varying speed and an initial water level of +0.50m NAP.